Dynamic Thin Film-Intensified Direct Transesterification of Oleaginous Biomass to Biodiesel

by

Eko Kornelius Sitepu

Thesis
Submitted to Flinders University
for the degree of Doctor of Philosophy

Department of Medical Biotechnology
College of Medicine and Public Health
Flinders University of South Australia
May 2020

Contents

LIST OF TABLES

List of Figures

Abstract

Utilization of liquid renewable energy is rising to satisfy increasing demands in the transport sector, as fossil fuel reserves are rapidly depleting. Although bioethanol can contribute to biofuel blends for the general transport sector, biodiesel is the only suitable biofuel for heavy machinery and in the shipping industry; yet high biodiesel production costs limit its uptake. Traditional biodiesel production is a multiple step process which is not cost-effective, and especially requires drying or dewatering of oleaginous biomass, oil extraction and purification, high temperature and prolonged reaction times. Direct transesterification (DT) of oleaginous biomass to biodiesel can significantly reduce production costs which can be further reduced by using wet biomass. The effectiveness of the DT process using some oleaginous biomass has been demonstrated and is predominantly conducted under high temperature and pressure, particularly when using wet biomass to avoid negative effects of water. Maintaining these conditions under prolonged reaction times increases the biodiesel price which therefore requires subsidy and tax exemption to compete with petro-diesel fuel. This research investigated the suitability, energy efficiency and green chemistry pathway attributes of DT assisted by novel microfluidic platforms, the vortex fluidic device (VFD) and the turbo thin film device (T^2FD), for biodiesel production from a range of representative oleaginous biomass, such as *Chloroparva pannonica* (microalga), *Mucor plumbeus* (fungus) and soybean seeds under room temperature and atmospheric pressure conditions.

Fatty acid extraction and fatty acid to FAME conversion efficiencies were used at different parameter settings to evaluate performance of the processing technology in continuous flow - and in confined mode for the VFD. Single factor experiments evaluated the effects of catalyst concentration and water content of biomass, while factorial experimental designs determined the interactions between catalyst concentration and biomass to methanol ratio, flow rate, and rotational speed. For the VFD-assisted DT of *C. pannonica* biomass, a response surface method based on Box-Behnken experimental design was used to determine effects of water content, ratio of biomass to methanol and residence time. The success of the VFD microfluidic platform led to the design of high throughput, higher shear T^2FD. The presence of high shear stress in the thin film of liquid with the adjustable thickness of 100 to 200 μm in T^2FD is the result of high rotational speed of internal surfaces; that is a titanium blade is moving relative to a stationary stainless-steel block, which also improves the interaction of reactants. Irrespective of raw materials and

process-intensification technology, conversion efficiencies were >90%, showing a broad tolerance to parameter settings and water content.

Finally, process performance was evaluated by determining energy efficiency and green chemistry process metrics. Compared to the traditional two-step, one step, and one-step microwave- and ultrasound-assisted biodiesel production pathways, VFD and T^2FD-assisted base-catalysed DT of microalgal biomass saved ~98, 60, 98 and 94% of energy, respectively, with the processing occurring at room temperature and ambient pressure, while the environmental factor improved by ~80%. These outcomes are promising for directing biodiesel process pathway development for scale-up to commercial production. Outcomes of this research also identified promising future research avenues that can further improve environmental and economic metrics, particularly for the T^2FD-intensified DT of oleaginous biomass, using novel green chemistry-generated re-usable catalysts and less toxic substances that serve both purposes of being solvents and reactants.

Declaration

I certify that this thesis does not incorporate without acknowledgment any material previously submitted for a degree or diploma in any university; and that to the best of my knowledge and belief it does not contain any material previously published or written by another person except where due reference is made in the text.

Signed: Eko Kornelius Sitepu

Date: 4th March 2019

Acknowledgements

First and foremost, praise and thanks to the God, for His grace and blessing throughout my PhD journey.

I would like to acknowledge the Australian government for a scholarship given through the Australia Awards Scholarship programme. I would like to express my deep and sincere gratitude to my PhD supervisors, Prof. Wei Zhang, A/Prof. Youhong Tang, A/Prof. Sophie Leterme, A/Prof. Kirsten Heimann and Prof. Colin Raston for giving me the opportunity to do research and for providing guidance and support throughout my research. I would like also to thank Prof. Chris Franco, Head of Medical Biotechnology Department, Hanna Krysinska, Su Peng, Kushari and Jane Keane for their genuine support during my research work. I also thank all the members of the Centre of Marine Biotechnology Development group and Professor Raston's research group. My special thank goes to Darry Jones who helped and allowed me to use the turbo thin film device, Liu Fei Tan for providing microalgae *Chloroparva pannonica* biomass and Dr. Zhanying Zhang from the Queensland University of Technology for providing fungi *Mucor plumbeus* biomass. Also, I express my thanks to Kendall Corbin, Xuan Luo and Scott Pye for their help in my first paper.

I am extremely grateful to my wife and children for their love and prayers, their patience and sacrifices during this PhD journey, and to my deceased parent and parent-in-law who always supported me until the end of their lives.

Finally, many thanks to all the people who supported me, particularly Trinity Lutheran Church Pasadena members (Pastor Detlev Vosgerau, Pastor Matt Huckle, Colin Hayter, Maria and Graeme Payne), Indonesia Bataknesse South Australia Association and Indonesian Student Association in Australia (PPIA).

Eko K. Sitepu

Chapter 1
GENERAL INTRODUCTION

1.1 Research project background

Global environmental issues, including climate change-inducing emissions of greenhouse gases generated by the utilization of fossil fuels, and the rapid decline of crude oil reserves have promoted research on liquid renewable energy (Escobar et al., 2009). Biofuels derived from organic sources have a lower carbon footprint and could in theory replace fossil fuels (Alipour et al., 2017), yet fossil fuel oil remains the main liquid energy resource, but the contribution of biofuels is rising, accounting for 4% of the current energy consumption in transport in 2014 and is predicted to increase to 10% by 2020 (Frankl, 2017). The European Union has set the target of 10% biofuels for transportation (García-Olivares et al., 2018, Murphy and Thamsiriroj, 2011). Bioethanol and biodiesel are the most commonly used liquid biofuels, currently delivering 2% of the global transportation energy (Murphy and Thamsiriroj, 2011). Although biogas and bioethanol have a sufficiently high energy density for applications in general automobile transportation, they cannot replace the fuel density requirements of heavy machinery in the shipping industry (Knothe, 2010). The fact that diesel engines were invented to run on vegetable oils provide the advantage that biodiesels can be used without requiring diesel engine modifications (Xu and Mi, 2011). Standards are nonetheless applied to biodiesels to ensure engine longevity by reducing wear and tear, optimal performance, and to limit emissions (Islam et al., 2015a). Vegetable oils have a high viscosity, low cetane number and low flash point, and biodiesel blends can be tailored to improve properties that make them more suitable for modern diesel engines.

Despite biodiesel being a potential source of renewable transportation fuel, the current utilization of biodiesel remains low due to high production costs (Haas et al., 2006). The average prices of biodiesel (B100) and petro-diesel in the United States of America were US$0.94 and US$0.86 per litre in July 2018, respectively (Bourbon, 2018). Currently, biodiesel can only compete with petroleum diesel if it is subsidized by government or given a tax exemption (Demirbas and Balat, 2006). Direct subsidies and tax exemption could increase the utilization of biodiesel as the price could be lower than for petrol fuel diesel (Lin et al., 2011). Multiple production steps, including the preparation of oils as raw materials have been determined to be the major contributors to biodiesel production costs

(Haas and Wagner, 2011). A model developed by Haas et al. predicted that 88% of the total biodiesel production costs are the high cost for vegetable oil feedstocks (Haas et al., 2006). This also applies to the use of waste animal fats (tallow), contributing ~80% to the total biodiesel production costs, while only ~15% is spent on fixed and capital costs (Duncan, 2003). Furthermore, investigation into whether biodiesel production plant size affects costs determined that the production capacity of biodiesel plant must be between 50 – 80 kilo ton per year to be economically feasible (Apostolakou et al., 2009).

The use of large amounts of vegetable oils for biodiesel and edible crop biomass for bioethanol production initiated the food vs oil debate, resulting in intensified research into 2nd (waste cooking oil, tallow and non-edible oil seed crops) and 3rd generation (renewable feedstock produced on non-arable land) biodiesel feedstock (Ahmad et al., 2011). In the last 10 years, research into 3rd generation feedstock has again hit the spotlight, due to the question, what type of feedstock could potentially replace future total liquid fuel needs without negative impacts on water, energy and arable land resources (Go et al., 2016). Using oleaginous microorganisms, such as microalgae, yeast and fungi could meet these criteria, as biomass could be easily produced on non-arable land using industrial waste waters, brackish or marine waters. These organisms exhibit high growth potential and can be more lipid-rich than oleaginous seed crops (Shuba and Kifle, 2018). Nonetheless, to be economically feasible, the lipid content of microalgal biomass should be at least 35% (El Shimi and Moustafa, 2018). The requirement of harvesting/dewatering of the biomass has been identified as a major energy obstacle for energy-smart production of microbial biodiesel, consuming ~85% of the total required energy consumption (Lardon et al., 2009) and accounting for 50% of total production costs (He et al., 2016). Costs for microbial biodiesel production could be lowered if wet biomass could be used as the raw material (Cheng et al., 2013) and it would also result in decreased total processing time (Chopra et al., 2016).

Conventional biodiesel production relies on the transesterification of extracted FAs to FAMEs. While the extraction costs for oils from seed crops is economical (Sawada et al., 2014), extractions are cost- and energy-intensive for feedstock requiring drying (Taher et al., 2014, O'Connell et al., 2013)The estimated energy consumption for dewatering of microalgal biomass was 85 to 90% of the total energy consumption (Lardon et al., 2009, Xu et al., 2011). A Life Cycle Analysis (LCA) determined a negative energy balance (energy input: 3,292 MJ vs energy output: 1,000 MJ) for production of 24 kg of microalgal biodiesel, primarily due to biomass harvesting and drying using a filter press for initial

dewatering and natural gas drying (Sander and Murthy, 2010). An LCA on *Chlorella* biomass production using brewery wastewater and improved mixing technology for open pond systems and solar drying would lower energy input for biomass production by 3-fold (Abu-Ghosh et al., 2015), which would provide a positive energy balance. It has to be queried though, if solar drying can be utilised for biodiesel production at scale (Sander and Murthy, 2010).

In general, however, conventional biodiesel production has a negative environmental impact due to the use of hexane as a solvent for extraction (Mubarak et al., 2015). Hexane is classified as a hazardous air pollutant, as it has low solubility and is highly volatile, resulting in quick transport to the atmosphere. Through reaction with nitrogen dioxide and ozone, it contributes to the production of photochemical atmospheric smog (Kaul et al., 2010). In addition, there are environmental concerns when using traditional extraction and transesterification methods, even for oil seeds. For example, palm oil-derived biodiesel was heralded as a sustainable renewable feedstock for biodiesel production (Pande et al., 2012), but a LCA reported that the palm oil mill accounted for ~60% of the total greenhouse gas emissions, releasing 2.83 kg CO_{2eq} per litre palm biodiesel and requiring an energy and water input of 30.49 MJ and 23.64 m^3 L^{-1}, respectively (Kittithammavong et al., 2014).

Therefore, simplifying the biodiesel production process through eliminating extraction and purification of oil/lipid could reduce total biodiesel production cost (Go et al., 2016). Direct transesterification (DT) of crop/biomass has been demonstrated to be possible for a variety of feedstocks, achieving high fatty acid extraction and fatty acid to fatty acid methyl ester conversion yields (Haagenson et al., 2010, Haas and Wagner, 2011, Cheng et al., 2013, Dianursanti et al., 2015, Dasari et al., 2017). Furthermore, techno-economic analysis of the DT of rapeseed showed that the rate of return was ~50% higher than for the conventional method (Abo El-Enin et al., 2013). Therefore, DT offers a promising approach to increase both the production and utilization of biodiesel.

1.2 Aims and objectives

The research in this thesis aimed to simplify biodiesel production from microbial biomass and seed crop using novel dynamic microfluidic thin film platforms, in particular the vortex fluidic device (VFD) and the turbo thin film device (T^2FD), for the DT of fatty acids to biodiesel. The VFD-mediated processing provides benefits through enhanced mass

transfer, due to a large surface area presented in the dynamic thin film. The VFD was shown to facilitate biological, chemical and materials processes at room temperature. For example, graphene synthesis and microencapsulation of active compounds has been successfully carried out through VFD-processing (Chen et al., 2012, Wahid et al., 2013, Eroglu et al., 2013, Britton and Raston, 2014, Yuan et al., 2015, Tong et al., 2015, Wahid et al., 2015, Britton et al., 2016, Kumari et al., 2016, Vimalanathan et al., 2016). Moreover, the VFD was demonstrated to intensify the transesterification of sunflower oil with high biodiesel conversion yields and a short residence time at room temperature (Britton and Raston, 2014). The success of the VFD microfluidic platform led to the design of high throughput; higher shear thin film processing technology, termed the turbo thin film device (T^2FD) where the dynamic thin films can be adjusted between 100 to 200 μm. The presence of high shear stress in the thin film of liquid is the result of high rotational speed of internal fins in a titanium blade moving relative to a stationary stainless-steel block, with the process using this device also improving the interaction of reactants. Both the VFD and T^2FD processes deliver high shear as a form of mechanical energy at room temperature to drive the processing, and this is a distinctive advantage over former DT processing approaches.

1.3 The Structure of the thesis

This thesis consists of 6 chapters, including 2 chapters of experimental results and 1 chapter of general discussion and future directions. Chapter 1 (this chapter) is a general introduction to this thesis with a focus on briefly outlining current issues of biodiesel production and the aim/objectives of the thesis. Chapter 2 is a literature review, critically assessing the latest information on DT biodiesel production. This chapter aimed to critically evaluate the impact of feedstock and processing variables for the DT process. The author's three published articles (which comprise Chapters 3 and 4) are also critiqued in this literature review, as the review was published in Renewable and Sustainable Energy Reviews (IF > 11) (Sitepu et al., 2020), which was required to then make recommendation for future high impact research in this field. Chapter 3 describes the thin film devices and the procedures to examine the ability of the platforms to assist the DT of oleaginous biomass. The procedures are divided into general and the DT processes which also have been specified to each biomass.

The DT of oleaginous biomass / seed is studied using 2 different thin film devices such as VFD and T^2FD (the methodology of which is presented in chapter 3). Therefore the

experimental section is divided into 2 chapters based on thin film-intensified DT platforms used for oleaginous biomass / seed to biodiesel conversion. The experimental results of the DT of microalga *Chloroparva pannonica* biomass using VFD either in confined and continuous flow is discussed in chapter 4. This chapter was published in *Bioresource Technology* as Sitepu et al. (2018a) and won the 2018 Flinders University Best Higher Degree by Research Student publication.

Chapter 5 established optimal processing parameters for T^2FD-intensified DT of oleaginous biomass / seed such as microalga, fungi and soybean. Section 5.2 demonstrated the applicability of T^2FD-intensified DT for ground soybean seeds and in section 5.3 the wet microalgal biomass of *Chloroparva pannonica* is studied and this section was published in *Chemistry Communications* as Sitepu et al. (2018a). Section 5.4 examined processing parameters for T^2FD-intensified DT of *Mucor plumbeus* biomass to biodiesel. This chapter has been published in *Bioresource Technology* as Sitepu et al. (2019).

The last chapter summarises the key findings of the experimental chapters and critically discusses challenges of this research and, based on these, important future research directions are discussed.

Chapter 2
LITERATURE REVIEW

2.1 Introduction

Finite fossil fuel reserves cannot satisfy the growing demand for energy by industry and for transportation. Although fossil fuel oil remains the main liquid energy resource, the contribution of biofuels (bioethanol and biodiesel) is rising, delivering currently 2% of the global transportation energy (Murphy and Thamsiriroj, 2011), and could, in theory, replace fossil fuels (Alipour et al., 2017). The European Union has set the target of 10% biofuels for transportation (Murphy and Thamsiriroj, 2011, García-Olivares et al., 2018). Although biogas and bioethanol have sufficient high energy density for applications in general automobile transportation, they cannot replace the fuel density requirements of heavy machinery and in the shipping industry (Knothe, 2010). Despite biodiesel being a potential source of renewable transportation fuel, high production costs limit competitiveness in the transportation fuel market (Haas et al., 2006). The average prices of biodiesel (B100) and petro-diesel in the United States of America were US$0.94 and US$0.86 per litre in July 2018, respectively (Bourbon, 2018). Currently, biodiesel can only compete with petroleum diesel if it is subsidized by government or given a tax exemption (Demirbas and Balat, 2006).

Multiple processing stages, in particular extraction and purification, have been estimated to account for ~80% of biodiesel production costs (Haas et al., 2006). Therefore, simplifying the production process can increase the competitiveness of biodiesel (Go et al., 2016). Direct transesterification (DT) of crop/ biomass can produce high yields of fatty acids (FA) and FA to fatty acid methyl ester (FAME) conversion efficiencies (Haas and Wagner, 2011, Kasim and Harvey, 2011, Hailegiorgis et al., 2013, Cheng et al., 2013, Dianursanti et al., 2015, Hidalgo et al., 2015, Sitepu et al., 2018a, Sitepu et al., 2019). The effectiveness of DT has been demonstrated for many oleaginous feedstock under a variety of reaction conditions with or without either homogeneous or heterogeneous catalysts, enzymes and/or co-solvents at different temperatures and reaction times (Sivaramakrishnan and Incharoensakdi, 2017a, Nguyen et al., 2018, Son et al., 2018, Talha and Sulaiman, 2018, Sitepu et al., 2018a, Martínez et al., 2019, Zhang et al., 2019, Sitepu et al., 2019). In fact, Dasari et al. (Dasari et al., 2017) powered a diesel engine using DT-derived biodiesel from castor seeds which met biodiesel quality standards. Review of DT of microbial oils (Salam

et al., 2016, Yousuf et al., 2017, Kim et al., 2019, Goh et al., 2019) and crops (Kasim et al., 2010) demonstrated that the DT process is capable of producing fast, reliable and cheap biodiesel. Reviews to date, however, solely summarize current DT processes, but lack a focus on the systematic evaluation of effects of a combination of multiple processing parameters on the efficiency and cost-competitiveness of the process for a wide variety of possible feedstock.

As such, in addition to feedstock and feedstock processing considerations, comparatively little attention has been paid to energy requirements for biomass drying, catalyst choice, temperature, solvent use, and processing time or FA extraction yields and conversion efficiencies, which are critical to ensure biodiesel production can competitively, at least in part, replace fossil diesel. Therefore, this review will, systematically and critically assess these parameters for the different feedstock and DT processes that are available for biodiesel production. Research outcomes of this PhD research has been incorporated in this review to provide an up to date critical evaluation of all tested technologies and conditions in order to develop suggestions for impactful future research in this field.

2.2 Biodiesel feedstock

Preparation of oil (drying or dewatering of biomass, extraction and purification) as raw material for biodiesel production accounts for up to 75 to 88% of the total production cost (Haas et al., 2006, Lim and Teong, 2010, Kasim and Harvey, 2011). Selection of suitable oil feedstock can reduce these costs and increase the competitiveness of biodiesel. Peanut oil was the first biodiesel, driving the first invented diesel engine (Asadi et al., 2016). Other feedstock such as soybean, palm, coconut, sunflower, and rapeseed have also been tested (Corsini et al., 2015, Islam et al., 2015b). These seed crops are categorized as first generation biodiesel feedstock, because their applications are primarily in the food sector (Ahmad et al., 2011). However, unprecedented global population increase demands food – and freshwater security. While water requirements of sunflower, hemp and canola are 2 orders of magnitude lower than for other edible seed crops, fertiliser requirements are high (Table 2.1). Although it has to be noted that palm cultivation is a non-irrigated crop, relying on adequate rainfall (Table 2.1), the large negative environmental footprint (e.g. habitat destruction), makes it unlikely that palm oil can replace petroleum diesel at required volumes (Fargione et al., 2008). In addition, the production of biodiesel from food crops raised a food *vs* fuel debate, which resulted in increased research into non-food biodiesel feedstock.

Second generation biodiesel feedstock are derived from non-edible lipid-rich resources either from wastes (e.g. waste cooking oil, tallow) or biomass such as Jatropha, Castor, rubber, Mahua and tobacco (Ahmad et al., 2011, Islam et al., 2015b). Like biodiesel produced from edible seed crops, 2nd generation feedstock-derived biodiesel has similar properties to fossil diesel fuel (Atabani et al., 2013). The biodiesel properties of rubber seed (*Hevea brasiliensis*) met ASTM 6751-12 and EN14214 biodiesel standards (Abdulkadir et al., 2015). Furthermore, a 15% blend of castor seed-derived biodiesel/ fossil diesel had no adverse effect on diesel engine performance when tested in a direct-injection diesel engine (Dasari et al., 2017). In fact, exhaust gas emissions of CO (carbon monoxide), NOx (nitric oxides) and unburned HC (hydrocarbons from unburned diesel) decreased significantly with increasing biodiesel ratios in the blended fuel within the tested range (up to 15% blend). Despite lower fertiliser requirements compared to edible crop feedstock, water requirements met by rainfall are still high (Table 2.1). Therefore, uncertain future climatic conditions may destabilise any guarantee of feedstock supplies. In addition, similar to palm cultivation, except for Jojoba, production is restricted to warm subtropical and tropical climates (Table 2.1), entailing longer transport routes to existing refineries, which is a significant disadvantage both financially and energetically. In contrast, the penalty for production (fertiliser, water, energy) of waste cooking oil and tallow has already been paid for through utilization in the food sector, and the resource is readily available. Despite this advantage, 80% of the total biodiesel production cost still applies to collecting tallow as a feedstock (Duncan, 2003). To solve this problem, biodiesel manufacturers are focusing their attention on using low-cost feedstock such as waste cooking oil. Costs for waste cooking oil are two to three times lower than for refined vegetable oils (Canakci, 2007). This makes waste cooking oil an outstanding feedstock, as there is no significant difference in diesel engine performance in comparison to petro-diesel controls (Islam et al., 2015b). Supplies are, however, limited and higher levels of impurities need to be dealt with (Gebremariam and Marchetti, 2018). In addition, waste cooking oil contains 2 to 7% free fatty acids (FFA) (Gerpen, 2005), making processing exceedingly difficult due to saponification (soap formation), especially when an alkaline catalyst is used (Atadashi et al., 2012). Saponification-induced reduction of catalyst levels result in lower yields and adversely affects biodiesel purity (Ehimen et al., 2010).

Oleaginous microorganisms such as microalgae, fungi and yeast have been identified with potential for 3rd generation biodiesel feedstock (Shuba and Kifle, 2018). The reasons underpinning this potential are: (1) Some oleaginous microorganisms are characterised by

high biomass productivities, with some exhibiting a doubling time of <24h (Rashid et al., 2014). (2) Calculated product yields, based on growth performance of *Chlorella*, are likely higher, if cultivation is undertaken as a two-step process e.g. hetero- or mixotrophic cultivation in food processing wastewater for high biomass density outcomes, followed by phototrophic cultivation under nitrogen limitation for accumulation of triacylglycerides (TAG) (Abu-Ghosh et al., 2015). Calculated oil yields (5,000 L ha^{-1}) were comparable to palm oil; the currently best performing oil plant (5,950 L ha^{-1}) (Table 2.1) and the remediation of nutrient-laden wastewater has a distinctive advantage over chemical fertiliser requirements for palm cultivation. (3) Biomass can be produced on non-arable land utilising wastewater or saline resources (Raja et al., 2014).

Table 2.1**.** Examples of crop/biomass resources for biodiesel production. References (Priyadarshan et al., 2005, Gupta et al., 2012, Sawangkeaw and Ngamprasertsith, 2013, Ho et al., 2014, Abu-Ghosh et al., 2015, Bhuiya et al., 2016, Braunwald et al., 2016, Godswill et al., 2016, Kaya, 2016, Murphy, 2016, McKeon, 2016, Pham, 2016, Pratap et al., 2016, Suriya, 2016).

Crop / Biomass	Oil Content	Oil Yield (L ha^{-1})	Land/Soil Type	Climate	Water requirement	Fertilizer kg N ha^{-1} y^{-1})
Edible						
Palm	45 – 50	4,800	All soil types	Tropical	2,000[a]	98
Soybean	18 – 20	391	All soil types	Warm and moist	1,158[b]	15
Sunflower	35	457	All soil types, soggy	Warm	5[b]	91
Canola	40 – 45	1,200	All soil types	Cold and warm	87[b]	125
Coconut	65 – 68	3,260	Coarse sand	Warm	1,800 – 2,000[a]	49
Hemp Seed	20 – 36	363	sandy, silty or clay loam soil	Mild climate	30 – 40[a]	135
Peanut	45 – 50	1,059	Crumbly clay	Temperate and tropical	1,360[a]	20- 30
Camelina	40 – 43	583	All soil type except heavy clay and organic soil	Can be grown in different climate	-	70 - 100
Non-Edible						
Castor	40 – 45	1,188	Sandy loam soils	tropical and subtropical	500 – 600[a]	40
Jatropha	50 – 60	741	Aerated sands and loams	tropical and subtropical	250 – 1,200[a]	14 - 34
Jojoba	45 – 50	1,413	Coarse, light or medium textured soils	Cold and warm	-	-
Mahua	50 – 61	2,700	All soil types	Tropical and subtropical	550 – 1,500[a]	-
Rubber Seed	40 – 60		Laterite / sandy loamy	Warm	1,000 – 1,400[a]	70

Crop / Biomass	Oil Content	Oil Yield (L ha^{-1})	Land/Soil Type	Climate	Water requirement	Fertilizer kg N ha^{-1} y^{-1})
Microbial						
Chlorella	50	5000	Non arable	Warm	50,000[c]	Heterotrophic in brewery wastewater followed by autotrophic under nutrient limitation
Yeast	40	10,260	Non arable	Warm	600[d]	Freshwater (0.3)

[a] rainfall (mm Y^{-1}); Y: year

[b] water for irrigation (m^3 ha^{-1})

[c] brewery wastewater

[d] freshwater with in system recycling

The use of salinity-tolerant microalgal species would reduce freshwater requirements for biomass cultivation, a beneficial aspect given freshwater scarcity in arid countries and increased water demands of the growing population (Schenk et al., 2008). In addition, microalgae farming would not compete with land requirements for agriculture or city development (Yen et al., 2013). (4) Compared to conventional crops, the areal foot print for production can be small, i.e. less than a third of that required for palm or soy production through cultivation in vertically arranged photobioreactors (Chisti, 2007). For example, approximately 2-fold higher oil yields can be obtained from yeast compared to palm on the same area using closed stirred tank reactors (Table 2.1). (5) Some microorganisms have a similar fatty acid profile to vegetable oil and there have been efforts to produce biodiesel from oleaginous microorganisms, with many predicting biodiesel quality via fatty acid profiling (Islam et al., 2015a). There are various studies that assess diesel engine performance of microorganism-derived biodiesel or biodiesel blends (Islam et al., 2017). A diesel engine performance study using biodiesel derived from heterotrophically produced *Crypthecodinium cohnii*, an organisms with a high level of long chain polyunsaturated fatty acids, showed that blends of up to 50% could be used without affecting engine performance and that ASTM 6751-12 and EN14214 were largely met (Islam et al., 2015b).

2.3 Feedstock processing technologies

Conventional biodiesel production relies on the transesterification of extracted FAs to FAMEs (Fig. 2.1A). While the extraction costs for oils from seed crops is economical (Sawada et al., 2014), extractions are cost- and energy-intensive for feedstock requiring drying (O'Connell et al., 2013, Taher et al., 2014). Estimated energy consumption for

dewatering of microalgal biomass was 85 to 90% of the total energy consumption (Lardon et al., 2009, Xu et al., 2011). A Life Cycle Analysis (LCA) determined a negative energy balance (energy input: 3,292 MJ *vs* energy output: 1,000 MJ) for production of 24 kg of microalgal biodiesel, primarily due to biomass harvesting and drying using a filter press for initial dewatering and natural gas drying (Sander and Murthy, 2010). An LCA on *Chlorella* biomass production showed that using brewery wastewater and improved mixing technology for open pond systems and solar drying would lower energy input for biomass production 3-fold (Abu-Ghosh et al., 2015), which would provide a positive energy balance. It has to be queried though, if solar drying can be utilised for biodiesel production at scale (Sander and Murthy, 2010).

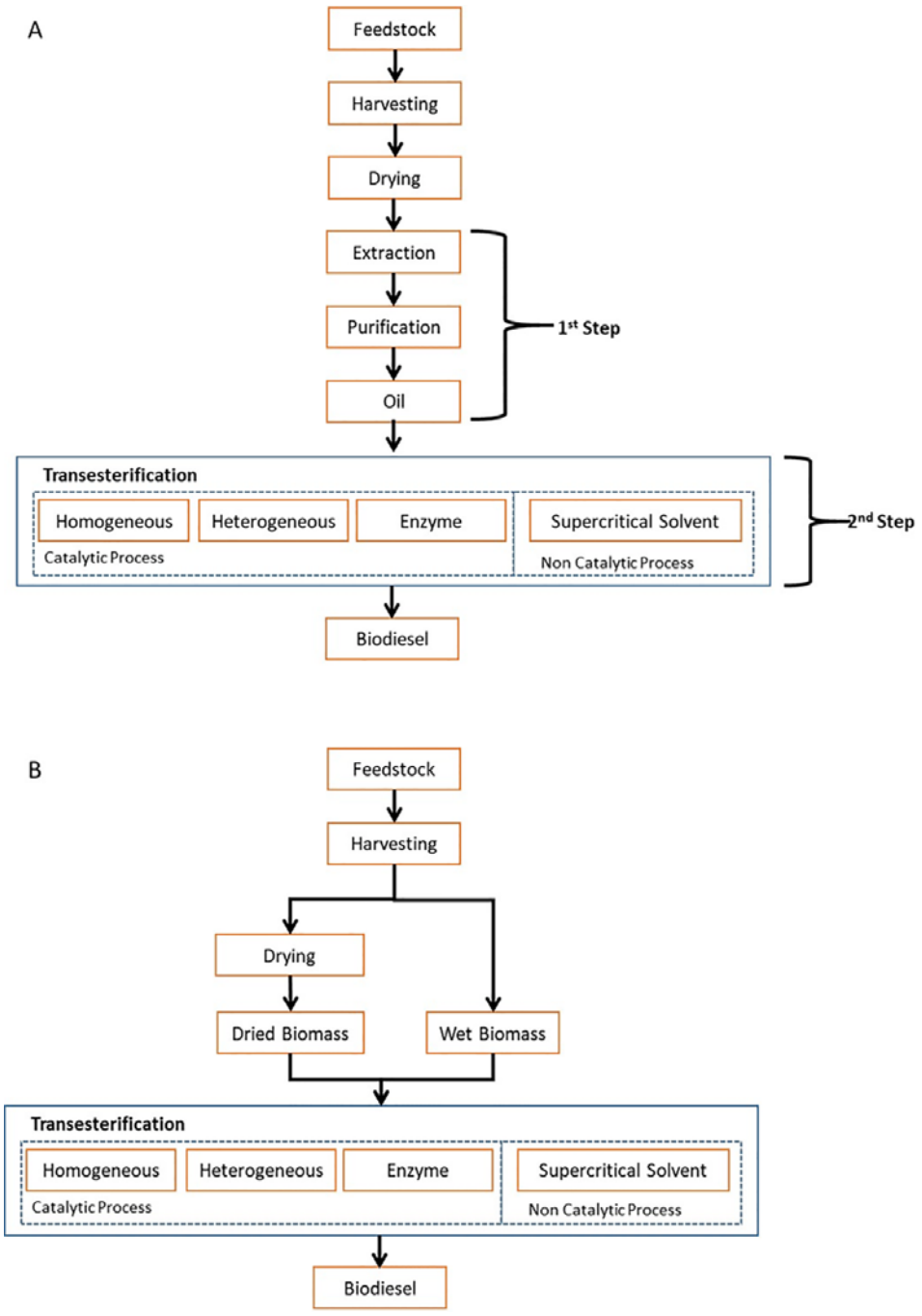

Figure 2.1. Biodiesel production from microorganism using the traditional approach **(A)** and direct transesterification methods **(B)**

In general, conventional biodiesel production has a negative environmental impact due to the use of hexane as a solvent for extraction (Mubarak et al., 2015). Hexane is classified as a hazardous air pollutant, due to low solubility and high volatility, resulting in quick evaporation to the atmosphere. Through reaction with nitrogen dioxide and ozone, it contributes to the production of photochemical atmospheric smog (Kaul et al., 2010). In addition, there are environmental concerns when using traditional extraction and transesterification methods, even for oil seeds. For example, palm oil-derived biodiesel

was heralded as a sustainable renewable feedstock for biodiesel production (Pande et al., 2012), but a LCA reported that the palm oil mill accounted for ~60% of the total greenhouse gas emissions, releasing 2.83 kg CO_{2eq} per litre palm biodiesel and requiring an energy and water input of 30.49 MJ and 23.64 m^3 L^{-1}, respectively (Kittithammavong et al., 2014).

Soxhlet extraction of lipids can save on solvent use, as the solvent is recycled within the system, but the process requires heating to boiling point, and an extraction time of 4 h typically applies (Ahmad et al., 2011). To avoid energy-intensive biomass drying and to shorten extraction times, accelerated solvent – (Ahmad et al., 2011, Islam et al., 2014) or subcritical water extraction (Ponnusamy et al., 2014) can be employed using wet biomass. These processes still require heating (90-120°C) and elevated pressure (11.7 MPa) to increase the interaction between the solvent and membrane lipids, yet extraction times are 16-fold lower compared to Soxhlet extraction. Importantly, water content had no significant effect on total yields under these conditions (Islam et al., 2014). A LCA on the effect of subcritical water extraction to produce 1 kg of microalgae biodiesel under optimised conditions required 28 MJ of energy, 68% of which was consumed in the extraction process (Ponnusamy et al., 2014). This clearly indicates that innovative biodiesel production should aim to eliminate the requirement for FA extraction to achieve significant energy savings.

Direct transesterification eliminates the need for FA extraction (Fig. 2.1B), as it produces alkyl esters directly from oil-bearing material through immediate contact between the alcohol and catalyst (Kasim and Harvey, 2011). Therefore, extraction and the transesterification reaction proceed in a single step, with the alcohol acting as both an extraction solvent and a transesterification reagent (Kildiran et al., 1996, Georgogianni et al., 2008, Shuit et al., 2010). Since 1985, numerous researchers have investigated the performance and feasibility of DT. Direct transesterification using homogenized sunflower seeds as substrate was first evaluated by Harrington and D'Arcy-Evans, who achieved a 20% increase in yield with the produced esters being identical to those produced in conventional transesterification (Harrington and D'Arcy-Evans, 1985). Since then, a number of articles concluded that DT is more efficient and effective and in some cases results in higher yields than conventional methods (Carvalho Júnior et al., 2011, Abo El-Enin et al., 2013, Amalia Kartika et al., 2013, Cao et al., 2013, Abdulkadir et al., 2015, Chen et al., 2015, Bauer et al., 2017). Direct transesterification can be carried out either in the presence or absence (non-catalytic processes) of a catalyst (Fig. 2.1B). Catalytic

transesterification reactions either utilise homogeneous and heterogeneous catalysts, either acid or base, while heating of the alcohol or carbon dioxide to subcritical temperatures (under appropriate pressure) is used for non-catalytic DT (Levine et al., 2010, Lim et al., 2010, Go et al., 2014b, Reddy et al., 2014).

In DT, cell walls are a major hindrance for the diffusion of solvents, adversely affecting potential biodiesel yields. The molar ratio of methanol to lipids/ biomass, temperature, reaction time and catalyst concentrations have to be optimized in order to enhance the rate of cell wall disruption and solvent/ catalyst diffusion. Mechanical pressing, high-pressure homogenization and supercritical fluid extraction have been used to break rigid cell walls, releasing lipids to the reactant (Choi et al., 2014). However, high energy input and time are major obstacles for all these methods (Martinez-Guerra et al., 2014b). Microwave and ultrasound are possible solutions to this problem, as these intensification processes enhance reaction rates in DT (Georgogianni et al., 2008, Koberg and Gedanken, 2012, Koutsouki et al., 2015). Even though microwave irradiation accelerates reaction rates, the energy produced is insufficient for breaking bonds (Talebian-Kiakalaieh et al., 2013, Koutsouki et al., 2015), but sufficient for the alcohol to reach its supercritical state (Patil et al., 2011b) (see Section 2.4.2.7). In contrast, ultrasound releases sound wave energy, resulting in elevated temperature and pressure, assisting cell wall disruption (Yu et al., 2010, Talebian-Kiakalaieh et al., 2013). In addition, cavitation effects produce turbulence in the liquids, further enhancing cell wall disintegration and solvent/ lipid interactions (Cravotto et al., 2008). Assessment of microwave and ultrasound-intensified DT for various biomass under dry and wet conditions suggests that outcomes range from moderate (~30-50%) to rather high levels of FA yields (≥90%) (Table 2.2).

For microwave-intensified DT, high FA yields were only obtained for dry biomass of Jatropha seeds, and for wet biomass of the fungus *Cryptococcus curvatus* using base catalysts (Table 2.2). Reaction times were typically shorter at 12 min; temperature (~50 – 60°C) and biomass to methanol ratio (1:8) were comparable to non-intensified DT processing, but catalyst concentrations (28%) were extraordinarily high. The process did not yield more than moderate DT rates for wet and dry microalgal biomass, regardless of the nature of the catalyst and inclusion of co-solvents, with only one microwave-intensified process achieving 75% FA yields for wet *Nannochloropsis* biomass, using a base catalyst (Table 2.2).

For ultrasound intensified DT, high FA yields were only obtained for dry biomass of *Cynara cardunculus* and the fungus *Trichosporon oleaginosus*, using base catalysts, and for wet biomass of the yeast *Yarrowia lipolytica*, using the catalyst sulphuric acid (Table 2.2). Little data is available on ultrasound-intensified DT of dry microalgal biomass and the process has not been investigated for wet microalgal biomass. Fatty acid yields from dry biomass of *Chlorella* and *Scenedesmus*, using base and the heterogeneous catalysts tungsten- and zirconium oxide, yielded only 19 and 21% with reaction times of 6 and 20 min, respectively, and biomass to methanol ratio was high 1:60 for *Scenedesmus* (Table 2.2). Fatty acid yields (19.5%) were also not impressive when using microwave- and ultrasound-intensified DT of dry *Chlorella* biomass, using the heterogeneous catalyst KF/CaO (Table 2). In contrast, ultrasound-intensified and acid-catalysed DT of dry biomass of *Chlorella* obtained an FA yield of 78%, but it included diethyl ether as a co-solvent and required a catalyst concentration of 4%, while reaction time, temperature and biomass to methanol ratio was comparable to standard DT conditions (Table 2).

Another green chemistry DT method has been evaluated in this PhD research. These DT processing platforms rely on microfluidic shear stress in thin films, producing biodiesel from a variety of wet biomass in continuous flow mode at room temperature and ambient pressure (Table 2.2) (Sitepu et al., 2018a, Sitepu et al., 2018b, Sitepu et al., 2019). These microfluidic devices provide a large surface contact area between reactants and exhibit enhanced mass – and heat transfers, which shortens reaction times (Britton et al., 2017, Sitepu et al., 2018b, Sitepu et al., 2019). In a vortex fluidic device (VFD), Figure 2.2A, a dynamic thin film with a thickness of ~250 µm forms when a tube containing liquid, inclined at an angle of 45°, is rotated at high speed (Eroglu et al., 2013, Britton and Raston, 2014). The angle corresponds to the maximum cross vector of centrifugal force and gravity in a VFD. The VFD can be operated with finite volumes of reactants (confined mode) or in continuous flow mode where jet feeds deliver reactants to the hemispherical bottom of tube (Yasmin et al., 2013). A new design of a microfluidic platform, the turbo thin film device (T^2FD), Figure 2.2B, has been developed based on a similar concept to the VFD, to improve reaction conditions under continuous flow operation (Sitepu et al., 2018b). The T^2FD consists of a motor connected to a blade and a base. The gap between blade and base can be adjusted, which allows reagents to form a thin film with a thickness between 100 to 200 µm. Periodic gaps in the blade allow reagents to flow to the base. A dynamic thin film spontaneously occurs when the reagents pass the blade, resulting in enhanced mass transfer. Highest FA extraction yields (72 mol%) and FA to FAME conversion

efficiencies (97%) were achieved with a residence time of 2 min with fungal biomass of *Mucor plumbeus* with a water content of 50%, using a base catalyst (Table 2.2).

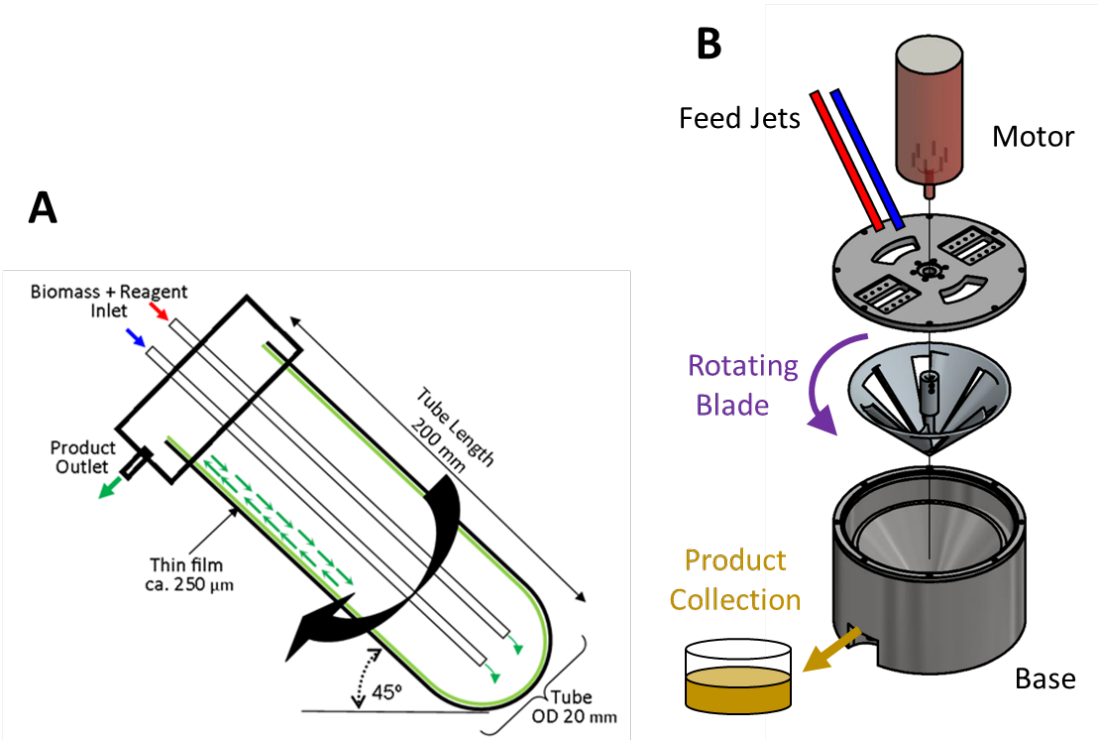

Figure 2.2. Diagram of the VFD (A) and T2FD (B) in continuous flow method adapted from (Sitepu et al., 2018a, Sitepu et al., 2019)

Catalysed DT is traditionally used more often for biodiesel production than non-catalytic processes (supercritical solvent DT), due to the requirement of high temperature and pressure and thus higher energy demands and production costs for the latter (Leung et al., 2010, Bernal et al., 2012). High pressure and temperature, however, assist in lysing of seed cell walls, improving diffusion of the alcohol and reaction with lipids. At a critical point of a solvent, which is achieved at appropriate pressure and temperature, a single fluid phase is formed, facilitating the mixing of lipids and methanol (Leung et al., 2010). Application of supercritical methanol transesterification of *Jatropha curcas* oil using the traditional two-step process obtained a 100% biodiesel yield in 4 min at 320°C and 8.4 MPa (Hawash et al., 2009). A similar result was also achieved when supercritical methanol transesterification was applied to *Jatropha curcas* seeds with a reaction time of 30 min (Lim and Lee, 2013). These results led to the conclusion that supercritical solvent-assisted transesterification was superior to the traditional approach with regards to reaction time, ease of product separation and yields.

2.4 Factors affecting direct transesterification yields and conversion efficiencies

A variety of factors – dependent on feedstock, the physical properties of feedstock (e.g. wet vs dry) and processing technology used – have a combined effect on DT yields and conversion efficiencies; i.e. the choice of catalyst and concentration, solvents, reaction time, temperature, and biomass to solvent ratios. It is, however, important to consider the effect of the single factors first, before evaluation of the combined effect to understand the implications on outcomes and to make informed decisions for cost- and energy-efficient biodiesel production. Therefore, this review will briefly assess the impact of single factors.

2.4.1 Effect of water content

DT of oily seeds typically is not affected by water content, as the feedstock contains little water (Table 2.2) that does not interfere with the transesterification reaction (Griffiths et al., 2010). In contrast, as outlined above, the water content of microbial biomass is typically too high for most processing technologies, requiring cost- and energy-intensive drying of the biomass. Excess water can result in hydrolysis of triglycerides to free fatty acids (FFA) (Freedman et al., 1984), affecting the choice of catalyst, i.e. saponification occurs if a base catalyst is used (Suwannakarn et al., 2009). Furthermore, water is also a by-product of the transesterification reaction, due to the condensation reaction of carboxylic acid and hydroxyl group of the alcohol, particularly in acid-catalysed transesterification reactions (Liu et al., 2006). In contrast, ~2% of water (based on lipid weight) had a positive effect when the heterogeneous catalyst CaO was used in DT, as protons from water react with O^{2-}, resulting ultimately in the formation of the methoxide anion and FAME production (Liu et al., 2008). Higher water contents, however, still resulted in saponification. Therefore, the effect of processing technologies in the DT of microbial biomass has focused on parameter optimisation using dry microbial biomass (Table 2.2).

Modern processing technologies and catalyst research focus on reducing the negative impacts of water to eliminate energy – and cost penalties. A complete summary of microbial oil yields and FA to FAME conversion efficiencies is given in Table 2.2, which highlights that high yields and conversion efficiencies can be achieved under dry and wet conditions using catalytic DT. The use of acid or acetyl chloride as catalysts were the most successful for obtaining high FA yields from wet biomass of the marine microalga *Nannochloropsis*, ranging from 90-95% to 100%, respectively, while microwave-assisted extraction in the presence of base catalysts or base and acid catalysts gave lower yields of

75 and 43, respectively (Table 2.2). Outcomes could be influenced by other species present, but another possible explanation is the chemically inert nature of the cell wall, which is bi-layered, with the outer part being 20 nm thick, consisting of a tri-laminar sheath of aliphatic C_{30}-straight chain saturated hydrocarbons joined by ester bonds, either at the terminal or one or two mid chain positions (Geldin et al., 1999, Scholz et al., 2014). This would explain why microwave processing was less effective. In general, however, microwave-assisted extraction of wet microalgal and fungal biomass suffers from low to average yields under wet and dry conditions (Table 2.2). Average FA yields of ~40-56% were also achieved with VFD- and T^2FD-assisted extraction of dry and wet microalgal and fungal biomass, but >90% FA to FAME conversion efficiencies were realised (Table 2.2). In this context, it is important to note that, unlike microwave-assisted DT, the VFD and the T^2FD-intensified processes do not require heating and proceed at ambient pressure, with residence times of 2 and 5 min under continuous flow conditions, respectively (Table 2.2).

Non-catalytic DT processes, such as supercritical solvent (either methanol or ethanol) have been developed specifically for wet microbial biomass, utilising water as a co-solvent (Kusdiana and Saka, 2004), but a positive effect was only evident for *Nannochloropsis* biomass (Table 2.3). Biodiesel yields from dry biomass were 2 – 9% higher for dry biomass (Jazzar et al., 2015a) and high yields of 84% have been reported for *Nannochloropsis* biomass with a water content of 90% (Table 2.3). A LCA, contrasting conventional biomass production (raceway), harvesting/ dewatering, drying, extraction and transesterification with bioreactor-grown and supercritical methanol DT of *Chlorella*, highlights that the 65% of energy requirements for the latter process can be covered by anaerobic digestion of residues and the entire process delivers energy savings of 85% (Brentner et al., 2011).

In summary, DT of wet biomass will be the preferred option to overcome the economic and energy constraints to commercial-scale biodiesel production (Razon and Tan, 2011). However, the choice of raw material (dry or wet) for biodiesel production will also depend on reaction conditions (e.g. ease of upscaling etc.), including reaction times and temperature, ratio of methanol to lipid or biomass and catalyst concentration, which are discussed further below.

2.4.2 Catalysts

In addition to non-catalyst-based processes, such as supercritical solvent processing, various catalysts are being trialled in the DT of wet biomass – homogeneous catalysts (Velasquez-Orta et al., 2012, Zhang et al., 2015b, Kakkad et al., 2015b), heterogeneous catalysts (Taufiq-Yap and Teo, 2014, Carvalho et al., 2017) combinations of homogeneous and heterogeneous catalysts (Zhang et al., 2012, Ma et al., 2015a), and enzymes (Huang et al., 2015) (Figure 2.1B).

2.4.2.1 Catalyst function in direct transesterification

Methanol is a poor solvent for lipids (Wahlen et al., 2011). For example, only 14.5 and 22% of Jatropha and cottonseed oil was extracted into methanol after 1 and 5 h, respectively (Qian et al., 2008, Kasim and Harvey, 2011). The quantity of cottonseed oil in methanol increased to 99.7% when 0.1 M sodium hydroxide was added as a catalyst, achieving a 98% conversion of FA to FAME (Qian et al., 2008), while the same FAME yield was also obtained using acid as a catalyst for Jatropha (Shuit et al., 2010).

In DT, the catalyst increases the transesterification rate and additionally aids in cell wall degradation, releasing more lipids into the reaction mixture (Kildiran et al., 1996, Macías-Sánchez et al., 2015). The shape and size of cells walls change during the processing; for example, cell diameters of *Chlorella* sp. decreased from 3.58 μm to 1.92 μm upon addition of sulfuric acid (Velasquez-Orta et al., 2013), while the use of a base catalyst was more effective in destroying the cell walls of *Chlorella* sp. (Kumar et al., 2014). Use of sodium hydroxide in the first stage of the DT process followed by sulfuric acid in the second stage achieved complete destruction of *Chlorella* cells.

2.4.2.2 Choice of catalysts and catalyst concentration

Common catalysts widely used in transesterification reactions are alkalis and acids, both in the form of homogeneous and heterogeneous substances and enzymes (Boro et al., 2012). Homogeneous alkaline catalysts such as sodium hydroxide, potassium hydroxide, carbonates, and derivatives of alkoxides such as sodium methoxide or sodium ethoxide were the preferred catalysts, achieving high purity and high yields of biodiesel with short reaction times (Ma and Hanna, 1999). Drawbacks of homogeneous alkaline catalysts are expensive- and time-consuming purification and environmental concerns relating to the disposal of highly basic waste streams (Granados et al., 2007). Furthermore, highly

purified triglycerides must be used as raw material to avoid soap formation, which decreases the quality and yield of biodiesel. The FFA concentration in triglycerides should be less than 1% when using an alkaline catalyst (Dias et al., 2008). In contrast, acid-catalyzed transesterification, i.e. use of sulphuric acid and hydrochloric acid, is more resilient to high FAA contents, as they can simultaneously catalyze both esterification and transesterification (Aranda et al., 2008).

Catalyst concentration is an important factor directly influencing the yield of biodiesel. Of the three different acetyl chloride catalyst concentrations (2.5, 5 and 10.5%) tested in the DT of wet *Nannochloropsis gaditana* biomass, 5% catalyst produced maximum yields (Macías-Sánchez et al., 2015). Reduction of FAME yields when exceeding optimal catalyst concentrations has been attributed to side reaction with polyunsaturated fatty acids, which can be present at high concentrations in microalgal biomass (Macías-Sánchez et al., 2015). Similarly, exceeding optimal levels of heterogeneous catalysts can lead to agglomeration of catalyst, reducing mass transfer and surface interaction between the reactants (Ma et al., 2015a, Koutsouki et al., 2015).

2.4.2.3 Acid catalysts

Although acid catalysts are not commonly used in biodiesel production, due to slow reaction rates and the requirement for larger quantities of solvents, a higher tolerance for FFA and water content is an advantage when using microbial biomass for biodiesel production (Atadashi et al., 2012). Microbial lipids can contain a high level of FFA (Table 4). Some microalgal species such as *Chaeotoceros gracilis* and *Chaeotoceros calcitrans* contain FFA as their major constituent (Volkman et al., 1989). The amount of FFA can also increase during storage. Lipids, particularly those containing polyunsaturated fatty acids, could be degraded to form FFA through oxidation, hydrolysis or polymerization reaction caused by the presence of enzymes, light, heat, ionization, or moisture (Alencar et al., 2010, Zhang et al., 2010).

Most acid-catalysed DT reactions with microbial feedstock utilized sulphuric acid, commonly resulting in high yields of biodiesel (Table 2.2). Although high biodiesel yields (92 and 98%) were achieved for dry *Chlorella* biomass, outcomes were highly variable (lowest FA yields of 25 and 26% (Table 2.2). This may indicate a significant effect of either species, identification accuracy, or production-controlled biomass quality. FA yields decreased further to 22% when the process was microwave-intensified (Table 2.2). A high FFA content in *Chlorella* dry biomass was successfully converted to FAME using sulphuric

acid as a catalyst, resulting in a FA to FAME conversion efficiency of 97% with a reaction time of 60 min at 60°C, but FA extraction yields were only 25% (Velasquez-Orta et al., 2013). In contrast, the use of sulphuric acid for DT of wet *Chlorella* biomass yielded poor outcomes of 8-9% FA yields, unless the process was microwave-assisted (37%) or hexane was used as a co-solvent (92%) (Table 2.2). Acid-catalysed DT of dry *Scenedesmus* biomass gave FA yields ranging from 48-85%, comparable to outcomes for *Nannochloropsis* (Table 2.2). In contrast, DT of wet biomass of *Nannochloroposis salina* or *N. gaditana* using sulphuric acid, hydrochloric acid (with chloroform as a co-solvent for the latter) or acetyl chloride as catalysts resulted in yields of >90% and FA to FAME conversion efficiencies of ≥95% (Table 2.2) (Kim et al., 2015a), but higher reaction temperatures of 100 and 95°C were required. Compared to sulphuric acid, hydrochloric acid has a lower boiling point, an advantage for easier recycling of the catalyst (Kim et al., 2015a). Acid-catalysed biodiesel yields varied widely for fungal/ yeast biomass under dry (6 to 97%) and wet conditions (46 to 94%) (Table 2.2), highlighting the effect of biomass choice on DT outcomes.

Several higher value chemicals could be potentially developed in sulphuric acid-catalysed DT of wet *N. gaditana* and *N. oceanica* biomass when processed at a reaction temperature of 125°C, which could offset production costs and lower the biodiesel market price (Sathish et al., 2014, Kim et al., 2015a), but FA yields (17%) would need to increase significantly (Table 2.2). High-value co-chemical products are ethyl levulinate (23.1%), ethyl formate (10.3%) and diethyl ether (52.1%). These chemicals are a product of acid hydrolysis of the cellulosic inner wall of the bi-layered cell wall and have applications as flavouring agents, fumigants, or solvents, but quantities isolated decreased with increasing water content.

2.4.2.4 Base catalysts

Sodium hydroxide and potassium hydroxide are the common base homogeneous catalysts for transesterification reactions, as high yields are achieved under mild conditions, e.g. ambient temperatures (Pinto et al., 2005, Haas and Scott, 2007, Dupont et al., 2009, Zeng et al., 2009) and up to 4,000-times faster reaction times compared to acid-catalysed conditions (Fukuda et al., 2001), but saponification due to high FFA contents can pose a problem.

The use of a base catalyst in the DT of dry *Chlorella* biomass gave >2-fold lower FA yields (21%) compared to acid-catalysed DT (FA yield 98%) and using hexane as a co-solvent in

acid-catalysed DT of wet biomass (Table 2.2). Outcomes improved by 18% using sequential catalysis, starting with a base catalyst followed by sulphuric acid (Table 2.2), which might indicate either more efficient cell wall degradation or a higher conversion of FFA in acid-catalysed DT. In contrast, potassium hydroxide-catalysed DT of dry *Nannochloropsis* biomass achieved FA yields of 91%, being 18% higher compared to acid-catalysed DT; while microwave-intensified base-catalysed DT achieved less than 45% (Table 2.2). On the other hand, sodium hydroxide-catalysed DT of wet *Nannochloropsis* biomass was 20% lower compared to acid-catalysed DT and yields were halved for microwave-intensified DT in a two-step catalytic approach, using sodium hydroxide followed by sulphuric acid, the latter being comparable to microwave-assisted DT of dry biomass (Table 2.2). These results demonstrate that, in order to select a process, the influence of feedstock choice must be ascertained.

Compared to acid-catalysed DT of dry biomass of *Scenedesmus* (85%) (Table 2.2), sodium hydroxide-catalysed DT yielded only 55% biodiesel per gram lipid but with a five-fold lower reaction time (2 *vs* 10 h) at similar temperatures (Table 2.2), but purification was 2.5-times more efficient for the acid-catalysed produced biodiesel (Kim et al., 2014). These outcomes highlight that the contribution of each parameter to biodiesel production costs and energy-efficiency must be explored to arrive at informed decisions for feedstock and feedstock condition (wet *vs* dry), as well as processing technologies and process parameter choices.

Base-catalysed DT and microwave-intensified base-catalysed DT with hexane as a co-solvent of dry yeast/fungal biomass (*Rhodosporidium toruloides* and *Trichosporon oleaginosus*) obtained FA yields of 98 and 93.5%, respectively (Table 2.2). In contrast, potassium hydroxide-catalysed DT of wet biomass of *Rhodosporidium diobovatum* with ionic liquid as a co-solvent produced less than half the yield (Table 2.2). Due to differences in species used, it cannot be determined whether the outcomes were affected by the water content or an effect of differences in DT parameters. This demonstrates that there is an urgent need for a systematic and complete analysis of DT processing parameters for promising species, which should ideally be complemented by modelled techno-economic and LCA outcomes.

2.4.2.5 Heterogeneous catalysts

Biodiesel purification after transesterification is a common problem associated with the use of homogeneous catalysts (Boey et al., 2011). Water, typically used for biodiesel

purification, requires wastewater treatment before discharge (Ma et al., 2015a). Other issues include corrosion, recyclability of base catalysts and recovery of glycerol, which also increase cost and environmental footprint of biodiesel production (Pinto et al., 2005, Dupont et al., 2009, Lee et al., 2009). In contrast, heterogeneous catalysts are solids with high activity and separation characteristics, eliminating washing with water (Demirbas and Balat, 2006, Liu et al., 2008). Heterogeneous catalysts have, therefore, been extensively investigated in the last few years, particularly for DT of microbial biomass. One of the largest foreseeable problems concerning cost- and energy-efficiency are very high temperature requirements for prolonged periods for activation of heterogeneous catalysts.

For biodiesel production from seed oil, microwave-intensified DT with strontium oxide and chloroform as a co-solvent using Castor seeds resulted in a 12% increase in yields and 36-fold reduced reaction times (Table 2.2). These results sound promising, but recycling required ramping the temperature by 10°C per min in a furnace under argon gas to 710°C, which was kept for 1 h (Koberg and Gedanken, 2012). Cost-benefit analysis and/or techno-economic and LCA is required to determine, if improvements made would pay dividend.

For heterogeneous catalyst-catalysed DT of *Chlorella*, effect on yields and conditions are unclear, as studies used different catalysts and species under wet and dry conditions (Table 2.2). In general though, FA yields (19.5 to 32%) for dry biomass were comparable to those using homogeneous acid and base catalysts. FA yields (87%) were slightly lower for microwave-intensified DT of wet biomass using graphene oxide, but change of catalyst to sulfonated graphene oxide gave 3-fold lower yields (Table 2.2). For dry *Nannochloropsis* biomass, biodiesel yields were much lower than in acid-catalysed DT (73%), achieving 28, 21 and 37% for magnesium-zirconium alloy, ultrasound-assisted strontium oxide and microwave-intensified strontium oxide-catalysed reactions, respectively (Table 2.2). Results were also disappointing for microwave-assisted (15%) and ultrasound-intensified tungsten oxide/strontium oxide-catalysed DT (21%) of dry *Scenedesmus* biomass (Table 2.2). In contrast, microwave-assisted DT of wet *Chlorella pyrenoidosa* biomass resulted in yields of 87% in the presence of graphene oxide (Table 2.2), representing the best results achieved to date using heterogeneous catalysts and wet microalgal biomass. Given the generally disappointing outcomes, it is paramount to model effects on energy balances and environmental burden. For example, to achieve a 15% FA yield from dried *Chlorella vulgaris* biomass using the heterogeneous catalyst (KOH/Al_2O_3), KOH was loaded onto Al_2O_3 using the wet impregnation method tolerating only up to 3% of

water, and KOH loading and the calcination temperature were optimised for the highest catalytic activity. This required a 2 h calcination time at 700°C and a 6 h reaction time at 60°C for 35 wt% KOH loading, (Ma et al., 2015a). In contrast, synthesis of graphene oxide required only 2 h at 35°C under acidic conditions using graphite and potassium permanganate, achieving an FA yield of 87% from wet biomass of *Chlorella pyrenoidosa* (Cheng et al., 2016). Although there may be species-specific effects, data to date indicate that biodiesel production from *Chlorella* should be performed using acid-catalysed DT, as this produced the highest FA yields from dry and wet biomass.

2.4.2.6 Enzymes

Several problems were identified in the use of chemical catalysts in biodiesel production such as a high energy input, effects of water and FFA contents, reusability of the catalyst, purification of both biodiesel and glycerol as a by-product, and environmental impact (Gog et al., 2012). The use of biocatalysts can overcome these problems. Lipases can catalyse both transesterification and esterification reactions (Noureddini et al., 2005, Li et al., 2006, Dizge et al., 2009, Huang et al., 2015, Sangaletti-Gerhard et al., 2015), with the advantage of requiring low reaction temperatures (20 – 50^{0}C), producing high-grade glycerol, and the enzymes can be recycled when immobilised on solid supports (Gog et al., 2012, Aguieiras et al., 2015). Although current production costs are higher than for chemically catalysed DT, some enzymatic biodiesel production plants have been established in China, Israel and the United States of America (Du et al., 2008, Christopher et al., 2014).

Different lipases have been trialled in DT of dry microlagal biomass, producing disappointing (8%) to acceptable FA yields (88%) (Table 2.2). The most disappointing outcome was achieved for *Chlorella vulgaris* using Novozyme 435 and pressurized propane as a co-solvent, requiring 8 h reaction time at 50°C and propane at a pressure of 18,000 kPa (Marcon et al., 2017). In contrast, Novozyme 435-catalysed DT of dry *Aurantiochytrium* sp. biomass achieved a FA yield of 48%, requiring a reaction time of 12 h at 50°C using dimethyl carbonate as a reactant (Kim et al., 2016). Best results for dry microalgal biomass was achieved with *Botryococcus* using Novozyme CAL-B Celite as a catalyst and dimethyl carbonate as the reactant, achieving an FA yield of 88% at a reaction temperature of 50°C and a reaction time of 4 h (Table 2.2). These results demonstrate that, in addition to a strong influence of species and reactant, lipase choice needs to be considered concerning reaction times. Furthermore, species choice has to take biomass productivities into account, which are for many strains of *Botryococcus* too low for serious consideration for biodiesel production at scale (Gouveia et al., 2017)

FA yields of 72% were also achieved for wet biomass of *Chlorella vulgaris*, using an immobilized *Burkholderia* lipase (3369 U/g oil) at 40°and hexane and methanol as an extractant and reactant, respectively (Table 2.2). Nano-core Fe_3O_4 and TEOS were used to form a mesoporous nanocomposite of Fe_3O_4-SiO_2 as a support for the lipase catalyst, providing the opportunity for reuse. The yield of biodiesel remained similar at 69, 68 and 58% in reuse cycles four, five and six (Tran et al., 2013), but reaction times were excessive (48 h). In any case, results are promising and impacts of catalyst cost and reaction time on production costs, footprint requirements and implications for scale should be investigated.

2.4.2.7 Non-catalytic direct transesterification

Critical solvent-based DT of Jatropha and soybean did not achieve competitive FA yields (Table 2.3). Similarly, FA yields for wet microalgal and fungal biomass were typically around 50% (Table 2.3). An exception is critical solvent-DT of wet *Nannochloropsis* biomass, achieving an FA yield of 84% and a FA to FAME conversion efficiency of 84% at a reaction temperature of 255°C in 25 min., while yields of 50% were achieved at slightly different water content and processing conditions. Whether one off higher yields are a consequence of species, triglyceride content and/or culture growth phase remains to be determined. This aside, a critical analysis of energy requirements for the entire process is required to ascertain whether supercritical solvent-based DT is a viable option for biodiesel production from wet biomass or difficult to process cells. In this regard, it needs to be considered that pure products and by-products were obtained without purification (Patil et al., 2012a).

2.5 Operating conditions for direct transesterification

2.5.1 Ratio of lipids/biomass to alcohol

In transesterification reactions, a stoichiometry of 3 moles of methanol per mole triglyceride is consumed to produce 3 moles of FAME, but an excess of the alcohol is required to ensure complete conversion (Ma and Hanna, 1999, Shiu et al., 2010, Hailegiorgis et al., 2015). The molar ratio of alcohol to triglyceride is further affected by the type of catalyst, being a ratio of 6:1 in most base-catalysed reactions, and exceeding the optimal ratio tends to make the separation of glycerol difficult (Ma and Hanna, 1999, Fukuda et al., 2001, Leung et al., 2010, Zakaria and Harvey, 2012). For DT, however, a higher molar ratio is required to completely immerge the biomass and for effective

agitation (Zakaria and Harvey, 2012). In addition, short chain alcohols are a poor solvent for lipid extraction, and, based on Fick's Law, requiring an excess of alcohol to extract lipids (Zakaria and Harvey, 2012). Non-catalytic supercritical solvent DT, where the alcohol acts as solvent, reactant and catalyst precursor, also requires higher alcohol/ lipid ratios (Reddy et al., 2014, Jazzar et al., 2015a), which can decrease the critical temperature of the mixture (Patil et al., 2011b, Jazzar et al., 2015a). 9 mL per gram biomass appears to be most frequently used (Table 3), which is equivalent to a molar ratio of 1:882 based on triolein as the main fatty acid, while higher ratios can interfere with the separation of glycerol (Jazzar et al., 2015a).

A 200-fold higher molar ratio was applied in the acid-catalysed DT of dry *Chlorella* biomass, resulting in dramatically different outcomes of FA yields, which is most likely due to feedstock choice rather than reaction time (*Chlorella* sp. 92% after 19 h *vs Chlorella vulgaris* 26% after 20 h) (Table 2.2). In addition to the choice of species, a potential impact of reaction time, rather than biomass/ methanol ratio, is evident in acid-catalysed FA yields of dry *Chlorella* biomass (98, 18, 25% after 4, 2 and 1 h) for biomass/ methanol ratios of 1:3, 1:20, and 1:4, respectively (Table 2.2). Similarly, a combined effect of species, co-solvent, reaction time and temperature could be the cause of the difference in FA yield in acid-catalysed DT of wet *Chlorella* biomass (Table 2.2). A biomass/ methanol ratio of 1:40 resulted in FA yields of 9% *vs* 92%, the latter process employed hexane as a co-solvent, 6-fold longer reaction times (2 h) and 30°C higher temperatures (90°C). Establishing an impact of biomass/ methanol ratio is not possible for studies using different catalysts, as catalysts directly affect lipid extraction efficiencies through different interactions with the cell wall, an important factor in DT. Therefore, the best ratio for acid- or base-catalysed DT cannot be established for dry or wet biomass of *Nannochloropsis*, or the base-catalyst under wet or dry biomass conditions for *Chlorella* (Table 2.2). Using base-catalysed VFD- and T^2FD-intensify DT of microalgal and fungal biomass (this PhD research), however, no large impact of biomass/ methanol ratio was evident (Sitepu et al., 2018a, Sitepu et al., 2018b). Nonetheless, the data demonstrate that compared to dry DT, DT of wet microalgal biomass requires a higher amount of methanol to lessen the impact of water (Table 2.2).

2.5.2 Temperature

Increased temperatures reduce the viscosity of the lipid/ methanol mixtures, enhancing the interaction between triglycerides, methanol and the catalyst (Fukuda et al., 2001, Leung et al., 2010). This was demonstrated for conventional transesterification of soybean oil

carried out at temperatures of 32, 45 and 60°C (Freedman et al., 1984) and for DT of soybean seed at 23 and 60°C (Haas et al., 2004). It appears, however, that 100% FA yields can also be achieved in DT of dry soybean flakes at room temperature (Table 2), likely due to increasing the reaction time from 8 to 10 h and lowering the biomass to methanol ratio from 1:4 to 1:2.4. Similarly, potassium hydroxide-catalysed DT of dry *Arthrospira* biomass at room temperature achieved a FA to FAME conversion efficiency of 86% in 1 h at a biomass to methanol ratio of 1:2, using a large volume of toluene as a co-solvent (Table 2.2).

In contrast, temperatures between 95 to 120°C were required for acid-catalysed DT of wet microalgal biomass of *Chlorella pyrenoidosa* and *Nannochloropsis salina* and *N. gaditana* to achieve FA extraction yields of ≥90% (Table 2.2), requiring higher lipid/ biomass to solvent ratios, as water decreases the concentration gradient of the solvent (Zakaria and Harvey, 2012). Cao et al. suggested that water acts as a protectant of the microalgae cell wall, preventing methanol-lipid contact (Cao et al., 2013), which can be offset by employing higher process temperatures (Sathish et al., 2014).

Non-catalyst, supercritical methanol-based DT requires temperatures between 255 and 265°C (Table 2.3) and elevated pressures of 12 to 35 MPa (He et al., 2007, Patil et al., 2012a) to reach the critical temperature of methanol. For microwave-assisted supercritical solvent DT of wet microalgal biomass, best results were obtained for *Nannochloropsis* with a water content of 90%, achieving a FA yield of 84% at a temperature of 255°C and 1200 psi, a reaction time of 25 min and a biomass to methanol ratio of 1:9 (Table 2.3). On the other hand, supercritical solvent extraction of *N. salina* biomass using ethanol and a lower water content (60%), a reaction time of 20 min and an even higher temperature (265°C) only achieved an FA yield of 35% (Table 2.3). The highly variable FA yields for *Chlorella* and *Nannochloropsis* biomass can be explained by differences in the use of solvent, species or FA profiles. *Nannochloropsis* spp. biomass contains high concentrations of the long-chain polyunsaturated eicosapentaenoic acid (EPA; C20:5) (Reddy et al., 2014), which may be prone to trans-isomerisation, reactions that involve carbon double bonds and occur at high temperature and pressure (Levine et al., 2010, Jazzar et al., 2015a). Effects of solvent choice may be evident in supercritical solvent DT of *Chlorella;* almost 2-fold higher FA yields were achieved with ethanol compared to methanol, but there were also differences in temperatures (325 *vs* 175°C) and water content (Table 2.3).

2.5.3 Time

Reaction time is an important criterion, because it strongly influences the size of refineries required at scale and, as such, impacts on the investment required. For DT-generated biodiesel from seeds, microwave-assisted base-catalysed DT of Jatropha gave FA yields of 90% in only 12 min, compared to 103 min for base-catalysed DT using the detergent Triton B (Table 2.2). This could be due to the fact that the solvent interacts with cell wall/ membrane lipids first, before gaining access to the stored triglycerides and other membrane lipids (Qian et al., 2008). Reaction time in the DT process of biomass depends on the type of catalyst used and is also strongly influenced by reaction temperature (Ehimen et al., 2010, Jazzar et al., 2015a). Biodiesel yields of *Chlorella* at reaction times of 75 min and 1,200 min were not different (Velasquez-Orta et al., 2012), suggesting that the reaction reached equilibrium (Zakaria and Harvey, 2012). Similarly, acid-catalysed DT of dry *Chlorella* biomass achieved more than 90% of FA yields at reaction times of 240 and 1,140 min (Table 2.2). In contrast, base-catalysed DT of dry *Chlorella* biomass yielded on 21% FA, but the reaction time was also significantly reduced from 1,140 min to 75 min (Table 2.2). The opposite applies to biodiesel production from dry *Nannochloropsis* biomass, demonstrating additional effects of cell wall architecture and chemistry. To achieve FA yields of 73% through acid-catalysed DT of *Nannochloropsis oculata* biomass, a reaction time of 1,140 min was required, whereas the base-catalysed reaction only required a fifth of the reaction time (Table 2.2), but comparison is problematic given the use of hexane as a cosolvent. In contrast, a 5-times faster reaction time with almost similar FA yields was obtained for base-catalysed DT of dry *Scenedesmus* biomass (Table 2.2). Furthermore, the generally poor FA yields obtained from DT of dry microalgal biomass using heterogeneous catalysts could be an indication that much longer reaction times are required than the ones applied (Table 2.2).

Water content is another parameter, which together with the choice of catalyst affects the required reaction times. For instance, FA yield outcomes significantly improved for both *Nannochloropsis* and *Chlorella* in acid-catalysed DT of wet biomass (Table 2.2). An FA yield of more than 90% was achieved for acid-catalysed DT of wet *Nannochloropsis* biomass with reaction times of 75 min at 90°C compared to 30 min at 105°C (Kim et al., 2015b). Therefore, energy benefits must be elucidated to determine whether elevation of temperature and reduced reaction times has benefits over applying lower temperatures over longer reaction times. This is particularly important for non-catalyst supercritical solvent-DT, as reaction times can be reduced to 25 min for the processing of wet

Nannochloropsis biomass, requiring a reaction temperature of 255°C (Table 2.3). In contrast, based-catalysed DT-derived FA yields were low for all microalgae investigated using wet biomass (Table 2). It remains unclear, however, whether this is due to the choice of catalyst or the significantly reduced reaction time compared to base- and acid-catalysed DT outcomes for dry microalgal biomass (Table 2.2).

2.5.4 Co-solvent

As mentioned earlier, DT of microalgae biomass requires larger volumes of methanol, which, even though methanol can be recycled and reused, affects the total cost of biodiesel production (Qian et al., 2008). Due to this, research investigated the effects of using co-solvents to reduce methanol consumption (Table 2.2). In general, it is unclear whether low FA yields represent the combined effects of the choice of species, operational parameters or process design. For seeds and acid- and base-catalysed DT of dry microalgal and fungal biomass, investigated co-solvents (dimethoxymethane, hexane, chloroform and the detergent Triton B) had no positive effect, with the only exception of base-catalysed DT of dry *Nannochloropsis* biomass, achieving 90% FA using hexane as a co-solvent (Table 2.2). Similarly, although studies are limited, intensified DT processing for dry microbial feedstock using co-solvents and homogeneous or heterogeneous catalysts did not significantly improve FA yields, with the exception of ultrasound-intensified acid-catalysed DT of dry *Chlorella* biomass using the co-solvent diethyl ether, achieving a 78% yield (Table 2.2). Although FA yields could not be determined, the use of toluene as a co-solvent reportedly improved FA to FAME conversion efficiency for base-catalysed DT of *Arthrospira* at room temperature without stirring and impressively low biomass to methanol ratio (1:2) and reaction time (1 h) (Table 2.2) (Xu and Mi, 2011).

Similarly, the use of co-solvents in the DT of wet microbial biomass generally did not significantly improve yields (Table 2.2). Acid-catalysed DT of wet *Chlorella* biomass in the presence of the co-solvent hexane yielded 92% FA at a reaction time of 3 h and 120°C (Table 2.2). In contrast, the use of a heterogeneous catalyst (graphene oxide) in a microwave-assisted DT yielded only 87% FA at a 90°C and a reaction time of 40 min (Table 2.2). FA yields, were lower (72%) in enzyme-catalysed DT with hexane as a co-solvent, requiring 48 h, but reaction temperature could be reduced to 40°C. The overall benefits in terms of energy- and cost savings of these processes still require comprehensive techno-economic and LCA modelling, before a recommendation on processing parameters for wet or dry microbial biomass can be made.

2.6 Summary and remaining challenges

Some published data demonstrate that catalytic and non-catalytic DT could be an effective and efficient method to produce biodiesel from a variety of wet and dry feedstock, but from a techno-economic perspective, each processing technology has its own advantages and disadvantages. High FA yields and FA to FAME conversion efficiencies (≥90%) were reported for 15% and 68% of all available studies, respectively, while 15% and 27% were promising (89 – 60%), 20% and 3% were moderate (59 – 40%) and 49% and 1% inefficient (≤39%), respectively.

On a feedstock basis, microwave-intensified base-catalysed DT of Jatropha and *Cynara cardunculus* (a non-edible mediterranian plant) produced highest FA yields, while outcomes for other terrestrial biomass were moderate. For DT of dry and wet microalgal biomass, FA yields were highly variable, but catalyst choice appears to be important. High and promising FA yields were achieved for *Chlorella* and *Nannochloropsis*, respectively, using an acid catalyst. Inclusion of a co-solvent could change the choice of catalyst, as FA yields improved for dry *Nannochloropsis* feedstock from moderate to high, using potassium hydroxide as a catalyst and hexane as a co-solvent. As some microalgal species were only analysed under one or two particular conditions, it is impossible to assess whether a similar catalyst preference would be identifiable. This also applies to fungal and yeast biomass, except for the yeast *Rhodosporidium toruloides* where high FA yields were obtained under both acid- and base-catalysed DT. Other fungal and yeast biomass achieving high FA yields were acid-catalysed DT of dry biomass of *Lipomyces starkeyi*, *Mortierella isbellina*, and *Pichia guilliermondi*. Ultrasound-intensified DT appears to be more efficient for processing of dry and wet fungal/yeast biomass, but this is based on limited data. For *Yarrowia lipolytica* ultrasound-intensified sodium hydroxide-catalysed DT of wet biomass obtained high FA yields, while acid-catalysed DT gave only moderate results. High yields were also obtained for ultrasound-intensified base-catalysed DT of *Trichosporon oleoginosus*.

In summary, homogeneous acid catalysts appear to be more suitable for wet feedstock in batch reflux systems, but reaction times, high temperature and environmental concerns of waste streams could prevent implementation at scale. In contrast, homogeneous base catalysts show better catalytic activity with dry feedstock, except when using turbo-thin film-assisted DT, i.e. the T^2FD, where a water content of 67% of the microalgal feedstock did not interfere with conversion efficiencies (>90%), but FA yields were moderate (this

PhD research). In this context, consideration should be given to existing infrastructure, i.e. base-catalysed transesterification is commonly used, necessitating only slight modification for reactor designs. Of consideration also are the use of heterogeneous catalysts, which produce high purity products due to phase separation in simple processes, but cost and time constraints do apply.

Current data demonstrate that processing parameters need to be optimised separately for different feedstock (including assessment of microbial strain-dependent variability), biomass water content, catalyst choice, utilization of co-solvents, reaction times, temperature and intensified DT processing technologies. This makes it inherently difficult to provide conclusive recommendations for commercial process applications. To bring DT-generated biodiesel production from 3rd generation feedstock a significant step closer to commercial reality, future research needs to place emphasis on modelling feedstock availability (e.g. required investment, environmental footprints etc.), the suitability of intensified DT processing technologies for feedstock with high water contents, as well as catalyst/ co-solvent choice in comprehensive techno-economic and LCAs. Given costs involved for creating the infrastructure for feedstock production, techno-economic and LCAs need to consider the viability of co-product development (e.g. protein, pigments, carbohydrates etc.) at scale in a biorefinery approach. Such analyses need to include sensitivity analyses on the impact of biomass productivity, lipid and co-product contents, FA yields and FA to FAME conversion efficiencies. Such approaches will instil confidence in investors, which is needed to substantially increase biodiesel contribution to the fuel requirements of the transportation sector.

2.7 Conclusion

Current data demonstrate that a variety of DT processing technologies are suitable for biodiesel production independent of feedstock choice and water content, despite large variabilities for a given feedstock. Observed variabilities in FA yields may be the result of single factors, such as suitability of catalyst/solvent or DT process technology for a given feedstock and its water content and/ or the interactive influence of multiple parameter settings. Given the complexity of interactions in intensified and non-intensified DT processing, future parameter-optimisation studies should focus on the most promising feedstock to enable the required comprehensive techno-economic and LCAs mentioned above, including the feasibility of establishing biorefineries for co-product development. It will also be necessary to establish model accuracies for production at scale, which will

require the installation of pilot plants. Ideally, in addition to suitability of DT processing approaches for wet feedstock, selection should consider the suitability of a process for a variety of feedstock, e.g as demonstrated for turbo-thin film devices like the VFD and T^2FD (this PhD research), as feedstock production at scale is likely to face geographic/ climatic constraints.

Table 2.2. Comparison of the catalytic DT process of oleaginous crop / biomass

Crops / Biomass	Catalyst	Co-Solvent	Water (wt.%)	Reaction Time (min)	Temp. (°C)	Ratio of Biomass to Methanol (w/v)	FA Yield (%)	FA to FAME Conversion Efficiency (%)	Ref.
Dry Seed/Biomass **1st Generation of biodiesel resources**									
Homogeneous Acid Catalyst									
Sunflower	H_2SO_4		NA	240	65	1:20	43	NA	(Harrington and D'Arcy-Evans, 1985)
Homogeneous Base Catalyst									
Sunflower	NaOH 0,5 M	DMM	NA	13	RT	1:101.4[a]	45	98	(Zeng et al., 2009)
Palm	KOH 3,85% (w/v)		NA	576	60	1:225[a]	48.5	97	(Jairurob et al., 2013)
Heterogeneous Base Catalyst									
Palm	CaO 1 g		NA	180	65	1:8	43	86	(Tarigan et al., 2017)
2nd Generation of biodiesel resources									
Homogeneous Acid Catalyst									
Rubber Seed	H_2SO_4 0.87 M		NA	240	56	1:50	37.2	93	(Muhammad et al., 2017)
Homogeneous Base Catalyst									
Castor	NaOH 1.19 wt.%		NA	180	30	1:200[a]	45	97	(Dasari et al., 2017)
Jatropha	KOH 0.075 M	Hexane	NA	300	50	1:6	39.4	~100	(Amalia Kartika et al., 2013)
Jatropha	NaOH 1.52 wt.%	Triton B	NA	103	37	NA	89	~100	(Hailegiorgis et al., 2013)
Jatropha	NaOH 0.15 N		NA	30	60	1:400[a]	82	95	(Kasim and Harvey, 2011)
Homogeneous Base Catalyst Intensified									
Cynara cardunculus	NaOH 9.5% (w/w) Ultrasound		NA	20	NA	1:550[a]	85	97	(Koutsouki et al., 2015)
Jatropha	KOH 5 N Microwave		NA	12	65	1:8	90	97	(Jaliliannosrati et al., 2013)
Heterogeneous Catalyst Intensified									
Castor	SrO 0.3 g Microwave	$CHCl_3$	NA	5	60	1:3	57	~100	(Koberg and Gedanken, 2012)
3rd Generation of biodiesel resources									
Microalgal									
Homogeneous Acid Catalyst									
Botryococcus braunii	H_2SO_4 21.5 wt.%	$CHCl_3$	NA	300	65	1:40	81	NA	(Hidalgo et al., 2014)
Botryoccis braunii	H_2SO_4 19.725 wt.%	Hexane	NA	300	65	1:151[a]	55	93	(Hidalgo et al., 2015)
Chlorella	H_2SO_4 0.04 mol		NA	60	60	1:4	25	92	(Ehimen et al., 2010)
Chlorella	H_2SO_4 0.35 M		NA	1140	60	1:600[a]	92	NA	(Velasquez-Orta et al., 2013)
Chlorella	H_2SO_4 10%	Hexane	NA	120	90	1:20	18	90	(Zhang et al., 2015a)
Chlorella	H_2SO_4 20 wt%		NA	240	60	1:3	98	NA	(Viêgas et al., 2015)
Chlorella vulgaris	H_2SO_4 0.35 M		NA	1200	60	1:600[a]	26	97	(Velasquez-Orta et al., 2012)
Commercial algal biomass	H_2SO_4 23.5 mmol		NA	120	65	1:4	17	83	(Haas and Wagner, 2011)
Nannochloropsis oculata	H_2SO_4 0.8 mM		NA	1140	60	1:600[a]	73	NA	(Velasquez-Orta et al., 2013)

Crops / Biomass	Catalyst	Co-Solvent	Water (wt.%)	Reaction Time (min)	Temp. (°C)	Ratio of Biomass to Methanol (w/v)	FA Yield (%)	FA to FAME Conversion Efficiency (%)	Ref.
Nannochloropsis oculata	HCl	$CHCl_3$	NA	120	80	1:100	23	NA	(Carvalho Júnior et al., 2011)
Scenedesmus	H_2SO_4 5% (v/v)		NA	600	70	1:22	85	97	(Choi et al., 2015)
Scenedesmus	H_2SO_4 5% (v/v)		NA	600	70	1:15	48	NA	(Kim et al., 2014)
Scenedesmus	H_2SO_4 5.46% (v/v)		NA	600	70	1:22	69	NA	(Choi et al., 2014)
Homogeneous Acid Catalyst Intensified									
Chaetoceros graciis	H_2SO_4 1.8% (v/v) Microwave		NA	10	80	1:25	22	82	(Wahlen et al., 2011)
Chlorella	H_2SO_4 0.04 mol Ultrasound	DE	NA	480	60	1:105[a]	78	NA	(Ehimen et al., 2012)
Homogeneous Base Catalyst									
Chlorella	NaOH 0.67% (w/w) then H_2SO_4 2.07% (v/w)		NA	40	90	1:30	39	95	(Kumar et al., 2014)
Chlorella vulgaris	NaOH 0.15 M		NA	75	60	1:600[a]	21	78	(Velasquez-Orta et al., 2012)
Nannochloropsis	KOH 2% (v/w)	Hexane	NA	240	60	1:400[a]	91	NA	(Dianursanti et al., 2015)
Scenedesmus	NaOH 0.5%		NA	120	60	1:50	55	NA	(Kim et al., 2014)
Spirulina Athrospira	KOH 4.85%	Toluene	NA	60	RT	1:2	NA	86	(Xu and Mi, 2011)
Homogeneous Base Catalyst Intensified									
Chlorella	NaOH 2 wt% Microwave		NA	6	75 – 80	1:12	19	96	(Martinez-Guerra et al., 2014b)
Chlorella	NaOH 2 wt% Ultrasound					1:9	19	95	
Chlorella	NaOH 1% Microwave	Hexane	NA	6	78	1:250[a]	19	96	(Martinez-Guerra et al., 2014a)
Nannochloropsis	KOH 2 wt.% Microwave		NA	4	60 – 64	1:12	NA	NA	(Patil et al., 2011a)
Nannochloropsis salina	KOH 2.5 wt.% Microwave		NA	10	65	1:13	40	NA	(Patil et al., 2012b)
Heterogeneous Catalyst									
Chlorella sorokiniana	Amberlyst-15 30 wt.% KOH[e] 0.3 wt.%		NA	70	90	1:6	32	95	(Dong et al., 2013)
Chlorella vulgaris	KOH/Al_2O_3 10 wt.%		NA	300	60	1:8	15.3	90	(Ma et al., 2015a)
Nannochloropsis	Mg-Zr 10 wt.%		NA	240	65	1:45 DCE	28	NA	(Li et al., 2011)
Heterogeneous Catalyst Intensified									
Chlorella vulgaris	KF/CaO 12 wt.% Microwave Ultrasound		NA	45	60	1:8	19.5	93	(Macías-Sánchez et al., 2015)
Nannochloropsis	SrO 0.3 g Microwave	$CHCl_3$	NA	5	60	NA	37	NA	(Koberg et al., 2011)
Nannochloropsis	SrO 0.3 g Ultrasound						21	NA	
Scenedesmus	WO_3/ZrO_2 4 wt.% Microwave		NA	20	80	1:45	15	52	(Guldhe et al., 2014a)

Crops / Biomass	Catalyst	Co-Solvent	Water (wt.%)	Reaction Time (min)	Temp. (°C)	Ratio of Biomass to Methanol (w/v)	FA Yield (%)	FA to FAME Conversion Efficiency (%)	Ref.
Scenedesmus	WO_3/ZrO_2 4 wt.% Ultrasound		NA	20	50	1:60	21	71	
Enzyme Catalyst									
Aurantiochytrium	Novozyme 435 30 % (w/w)		NA	720	50	1:5 (DMC)	48.4	90	(Kim et al., 2016)
Botrycoccus	Novozyme CAL-B 10 wt.% Celite		NA	240	50	1:5 Dimethyl carbonate	88	NA	(Sivaramakrishnan and Incharoensakdi, 2017a)
Chlorella vulgaris	Novozyme 435 20 wt.%	PP	NA	480	50	1:12	8	76	(Marcon et al., 2017)
Chlorella	LiOH – pumice 20 wt.%		NA	180	80	1:12	47	NA	(de Luna et al., 2017)
Chlorella zofingiensis	*Candida antartica* Lipase B 400 U	IL	NA	6900	60	NA	16	NA	(Bauer et al., 2017)
Fungi									
Homogeneous Acid Catalyst									
Aspergillus sp	HCl 10% (v/v)	$CHCl_3$	NA	480	90	1:12	NA	NA	(Venkata Subhash and Venkata Mohan, 2011)
Aspergillus candidus	H_2SO_4 0.2 M	$CHCl_3$	NA	480	65	1:12	NA	NA	(Kakkad et al., 2015a)
Lipomyces starkeyi	H_2SO_4 0.2 M		NA	1200	70	1:20	97	NA	(Liu and Zhao, 2007)
Mortierella isabellina	H_2SO_4 0.2 M		NA	1200	70	1:20	91	NA	(Liu and Zhao, 2007)
Mucor circinelloides	BF_3 H_2SO_4 HCl	$CHCl_3$	NA	480	65	1:10	20 20 20	99 ~100 99	(Vicente et al., 2009)
Pichia guilliermondi	H_2SO_4 4 % (v/v)		NA	360	60	1:20	92	NA	(Chopra et al., 2016)
Rhodosporidium toruloides	H_2SO_4 0.2 M		NA	1200	70	1:20	98	NA	(Liu and Zhao, 2007)
Rhodosporidium toruloides	H_2SO_4 0.2 M		NA	1200	70	1:20	9.8	98	(Koutinas et al., 2014)
Yarrowia lipolytica	H_2SO_4 0.2 M	$CHCl_3$	NA	480	50	1:25	22	NA	(Katre et al., 2018)
Homogeneous Acid Catalyst Intensified									
Rhodosporidium toruloides	H_2SO_4 6 % (v/v) Microwave		NA	10	60	1:16	6	71	(Ling et al., 2016)
Homogeneous Base Catalyst									
Rhodosporidium toruloides	NaOH 0.1 N		NA	600	50	1:20	98	NA	(Thliveros et al., 2014)
Homogeneous Base Catalyst Intensified									
Mucor plumbeus	NaOH 3 wt.% T^2FD		NA	2	RT	1:12	67	97	(Sitepu et al., 2019)
Trichosporon oleaginosus	NaOH 1 wt.% Ultrasound	Hexane	NA	720	55	1:32	93.5	92	(Zhang et al., 2014)
Heterogeneous Catalyst									
Mucor circinelloides	Heteropoly acid 10 wt.%		NA	240	200	1:120	NA	NA	(Carvalho et al., 2017)
Wet Seed/Biomass **1st Generation of biodiesel resources**									
Homogeneous Acid Catalyst									

Crops / Biomass	Catalyst	Co-Solvent	Water (wt.%)	Reaction Time (min)	Temp. (°C)	Ratio of Biomass to Methanol (w/v)	FA Yield (%)	FA to FAME Conversion Efficiency (%)	Ref.
Soybean	H_2SO_4		9	180	65	1:3	9.3	42	(Kildiran et al., 1996)
Soybean	H_2SO_4 1.2 N		2.8	600	65	1:1.2	21	8	(Wyatt and Haas, 2009)
Homogeneous Base Catalyst									
Canola	KOH 1.05 M		7	360	60	1:275[a]	15.4	80	(Haagenson et al., 2010)
Soybean	NaOH 0.1 N		9.4	600	RT	1:2.4	100	100	(Haas and Scott, 2007)
Homogeneous Base Catalyst Intensified									
Sunflower	NaOH 2 wt.% Ultrasonic ator		6.1	40	60	1:3	20	98	(Georgogianni et al., 2008)
2nd Generation of biodiesel resources									
Homogeneous Base Catalyst									
Jatropha	NaOH 0.1 M		4	60	65	1:7.8	33	98	(Kaul et al., 2010)
3rd Generation of biodiesel resources									
Microalgal									
Homogeneous Acid Catalyst									
Chlorella	H_2SO_4 10 % (v/v)		84	30	90	1:40	9	81	(Sathish et al., 2014)
Chlorella pyrenoidosa	H_2SO_4 0.5 M	Hexane	90	180	120	1:40	92	93	(Cao et al., 2013)
Nannochloropsis salina	H_2SO_4 5 % (v/v)		76.5	60	100	1:10	95	~100	(Kim et al., 2015b)
Nannochloropsis gaditana	CH_3COCl 5 % (v/v)		75	105	100	1:171[a]	100	NA	(Macías-Sánchez et al., 2015)
Nannochloropsis gaditana	HCl 35 wt.%	$CHCl_3$	80	120	95	1:10	90	NA	(Kim et al., 2015a)
Nannochloropsis oceanica	H_2SO_4 10 % (v/v)	$CHCl_3$	65	90	95	1:15	17	91	(Sathish et al., 2014)
Homogeneous Acid Catalyst Intensified									
Chlorella gracilis	H_2SO_4 2 % (v/v) Microwave		100	20	80	1:40	37	84	(Wahlen et al., 2011)
Chlorella pyrenoidosa	H_2SO_4 2.5 % (v/v) Microwave		80	10	60	1:4	8	NA	(Cheng et al., 2013)
Homogeneous Base Catalyst									
Chlorella	NaOH 2 M then H_2SO_4 1.8 M		90	35	100	1:3	20	NA	(Fang et al., 2018)
Chlorella	NaOH then HCl		70	40	90	1:30	43	NA	(Kumar et al., 2014)
Pavlova lutheri	NaOH 2 wt.%		77	240	60	1:12	17	67	(Álvarez et al., 2017)
Homogeneous Base Catalyst Intensified									
Chloroparva pannonica	NAOH 3 wt.% VFD		67	2	RT	1:6	41	96	(Sitepu et al., 2018a)
	NaOH 1 wt.% T2FD			5				97	(Sitepu et al., 2018b)
Chlamydomonas	NaOH 0.5 wt.% Microwave	Hexane	68.7	15	45	1:6	101	~100	(Chen et al., 2015)
Nannochloropsis	NaOH Microwave		20	10	50	NA	75	NA	(Chee Loong and Idris, 2017)
Nannochloropsis	NA	IL	80	15	65	NA	37	~100	(Wahidin et al.,

Crops / Biomass	Catalyst	Co-Solvent	Water (wt.%)	Reaction Time (min)	Temp. (°C)	Ratio of Biomass to Methanol (w/v)	FA Yield (%)	FA to FAME Conversion Efficiency (%)	Ref.
									2016)
Nannochloropsis	NaOH H_2SO_4 Microwave		20	960	50	NA	NA	NA	(Teo and Idris, 2014)
Heterogeneous Catalyst Intensified									
Chlorella pyrenoidosa	Graphene Oxide 5 wt.% Microwave	$CHCl_3$	75	40	90	1:4	87	95	(Cheng et al., 2016)
Chlorella pyrenoidosa	Sulfonated graphene oxide 5 wt.% Microwave	$CHCl_3$	77	40	90	1:4	24	84	(Cheng et al., 2017)
Enzyme Catalyst									
Chlorella vulgaris	*Burkholderia* sp C20 1203 Ug^{-1}	Hexane	71.39	2880	40	1:68[a]	72	97	(Tran et al., 2012)
Fungi									
Homogeneous Acid Catalyst									
Yarrowia lipolytica	H_2SO_4 0.4 M	$CHCl_3$	53	60	50	NA	46	72	(Cheirsilp and Louhasakul, 2013)
Homogeneous Acid Catalyst Intensified									
Yarrowia lipolytica	H_2SO_4 360 mM Ultrasound	Detergent	83.8	10	25	1:360[a]	94	NA	(Yellapu et al., 2017)
Homogeneous Base Catalyst Intensified									
Cryptococcus curvatus	KOH 5 wt.% Microwave		80	4	NA	1:50	92	64	(Cui and Liang, 2014)
Mucor plumbeus	NaOH 3 wt.% T2FD		50	2	RT	1:9	72	91	(Sitepu et al., 2019)
Rhodosporidium diobovatum	KOH 20 %	IL	76	150	65	1:17	38.8	97	(Ward et al., 2017)

[a]Ratio molar oil to methanol

DE = diethyl ether, DMM = dimethoxymethane, DMC = dimethylcarbonate, IL = ionic liquid; NA = information not available, PP = pressurized propane, Triton B = Benzyl-trimethylammonium hydroxide.

Table 2.3. Supercritical solvent based DT of oleaginous crops and microbial biomass

Crops / Biomass	Type of Alcohol	Co-Solvent	Water (wt.%)	Reaction Time (min)	Temp. (°C)	Ratio of Biomass to Methanol (w/v)	FA Yield (%)	FA to FAME Conversion Efficiency (%)	Ref.
Soybean	Methanol	Toluene	NA	180	350	1 : 10	17.2	86	(Xu et al., 2016)
Jatropha	Methanol		NA	30	280	1:40	62	98	(Ishak et al., 2017)
Jatropha	Methanol		10	60	250	1:12	57	98	(Go et al., 2014a)
Chlorella vulgaris	Ethanol		46	120	325	1 : 10	53.3	100	(Levine et al., 2010)
Chlorella vulgaris	Methanol		80	240	175	1 : 4	29	90	(Tsigie et al., 2012)
Nannochloropsis	Methanol		90	25	255	1 : 9	NA	NA	(Patil et al., 2011b)
Nannochloropsis	Methanol		75	50	265	1 : 10	45.62	NA	(Jazzar et al., 2015b)
Nannochloropsis	Methanol		90	25	255	1 : 9	84	84	(Patil et al., 2012a)
Nannochloropsis gaditana	Methanol		80	90	225	1 : 6	59	NA	(Sitthithanaboon et al., 2015)
Nannochloropsis gaditana	Methanol		80	50	255 - 265	1 : 10	46	NA	(Jazzar et al., 2015a)
Nannochloropsis salina	Ethanol		60	25	260	1 : 9	30.9	NA	(Patil et al., 2013)
Nannochloropsis salina	Ethanol		60	20	265	1 : 9	35	67	(Reddy et al., 2014)
Neochloris oleoabundans	Methanol		25	30	280	1:3	35	NA	(Hegel et al., 2017)
Schizochytrium limacium	Methanol		NA	120	211.6	1 : 75	37.5	NA	(Bi et al., 2015)
Rhodosporidium torulaides	Methanol CO_2 2 MPa injected		NA	300	100 then 60	NA	66.5	95	(Cao et al., 2012)

Table 2.4 Free fatty acids contained in some species of microalgae

Species	Percentage of FFA	Units	References
Nannochloropsis gaditana	12.1 ± 0.2	wt% of dry biomass	(Castillo López et al., 2015)
Chlorella sorokiniana	46.85	% of the total lipids	(Dong et al., 2013)
Dunaliella tertiolecta	167.2505	mg KOH	(Krohn et al., 2011)
Nannochloropsis oculata	83.4012	mg KOH	(Krohn et al., 2011)
Chlorella	5.11	wt% oil weight	(Ehimen et al., 2010)
Scenedesmus	20	Mg KOH/g	(Guldhe et al., 2014a)
Chlorella vulgaris	1.91	wt%	(Macías-Sánchez et al., 2015)
Nannochloropsis gaditana	28.7	wt%	(Macías-Sánchez et al., 2015)
Chlorella	21	wt% oil weight	(Viêgas et al., 2015)

Chapter 3
RESEARCH METHODOLOGY

This chapter presents the methodology used to examine the effectiveness of dynamic thin film-assisted DT of oleaginous biomass. The first section describes the thin film devices used in this research and the procedures to study the DT process are shown in the last section.

3.1 Thin film devices

3.1.1 Vortex fluidic devices

Application of vortex fluidic device (VFD)-mediated extraction and conversion (Figure 3.1) is an emerging environmentally friendly processing platform, as many chemical and biochemical reactions benefit from enhanced mass and heat transfer due to large surface area present in the dynamic thin film (~300 μm). The thin film forms when a borosilicate glass tube 20 mm OD containing liquid, inclined at an angle of 45˚, is rotated at high speed (i.e. 6000 – 8000 rpm) (Eroglu et al., 2013), with this angle corresponding to the maximum cross vector of centrifugal force and gravity. Stewartson/Ekman layers on the sidewall of tube arise from the high rotation speed of the liquid operating against gravity (Kumari et al., 2016). Overall, the VFD is a versatile microfluidic platform which imparts controlled mechanical energy into the dynamic thin film. This controlled and energetically favourable processing platform has been applied to a number of biological and chemical processes such as refolding of proteins, synthesis of graphene from graphite, coating a magnetic responsive polymer or graphene onto microalgae cells, synthesis of silica xerogel, microencapsulation of bacteria cells in graphene oxide, slicing carbon nanotubes, controlling organic reactions, enhancing enzymatic reactions and more (Britton et al., 2017).

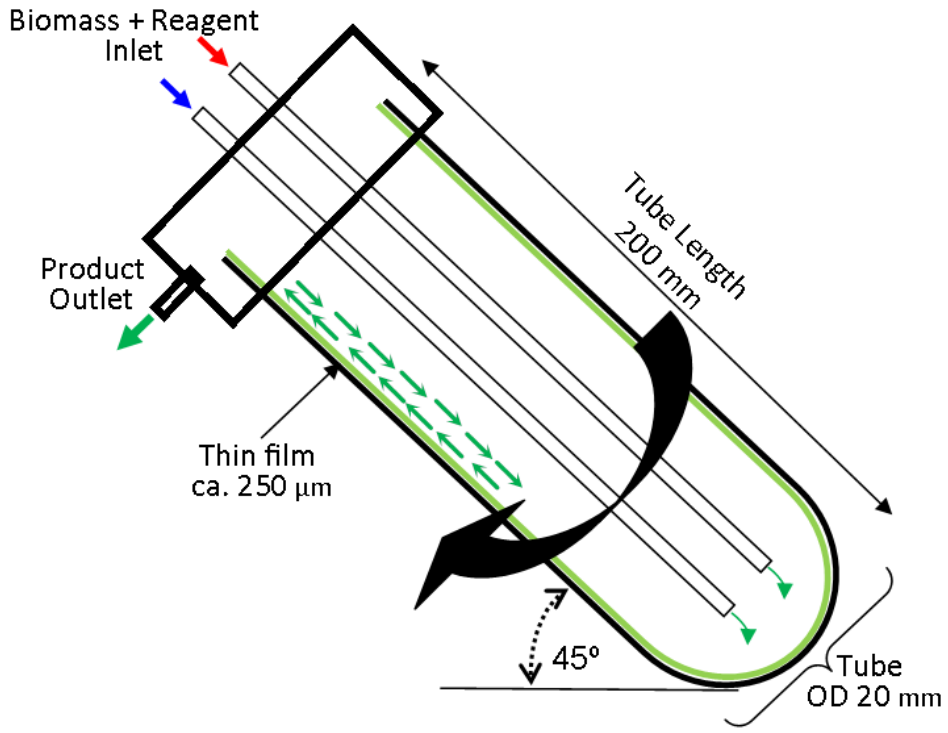

Figure 3.1. Schematic representation of the VFD operating in continuous flow for microalgae biodiesel production.

The VFD can operate in two modes. For reactions with a finite volume of reactants, the VFD is operated in the confined mode, where the liquid is processed in a sealed, rotating tube. Alternatively, in the continuous flow mode, jet feeds are used to continuously deliver reactants to the hemispherical bottom of the tube, or at specific positions along the tube (Britton et al., 2017). The residence time of liquid in the tube is important in that it can affect the conversion rate. Under continuous flow mode, residence time is controlled by flow rate, rotational speed and tilt angle, and for a fixed rotational speed and tilt angle it is expressed as follows (equation 3.1) (Jones and Raston, 2017):

$$Residence\ Time = \frac{Fluid\ Retained\ in\ Device}{Incoming\ Fluid\ Flow\ Rate} \qquad \text{(eq. 3.1)}$$

Moreover, the thickness of film decreases for a specific speed along the tube towards the exit housing, and changes with speed, with the average thickness 530 µm at 6000 rpm and 294 µm at 8000 rpm (Jones and Raston, 2017).

3.1.2 Turbo thin film devices

The success of the VFD microfluidic platform, for which upscaling is challenging, led to the design of the high throughput, high shear turbo thin film device (T^2FD) (Figure 3.2), where the maximum thickness of the dynamic thin film can be adjusted from 100 to 200 µm. The

DT of wet *Chloroparva pannonica* biomass with a conversion efficiency of ~98% was achieved under continuous flow operation with a residence time of ~ 2 min at ambient temperature and pressure (Sitepu et al., 2018a). The T^2FD consists of two main parts: a 3D-printed titanium-rotating blade, and a stainless-steel base. When a biomass/reactant mixture enters the T^2FD, the internal fins on the rotating blade push the mixture into the base resulting in high shear stress within the thin film, which releases lipids that directly react with methanol in the presence of a catalyst to yield fatty acid methyl ester (FAME). The localised average shear stress ($\overline{\gamma}$) in a film is described by equation 3.1 (Schilde et al., 2011),

$$\overline{\gamma} = \frac{\Delta v}{d}, \qquad \text{(eq. 3.1)}$$

where Δv is the velocity difference across the stationary base and rotating surface fluid boundaries that are separated by the gap distance, *d*. Because of the conical shape of the rotor and base, which both have matching apex angles of 90°, the average shear stress increases as the fluid moves up the conical surface. Here the average shear is a function of the radial distance from the axis of rotation (r) and the rotational angular velocity (ω),

$$\overline{\gamma}(r) = \frac{r\omega}{d}. \qquad \text{(eq. 3.2)}$$

In this in-house developed system, the blade has been designed with periodic gaps that allow the fluid to flow into the rotor-base gap. Here the atmosphere above the liquid can also be drawn under the blades, and into the thin film. After the mixture passes under the blade, the thin film relaxes, leading to significantly improved mass transfer across the large vapour-liquid interface. Observations resulting from this study confirmed that the centrifugal motion of the rotor drives the fluid outwards and up the conical surface of the base in a helical-like motion. Here the conical shape of the base introduces a component of the gravitational force that opposes the outward motion of the fluid. As such, depending on the rotational speed and liquid flow rate, the fluid may (i) form a continuous turbulent film, (ii) experience viscous fingering or (iii) form droplets, streaking, and phase deformation (Jha et al., 2011). The shear stress that the fluid experiences through repeated contact with the rotating blade surfaces creates intense micro-mixing within the fluid, as the large shear rate typically exceeds the critical shear rate required for single phase formation, i.e. homogenization (Hashimoto et al., 1995). All these features create a

novel hybrid chemical processing environment, whereby the fluid(s) injected into the device are subjected to a unique mix of high shear and efficient mass transfer.

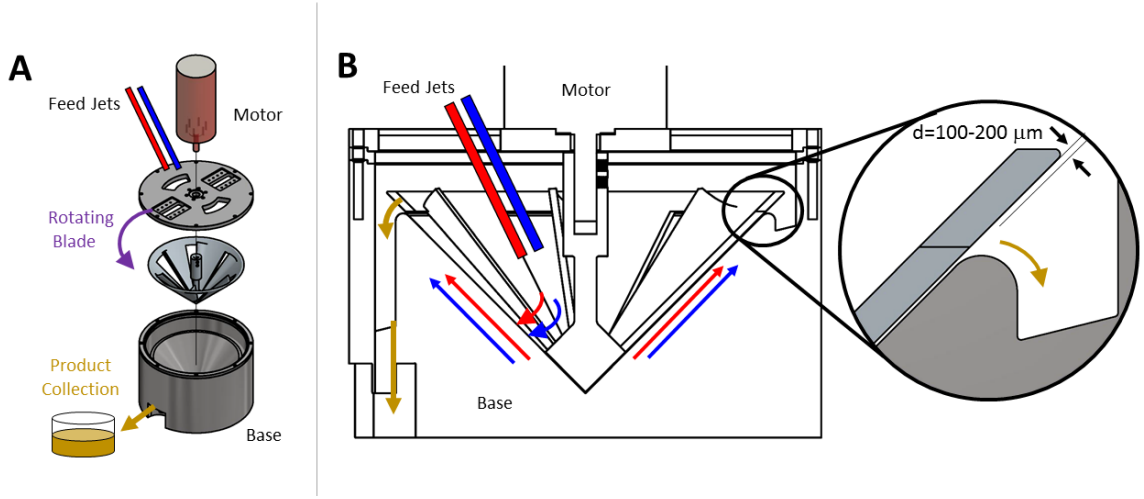

Figure 3.2. (A) An exploded diagram of the key components of the T^2FD. (B) A cross-sectional segment of the device illustrating the assembled device and the fluid paths into and out of the device, with the inset showing the rotor base gap - d. Adapted from Sitepu et al., (2018a).

3.2 Materials

Soybean seeds were purchased from the Central Markets in Adelaide, South Australia (34.9295°S, 138.5973°E) and were ground to a homogenous powder using a coffee grinder (Homemaker, model PCML2013TS) set to fine (particle size <200 µm). Methanol (purity: >99%), sodium hydroxide (purity: 98%), and hexane (purity: 95%) were purchased from Sigma Aldrich (Castle Hill, Australia).

3.2.1 Microalgae cultivation and validation of vortex fluidic device-induced cell breakage

The microalga *Chloroparva pannonica* (FC40) biomass was obtained from the South Australian Research and Development Institute (SARDI, Adelaide, Australia) and grown in f/2-Si medium (Andersen et al., 2005) in an 11 L photo-bioreactor with two cool white fluorescent lights (M5F128, Nelson Lamps, Australia) under a 12:12 h photo period with CO_2-supplementation during the light phase only. Biomass was harvested after 7 days of cultivation by centrifugation (6000×*g*, 10 min, Beckman J-6M, Beckamn Coulter, Indianapolis 46628, USA), then freeze-dried (VirTis BenchTop K, SP Industries, NY 12484, USA) until constant weight and stored at 4 °C until use. After lyophilisation, the

biomass needed was ground with a pestle and mortar and sieved to 250 µM for delivery to the VFD tube.

Scanning electron microscopy was used to ascertain VFD-induced shear-force and solvent (methanol)-assisted cell breakage of *C. pannonica*. Live cells of *C. pannonica* were spheroidal with diameters of ~3.4 µm. Post VFD-examination showed that the cells were reduced in size and collapsed for both acid- and base-catalysed DT processing, indicative of cell rupture, providing access for the solvent to lipid content of the cells.

3.2.2 Fungal biomass cultivation and validation of turbo thin film device-induced cell breakage

Mucor plumbeus biomass was cultivated using diluted molasses as the growth medium in a 1,000 L stirred tank fermenter at the Mackay Renewable Biocommodities Pilot Plant – a facility of Queensland University of Technology, Australia. The molasses medium contained a sugar concentration of ~30 g L^{-1} (glucose equivalent), 0.5 g L^{-1} $(NH_4)_2SO_4$ and 0.25 g L^{-1} KH_2PO_4. Fungal biomass was produced at 28 °C, pH 6.0 over a cultivation period of 6 days with oxygen levels maintained at above 20% by aeration (Ahmad et al., 2017). Microbial oil production was performed under nitrogen-limiting condition. As a result, sugar consumption was slow, requiring longer cultivation time for the utilisation of sugars. At the end of the cultivation period, the fungal biomass was harvested on a filter cloth, and washed with tap water for removal of residual growth medium. The washed fungal biomass was subsequently pressed in a juice press to remove excess water, followed by air-drying. The dried fungal biomass was kept at 4 °C until use.

In order to investigate the cell disruption effect of the T^2FD, the fungal biomass was analysed by scanning electron microscopy (Inspect F50, Thermo Fisher Scientific, Australia) before and after T^2FD-processing. As expected, fungal hyphae initially had a tubular shape, with a relatively smooth surface and undamaged. After passage through the T^2FD, fungal hyphae were fully disrupted (data not shown). Consequently, T^2FD-induced cell breakage should release stored and membrane lipids into the solution, making them accessible for catalytically conversion to biodiesel in the transesterification reaction.

3.3 General procedures

3.3.1 Lipid quantification

The Folch method (1957) was used to quantify lipid content in the microalga *C. pannonica*. Briefly, 0.05 g dry biomass was mixed with 1.4 mL 0.9% saline and 2 mL methanol. After 5 min rest, 4 mL of chloroform was added and the mixture was shaken. After 5 min phase separation was induced by centrifugation at 3000×*g* for 10 min (Allegra® X-12, Beckman Coulter, California 92834, USA). The chloroform layer was collected and the solvent evaporated under a stream of nitrogen. Total lipid was determined gravimetrically.

3.3.2 Fatty acid profile

After transesterification of the microalgal fatty acids derived from the dry biomass, 1 μL of fatty acid methyl ester (FAME) was injected into the GC using a 5 μL microsyringe. The fatty acid profile was determined using a gas chromatograph-mass spectrometer (GC/MS) (Agilent Technologies 7890A gas chromatograph with 7683B autosampler, coupled to an Agilent Technologies 5975C mass spectrometer), equipped with an SGE Analytical BP21 capillary column (length 15 m x 0.25 mm i.d.). Helium was the carrier gas delivered in constant flow mode at 1 mL/min. Split injection was used with a split ratio of 100:1 for the biodiesel standard (ERM-EF001) and 20:1 for the biodiesel samples. The injection port temperature was maintained at 240 °C while the detector temperature was operated at 250 °C. Integration was carried out on the FID output using the Agilent Chemstation software. Biodiesel samples prepared by direct transesterification using the VFD, as described above were analysed by Fourier-Transformed- Infrared spectroscopy (FT-IR) and Proton-Nuclear Magnetic Resonance (^{1}H-NMR) spectroscopy instead of GC/MS, as this is a validated process for the biodiesel industry (Tariq et al., 2011).

3.3.3 Conventional extraction and transesterification of fungal biomass

To investigate the efficacy of the T^{2}FD extraction and transesterification process, *M. plumbeus* dry biomass was processed following a protocol for *Rhodosporidium toruloides* (Thliveros et al., 2014). Briefly, 2 g dry biomass of *M. plumbeus* was mixed with methanol containing 4 wt./v % sodium hydroxide as a catalyst at a ratio of 1:20 and reacted at 50 °C for 10 h. Another control sample was prepared using sulphuric acid as the catalyst following a protocol for biodiesel production from *Pichia guilliermondii* (Chopra et al., 2016). Briefly, 2 g dry biomass of *M. plumbeus* was mixed 1:20 with methanol containing 4

v/v% sulphuric acid and reacted at 60 °C for 6 h. After cooling, 20 mL hexane was added to these samples to extract the FAME and the hexane phase was dried *in vacuo*. For ^{1}H-NMR, the sample was reconstituted in 800 µL deutero-chloroform (chloroform-d, Sigma-Aldrich, Castle Hill, NSW) and analysed by ^{1}H-NMR on a 600 MHz Bruker spectrometer set at 64 scans and 1 second D1 delay, while the extract was directly analysed after drying by FT-IR.

3.3.4 FT-IR and ^{1}H-NMR analysis

The presence of FAMEs was confirmed using FT-IR (Perkin Elmer FT-IR 100, Perkin Elmer, Connecticut 06484-4794, USA) equipped with attenuated total reflectance (ATR) probe. The biodiesel spectra were observed in the range of 4000 – 400 cm^{-1}. As published, ^{1}H-NMR can be employed to measure conversion yields (Niju et al., 2014, Sarpal et al., 2016). ^{1}H-NMR was carried out on a 600 MHz Bruker spectrometer with typical condition of 64 scans and 1 second D1 delay. Amounts of unsaturted and saturated fatty acids (mol%) were quantified from ^{1}H-NMR spectra using equations developed by (Knothe and Kenar, 2004), who validated the methodology through comparison with GC/MS-derived data (w%). Extraction efficiencies of quantifiable saturated and unsaturated fatty acids (mol%) were calculated using GC-MS data (w%) obtained from chloroform/methanol-extracted biomass and hexane/methanol transesterified fatty acids, as the differences between mol% and w% are insignificant (Knothe and Kenar, 2004). Conversion efficiencies were calculated based on the integration value of the specific chemical shift of methoxy protons (OMe) and α-methylene protons (α-CH_2), using equation 3.2 (Tariq et al., 2011).

$$C = \frac{2A_{Me}}{3A_{CH_2}} X\ 100 \qquad \text{(eq. 3.3)}$$

where C = percentage conversion of triglyceride (TG) to fatty acid methyl ester, A_{Me} = integration value of the methoxy protons of methyl ester and A_{CH_2} = integration value of α-methylene protons.

3.3.5 Statistical analysis

Statistica v13.6 was used to statistically determine significant effects of catalyst concentration, ratio of biomass / seed powder to methanol, flow rate and rotational speed. Data were first analysed for homogeneity of variance and normality using the Cochran-

Bartlett test and q-q plots. Data conforming to these assumptions were analysed via one-way or factorial ANOVA, followed by Tukey post hoc analysis to determine conditions driving the significance. Data that did not satisfy the assumption of homogeneity were analysed via Newman-Keuls tests. Effects were reported as significant at $\alpha = 0.05$. All experiments were conducted in triplicate. Data are represented as means ± standard deviation.

3.4 Thin film devices-assisted direct transesterification of oleaginous biomass to biodiesel

3.4.1 Direct transesterification of microalgal biomass using vortex fluidic device

The fatty acid methyl ester (FAME), free fatty acid and triglyceride contents, as well as the fatty acid profiles of these were determined for *C. pannonica* dry biomass following standard extraction, transesterification and gas chromatography protocols. Values were corrected for the recovery of the internal standard (C17:0).

Direct transesterification of *C. pannonica* biomass using VFD was first studied in the confined mode, using 150 mg dry microalgae or prepared to contain variable water content, mimicking water content of harvested biomass. Dry biomass was VFD-transesterified using either methanol-NaOH or methanol-sulphuric acid at volumes of 1,200, 1,000, 750 and 550 µL (methanolic solution) resulting in biomass:methanolic solution ratios of 1:3.7, 1:5, 1:6.7 and 1:8 (w/v) in the VFD tube (20 mm borosilicate tube) at a constant 7% catalyst and tube rotational speed of 6,000 rpm for 60 min. and processed at 6,000 rpm for 60 min. Catalyst concentrations were maintained at 7%, as was biomass:methanonlic solution ratio (1:5), for experiments investigating the effect of rotational speed (4,000, 5,000, 6,000, 7,000, and 8,000 run at 60 min reaction time) and reaction time (15, 30, 45, 60, and 75 min run at a rotational speed of 6,000 rpm).

To produce biomass with variable water content, biomass was rewetted on an–orbital shaker (Ratex, Adelab Scientific, Adelaide 5031, Australia) at room temperature and 150 rpm for at least 30 min. Methanol-NaOH at volumes of 1,200, 1,000 and 750 µL (methanolic solution) resulting in biomass:methanolic solution ratios of 1:5, 1:6.7 and 1:8 (w/v) was added to the VFD tube and the content was processed at 6,000 rpm for 15, 30 and 45 min, following a Box-Behnken response surface design. At the completion of the reaction, 2 mL of hexane was added to extract the biodiesel from the mixture. The mixture was then transferred to a separation funnel and washed twice with 2 mL MilliQ water

(Rephile, Adelab Scientific, Adelaide 5031, Australia**)**. Following centrifugation (12,000 rpm, 5 min, microcentrifuge Sigma I-13, Quantum Scientific, Queensland 4173, Australia) the hexane layer was collected and then it was removed under nitrogen stream to dry biodiesel. The biodiesel was stored in a desiccator until analysed.

Under continuous flow processing, two jet feeds were used to separately deliver the reactants to the bottom of VFD tube. Microalgae biomass is difficult to suspend in methanol, and this necessitated the use of a peristaltic pump to deliver the mixture of biomass and methanol via a jet feed into the VFD tube. A syringe pump was used to deliver the catalyst dissolved in methanol to the base of the VFD tube (Figure 3.1). The two jet feeds delivered the reagents at various flow rates (0.1; 0.55 and 1 mL/min) to the bottom of the VFD tube, which rotated at 6,000 rpm (Figure 3.1). Wet microalgal (500 mg) was mixed 1:2 to 1:6 (w/v) with methanol and the mixtures were delivered at a flow rate of 0.2 mL/min through one jet feed using a peristaltic pump. Methanolic solution was added to yield final biomass to methanol ratios of 1:4 to 1:12 which was injected to the VFD tube through the other jet feed using a syringe pump. A rotational speed range was chosen to ensure that the vortex is maintained in the VFD tube, which governs output flows. The biodiesel product was extracted as previously described.

3.4.2 Direct transesterification of ground soybean seeds using the turbo thin film device

Two grams of soybean powder were mixed with methanol to homogeneity in a modified 60 mL syringe containing a magnetic stir bar at ratios of 1:6, 1:9, 1:12, and 1:15 (wt/v), while another 60 mL syringe contained methanolic solution of sodium hydroxide at 0, 0.5, 1, 3, 5, 7, 9, and 12 wt/v %. Effects of flow rate (1, 2, 3, 4, and 5 mL/min) and rotational speed (2000 to 6000 rpm at increments of 500 rpm), and biomass:methanol ratio were investigated at 1 and 3 wt/v % of the catalyst sodium hydroxide. The soybean seed powder/ methanol mixture and methanolic catalyst solution were delivered to the T^2FD by using syringe pumps (Adelab Scientific, 12VDC, Australia). FAME products were extracted using 10 mL of hexane, washed two times with 25 mL of MiliQ water (Rephile, Adelab Scientific, Australia), and followed by evaporation of hexane *in vacuo*. FAME products were stored in a desiccator prior to analysis.

3.4.3 Direct transesterification of wet microalgal biomass using the turbo thin film device

Biomass of the microalga *Chloroparva pannonica* was cultivated in photobioreactor in Flinders University (Adelaide, South Australia) using f/2-Si medium. The biomass was harvested by centrifugation at 7,500 rpm for 10 min and then the concentrated paste biomass was stored in cold room prior before use. The water content in the concentrated paste was determined by gravimetric analysis after freeze drying for 3 days. All data points were obtained from three separate experiments performed under identical condition with each experiment using 2 g of wet concentrated biomass paste which was mixed with predefined volumes of methanol. The reaction variables studied were catalyst concentration in methanol (0 – 12%; wt./v), flow rate (1 – 5 ml/min), rotation speed (2,000 – 7,000 rpm) and ratio biomass to methanol (1:6 – 1:18). A peristaltic pump was used to deliver the biomass - methanol slurry while a syringe pump delivered methanol – catalyst with various flow rate to the T^2FD which was rotated at specific rotation speed. The biodiesel was collected from the mixture product with hexane followed with purification and evaporation. Biodiesel was stored in a desiccator before analyse. The formation of biodiesel was confirmed using spectrophotometer FT-IR and the conversion yield was calculated based on the difference integration value of proton methoxy ($-OCH_3$) and methylene ($-CH_2-$) generated from ^{1}H-NMR spectrophotometer.

3.4.4 Direct transesterification of fungal biomass using the turbo thin film device

For biodiesel production, water was added to reconstitute the biomass to mimic naturally occurring water content (Kim et al., 2015a). The fungal biomass slurry was premixed with methanol in a modified 60 mL syringe containing a magnetic stir bar, which was located above a magnetic stirrer to achieve homogeneity of the mixture. The homogeneous fungal biomass-water-methanol mixture was pumped to the T^2FD using a syringe pump (Adelab Scientific, 12VDC, Australia). The catalyst, sodium hydroxide in methanol, was delivered via another syringe pump at the investigated concentrations. In all experiments, the matched and quoted flow rates were used for both the biomass slurry and the catalyst in methanol, as high FA to FAME conversion efficiencies were achieved, allowing to minimise solvent use. Biodiesel conversion was optimized by exploring different reaction conditions. For each experiment, 2 g of fungal biomass was prepared as a biomass/methanol mixture at biomass to methanol ratios of 1:6, 1:9, 1:12, 1:15, 1:18 and 1:25 wt./v. Flow rates (1, 2, 3, 4, 5, 8 and 10 mL/min), rotational speed of the turbo blade

(2,000 to 6,000 rpm, with increments of 500 rpm), catalyst concentrations (0, 0.5, 1, 3, 5, 7, 9 and 12 wt./v %) and water content (5, 25, 50 and 75% of dry weight (DW)) were systematically varied. After collection of the methanol and catalyst-reacted cell lysate from the T^2FD (~10 mL), the biodiesel was extracted with 10 mL of hexane. The hexane was removed *in vacuo* and the product stored in a desiccator prior to analysis. All experiments were performed in triplicate, with reported values and uncertainties being the average and standard errors, respectively.

Chapter 4

VORTEX FLUIDIC DEVICE-ASSISTED DIRECT TRANSESTERIFICATION OF WET MICROALGAL BIOMASS

4.1 Introduction

Microalgae have been recognized as an abundant resource that can be used for biodiesel production due to their rapid growth rate and high lipid yield per hectare compared to oil crops (Chisti, 2007), with limited competition for arable land use for food production (Ahmad et al., 2011). Current microalgae-based biodiesel production methods are labour and energy intensive, and require extensive processing including cultivation, harvesting, dewatering, lipid extraction and transesterification. In this multi-step processing, dewatering and lipid extraction have been identified as being the most energy-intensive and costly steps (Misra et al., 2014). Lardon et al. (2009) estimated that the dewatering process accounted for 84.9% of the total energy consumption required. He et al. (2016) calculated that the cost of drying and extraction of lipids from *Chlorella sp*. accounted for 48.4% of the operating cost of microalgae oil production in a semi continuous system.

In order to improve the cost- and energy-efficiency of biodiesel production, direct transesterification (DT) of microalgae biomass to biodiesel has been developed using both catalytic and non-catalytic processes (Ehimen et al., 2010). By eliminating the extraction and purification of oil steps in the DT process, the energy inputs required can be drastically reduced compared to conventional processes. Supercritical methanol extraction and transesterification has been shown to be suitable and an energy saving approach to biodiesel production from microalgae, saving 71MJ by eliminating drying and hexane extraction for a 10,000 MJ microalgal biodiesel production (Heimann, 2016). Thus eliminating hexane extraction will improve the overall green chemistry metrics of the process, simultaneously reducing the use of chemicals and other fixed costs (Carvalho Júnior et al., 2011). These reductions are projected to reduce biodiesel production costs by up to 75% (Haas and Wagner, 2011), thereby increasing the economic viability and competitiveness of microalgae-based biodiesel relative to fossil fuel.

Wet algal biomass has been used previously for biodiesel production, albeit under specific conditions, frequently requiring acid as the catalyst (Wahlen et al., 2011) or the use of a supercritical solvent (non-catalytic) (Jazzar et al., 2015a). DT of wet *Nannochloropsis*

gaditana biomass containing 75% water results in 100% conversion after 105 min at 100 °C (Macías-Sánchez et al., 2015), whilst 84% was achieved with supercritical methanol extraction (Patil et al., 2012a). Subcritical hydrothermal liquefaction is the most frequently studied microalgal biodiesel production route; however, high temperature (120 ºC) (used to prevent water from inhibiting the interaction between methanol and microalgae lipids (Cao et al., 2013) and to reduce methanol usage (Zakaria and Harvey, 2012)), and super nutrient-rich process water generated are potential limitations to implementation at scale (Heimann, 2016). Consequently, the development of an energy-efficient, rapid and high yielding method for direct biodiesel production from wet microalgae is yet to be realised. A major challenge is the translation of lab-based research to large-scale production.

Biodiesel can be produced from sunflower oil at room temperature in the VFD under continuous flow mode (Britton and Raston, 2014). This process is highly effective (99.9% conversion), requiring only a few minutes of residence time, using sodium hydroxide in methanol as the catalyst, and a low volume ratio of methanol to oil (1:1) (Britton and Raston, 2014). The VFD can also facilitate conversion of free fatty acids to biodiesel at room temperature (Britton and Raston, 2015). However, both of these studies use oil as the raw material. In contrast, the present study demonstrates for the first time that the VFD can be used to produce biodiesel directly from wet microalgal biomass (*Chloroparva pannonica*) using a homogeneous catalyst. *Chloroparva pannonica* was used due to the possibility to produce a valuable carotenoid co-product (Somogyi et al., 2011, Tan, 2016).

Firstly, the DT process of dry biomass using sulfuric acid or sodium hydroxide as the catalysts in methanol was studied. Four operating parameters were systematically explored, namely the ratio of biomass to methanol, the catalyst concentration in methanol, the reaction time and the rotational speed of the VFD tube. In defining the optimal conditions for biodiesel production under confined mode of operation, the catalyst that resulted in the highest conversion yield was then used in the continuous flow mode. The ratio of biomass to methanol, flow rate, rotational speed and tilt angle were identified as critical for biodiesel conversion in continuous flow, and they were systematically varied to identify the optimal combination of parameters for direct transesterification of dry microalgae biomass.

Based on the result generated using dry biomass, the DT of biomass with variable water content using sodium hydroxide in methanol as the catalyst was explored in confined and continuous mode. A response surface method based on Box-Behnken experimental

design was used to investigate the effects of the different operating parameters. Biodiesel formation was confirmed using FT-IR and ^{1}H-NMR with the latter used to determine the conversion yield. In addition, the effect of a VFD-intensified DT-processing on the microalgal cell wall disruption was investigated using scanning electron microscopy (SEM), as it correlates with lipid release.

4.2 Results and discussion

Total lipid content determined by GC-MS of the *C. pannonica* biomass was 23.4%, of which 42.7% were free fatty acids, 57.3% were triglycerides. Although the total lipid content was 7-fold higher than previously determined for *C. pannonica* (35 – 45mg of lipids per 100g of biomass), the fatty acid profile was similar (Somogyi et al., 2011).

Table 4.1 Fatty acids profile of microalga *Chloroparva pannonica*

Fatty Acid		**Percentage**
Saturated		
$C_{16:0}$	Palmitic	16.7
$C_{18:0}$	Stearic	0.7
Monounsaturated		
$C_{18:1}$	Oleic	33.1
Polyunsaturated		
$C_{18:2}$	Linoleic	24.7
$C_{18:3}$	Linolenic	21.9

Extraction efficiencies based on quantification of ^{1}H-NMR spectra of fatty acids derived from DT of VFD-extracted biomass and comparison with GC/MS analysis of FAME profiles using standard biomass extraction and transesterification protocols following published equations (Knothe and Kenar, 2004) were on average 41.5 mol%, ranging from 38.3 to 49.5 mol%. Extraction efficiencies were negatively affected, as Linolenic acid was not extracted in sufficient amounts for reliable quantification, irrespective of whether dry or wet biomass was used, or of the mode of operation (confined vs. continuous flow). In addition, extraction conditions biased extraction for C18:1 vs. the co-extraction of C18:3 and C16:0, further limiting complete extraction, and the Stearic acid (C18:0) content could not be reliably determined from ^{1}H-NMR spectra, due to low concentrations present in the *C. pannonica* biomass.

4.2.1 Dry biomass direct transesterification - confined mode

The DT of dry microalgae biomass facilitated by VFD was first investigated in the confined mode of operation, which is a reliable starting point before designing processing operations for continuous flow (Britton and Raston, 2014). The catalytic activity of both sulphuric acid and sodium hydroxide as catalysts in methanol was also studied using the confined mode.

Sample volume range was limited by the VFD vessel, with 550 μL being insufficient for the biomass to be immersed in the tube (preventing uniform processing) and 1200 μL being the maximum volume still permitting formation of a vortex. The establishment of a vortex from the base of the tube during the processing is critical, noting the VFD is distinctly different to a vortex mixer, which operates vertically and only under confined mode. Non-establishment of a vortex in the VFD changes fluid dynamics and progression of the reaction may be unpredictable and not reproducible (Eroglu et al., 2013).

Average extraction efficiency of the major fatty acids from dry biomass of *C. pannonica* was 43 mol%, ranging from 38 to 49.5 mol%. Extraction efficiencies of major fatty acids were affected by operational mode and catalyst used for dry biomass processed in the VFD. Palmitic acid (C16:0) and α-Linolenic acid (C18:3) co-extracted with 85 and 91% efficiency using the acid catalyst, a biomass to methanol ratio of 1:5, a processing time of 60 min, a rotational speed of 6,000 rpm and an acid catalyst concentration of 7%, but extraction of Oleic acid was only 49 mol% (C18:1). Under the same parameter settings, an increase in rotation speed to 8,000 rpm or decrease of reaction time yielded highest extraction efficiencies for C18:1 (84.5% and 74%, respectively). Extraction of C18:3 (40 and 58 mol%, respectively was decreased, whilst extraction of C16:0 (62 mol%) was only negatively affected at the increased rotational speed. An increase in incubation time also achieved 82 mol% extraction efficiency of C16:0 and almost 20% higher extraction efficiency of C18:1, while it was 23% lower for C18:3 compared to highest efficiencies achieved for the latter two fatty acids. Use of the base catalyst under the above conditions resulted in unquantifiable ^{1}H-NMR spectra for some samples, the loss of which did not correlate with any given extraction parameter. Generally, extraction of C18:1 of 74 mol% efficiency was achieved at the same parameter settings as for the acid catalyst which, in contrast to here (C18:3 49 mol%, C16:0 54 mol%), yielded highest C18:3 and C16:0 extraction efficiencies. No parameter setting yielded the same extraction efficiencies as achieved with the acid catalyst (max C18:3, 76 mol% and C16:0, 83 mol%). Extraction

efficiencies were similar to those obtained using microwave- or ultrasound-assisted DT of dry biomass of *Nannochloropsis* sp. or *Enteromorpha compressa* with either methanol as a solvent (Patil et al., 2011a) or the co-solvent tetra hydro furan (THF) (Suganya et al., 2014), respectively.

Highest conversion efficiency (92.8%) of fatty acids to FAME was achieved for a biomass to methanolic solution ratio of 1:6.7 (w/v) using the base catalyst, while 86.6% was achieved with the acid catalyst using a ratio of 1:8 (w/v) (Figure 4.1A). These results are similar to conversion efficiencies achieved using conventional direct transesterification methods (Ma et al., 2015b), however, unlike the VFD, continuous stirring of the reactant mixture, prolonged heating of the reactor at the boiling point of methanol (65°C) and an increased input of catalyst were required (12 vs. 7% w/v here).

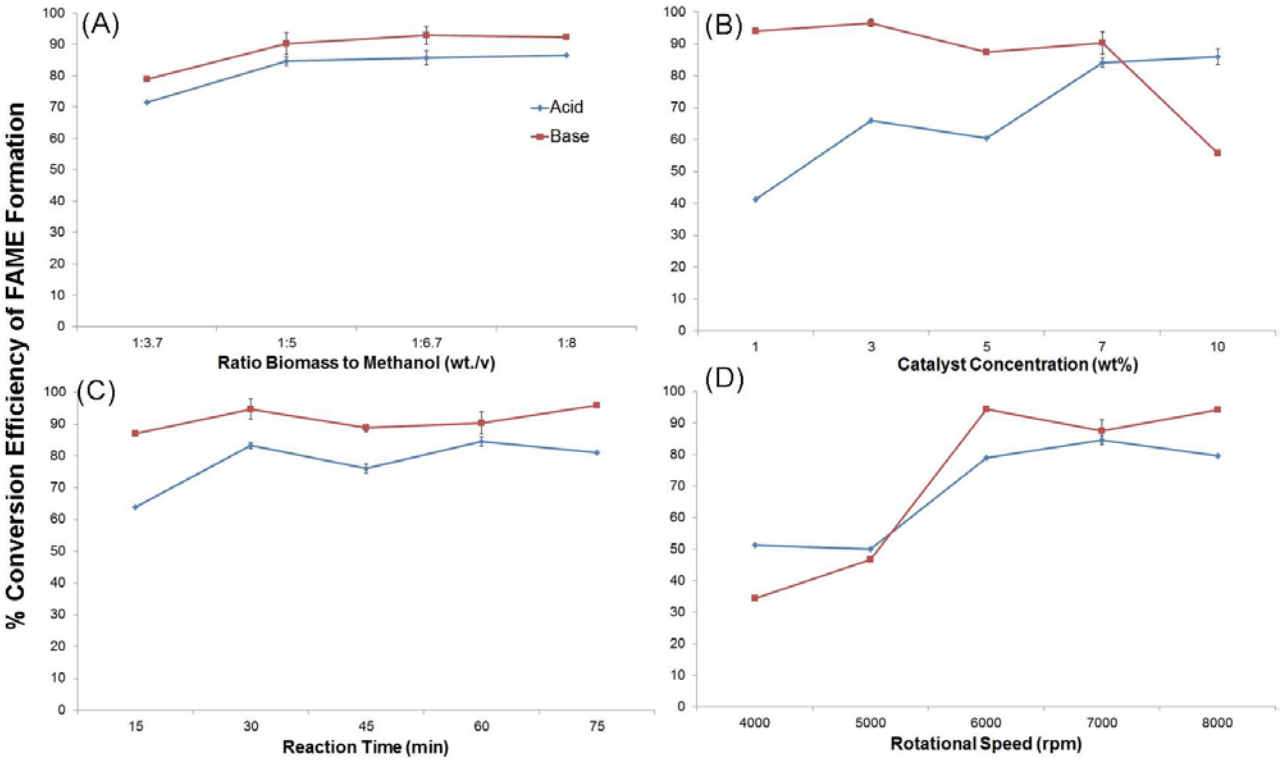

Figure 4.1 Effect of processing parameters for VFD-assisted DT of dry biomass of *Chloroparva pannonica* operated in confined mode: (A) Ratio of biomass to methanol (w/v); (B) catalyst concentration (%); (C) reaction time (min); and (D) rotational speed (rpm). n = 2 ± standard deviation.

Theoretically, the molar ratio of alcohol to triglycerides for transesterification is 3:1. In traditional batch-processing, however, an excess of alcohol is used to drive the reaction and to ensure that all triglycerides are converted to FAMEs (Leung et al., 2010). Previous studies established that the conversion of free fatty acids was affected by the volume of methanol used in the esterification reaction (Britton and Raston, 2015). In the present

study, a further increase in the amount of methanolic solution did not affect the biodiesel conversion efficiencies. Previous studies also determined that increasing the amount of methanol, resulting in lower catalyst concentrations, decreased the conversion yield and could negatively impact on downstream separation processing (Kasim and Harvey, 2011). Therefore, a ratio of biomass to methanolic solution of 1:6.7 was deemed optimal in our process.

A number of studies have shown that catalyst concentration can affect the yield of biodiesel production (Kasim and Harvey, 2011, Britton and Raston, 2014). Based on these findings, five different concentrations of acid and base catalysts 1, 3, 5, 7 and 10% were used at a biomass to methanolic solution ratio of 1:5, for a 60 min reaction time at a rotation speed of 7,000 rpm (Figure 4.1B). The highest biodiesel conversion efficiency was 96.6% at 3% (w/v) sodium hydroxide and a further increase neither enhanced the conversion efficiency nor increased the ester content, except at 10% (w/v), which resulted in a dramatic decrease in conversion efficiency to 55.7%, which could be due to excess alkaline-induced saponification (Kasim and Harvey, 2011, Zakaria and Harvey, 2012). Excess alkaline catalyst produces more triglycerides which react with the catalyst to form soap, resulting in a gradual decrease in FAME yields, as alkaline catalyst concentrations exceed threshold concentrations (Efavi et al., 2018).

Different processing outcomes were obtained using sulphuric acid as the catalyst, where increasing concentrations incrementally increased conversion efficiencies, with the highest conversion yield of 86% obtained at 10% (w/v). This finding supports the results of other studies on the DT of microalgae biomass (Wahlen et al., 2011, Velasquez-Orta et al., 2013). In summary, the use of an acid catalyst resulted in lower conversion efficiencies of fatty acids from dried microalgae biomass to FAME compared to a base-catalyzed transesterification, but fatty acid extraction efficiencies were higher.

High shear in the VFD corresponds to higher rotational speeds which improves mass, as well as heat transfer (Britton et al., 2017). In studying the effect of shear in the VFD, DT processing was conducted in the absence of a catalyst, achieving a conversion efficiency of 29.8% after 60 min at a rotation of 7,000 rpm and a biomass to methanol ratio 1:5 (w/v). The high shear disrupts the microalgae cell walls and membranes releasing fatty acids and enzymes (lipases and esterases), resulting in free fatty acids, explaining the high free fatty acid content observed. Auto-catalytic formation of FAME is a well-described phenomenon under these conditions (Gu et al., 2011, Jiang et al., 2013). While conversion efficiencies

to FAME of the non-catalytic DT process using the VFD only yielded 1/3 of those possible, the process would open the opportunity to utilise the remaining biomass as a high protein nutrient supplement, whilst producing biodiesel in an environmentally conscious way, additionally simplifying downstream purification processes.

Conversion efficiencies to FAME have been shown to positively correlate with reaction time (Jazzar et al., 2015a, Ma et al., 2015b), although the extent is strongly dependent on the processing technology employed. In this study, reaction time did not significantly influence conversion efficiencies when a base catalyst was used (87 to 95% w/v), but a strong increase was observed for a reaction time increase from 15 to 30 min for the acid catalyst (64 to 83% w/v) (Figure 4.1C). A virtually unchanged conversion efficiency for reaction times from 30 to 75 min suggests that reactions were not at equilibrium, which would have favored ester hydrolysis (Leung et al., 2010). This finding is in contrast to conventional DT processing of dry microalgae biomass, which usually requires longer than 60 min reaction times (Ehimen et al., 2010) at a higher temperature (60°C – 120°C) and higher biomass to the solvent ratio (6 – 40; w/v). For example, a conversion efficiency of 98.4% was achieved when using sulphuric acid as the catalyst after 240 min at 60 °C (Viêgas et al., 2015).

Based on the fact that triglycerides and methanol are immiscible, vigorous mixing is required to increase surface to surface interactions that govern the reaction process and conversion efficiencies (Ehimen et al., 2010). In a VFD, the interaction occurs simultaneously during the reaction (Britton and Raston, 2014, Britton et al., 2016, Luo et al., 2016) and an increase in the rotational speed in the VFD yielded higher biodiesel quantities from sunflower oil (Britton and Raston, 2014). This is attributed to the formation of thinner films at a higher rotational speed which are more intensely mixed (Luo et al., 2016), thereby increasing reactions rates (Viêgas et al., 2015). In the present study, increasing the rotational speed affected fluid dynamics in various ways, i.e. the liquid covered a greater length/surface area of the tube, resulting in a reduction of the thin film thickness formed upon rotation. Using a biomass to methanol ratio of 1:5 and 7% (w/v) acid or base catalyst concentration and a reaction time of 60 min, conversion efficiencies positively correlated with rotational speed up to 6,000 rpm, increasing from 51 to 79% for the acid catalyst and from 34 to 94% for the base catalyst, but remained relatively constant upon further increases to 8,000 rpm (Figure 4.1D). This result is similar to that for the esterification of free fatty acid to biodiesel, involving continuous flow VFD processing (Britton and Raston, 2015).

In summary, optimal conditions for DT of fatty acids from dry biomass of *C. pannonica* in confined operation mode were: biomass to methanol ratio of 1:6.7 (w/v), 10% and 3% (w/v) acid and base catalyst concentrations, respectively, 30 min reaction time and 6,000 rpm rotational speed. Fatty acid to FAME conversion efficiencies of 83.3% and 96.4% were obtained using sulphuric acid and sodium hydroxide as catalysts, respectively. The base catalyst showed higher conversion efficiencies at lower catalyst concentration, which is consistent with previous findings (Velasquez-Orta et al., 2012, Kim et al., 2014).

4.2.2 Dry biomass direct transesterification - continuous flow

Based on results obtained in the confined operation mode, continuous flow operation of the VFD was investigated using 3% (w/v) of sodium hydroxide as catalyst. Compared to DT of dry biomass of *C. pannonica* in confined mode, average extraction efficiencies of the extractable dominant fatty acids was lower than in continuous mode (39.6 mol%), ranging from 38 to 42 mol%. Highest extraction efficiencies of 93 to 96 mol% were achieved for C18:3, but unlike in confined mode using the base catalyst, C16:0 and C18:1 extraction efficiencies were 17 and 27% lower at opitmal settings for highest C18:3 recovery (biomass to methanol ratio 1:10, flow rates of 0.2, 0.4 and 05 mL/min, a rotational speed of 6,000 rpm and an angle of 45°). Parameter settings (rotational speed 5,000 and 7,000 rpm at a flow rate of 0.5 mL/min at the same biomass to methonal ratio and angle) that yielded the highest C18:1 extraction efficiencies still only achieved 19 to 36% of highest efficiencies achieved with the base catalyst in confined mode.

Unlike observed large effects of biomass to methanol ratio and rotational speed on fatty acid to FAME conversion efficiencies of dry biomass of *C. pannonica*, in confined mode of operation, these parameters had no discernible effect when continuous flow was applied, although the rotational speed of the VFD tube in the continuous mode affects the thickness of the film formed along the tube and the residence time (Yasmin et al., 2013, Jones and Raston, 2017). Unlike in continuous mode, in the confined mode using the base catalyst, conversion efficiency dropped slightly at a rotation of less than 6,000 rpm. The higher conversion efficiencies at a lower rotational speed under continuous flow could be due to extra shear stress from the viscous drag of the liquid moving up the tube, which enhances the interaction between the biomass and reactants, and thus is likely to increase the rate of the reaction. In the VFD, the maximum cross vector of gravity and centrifugal forces occur when the rotating tube is inclined at 45° (Chen et al., 2012, Britton and Raston, 2014, Kumari et al., 2016) and this corresponds to the optimum angle for many processes

(Britton et al., 2017). In the present study, the mounting angle of the VFD tube had no effect. Maximal achieved fatty acid to FAME conversion efficiencies were 97, 95 and 99%, respectively.

Under continuous flow, the flow rate controls the residence/reaction time of the reagents in the VFD tube (Britton et al., 2016, Luo et al., 2016). Seven different flow rates (ranging from 0.1 to 1 mL/min) were investigated on the DT processing of dry algal biomass in continuous mode, but effects were minimal, reaching a maximum of ~99% at 0.5 mL/min.

4.2.3 Wet biomass direct transesterification – confined mode

The drying or dewatering of microalgae biomass has a high energy penalty (He et al., 2016). Therefore, VFD-assisted DT of wet biomass of *C. pannonica* was investigated in confined mode determining fatty acid extraction efficiency and fatty acid to FAME conversion efficiency at biomass to methanol ratios of 1:5, 1:6.7 and 1:8.3, reaction times of 15, 30 and 45 min and water contents of 5, 47.5 and 90 (% w/w) at a rotational speed of 6,000 rpm and a catalyst concentration of 3% (w/v in methanol). A Box-Behnken design was used to investigate the interactions between varying parameters on fatty acid to FAME conversion efficiency so that the optimal conditions for biodiesel production could be identified. Average extraction efficiency for the major extractable fatty acids was 41 mol%, ranging from 40 to 43 mol%, which was slightly lower and higher than for dry biomass of *C. pannonica* extracted in confined mode and continuous mode using the base catalyst, respectively. Extraction efficiency of C18:1 was comparable with a maximum of 77.5 mol% at a 15 min shorter reaction time of 45 min, a slightly higher biomass to methanol ratio of 1:6.7 instead of 1:5, and a water content of 90%. The second lowest extraction efficiency of C18:1 was 50 mol% at a biomass to methanol ratio of 1:6.7, a 30 min reaction time and a 47% (w/w) water content, but there was no clear effect of parameter settings, as the same settings also resulted in the second highest extraction efficiency of 71 mol%. Extraction efficiencies for C18:3 ranged from 46 to 74 mol%, with the maximum being only marginally lower than recorded for confined mode operated VFD-assisted DT of dry biomass of *C. pannonica* using the base catalyst. Maximal extraction efficiencies for C16:0 ranged from 56 to 74 mol%, with the maximum being 19% lower than for dry biomass extracted in confined VFD mode. As for C18:1 extraction efficiencies, no clear effects of parameter settings were discernible for confined mode operated VFD-extracted biomass of *C. pannonica*. Wet DT using solvents like methanol and ethanol and 10% sulphuric acid as a catalyst has been carried out with microalgal, fungal and yeast

biomass (Hoarau et al., 2016, Suh et al., 2015). Extraction efficiencies were not reported and units used are not convertible to units used here. Regardless, DT of wet extraction of various types of wet biomass still required heating to 80 to 120 °C for up to 2 h, an energy-intensive step that is avoided in VFD-processing. Similarly, high pressure DT using hexane on a wet mixed green microalgal biomass required heating, but yielded extraction efficiencies of 70-86% (Islam et al., 2014), a point to consider in life-cycle analyses of biodiesel production. Microwave-assisted one step DT of wet *Chlorella* biomass yielded higher extraction efficiencies (~53%) (Cheng et al., 2013) than reported here for the VFD, but differences in energy requirements would need to be determined for both approaches.

Quadratic regression model-generated (equation 4.1) values of fatty acid to FAME conversion efficiencies were generally in a good agreement with empirical data (Table 4.1).

$$\text{Conversion Efficiency} = 94.25 - 1.73A - 0.97B + 0.81C - 0.23AB + 0.81AC - 1.01BC + 0.12A2 + 0.92B2 - 0.36C2 \quad \text{(eq. 4.1)}$$

where:

- A = Water content (w%); - B = Reaction time (min); - C = Ratio of biomass to methanol (w/v)

Table 4.2 Box-Behnken design matrix and response to VFD-assisted direct transesterification of wet microalgal biomass of *Chloroparva pannonica* operating in confined mode.

Run	Water Content (w%)	Reaction Time (min)	Ratio biomass to methanol (w/v)	FA to FAME Conversion Efficiency (%)	
				Experimental	Predicted
1	23.75	30	1:6.7	90.26	94.25
2	45	45	1:6.7	92.91	92.36
3	23.75	30	1:6.7	97.40	94.25
4	2.5	30	1:8.3	96.46	95.74
5	23.75	15	1:5	94.36	93.96
6	45	15	1:6.7	95.09	94.77
7	23.75	45	1:5	94.21	94.01
8	2.5	30	1:5	95.90	95.75
9	45	30	1:8.3	93.75	93.91
10	23.75	45	1:8.3	93.23	93.63
11	45	30	1:5	89.95	90.67
12	2.5	15	1:6.7	97.20	97.76
13	23.75	30	1:6.7	95.09	94.25
14	23.75	15	1:8.3	97.44	97.61
15	2.5	45	1:6.7	95.96	96.28

Correlation analyses and analysis of variance for the interaction of parameters (ANOVA, α = 0.05) on fatty acid to FAME conversion efficiencies of VFD-assisted DT of wet biomass of *C. pannonica* operated in confined mode confirmed that there was no significant effect of the parameter combinations chosen following a Box-Behnken design. Generally, irrespective of parameter setting, a high fatty acid to FAME conversion efficiency was achieved for VFD-assisted DT of wet biomass (>90%). Response surface analysis of water content vs. reaction time confirmed the broad range of parameter settings 95% and higher fatty acid to FAME conversion efficiencies, with the highest efficiencies (~97%) being predicted for 0% water content and a 15 min reaction time under the Box-Behnken design of parameter settings (Figure 4.2A). Similarly, broad parameter settings were recorded for >95% fatty acid to FAME conversion efficiencies for water content vs. biomass to methanol ratio (Figure 4.2B) and reaction time vs, biomass to methanol ratio (Figure 4.2C), with predicted maxima occurring at water contents of 0% and a biomass ration of 1.1 and a reaction of > 15 min and a biomass to methanol ratio of 1.3, respectively. The only parameter setting according to the response surface analysis that resulted in < 90% fatty acid to FAME conversion efficiency was a water content of 80% at a biomass to methanol ratio of 0.8 (Figure 4.2B).

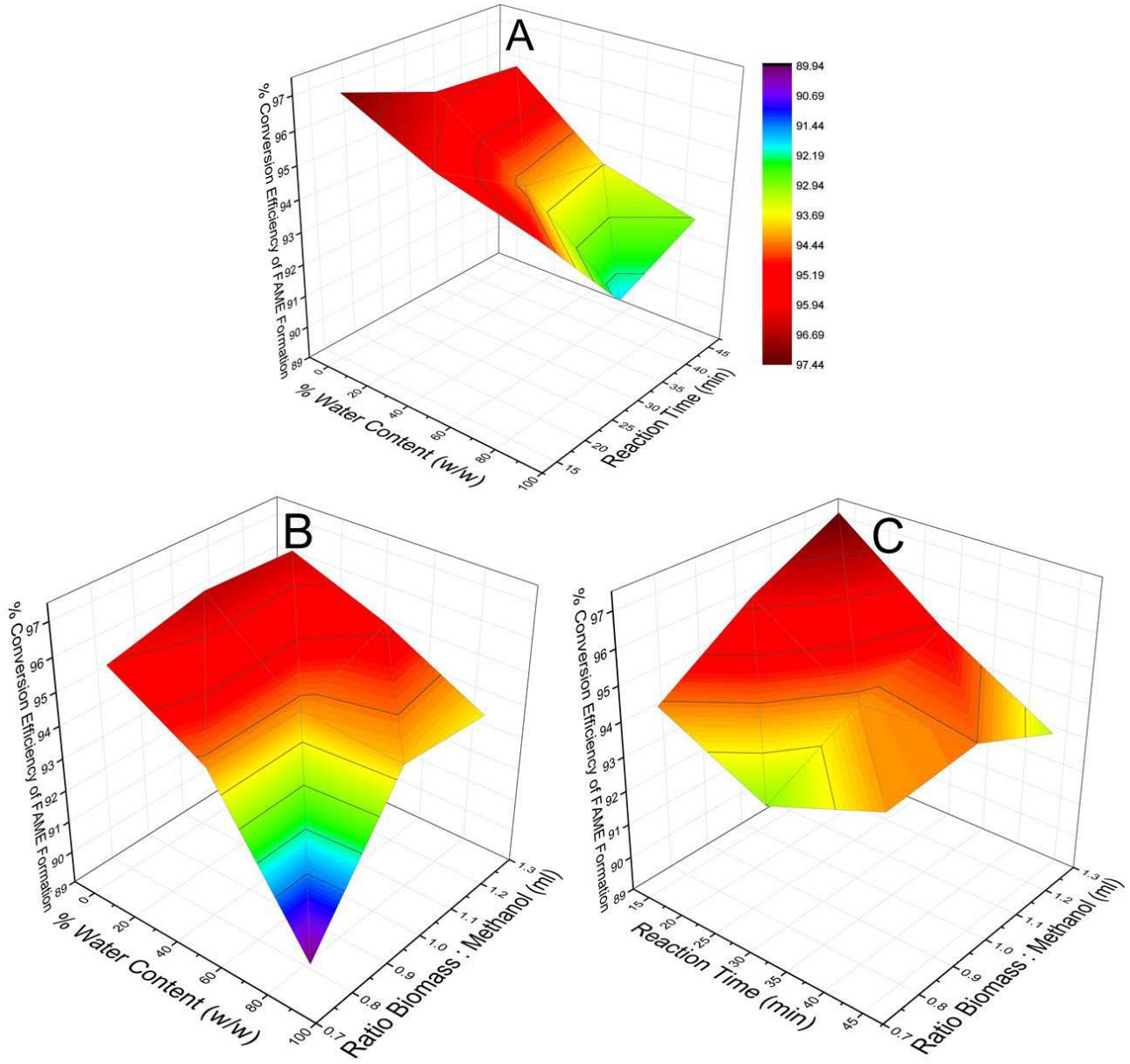

Figure 4.2 Surface response plots for fatty acid to FAME conversion efficiency of VFD-assisted DT of wet *Chloroparva pannonica* biomass operated in confined mode: (A) water content (w%) and biomass to methanol ratio (w/v); (B) biomass to methanol ratio and the reaction time (min); and (C) the reaction time and water content.

Accordingly, VFD-assisted DT of wet biomass of *C. pannonica* could be achieved within minutes without compromising on fatty acid to FAME conversion efficiency, most likely attributable to intense micro-mixing and a high level of shear stress within the tube at high rotational speeds (6,000 rpm), as this increases mass transfer (Britton et al., 2017). Thus there is potential to eliminate the necessity to dry the biomass and subsequently extract the lipids, which will dramatically reduce the energy consumption and facilitate commercialization of the process.

Although there was no statistical effect of parameter settings on fatty acid to FAME conversion efficiency, predicted optimal water content was 90%, reaction time 15 min and biomass to methanol ratio 1:8.3 (w/v), resulting in a predicted conversion efficiency of 97.1%. In order to verify the model predictions, the optimum response parameters were tested experimentally, resulting in an average conversion efficiency of 96.9 ± 0.9%, being within 1% of the predicted value.

4.2.4 Wet biomass direct transesterification – continuous mode

Continuous flow operation of the VFD offers a number of advantages including the integration of multiple steps into a high-throughput one-step reaction with ease of scale-up. Therefore, the effect of water content (80, 90, 100% w/w), flow rate (0.1, 0.55 and 1mL/min) (residence (reaction) time) and biomass to methanol ratio (1:6, 1:15 and 1:24, w/v) on fatty acid extraction efficiency and fatty acid to FAME conversion efficiency was further investigated for VFD-assisted DT of wet *C. pannonica* biomass at a fixed rotational speed of 6,000 rpm and 3% (w/v) base catalyst. Water content of the biomass can have negative (reduced extraction and conversion efficiencies of fatty acids) and positive effects (reduced costs of biodiesel production), the latter if process efficiency is not adversely affected.

Average extraction efficiency for the major extractable fatty acids was the same as for confined mode operated VFD-assisted extraction of wet biomass 41 mol%, ranging from 39 to 47 mol%, with maxima being slightly higher than for confined mode extracted wet biomass. Extraction efficiency of C18:1 was similar with a maximum of 78.5% at a significantly shorter residence time of ~2 min and a similar water content of 100% vs 90%, a flow rate of 0.55 mL/min) and a biomass to methanol ration of 1:24, which could be due to the ~4-times higher methanol content. The lowest extraction efficiency of C18:1 was 42 mol% at a biomass to methanol ratio of 1:15, a flow rate of 0.55 mL/min a water content of 90% (w/w), being 10% lower than the lowest C18:1 extraction efficiency recorded for wet biomass VFD-extracted in the confined mode of operation, which could be explained by the interacting effect of approximately half the water content and much lower methanol concentration. Similarly to wet extraction in VFD-confined mode, extraction efficiencies for C18:3 ranged from 46.5 to 75 mol%, with flow rate being the determining factor between high and low extraction efficiencies (1 vs. 0.1 mL/min) at a water content of 80% and a biomass to methanol ratio of 1:15. Maximal extraction efficiencies for C16:0 ranged from 55 to 70.5 mol%, with the minimum being similar to the confined mode operation, but the

maximum is 3.5% lower. The parameter settings for high and low extraction efficiencies of C16:0 in the continuous flow were quite different, i.e. for the maximum the water content was 100%, the flow rate of 0.55 mL/min and a biomass to methanol ratio of 1:24 vs. a water content of 80%, a flow rate of 1 mL/min and a biomass to methanol ratio of 1:15. Interestingly, parameter settings of a water content of 80%, a flow rate of 1 mL/min and a biomass ratio of 1:15 resulted in an extraction bias for C18:1 over C18:3 and C16:0, similar to observation for dry biomass extraction in the confined mode using the base catalyst.

A response surface methodology model was fitted to data for fatty acid to FAME conversion efficiency to investigate the effect of three experimental parameters, namely water content, biomass to methanol ratio, and flow rate on the conversion yield. From the Box-Behnken model, the quadratic regression was calculated using equation 4.2. The relationship between the predicted and observed conversion yield showed good linearity (Table 4.2).

$$\text{Conversion efficiency} = 96.27 - 0.51A - 0.98B - 0.29C - 1.48AB - 0.85AC + 0.13BC - 0.98A2 + 0.34B2 + 0.42C2 \quad \text{(eq. 4.2)}$$

Table 4.3 Box-Behnken design matrix and response to VFD-assisted—direct transesterification of wet microalgal biomass of *Chloroparva pannonica* operating in continuous mode.

Run	Water Content (w%)	Flow Rate (mL/min)	Ratio Biomass to Methanol (w/v)	FA to FAME Conversion Efficiency (%)	
				Experimental	Predicted
1	45	0.55	1:15	94.1	96.3
2	50	0.55	1:24	93.3	94.1
3	45	0.55	1:15	97.6	96.3
4	45	1	1:6	96.0	96.2
5	40	0.1	1:15	96.4	95.6
6	40	0.55	1:24	95.8	96.8
7	50	0.1	1:15	98.1	97.6
8	45	0.1	1:6	96.9	98.4
9	45	1	1:24	97.4	95.9
10	50	1	1:15	91.9	92.7
11	45	0.1	1:24	97.8	97.6
12	40	0.55	1:6	96.4	95.7
13	45	0.55	1:15	97.1	96.3
14	40	1	1:15	96.1	96.6
15	50	0.55	1:6	97.3	96.3

The ANOVA analysis showed that there was no significant effect within or between any of the operating parameters considered in this study. The model suggests that water content

would not affect conversion efficiencies at a slow flow rate < 0.1 mL/min, but higher flow rates would negatively impact (Figure 4.3A), which could be a consequence of the reduction in reaction (residence) time. A thin film formed rapidly upon delivery of the reagents to the VFD tube using the jet feeds, inducing intense micro-mixing and high shear stress. Under these conditions, high water content could inhibit transesterification, affording lower conversion efficiencies. Accordingly, when moderately low biomass water content resulted in higher conversion efficiencies at faster flow rates and decreased at higher water content. Increased water content had little effect on fatty acid to FAME conversion efficiencies at higher of biomass to methanol ratios (Figure 4. 3B). Conversion efficiencies were predicted to decrease, however, at a simultaneous increase of both water content of the algal biomass and ratio of biomass to methanol. The model predicts that increasing the flow rate would significantly reduce conversion efficiencies at either low or high ratios of biomass to methanol (Figure 4.3C). Residence time dictates reaction time, influences micro-mixing and effective shear stress (Britton et al., 2016). At high flow rates, the film is thicker and the mechano-energy exposure to the reactants is reduced, which could result in lower conversion efficiencies.

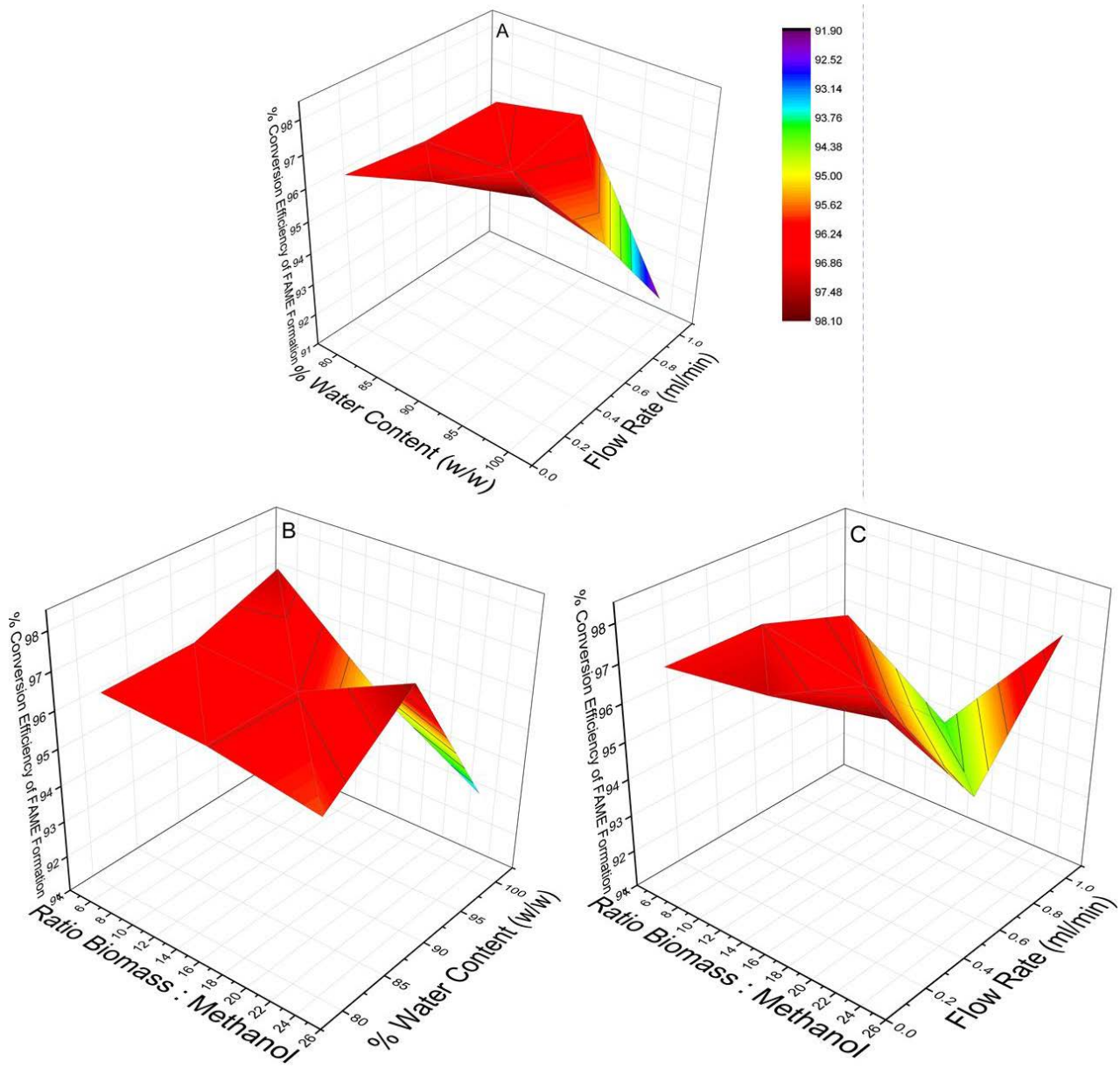

Figure 4.3 Surface response plots for fatty acid to FAME conversion efficiency of VFD-assisted DT of wet *Chloroparva pannonica* biomass operated in continuous mode, for (a) water content (w%) and ratio of biomass to methanol (w/v); (b) flow rate (mL/min) and water content; and (c) flow rate and ratio of biomass to methanol.

Careful scrutiny of the impact of independent variables on fatty acid to FAME conversion yields suggests that a conversion efficiency of 99.2% could be achieved at a water content of 50% (w/w), a flow rate 0.1 mL/min and a biomass to methanol ratio at 1:6 (w/v). The model output was verified by testing these conditions experimentally, which resulted in a conversion efficiency of 96.9 ± 0.9%.

The above results suggested that water content of the microalgal biomass did not significantly affect fatty acid to FAME conversion in continuous flow mode operated VFD-assisted DT, which was further tested at 0.5 mL/min flow rate for a 1:6 ratio of biomass to

methanol, 6,000 rpm rotation speed and 3% (w/v) of sodium hydroxide in methanol as the catalyst. A test series of four biomass samples, containing water contents of 25, 50, 75 and 100%, however, determined that conversion decreased from ~98 to just over 90% with increasing water content. These outcomes were further confirmed using fresh bioreactor-raised biomass of *C. pannonica* harvested by centrifugation, resulting in a water content of 67%, achieving 96% conversion efficiency at a residence time of 2 min. An advantage of the VFD microfluidic platform for DT of wet microalgal biomass is the capability for continuous flow operation achieving >90% fatty acid to FAME conversion efficiencies for a broad range of parameter settings. This renders the VFD as a new potential wet extraction and DT platform technology for conversion of microalgal lipids to biodiesel, particularly in light of DT of wet microalgal biomass approaches such as high pressure extraction which cannot be operated in continuous flow (Islam et al., 2014).

4.2.5 Biodiesel characterization

FT-IR was used to identify the functional groups relating to various stretching and bending vibrations (fingerprint) of biodiesel and compared to the spectrum for sunflower oil. The FT-IR spectra of both triglyceride and microalgal FAME (biodiesel) were similar, except for the presence of the FAME-specific methoxy (-OCH_3) group. The main absorption peaks of microalgae biodiesel were at 2954 – 2854 cm^{-1}, 1744 cm^{-1}, 1377 cm^{-1}, 1460 cm^{-1} and 1196 cm^{-1}. The strong absorption peak at 1744 cm^{-1} is specific for νC=O, while the peak at 1377 cm^{-1} corresponds to νC-O. The formation of FAME was confirmed by the peaks at 1460 cm^{-1} and 1196 cm^{-1}, which corresponds to -CH_3 asymmetric and O-CH_3 stretching (Tariq et al., 2011).

To confirm the FT-IR analyses, methoxy protons (OCH_3) of the FAME product and the α-methylene protons (α-CH_2) were quantified for both the microalgal FAME and the sunflower triglycerides from ^{1}H-NMR spectra. As expected, no peaks representing the methoxy proton resonance at 3.6 – 3.7 ppm were observed for the sunflower oil in contrast to the microalgal FAME. Thus ^{1}H NMR spectroscopy is consistent with the formation obtained by FT-IR. It is therefore not surprising that the biodiesel industry is interested in developing Fourier-transformed FT-IR spectroscopy techniques to monitor and optimise FAME formation in the transesterification processing step (Yuan et al., 2014).

4.3 Conclusion

VFD-intensified DT of microalgal biomass is a novel method for one step biodiesel production. No significant impact of catalyst, parameter setting, or mode of operation was detected for fatty acid extraction or conversion to FAME efficiencies. Average extraction efficiencies of extractable fatty acids 41 mol%, which was low because C18:2 did not extract. Continuous flow-operated VFD achieved a 96% conversion efficiency for fresh biomass (67% water content) at a residence time of 2 min. The tolerance of the DT to a wide range of crucial parameters in the continuous flow-operated VFD overcomes a critical hurdle for up-scaling of the process.

Chapter 5

TURBO THIN FILM DEVICE-ASSISTED DIRECT TRANSESTERIFICATION OF OLEAGINOUS BIOMASS TO BIODIESEL

5.1 Introduction

Given the depletion of petroleum-derived fuels and increasing environmental concerns regarding pollution, research in renewable energy has escalated and much effort has been devoted to the production of biodiesel (Faried et al., 2017). Semi-refined and refined vegetable oils are very often used as starting materials for biodiesel production, which is not sustainable due to the diversion of valuable food resources. The traditional approach to biodiesel production from plant materials consists of biomass drying, oil extraction, fatty acid (FA) transesterification and purification, of which the oil extraction and drying steps are the most energy intensive ones, contributing with 28 and 21%, respectively (He et al., 2016). The use of waste cooking oils, animal fats and plant seeds eliminates the energy-intensive drying step and they are therefore suitable candidates for biodiesel production. Among the oil seeds, palm oil production has been heralded as a solution to increase biodiesel production, but a large environmental footprint, i.e. habitat destruction and versatile applications in food and other products (Pande et al., 2012) has generated a negative public acceptance on the one hand and eroded the competitive price on the other hand (Fargione et al., 2008).

Soybeans, although used in various feed applications, are among the first generation of biodiesel feedstock due to a 3.2 – 5.4 fossil fuel energy ratio, which is derived from renewable energy produced per unit fossil energy consumed over its life cycle, which takes into account feedstock production and transportation, biomass processing including biodiesel conversion and distribution (Sieverding et al., 2015). Therefore, soybean-derived biodiesel has a large market share in the world market, with the United States and Brazil being major producers (da Silva César et al., 2019). Furthermore, modernisation of farming practices and soybean processing in the biodiesel industry is expected to further increase the fossil energy ratio (Pradhan et al., 2011). Moreover, 83% of the protein content of soymeal can be maintained in biomass residue processed by direct transesterification (DT, see below) (Wyatt and Haas, 2009), with the lipid-free soybean

meal yielding the same weight in rainbow trout as the unextracted soymeal (Barrows et al., 2008). This highlights that there may be no loss of product application, e.g. food vs fuel. Despite this and a large contribution of soybean-derived biodiesel to renewable liquid fuel supplies, research on the DT of soybean seed to biodiesel is surprisingly rare. Studies to date have been conducted in batch mode at high temperature with long reaction times (Kildiran et al., 1996, Haas and Scott, 2007, Barrows et al., 2008, Wyatt and Haas, 2009). Prolonged reaction times at high temperature increase energy input and total biodiesel production cost (Skorupskaite et al., 2016). It is therefore paramount to investigate DT processing strategies that allow for simultaneous oil extraction and transesterification at ambient temperature and pressure under continuous flow to further increase net energy gains.

To eliminate the use of edible feedstock, current emphasis is placed on developing 2nd and 3rd generation biofuels from non-food source feedstock, such as waste cooking oil and animal fats, Jatropha and microalgae (Islam et al., 2013). Engine tests using biodiesels from various feedstock have determined their suitability for fossil diesel replacement, generally achieving a reduction in greenhouse gas emissions (Islam et al., 2015b, D´Agosto et al., 2017, Liu et al., 2017). With regards to environmental footprint, energy consumption of the process is another determinant of adoption into the market, primarily driven by a consumer-issued social licence. However, adoption into the market is presently driven by price, and the current US biodiesel price is still ~9% higher than for fossil-derived diesel with US$ 0.94 vs US$ 0.86 L^{-1} (Bourbon, 2018). The higher costs for biodiesel are driven by feedstock supply and price as well as biomass processing, the latter requiring a multi-step processing pathway, if plant materials are used. Conventional biodiesel production is costly, as the transesterification reaction requires heating, and, if biomass is used, drying and extraction, add additional costs (Cui and Liang, 2014). Haas and Wagner calculated that eliminating pre-processing oil feedstock could reduce the cost of biodiesel production by 88% (Haas et al., 2006) which would therefore significantly reduce the price of biodiesel. Furthermore, performing DT processing without the need for pre-processing could also reduce the use of chemicals, particularly hexane which has been classified as an air pollutant (Kaul et al., 2010). There are many reports on DT processing, particularly using microalgae biomass feedstock, either as a catalytic or non-catalytic process, with high conversion yields, as for example in the acid-catalysed processing of dry *Chlorella* sp. (Viêgas et al., 2015) and non-catalytic processing of wet *Chlorella vulgaris* (Levine et al., 2010). Direct transesterification of oleaginous microorganisms can reduce processing time

and restrict the use of harmful solvents to methanol only (Yousuf et al., 2017). Promising oil-rich feedstock are oleaginous microorganisms such as microalgae, fungi, and yeast, which have several advantages, including (i) year-round, rather than seasonal production on non-arable land, (ii) higher biomass productivities and (iii) higher lipid contents than food oil crops (Shuba and Kifle, 2018). Oleaginous microorganisms can grow in inexpensive media such as industrial waste waters (Deeba et al., 2016), glucose and acid hydrolysate of sugarcane bagasse (Brar et al., 2017), and dairy farm waste water (Sun et al., 2018). For example, *Cryptococcus humicola*, grown on glycerol as a carbon source, has a lipid content of ~71% (Souza et al., 2017).

The techno-economic outcomes for biodiesel production can be significantly improved using direct transesterification (DT) of wet biomass feedstock and developing less expensive raw material supply chains (Kumar, 2017).Thus, circumventing the need for drying microalgae prior to DT processing can overcome one of the bottlenecks in the commercialization of microbial biodiesel, by reducing the processing time and energy consumption of the overall process (Abu-Ghosh et al., 2015). Current DT processing requires operating at high temperature and pressures, especially when using wet biomass as the raw material. A conversion efficiency of 100% was reported for catalytic DT of wet biomass of *Nannochloropsis gaditana* at 100 °C (Macías-Sánchez et al., 2015) while a higher temperature (175 – 325 °C) was required for non-catalytic processing (Levine et al., 2010, Patil et al., 2012a, Tsigie et al., 2012). Direct transesterification of wet *Pichia guilliermondii* reduced the total production time by up to 8 h compared to the conventional two-step method by avoiding the drying step (Chopra et al., 2016). High biodiesel conversion efficiencies, however, still required long reaction times (6 h). Overall production times can also be shortened using high energy input microwave- and ultrasonication-intensified DT of wet biomass, yielding conversion efficiencies of 92% and 94.3% with reaction times of 4 min from wet *Cryptococcus curvatus* and *Yarrowia lipolytica* biomass, respectively (Yellapu et al., 2017). To date, however, most studies on DT of fungal biomass have been conducted at high reaction temperatures of 60 - 100ºC, representing a significant energy penalty. Therefore, developing a rapid DT process with low energy consumption is necessary to increase the competitiveness of direct biodiesel production. In addition, finding a method for DT of wet biomass that operates at room temperature and atmospheric pressure is paramount for reducing energy costs (Skorupskaite et al., 2016).

For the DT of microbial biomass, effective cell disruption with simultaneous extraction and transesterification of fatty acids is essential. High shear stress processing is particularly

useful for homogenising, dispersing and dissolving material, and a number of different types of devices are available for these purposes (Schilde et al., 2011). This includes thin film continuous flow processors, such as spinning disc and rotating processors (Chen et al., 2014), and more recently the vortex fluidic device (VFD) which has a boundary layer between the liquid and a gas and has shown distinct advantages in a number of applications (Britton et al., 2017). A remarkably versatile vortex fluidic device (VFD) was recently tested for rapid DT of wet microalgal biomass (*Chloroparva pannonica*, water content ~68%) to biodiesel, achieving rapid (~2 min residence time) and high (>96%) conversion efficiencies, when operated under continuous flow conditions at room temperatures (Sitepu et al., 2018a) (Chapter 4). It is, however, challenging to up-scale the device for industrial applications.

In contrast, rotating reactors are frequently used at industrial scale (Visscher et al., 2013). Here, we report the development of a novel rotating, high shear continuous flow turbo thin film microfluidic processing device (T^2FD) (Figure 3.2). The device comprises a rapidly rotating cone-shaped 3D printed titanium blade held above a stainless block with added liquid drawn between the blade and block and exiting at the top of the blade. Operation of the device is simple with solutions continuously pumped into the base where they are dispelled outwards by the rapidly rotating polished titanium blade. As the blade rotates, the internal fins on the blade force the liquid outwards into a tuneable gap between the rotor and base, ≥ 100 μm, where high shear stress is generated resulting in short diffusion path lengths for reactants (Britton et al., 2016). The thickness of the diffusion boundary layer is decreased by increased flow velocities in thin films (Selmi et al., 2017), modulated here by rotational speed. This inverse relationship leads to shorter response/reaction times, resulting in more efficient reactions. The fluid dynamics of the T^2FD are discussed in detail in the section 3.1.2.

This chapter presents the results obtained using T^2FD-intensified DT for a variety of dry and wet biomass feedstocks. Section 5.2 presents the results using pulverised soybean seed using the T^2FD in a continuous mode with methanol as a solvent and methanolic sodium hydroxide solution as the catalyst. The influence of catalyst concentration was studied in single factor experiments, while a two-factor design was applied to other operating parameters such as flow rate and rotational speed with catalyst concentration as a co-factor. The effect of ratio of soybean seed powder (biomass) to methanol was also investigated with catalyst concentration as a co-factor.

In section 5.3, we investigated the efficiency of the T^2FD processing platform for rapid DT of wet *Chloroparva pannonica* (Figure 3.2). The sensitivity of DT conversion efficiencies to processing parameters, such as catalyst concentration (NaOH in methanol (0 – 12%; wt./v), flow rate (1 – 5 mL/min), rotational speed (2,000 – 7,000 rpm) and the ratio of biomass to methanol (1:6 – 1:18) was systematically explored in triplicate, varying one parameter at a time. Through this optimisation, we were able to establish rapid, high conversion efficiencies to biodiesel from the wet feedstock at room temperature and atmospheric pressure.

Section 5.4 reports the outcomes of T^2FD-intensified DT of dry and wet fungal biomass operated in continuous mode at ambient temperature and pressure, using methanol as a solvent and sodium hydroxide as the catalyst. Effects of processing parameters such as the ratio of biomass to methanol, flow rate, rotation speed and the catalyst concentration were systematically investigated to optimize the process. Finally, energy requirements were estimated and compared to two step-dry biomass DT and single step wet biomass DT (Chopra et al., 2016).

5.2 Continuous direct biodiesel production from soybean seeds by micro-fluidic turbo thin film processing

5.2.1 Results and discussion

Soybean seed powder used in this experiment had a low total lipid content of 10.2 wt% (0.102 g total lipid g^{-1} biomass dry weight). In comparison, the reported total lipid content of commercial soy flakes was more than two-fold higher (22.6 wt% of dry weight basis) (Haas and Scott, 2007). Despite this, the FA profile obtained here was similar to reported profiles (Abdullah et al., 2017). The FA profile was dominated by linoleic acid (C18:2) and oleic acid (C18:1) at 39.2% and 20.3%, respectively. In contrast, the saturated fatty acids palmitic acid (C16:0) and stearic acid (C18:0) and the omega-3 fatty acid α-linolenic acid (C18:3) were more than two-fold lower with 8.9, 3.9 and 8.2 wt %, respectively, conforming to previous reports (Abdullah et al., 2017)

Quantified FAMEs obtained by the T^2FD-intensified DT using ^{1}H-NMR spectroscopy were compared to results obtained by traditional transesterification quantified by the GC/MS analysis (Knothe and Kenar, 2004). Using this method, C18:3 contents were overestimated by up to 2.2 mol% for most extraction conditions and were therefore excluded from further analyses. Total FA yields were on average 39.5 mol%, ranging from

35.6 to 53.9 mol%. This is slightly lower compared to FA yields obtained by the VFD- and T^2FD-intensified DT of *C. pannonica*, which achieved average yields of 41.5 and 42 mol% in a range of 38.3 to 49.5 and 39 to 44 mol%, respectively (see sections 5.3 and 5.4) (Sitepu et al., 2018a). Total FA extraction efficiency was 54.7% (including C18:3) or 42.3% (excluding C18:3), which is 14.0 or 26.4% lower than obtained for hexane extraction of soybean seed (Nikolić et al., 2009). This is low compared to 77.5% achieved with absolute ethanol extraction of soybean seeds at 40°C (Sawada et al., 2014). C18:2 yields were on average 76% lower (5.3 mol%) compared to 39.2 wt% obtained through traditional transesterification, with highest (~10 mol%) and lowest (2 mol%) obtained at a catalyst concentration of 1 and 0 wt/v%, a biomass to methanol ratio of 1:15 and 1:9, a flow rate of 3 mL/min and a rotational speed of 4,000 rpm, respectively. In contrast, average yields for C18:1 (~19 mol%) were only slightly lower compared to GC/MS determined contents (20.3 wt%), with highest and lowest yields of ~26.5 and 16.0 mol% achieved at a catalyst concentration of 1 wt/v%, a biomass to methanol ratio of 1:15 and 1:9, a flow rate of 3 mL/min and rotational speeds of 4,000 and 6,000 rpm, respectively. Extraction yields for C16:0 (~4.3 mol%) and C18:0 (~2.2 mol%) were ~50% of the contents determined by GC/MS (8.9 and 3.9 wt%, respectively), irrespective of operational conditions. Compared to fatty acid yields obtained with trichloroethylene by reflux, Soxhlet and Tilepape extraction yields for C18:2 were ~10-fold lower, less than half for C16:0 and C18:0. C18:1 extraction yields were, however, ~5% higher compared to reflux and Soxhlet, but ~8.5% lower compared to Tilepape achieved at a biomass to solvent ratio of 1:10 (Nikolić et al., 2009). Average extraction efficiencies of C18:2, C18:1, C16:0 and C18:0 were ~14 ± 0.2, 93 ± 1, 48 ± 0.3 and 56 ± 0.3%, respectively. This is 14, 90, 51 and 55% of average extraction efficiencies obtained by hot ethanol (70°C) extraction from soybean (99, 103, 94 and 102%, respectively) (Sawada et al., 2014). It needs to be emphasised though that the T^2FD-intensified DT is conducted at ambient temperature and pressure, saving on the energy costs required for hot extraction. The energy requirement for the T^2FD-assisted extraction is 2.44 kWh kg^{-1} biomass when operated at 4,000 rpm at a flow rate of 3 mL/min. In contrast, 35 kWh kg^{-1} biomass is required for lipid extraction using the conventional method of hexane extraction, which requires heating to 65°C (Sitepu et al., 2019). The impact of the very low extraction efficiency of C18:2, the major FA present in soybean seed, would require 7-times the biomass input, which is estimated to increase energy consumption to 17.3 kWh kg^{-1} when matching extraction achieved with absolute ethanol at 70°C. Thus in terms of energy requirement, the T^2FD-intensified DT of soybean seed powder is still over 2-fold lower. Complete future life cycle and techno-economic

modelling-based cost-benefit analyses of the T^2FD-assisted extraction, and similarly the VFD mediated extraction, and comparison to other methods, especially those that require heating, will be required to determine the cut off for minimal biomass oil content, extraction and conversion efficiencies.

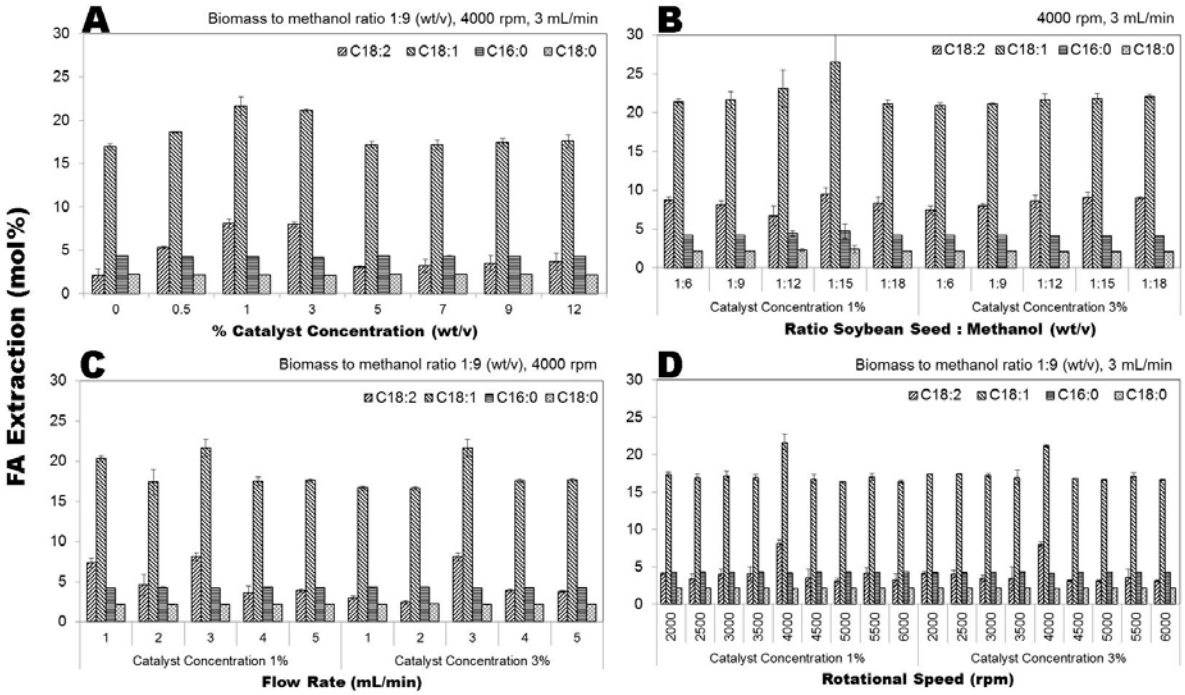

Figure 5.1. Effects of (A) catalyst concentration, (B) biomass to methanol ratio, (C) flow rate and (D) rotational speed on FA extraction of the continuous flow mode-operated, T^2FD-intensified DT of soybean seed powder. Experiments for B to D were performed at two catalyst concentrations of 1 and 3 wt/v% of sodium hydroxide in methanol.

5.2.1.1 Effect of catalyst concentration

All FA extraction yields were significantly affected by catalyst concentration due to higher yields obtained at catalyst concentrations of 0.5, 1 and 3 wt/v %, whilst yields at higher catalyst concentrations were similar to those achieved in the absence of the catalyst, as shown in Figure 5.1A. Many studies have shown that sodium hydroxide pre-treatment of plant biomass results in structural decomposition due to hydrolysis of hemicellulose and lignin, resulting in improved surface area and volume for reaction in the treated biomass (Harun and Geok, 2016). Similar to our results, a study using rice straw showed that concentrations of 6 and 12 wt/v % resulted in decreased solubilisation of cell wall materials (Harun and Geok, 2016). This was also shown for the extraction of polyhydroxybuturate (PHB) from *Alcaligenes latus*, a facultative anaerobic bacterium from vertebrate intestines, although at 100-times lower sodium hydroxide concentrations (Tamer et al., 1998). These outcomes were interpreted to be a result of optimal biomass to sodium hydroxide ratios

(Harun and Geok, 2016). Highest average C18:2, C18:1, C16:0, and C18:0 extraction efficiencies of 20.5 ± 1, 105 ± 3.5%, 48 ± 0.8, and 56 ± 0.9, respectively, were achieved at sodium hydroxide concentrations of 1 and 3 wt/v %, with yields ranging from 7.6 – 8.7, 21 – 23, 4.14 – 4.35, and 2.12 – 2.23 mol%, respectively (Figure 5.1A).

Numerous studies demonstrated that FA transesterification is minimal in the absence of a catalyst (Kasim et al., 2010). T^2FD-intensified DT on microalgal and fungal biomass, achieved conversion efficiencies of 7.6% and 1.6%, respectively, in the absence of the catalyst of sodium hydroxide, the latter being similar to this study of soybean seeds (~1%) (see sections 5.3 and 5.4). Conversion efficiencies increased 15- and 11-fold, respectively, at 0.5 wt/v % of catalyst (Sitepu et al., 2018a, Sitepu et al., 2019). As methanol is a poor solvent for lipid extraction, the catalyst has a dual action, namely disruption of intracellular cell structure thereby releasing lipids, and catalysis of the transesterification of FAs to FAME (Abo El-Enin et al., 2013). Homogenous base catalysts have shown higher catalytic activity in the DT process compared to heterogeneous catalysts (Kasim et al., 2010, Go et al., 2016, Sitepu et al., 2018a, Sitepu et al., 2019). The VFD-intensified DT of *C. pannonica* biomass achieved a conversion efficiency of 66% using sulphuric acid, while the use of sodium hydroxide as a catalyst achieved a conversion efficiency of 95% (chapter 4) (Sitepu et al., 2018a). Therefore, sodium hydroxide was used as a catalyst in the T^2FD-intensified DT of soybean seed powder for biodiesel production.

The effect of sodium hydroxide concentration in methanol (0 – 12 wt/v %) was determined for the continuous flow-operated T^2FD-intensified DT of soybean seed powder at a ratio of biomass to methanol of 1:9 (wt/v), a flow rate of 3 mL/min and a rotational speed of 4000 rpm (Figure 5.2A). FA to FAME conversion efficiency increased 107-fold at 0.5 wt/v % of sodium hydroxide in methanol compared to that of the non-catalyst condition, and increased 1.3-fold further as the catalyst concentration increased to 1 wt/v %. Higher catalyst concentrations had no further effect on FA to FAME conversion efficiencies. Therefore, catalyst concentrations of 1 and 3 wt/v % were chosen to examine the effects of other processing and operating parameters.

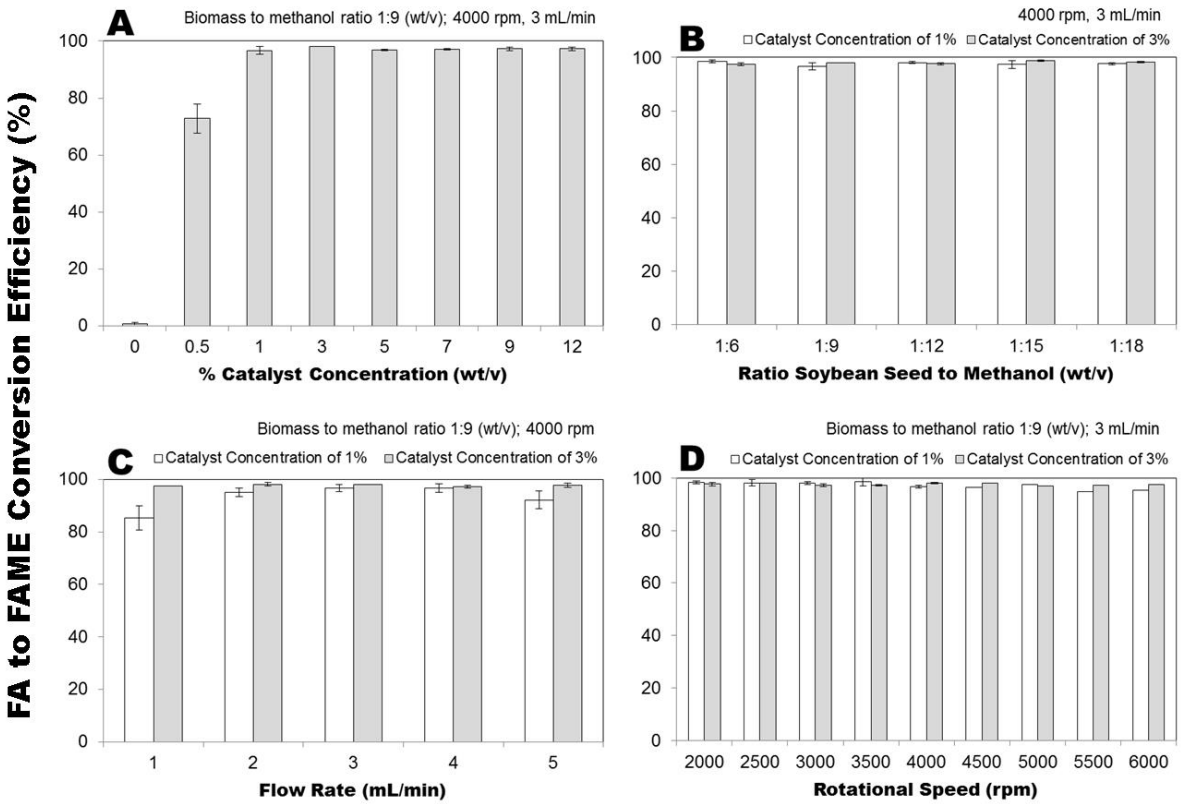

Figure 5.2. Effects of (A) catalyst concentration, (B) biomass to methanol ratio, (C) flow rate and (D) rotational speed on FA to FAME conversion efficiency of continuous flow mode-operated T^2FD-intensified DT of soybean seed powder. Experiments for B to D were performed at two catalyst concentrations of 1 and 3 wt/v % of sodium hydroxide in methanol.

5.2.1.2 Effect of biomass to methanol ratio

Oil to methanol molar ratio used in conventional transesterification processes is 1:3, while higher ratios are required in DT processes (Sitepu et al., 2018a). This is partially due to the low solubility of lipids in methanol, but also for complete immersion of the biomass, as well as for structural destabilisation of cell walls (Kasim et al., 2010, Sitepu et al., 2018a). For example, a biomass to methanol ratio of 1:10 (wt/v) was used in the DT of *Nannochloropsis salina* biomass (Kim et al., 2015b). For oil extraction from soybean seed, except when the methanol was replaced with other solvents (Nikolić et al., 2009), use of larger volumes of methanol requires evaporation of the solvent which can be achieved in a cost-effective manner, due to the low boiling point of methanol (Kasim et al., 2010). Based on previously published biomass to methanol ratios, a ratio range of 1:6 to 1:18 (wt/v) was investigated for FA extraction and FA to FAME conversion efficiency at a flow rate of 3 mL/min and a rotational speed of 4,000 rpm.

Biomass to methanol ratio had no significant effect on FA extraction yields (Figure 5.1B) or - efficiency for C18:1, C16:0 and C18:0, showing average extraction yields and efficiencies of 22 ± 2.2, 4.2 ± 0.3 and 2 ± 0.2 mol% and 109 ± 11, 47.5 ± 3.6 and 55.4 ± 4%, respectively. In contrast, a significant effect of biomass to methanol ratio ($p < 0.01$), but not catalyst concentration, was determined for the T^2FD-assisted extraction of C18:2, which also showed significant interaction of biomass to methanol ratio with catalyst concentration ($p < 0.02$). A Tukey post hoc analysis determined that the significance on yields and extraction efficiency was driven by a biomass to methanol ratio of 1:15 wt/v, at a catalyst concentration of 1 wt/v %, being significantly lower (7 ± 1 mol% and 17 ± 3%, respectively) compared to highest extraction yields and efficiencies at a biomass to methanol ratio of 1:15 and 1:18 wt/v at a catalyst concentration of 3 wt/v % and 1:18 wt/v at a catalyst concentration of 1 wt/v % (average of 8.5 ± 0.9 mol% and 23 ± 1.5%, respectively) (Figure 5.1B) (Table 2. Appendix section 5.2.). Similar to the results obtained here, biomass to methanol ratio also had no significant effect on the T^2FD-assisted C18:1 extraction of fungal biomass (see section 5.4) (Sitepu et al., 2019). The T^2FD-assisted extraction of C18:1 from soybean seed powder is in accordance with results obtained in confined mode-operated the VFD-assisted FA extraction of *C. pannonica* biomass, which biased extraction in favour of C18:1 (see chapter 4) (Sitepu et al., 2018a). Unlike the results obtained here, C18:1 extraction efficiencies decreased from 81 to 64% in the continuous flow-operated VFD-assisted extraction at a flow rate of 5 mL/min and a biomass to methanol ratio of 1:10 wt/v at the same catalyst concentration of 3 wt/v % (Sitepu et al., 2018a). This difference in outcomes could be due to device-specific interactions with the biomass or the extractability of C18:1 from different biomass sources. For C16:0, extraction efficiency was 14.5 to 20.5% lower compared to the VFD-assisted extraction of *C. pannonica* operating under continuous flow at a flow rate of 0.2 mL/min and biomass to methanol ratios of 1:12 and 1:8, respectively. In addition to biomass effects, this difference could be due to the 15-times slower flow rate used in the VFD, suggesting that slower flow rates should be explored for the T^2FD for biomass where C16:0 is a major FA, and this will be featured in future studies.

In contrast to the effects on C18:2 extraction yields and efficiency, soybean seed powder to methanol ratio had no significant effect on FA to FAME conversion efficiency using the T^2FD-intensified DT, achieving >96% at both catalyst concentrations. Biomass to methanol ratio also had no significant effect on FA to FAME conversion efficiencies in the T^2FD-intensified DT of fungal or microalgal biomass or the continuous mode-operated VFD-

intensified DT of microalgal biomass, achieving conversion efficiencies of more than 90% (see section 5.4) (Sitepu et al., 2018a, Sitepu et al., 2019). Therefore, to investigate effects of other operational parameters on FA extraction yields and efficiencies and FA to FAME conversion efficiency, a ratio of 1:9 was chosen, as this was the lowest amount of methanol required for producing a homogeneous mixture for delivery to the T^2FD.

5.2.1.3 Effect of flow rate

Continuous flow operation requires investigation on the effect of flow rate on biodiesel production, as it affects contact times of reactants. A positive correlation between increased biodiesel yields and prolonged residence time has been demonstrated to result in increased biodiesel yields and purity (Boon-anuwat et al., 2015). Increased residence time in continuous reactors, however, also results in higher energy consumption, which increases further at elevated operating temperature (Britton et al., 2016). Therefore, developing scalable, fast and reliable continuous reactors that give high quality biodiesel yield at ambient temperature and pressure would decrease total biodiesel production cost. Therefore, the effect of flow rate (1 to 5 mL/min) was investigated for the T^2FD-intensified DT of soybean seed powder to biodiesel at a biomass to methanol ratio of 1:9, and a rotational speed of 4,000 rpm at the two different catalysts concentrations of 1 and 3wt/v %.

Flow rate had a significant effect on extraction yields of C18:2, C18:1, C16:0 and C18:0 ($p < 0.001$), showing significant interaction with catalyst concentration. In contrast to a significant effect of catalyst concentration on extraction yields of C18:2 and C18:1, no significant effect was determined for C16:0 and C18:0. C18:2 extraction efficiencies were 18 ± 4% vs 3.4 ± 0.6 mol% and 8.7 ± 1.7%, respectively, at flow rates of 1 and 3 mL/min for a catalyst concentration of 1 wt/v%, and at 3 mL/min for a catalyst concentration of 3 wt/v% (Figure 5.1C). This led to significant effects of flow rate and interaction of flow rate and catalyst concentration (Tukey post hoc) (Table 2 Appendix Section 5.2). This is similar to results obtained for the T^2FD-assisted FA extraction of fungal biomass (section 5.4), where higher flow rates (8-10 mL/min) resulted in decreased C18:2 extraction efficiency at a catalyst concentration of 1 wt/v % (Sitepu et al., 2019). In contrast to a ~100% extraction efficiency of C18:2 in the T^2FD-assisted processing of fungal biomass (Sitepu et al., 2019) (section 5.4), extraction efficiencies of C18:2 were low for soybean seed powder, which has also been reported for both VFD- (chapter 4) and T^2FD-assisted extractions from *C. pannonica* (below detection limit) (section 5.3) (Sitepu et al., 2018a). Flow rate and

catalyst concentration had a similar effect on C18:1 extraction yields (Figure 5.1C) and efficiency, being 22 and 23% higher (21. 6 ± 1 mol% and 107 ± 4% vs 17.7 ± 1.2 mol% and 86.7 ± 6%, respectively) at a flow rate of 3 mL/min and catalyst concentrations of 1 and 3 wt/v %. In contrast, although statistically significant (Table 2 and 3 Appendix Section 5.2), extraction yields and efficiencies of C16:0 and C18:0 were only slightly higher at a flow rate of 4 mL/min and a catalyst concentration of 1 wt/v % and flow rates of 1, 2 and 5 mL/min at a catalyst concentration of 3 wt/v % (4.3 ± 0.03 and 2.2 ± 0.02 vs 4.2 ± 0.05 and 2.2 ± 0.02 mol% (Figure 5.2C) and 48.4 ± 0.4 and 56.5 ± 0.4 vs 47.7 ± 0.6 and 56 ± 0.9%, respectively), whilst they were not significantly different at a flow rate of 4 mL/min and a catalyst concentration of 3 wt/v %. In contrast to the T^2FD-assisted FA extraction of fungal biomass, where increased flow rates positively correlated with extraction efficiency of C18:1 (Sitepu et al., 2019) (section 5.4), improved extraction efficiencies were only achieved at lower flow rates for the T^2FD-assisted FA extraction of soybean seed powder, which is similar to results obtained for T^2FD- and VFD-assisted extractions from *C. pannonica* biomass (section 5.3 and chapter 4, respectively) (Sitepu et al., 2018a). The choice of flow rate had no significant effect on extraction efficiency of C16:0 from soybean seed powder, a situation mirrored in T^2FD- and continuous mode-operated VFD-assisted extraction from *C. pannonica* (Sitepu et al., 2018a) (section 5.3 and chapter 4, respectively), yet a positive correlation with extraction efficiency was demonstrated for fungal biomass (Sitepu et al., 2019). Taken together with outcomes for C18:2 extraction efficiencies, this suggests that there are differences in accessibility for methanol and/or the catalyst for reacting with C18:2 and C16:0 between plant and fungal biomass. Extraction efficiency for C18:0 could not be determined for microalgal biomass because of a low content (0.7 wt%) but also not for the fungal biomass despite being present in significant amounts (23.9 wt%), due to algorithm-based overestimation of total saturated fatty acid content (Sitepu et al., 2019).

FA to FAME conversion efficiency showed a parabolic response to flow rates for a catalyst concentration of 1 wt/v %, increasing from 85.2% ± 4.6 to 96.6% ± 1.5 for flow rates of 1 to 4 mL/min, before decreasing slightly for a flow rate of 5 mL/min. In contrast, changing the flow rate did not have significant effect on the FA to FAME conversion efficiency at a catalyst concentration of 3 wt/v %. This result was consistent with the previous research on the T^2FD-intensified DT of fungal and microalgal biomass (sections 5.4 and 5.3, respectively), as well as for the continuous mode-operated VFD-intensified DT of *C.*

pannonica (chapter 4) (Sitepu et al., 2018a, Sitepu et al., 2019). At low flow rates, residence time is increased and is mainly driven by rotational speed (Sitepu et al., 2019).

5.2.1.4 Effect of rotational speed

Homogeneous plant material mixtures and agitation are required for effective reactant contact for transesterification (Skorupskaite et al., 2016). For example, DT of *Spirulina plantesis* biomass yielded no biodiesel production without stirring, while it increased significantly at a stirring speed of 650 rpm (El-Shimi et al., 2013). In thin film microfluidic devices, like the T^2FD and VFD, mixing and biomass disruption is achieved by the rotational speed of either the blade or tube (chapter 3) (Sitepu et al., 2018a, Sitepu et al., 2019). For example, increasing rotational speed affected the FA to FAME conversion efficiency in the VFD-intensified DT of *C. pannonica* biomass operated in confined mode (chapter 4). The reactant film along the VFD tube becomes thinner with increasing rotational speed, simultaneously providing a larger contact area between the reactant and higher shear stress (Sitepu et al., 2018a).Therefore, the effect of rotational speed on FA yields and extraction efficiencies, as well as FA to FAME conversion efficiencies was investigated for the T^2FD-intensified DT of soybean seed powder at catalyst concentrations of 1 wt/v % and 3 wt/v %, a biomass to methanol of 1:9 and a flow rate of 3 mL/min.

Rotational speed had a significant effect on extraction yields (Figure 5.1D) and efficiencies of C18:2, C18:1, C16:0 and C18:0, which was driven by higher FA extraction yields and efficiencies at 4,000 rpm, at both catalyst concentrations for C18:2 and C18:1, but marginally lower outcomes for C16:0 and C18:1 under these operational conditions. For these parameters, FA extraction yields and efficiencies were more than two-fold higher for C18:2 (8 ± 0.4 mol% and 20.5 ± 1% vs 3.6 ± 0.7 mol% and 9.2 ± 1.8%, respectively), while they were only 26 and 10% higher for C18:1 (21.5 ± 0.7 mol% and 94.5 ± 14% vs 17 ± 0.5 mol% and 86 ± 8%, respectively). These results are similar to those obtained for C18:2 FA extraction efficiency from the T^2FD-intensified fungal biomass processing, at a catalyst concentration of 3 wt/v %, while a catalyst concentration of 1 wt/v % achieved 100% at 2,500 rpm which was maintained at higher rotational speed levels (section 5.4) (Sitepu et al., 2019). These results mirror outcomes obtained in the T^2FD-processed biomass of *C. pannonica* and *M. plumbeus* (sections 5.3 and 5.4) (Sitepu et al., 2018a, Sitepu et al., 2019), while the continuous flow VFD-processed extraction outcomes were poor (chapter 4) (Sitepu et al., 2018a). In contrast, although statistically significant, these operational

conditions led to only a marginal decrease of 3 and 0.7% on extraction yields and efficiencies for C16:0 and C18:0, respectively (4.3 ± 0.03 mol% and 48.3 ± 0.9% vs 4.2 ± 0.04 mol% and 48 ± 0.65%, respectively and 2.2 ± 0.02 mol% and 56.3 ± 1.02% vs 2.1 ± 0.02 mol% and 56 ± 0.75%, respectively).

Rotational speed had no significant effect on FA to FAME conversion efficiency at a catalyst concentration of 3 wt/v %, achieving conversion efficiency routinely at 97% (Table 3 Appendix Section 5.2). While it decreased slightly with increasing rotational speed exceeding 3,500 rpm for a catalyst concentration of 1 wt/v %, 98.5% was achieved at a rotational speed of 3,500 rpm (Figure 5.2D). Similarly, a significant effect of rotational speed on FA to FAME conversion efficiency was determined for the T^2FD-intensified DT of *M. plumbeus* biomass at a catalyst concentration of 1 wt/v % and no significant effect was determined at a catalyst concentration of 3 wt/v % (section 5.4) (Sitepu et al., 2019), the latter being also the case for the VFD-assisted DT of *C. pannonica* (chapter 4) (Sitepu et al., 2018a). In contrast, a catalyst concentration of 1 wt/v % had no significant effect on FA to FAME conversion efficiency in the T^2FD-intensified DT of *C. pannonica* (section 5.3) (Sitepu et al., 2018a).

5.2.2 Conclusion

Catalyst concentration, biomass to methanol ratio, flow rate and rotational speed had a significant effect on FA extraction yields/efficiencies using the T^2FD, but FA to FAME conversion efficiency was only significantly affected by catalyst concentration, being highest at 1 and 3 wt/v %, and flow rate, being highest at a catalyst concentration of 1 wt/v % at 4 mL/min, achieving 98 and 96%, respectively. Highest FA extraction yields between 49 and 54 mol%, including and excluding C18:3 extraction, were achieved at a biomass to methanol ratio of 1:15 wt/v, a catalyst concentration of 1 wt/v %, a flow rate of 3 mL/min and a rotational speed of 4,000 rpm. While methanol requirements are 33% higher than in the conventional DT, the required sodium hydroxide concentrations are 66% lower. Higher methanol consumption is less of an issue, due to cost-effective recovery and reuse options, but the recovery of the catalyst is problematic, adding additional cost and generating large amounts of waste water (Nasreen et al., 2018). Based on estimated energy consumption (Sitepu et al., 2018a), the T^2FD-intensified DT of soybean seed operated in the continuous flow mode can replace the traditional two-step biodiesel production, despite low extraction efficiency of the dominant fatty acid C18:2. The low extraction efficiency of the polyunsaturated fatty acids could also be desirable with regards

to biodiesel standards for cetane number, iodine values and oxidative stability of the biodiesel (Islam et al., 2015a).

5.3 Continuous flow biodiesel production from wet microalgae using a hybrid thin film microfluidic platform

5.3.1 Results and discussion

Similar to data obtained for *C. pannonica* wet biomass processing using the VFD (chapter 4) (Sitepu et al., 2018a), C18:2 was not extracted and extraction of C18:0 was not quantifiable due to low biomass contents; extraction efficiencies for the remaining main fatty acids were similar (~39-44%), as were fatty acid to fatty acid methyl ester conversion efficiencies for optimized parameters (≥90%). Catalyst concentration had a significant effect on fatty acid extraction and FA to FAME conversion efficiencies (Table 4 and 5 Appendix Section 5.3) (due to negative effects at 12 and 0 wt./v %, respectively (Figure 5.3A). As expected, increasing the catalyst concentration from 0% to 0.5% resulted in an increase in FA to FAME conversion efficiencies, from 7.6% to 84.0%. We note that 50 and 100% FA to FAME conversion efficiencies were reported for the DT of wet *Pavlova lutheri* (60 °C, 2% NaOH over 4h) (Álvarez et al., 2017) and *Chlamydomonas* biomass (microwave-assisted, 0.25% NaOH, 15 min) (Chen et al., 2015), respectively. In the present work we achieved a marked improvement in efficiency with high conversion in the T^2FD device at room temperature for a short residence time of < 1 min. Improved FA to FAME conversion efficiencies due to inclusion of the catalyst NaOH were also achieved for rape seed, as the catalyst breaks the seed wall, facilitating access of methanol to membrane and intracellular lipids (Abo El-Enin et al., 2013).

In the continuous flow operated T^2FD device, flow rate and rotational speed are important factors governing reaction time for FAME formation. A fast flow rate will result in a shorter residence time and thus a shorter reaction time. While flow rate had no significant effect on FA extraction efficiency, the slowest flow rate of 1 mL/min resulted in significantly reduced FA to FAME conversion efficiency (74% ± 8.5), while 3 mL/min was optimal (94.01 ± 1.19), but not significantly different to 2, 4 and 5 mL/min (Figure 5.3B). Although a slow flow rate increases reaction time, evaporative loss of methanol from the thin film in the T^2FD at the high rotational speed (6,000 rpm) could have limited dissolution of the lipid. At a catalyst concentration of 1%, a rotational speed of >5,500 rpm yielded slightly lower FA extraction

efficiencies, while FA to FAME conversion efficiencies were negatively affected at 5,000, 5,500 and 7,000 rpm (Figure 5.3E).

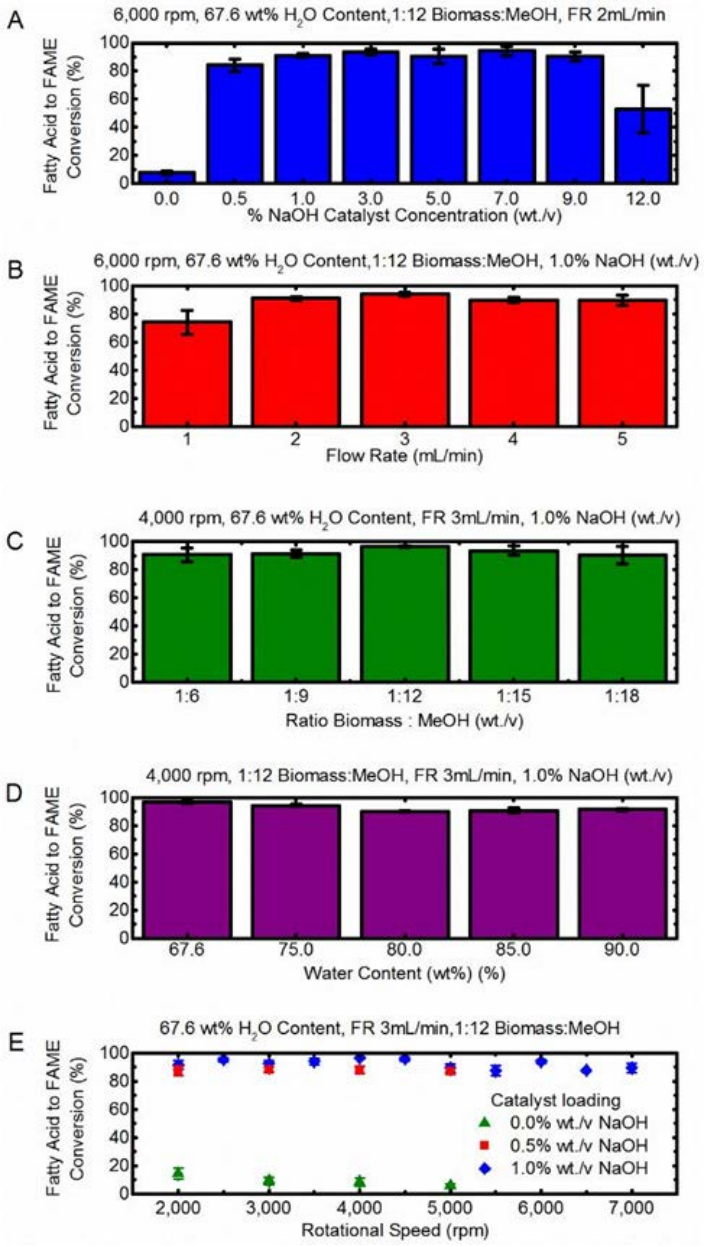

Figure 5.3. Effect of processing parameters on FA to FAME conversion efficiencies for DT of T^2FD-processed wet biomass of *C. pannonica*: (A) catalyst concentration; (B) flow rate (FR); (C) ratio biomass to methanol, (D) water content; and (E) rotational speed at various catalyst concentrations. Error bars represent standard deviation of 3 independent replications.

High rotational speed corresponds to shorter residence time and higher evaporation rates of methanol, both of which are likely to reduce the conversion efficiency. Consequently, the effect of biomass to methanol ratio was investigated at 4,000 rpm, as methanol acts both as a reactant and solvent in the DT process.

Fatty acid extractions as well as FA to FAME conversion efficiencies (Figure 5.2C) were optimal at a biomass to methanol ratio of 1:12. This result is similar to the optimal biomass to methanol ratio reported for DT of wet biomass of *Nannochloropsis oceanica* (1:13) (Yu et al., 2015). Lower efficiencies at higher methanol concentrations could be due to lower concentrations of catalyst while lower methanol concentrations could restrict accessibility of methanol to the fatty acids (Yu et al., 2015). Therefore, the ratio of biomass to methanol of 1:12 (wt./v) was selected for subsequent experiments.

To assess the combined dependence of catalyst concentration and rotational speed on conversion efficiency, we investigated a range of rotational speeds between 2,000-5,000 rpm for additional catalyst concentrations of 0 and 0.5% (see Figure 5.3E). Extraction efficiency of C18:3 and C16:0 were significantly affected by catalyst concentration, while C18:1 was affected by rotational speed. Highest extraction efficiencies of extractable FAs of 48-50% were achieved without catalyst. Likewise, catalyst concentration, but not rotational speed affected FA to FAME conversion efficiency, with 0% catalyst concentration having a significant negative effect. At 0% catalyst concentration, FA to FAME conversion efficiencies decreased as rotational speed increased, with the highest conversion of only 14.4% ± 3.9 observed for 2,000 rpm, while they were 87-89% at 0.5%. Vortex mixing under similar conditions (excluding flow rate, due to the operation being restricted to a confined mode, and rotational speed, which is not selectable) served as a control. After 5 min, no FA to FAME conversion occurred, demonstrating that vortex-induced mixing alone did not support DT of wet microalgae biomass.

For DT processing using an alkaline catalyst, an excess of water contained in the biomass could lead to saponification, which would lower the catalyst concentration, resulting in low FA to FAME conversion efficiencies (Ma and Hanna, 1999). However, it is necessary to eliminate the dewatering process in microalgae biodiesel production, as this process is high in energy consumption. As expected, the water content had a significant effect on extraction efficiencies of extractable FAs, and FA to FAME conversion (Figure 5.3D), which were negatively affected by increasing the water content.

We have demonstrated herein that a high conversion yield of 96.6 ± 0.7 occurred using wet biomass containing 67.7% water. But what happens if the water content is higher? To this end the wet biomass was first mixed with water (ratio biomass to water of 1:6, wt./v) before being delivered into the T^2FD, at a fixed flow rate of 3 mL/min while the flow rate of methanol containing 1% catalyst was varied from 3 to 6 mL/min (Figure 5.4). The biodiesel

conversion increased with an increase in the amount of methanol in the T^2FD, to 81.9% ± 1.8 for a flow rate of methanol of 6 mL/min. Thus raising the amount of methanol in the T^2FD can significantly reduce the effect of water, and overall, it is possible to produce biodiesel directly from a suspension of microalgae.

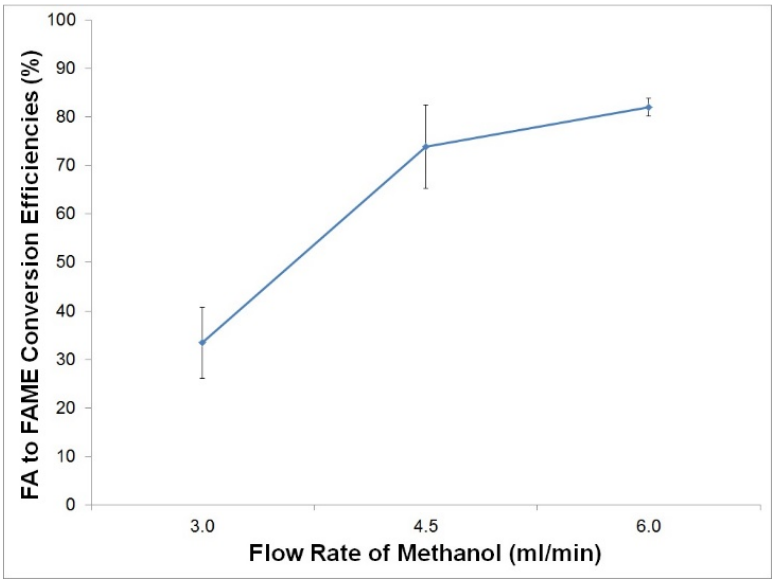

Figure 5.4 Effect of water on the formation of biodiesel from 2 g of wet biomass mixed with water (ratio biomass to water of 1:6, wt./v), flow rate of biomass in water 3 mL/min, catalyst concentration 1% and rotation speed 4,000 rpm. Error bars represent standard deviation taken from 3 individual experiments.

In conclusion, the new hybrid T^2FD microfluidic platform is effective in rapidly producing biodiesel directly from wet biomass of the microalga *Chloroparva pannonica*. The maximum biodiesel conversion yield of 96.6% ± 0.7 was obtained at room temperature and atmospheric pressure with a short residence time (< 1 min). The results establish that the high shear processing in the T^2FD is effective in enhancing DT of microalgae biomass even for a relatively high concentration of water, with the amount of methanol present playing a key role in the DT process. This T^2FD-mediated DT of wet biomass offers a novel and efficient way of producing biodiesel. Moreover, the rapid high conversion yield of direct biodiesel production using T^2FD at room temperature opens the possibility of economically feasible production of biodiesel.

5.4 Turbo thin film continuous flow production of biodiesel from fungal biomass

5.4.1 Results and discussion

The total fatty acid content of the *M. plumbeus* biomass was 25 ± 1.2% of its dry matter, composed of 41 ± 0.1 of saturated fatty acid (SFA), 43% of monounsaturated fatty acid

(MUFA) and 16 ± 0.1% of polyunsaturated fatty acids (PUFA). Unsaponifiable compounds such as tocopherol and sterols were not detected in the fungal oil, while saponifiable compounds composed of free fatty acid (56%), monoacylglycerols (2%), diacylglycerols (18%), and triacylglycerols (24%) were obtained. Based on GC/MS analyses of FAMEs after conventional extraction and transesterification, the fatty acid profile was dominated by oleic acid (C18:1; 43 ± 0.03%), followed by stearic acid (C18:0; 24 ± 0.1%), the ω-6 fatty acid linoleic acid (C18:2; 15 ± 0.1%), and palmitic acid (C16:0; 13 ± 0.1). In contrast, α-linolenic acid (C18:3n-3) and myristic acid (C14:0) were presented at very low levels (0.02 ± 0.002 and 0.3%, respectively). Other fatty acids presented at <2% of the total fatty acids were C12:0, C15:0, C20:0, C16:1(n-7) and C18:1(n-7), and the long-chain fatty acids C22:0, C24:0, C20:1(n-9), C20:2, C22:4(n-6) and C22:6(n-3) (docosahexaenoic acid, DHA).

5.4.1.1 Effect of catalyst concentration on conventional direct transesterification and turbo thin film device-intensified direct transesterification of Mucor plumbeus biomass

Catalyst concentration had a significant effect on the extraction of C18:2, C18:1 and C16:0 (Figure 5.5A). Extraction of C18:2 was significantly lower at 0 and 5 wt./v % of the catalyst, achieving extraction efficiencies of only 27 ± 5 and 87 ± 2%, respectively, whilst high catalyst concentrations led to 100% extraction efficiencies (Table 1 Appendix Section 5.4). In contrast, C18:1 was completely extracted in the absence of the catalyst, and extraction efficiencies ranged between 83 ± 2 and 90 ± 0.3 for the other catalyst concentrations, being lowest at catalyst concentrations of 9 wt./v %. Extraction efficiencies for C16:0 behaved similarly, and catalyst concentrations of 7 and 9 wt./v % resulted in reduced extraction efficiencies of 91 ± 2 and 88 ± 2, respectively. At catalyst concentrations < 5 wt./v %, the algorithm overestimated extractions of C16:0 by 3 to 58% (e.g. at catalyst concentrations of 0.5 and 1 wt./v % calculated extraction efficiencies were 159 ± 0.3 and 152 ± 2%, respectively). The amount of saturated fatty acids is derived by difference (e.g. 100% - amount of quantified unsaturated fatty acids), which is then multiplied by empirically established factors for C18:0 and C16:0 (Knothe and Kenar, 2004), which could explain these overestimations, being 27% for total saturated fatty acids compared to GC/MS quantified amounts. In addition, differences in the molecular weights of the fatty acids have been attributed to an overestimation of saturated fatty acids (mol%) compared to GC-derived wt% quantification (Sedman et al., 2010). As C16:0 was overestimated for all parameter settings, no further analyses or quantifications are shown.

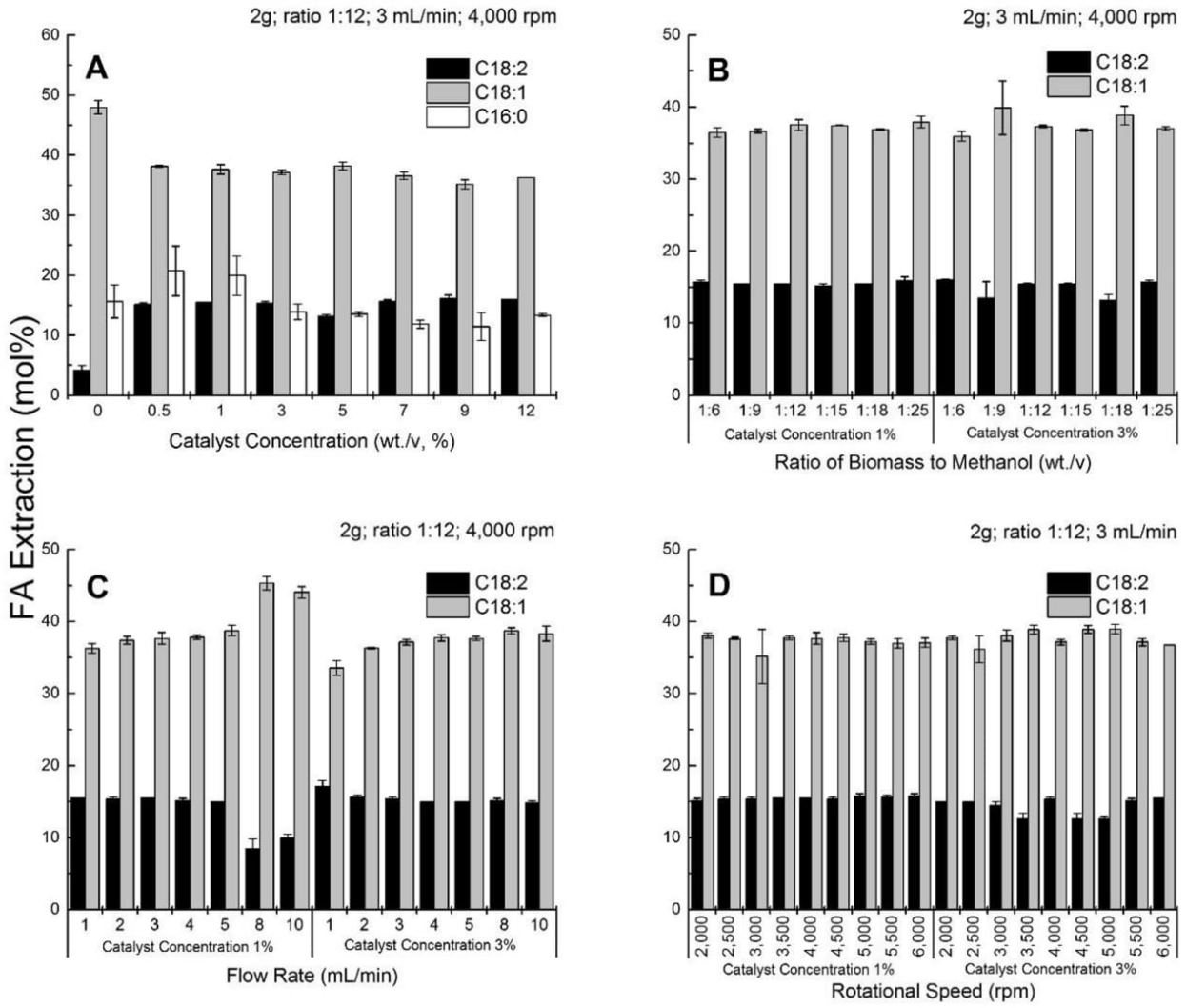

Figure 5.5 Effect of (A) catalyst concentration (NaOH) on fatty acid extraction efficiency (mol%) of T^2FD-intensified DT of *M. plumbeus* biomass operated in continuous mode. Fatty acid extraction was then investigated at catalyst concentrations of 1 and 3% (wt./v) for (B) variable biomass to methanol ratios, (C) flow rates, and (D) device rotational speed. Error bars represent SD; n = 3.

A homogenous base catalyst has greater catalytic activity than that of an acid catalyst in a transesterification reaction (Ma and Hanna, 1999). However, soap formation spontaneously occurs when the oil/biomass contains free fatty acids. Soap formation reduces the FA to FAME conversion yields and increases the cost of downstream biodiesel processing (Kasim and Harvey, 2011). In fact, in a control experiment, no conversion of FA to FAME was detected when *M. plumbeus* was directly processed using a conventional method (Thliveros et al., 2014) with 4 wt./v % sodium hydroxide as a catalyst, a biomass to methanol ratio of 1:20, and reaction temperature of 50 $^{\circ}$C for a reaction time of 10 h. In contrast, in another control experiment using sulphuric acid at 4 v/v % at the same biomass to methanol ratio, a reaction time of 6 h at 60 °C, quantification of ^{1}H-NMR spectra integration yielded a FA to FAME conversion efficiency of ~98 ± 0.3.

This suggests that the base catalyst under conventional DT operation induced saponification of fatty acids, whilst this did not occur using the acid catalyst (Kakkad et al., 2015a). However, this phenomenon did not arise when using the T^2FD, even at a base catalyst concentration of 12 wt./v % under continuous operation. Our previous studies using microalgal *Chloroparva pannonica* biomass containing 43% of free fatty acid, using either VFD (chapter 4) (Sitepu et al., 2018a) or T^2FD thin film microfluidic platforms (section 5.3) (Sitepu et al., 2018b), showed that saponification did not occur at low concentrations of sodium hydroxide. The FA to FAME conversion efficiencies for both studies decreased at high concentrations of the base catalyst, suggesting saponification did occur at excess sodium hydroxide concentrations (Sitepu et al., 2018a). Based on these studies, the effect of sodium hydroxide was analysed at concentrations from 0 to 12 wt./v % in the T^2FD for dry *M. plumbeus* biomass, which also contained high free fatty acids. Sodium hydroxide concentrations of ≥ 1 wt./v % in methanol achieved ≥ 90% FA to FAME conversion efficiencies using T^2FD-intensified DT of the fungal biomass, which were, however, significantly reduced at low catalyst concentrations (Table 2 Appendix Section 5.4). This is similar to T^2FD-intensified DT of *C. pannonica* biomass (section 5.3) (Sitepu et al., 2018a), while concentrations lower than 1 wt./v % base catalyst was not examined in the VFD-intensified DT of the algal biomass (Sitepu et al., 2018a). Based on these results, sodium hydroxide concentrations were set at 1 and 3 wt./v % in experiments investigating the interactive effects of both concentrations with the ratio of biomass to methanol, flow rate, and rotation speed (Figures 5.6A - C).

Figure 5.6 Effect of (A) variable biomass to methanol ratios, (B) flow rates and (C) rotational speed on FA to FAME conversion efficiency (%) of T^2FD-intensified DT of *M. plumbeus* biomass at catalyst concentrations of 1 and 3% operated in continuous mode. Error bars represent SD; n = 3.

5.4.1.2 Effect of biomass to methanol ratio on turbo thin film device-intensified direct transesterification of Mucor plumbeus biomass at catalyst concentrations of 1 and 3 wt./v %

The effect of biomass to methanol ratio on T^2FD-intensified fatty acid extraction (Figure 5.5B) and FA to FAME conversion efficiencies of *M. plumbeus* biomass (Figure 5.6A) was investigated at five different ratios in the presence of 1 and 3 wt./v % of the base catalyst at room temperature with a flow rate of 3 mL/min and a rotational speed of 4,000 rpm. Methanol is regarded to be a poor solvent for lipids, as the solubility of triglyceride in methanol is very low, i.e. an extraction of only 9% compared to hexane was demonstrated (Zeng et al., 2009). In DT, however, methanol acts both as an extraction solvent and a reactant (Kasim et al., 2010). Biomass to methanol ratio had no significant effect on C18:1 extraction, with efficiencies ranging from 84 ± 2 to 92 ± 3%, irrespective of the catalyst concentration (Table 1 Appendix Section 5.4). Biomass to methanol ratio did also not

greatly affect the extraction of C18:2, but a significantly lowered the extraction efficiency from 100% for other conditions to 87 ± 5% for a ratio of 1:18 at a catalyst concentration of 3 wt./v (Table 2 Appendix Section 5.4).

As mentioned above, excess methanol is necessary to drive the extraction and FA to FAME conversion in DT applications. FA to FAME conversion efficiencies were >90%; except for a biomass to methanol ratio of 1:25 at a base catalyst concentration of 1 wt./v %, (Figure 5.5A), demonstrating efficient conversion to biodiesel under continuous T^2FD operation. This is similar to VFD- and T^2FD-intensified FA to FAME conversion efficiencies of *C. pannonica* biomass for the similar biomass to methanol ratio range investigated (1:6 to 1:18) (chapter 4 and section 5.3) (Sitepu et al., 2018a).

5.4.1.3 Effect of flow rate

One of the main factors affecting FA extraction and FA to FAME conversion efficiencies is reaction time (batch processing) or residence time (flow rate in continuous flow devices) (Britton et al., 2016). At flow rates of 1-10 mL/min and catalyst concentrations of 1 and 3 wt/v %, extraction yields for C18:2 and C18:1 ranged from 9 ± 1 to 17 ± 1 and 34 ±1 to 45 ± 1 mol% (Figure 5.5C) with extraction efficiencies of 56 ± 9 to 100 and 80 ± 2 to 100%, respectively. A factorial ANOVA determined a significant effect of the catalyst concentration and flow rate on T^2FD extraction of C18:2, C18:1 and C16:0 from *M. plumbeus* biomass (Table 1 Appendix Section 5.4), and a significant interaction of catalyst concentration with flow rate. A Tukey post hoc analysis determined that the significance was driven by low extractions of C18:2 at flow rates of 8 and 10 mL/min at a catalyst concentration of 1 wt./v %, achieving extraction efficiencies of only 56 ± 9 and 66 ± 3% (Table 1 Appendix Section 5.4). Likewise, the same parameters were the main drivers of significance of extraction of C18:1, but here highest extraction efficiencies of 107 ± 2 and 104 ± 2% were achieved. A catalyst concentration of 3% at a flow rate of 1 mL/min also had a significant effect on the extraction of C18:2 and C18:1, but resulted in the highest and lowest yields of 17 ± 1 and 34 ± 1 mol%, respectively.

Fluid dynamics are highly dependent on flow rate and rotational speed, when the T^2FD is operated in continuous processing mode. A fast flow rate may reduce the residence time (when a continuous film is formed). As exposure to high shear stress drives the DT process (Zhou et al., 2017), a reduced residence time in the T^2FD may influence conversion efficiency. In contrast, although a slow flow rate provides more residence time

when a continuous film is formed at a fixed rotational speed, it could lead to lower FA to FAME conversion efficiencies. Here evaporative loss of methanol increases the base catalyst concentrations, which can potentially induce saponification (Niju et al., 2014). Despite these potentially adverse effects, using T^2FD-intensified DT of dry *M. plumbeus* biomass achieved conversion efficiencies between 92 and 96% at a rotational speed of 4,000 rpm, with a catalyst concentration of 3% and a biomass to methanol ratio of 1:12. No significant effect of flow rate was detected. This may suggest that the residence time under these low-flow conditions of the device is mainly driven by the rotational speed (Figure 5.6B). As the T^2FD is a high throughput device, capable of operating at much larger flow volumes, this result is consistent with the residence time being independent of the flow rate, as for this combination of flow rate and rotational speed a minimal volume of fluid is retained in the device. In contrast, high flow rates (8 and 10 mL/min) significantly reduced FA to FAME conversion efficiencies from ~89 (FR 1-5) to 75% at 1% catalyst concentration. Under these operational parameters of the T^2FD, FA to FAME conversion efficiencies at 1% catalyst concentration were in general, slightly but not significantly lower than that at 3% catalyst concentration (Figure 5.6B). Previous studies on the T^2FD-intensified DT of wet biomass of microalgal *C. pannonica* observed a negative impact on FA to FAME conversion efficiencies at higher rotational speeds (6,000 rpm) and a slow flow rate of 1 mL/min (section 5.3) (Sitepu et al., 2018a), a result contrary to that observed in VFD-intensified processing which achieved conversion efficiencies of ~99% (Chapter 4) (Sitepu et al., 2018a). This result could be attributed to increased evaporative loss of methanol in the T^2FD, exacerbating the effect of the water content of the wet microalgae biomass (Sitepu et al., 2018a). In contrast, the fungal biomass was dry and the negative effect of high flow rates on FA to FAME conversion efficiencies are likely the result of reduced reaction time. As flow rates of more than 5 mL/min were not investigated for T^2FD-intensified DT of *C. pannonica*, the effects cannot be compared. Mathematical modelling of high flow rates, however, also predicted a decrease in FA to FAME conversion efficiencies in VFD-intensified DT of wet *C. pannonica* biomass operated in continuous mode, which is thought to be a consequence of reduced mechano-energy exposure of the reactants in thicker films of liquid (chapter 4) (Sitepu et al., 2018a). The present results, in combination with the previous work (Sitepu et al., 2018a), reinforce the view that the fluid dynamics within the T^2FD involve a complex interplay between rotational speed and fluid volume available (flow rate). In this respect, the biomass slurry will have a distinctly different viscosity from the methanol, which will further complicate the fluid dynamics and may impact on FA extraction and FA to FAME conversion efficiencies.

5.4.1.4 Effect of rotational speed

Rotational speed is one of the critical operating parameters of the T^2FD, which can impact FA extraction and FA to FAME conversion efficiencies. Normally in VFD-generated thin films, increased rotational speed can enhance reaction rates through providing higher shear stress and larger surface contact area between reactants (Luo et al., 2016, Britton et al., 2017). At rotational speeds of 2,000 to 6,000 rpm in the T^2FD and catalyst concentrations of 1 and 3 wt/v %, extraction yields for C18:2 and C18:1 ranged from 13 ± 0.3 to 16 ± 0.3 and 35 ±1 to 39 ± 0.6 mol% (Figure 5.5D) with extraction efficiencies of 83 ± 5 to 100 and 83 ± 9 to 92 ± 2%, respectively. A major significant effect was only observed for C18:2 extraction at a catalyst concentration of 3 wt./v % and rotational speeds of 3,500, 4,500 and 5,000 rpm, which yielded the lowest extraction efficiencies of 83% (Table 1 Appendix Section 5.4). Similar extraction efficiencies of 83% for C18:1 at a catalyst concentration of 1% and 3,000 rpm contrasted with highest extraction efficiencies of >91% at a catalyst concentration of 3 wt./v %% at rotational speeds of 3,500, 4,500 and 5,000 rpm.

No significant effect of changing the rotational speed was observed for T^2FD-intensified FA to FAME conversion efficiencies (~96 - 97%) for a catalyst concentration of 3 wt./v % at a flow rate of 3 mL/min and a biomass to methanol ratio of 1:12 (wt./v) (Figure 5.6C) (Table 2 Appendix Section 5.4). In contrast, at a catalyst concentration of 1 wt./v % at the same operational settings, FA to FAME conversion efficiencies were generally lower (~74 - 90%) and significantly reduced at the highest rotational speeds of 5,500 and 6,000 rpm (~74 - 76%) (Figure 5.6C). For a catalyst concentration of 1 wt./v %, increasing the rotational speed led to the same outcomes compared to increasing flow rate, while on both occasions these parameters had no significant effect at a catalyst concentration of 3 wt./v %. This strongly suggests that 1 wt./v % catalyst concentration is insufficient at reduced residence/reaction times of T^2FD-intensified DT of dry *M. plumbeus* biomass. For all parameter settings tested, the highest FA to FAME conversion efficiencies (97% ± 0.5) were achieved for a catalyst concentration of 3 wt./v %, a rotational speed of 4,500 rpm, a biomass to methanol ratio of 1:12 (wt./v) and a flow rate of 3 mL/min (Figure 5.6C).

5.4.1.5 Effect of water content in fungal biomass

One of the main bottlenecks in biodiesel production is dewatering of the biomass, which requires high energy input (Salam et al., 2016). Even though air-drying is energy-efficient,

the process is prohibitively time-consuming, and highly dependent on unpredictable sunlight radiation, and typically land area-intensive (Guldhe et al., 2014b). Therefore, DT of wet biomass is desirable to overcome these limitations. To investigate the suitability of continuous mode-operated T^2FD-intensified DT of wet fungal biomass, parameter settings were chosen based on single parameter best outcomes. Outcomes of a Box-Behnken model for continuous mode-operated VFD-intensified DT of wet algal biomass were also considered. Here the Box-Behnken model predicted a decrease in FA to FAME conversion efficiencies at high biomass to methanol ratios, increased water contents and increased flow rates (Sitepu et al., 2018a). Accordingly, a biomass to methanol ratio of 1:9 (wt./v), a flow rate of 2 mL/min and a rotational speed of 4,500 rpm at a catalyst concentration of 3 wt./v % were chosen for T^2FD-intensified DT of *M. plumbeus* biomass of various water contents of 5, 20, 50, and 75% (w/w) water. Irrespective of biomass water content, extraction of C18:2 was complete, while an extraction efficiency of ~86% was achieved for C18:1 at these parameter settings. In contrast, Kruskal-Wallis ANOVA established a significant effect of water content on FA to FAME conversion efficiency, which was driven by significantly reduced efficiencies at highest water content of 75% (w/w) (46 ± 4% compared to 91 ± 1% to 94 ± 0.5% at the other water contents) (Table 2 Appendix Section 5.4). This may indicate inhibition of DT through saponification of fatty acids by base catalysts in the presence of water (Ma and Hanna, 1999) and/or reduced concentration of the catalyst at high water contents. Taking all results into account, T^2FD-intensified DT of wet or dry *M. plumbeus* biomass is feasible up to a water content of 50% (w/w). Energy requirements for biomass processing and biodiesel production should be lower than that for conventional transesterification or other DT processes requiring heating, as T^2FD-intensified DT of *M. plumbeus* biomass was achieved at room temperature with minimal dewatering requirements. Establishing an optimal water content, however, will be a trade-off between FA extraction, FA to FAME conversion efficiencies and energy cost for biomass drying.

5.4.1.6 Implications for biodiesel production from fungal biomass

Lipid content is likely to determine biodiesel production yields and is therefore a primary concern for economic feasibility assessment, but reported values vary widely even for the same species, e.g. for *Rhodosporidium toruloides* reported values range from as low as 10 to as high as 70 mg g^{-1} dry weight biomass (Liu and Zhao, 2007, Cao et al., 2012, Koutinas et al., 2014, Thliveros et al., 2014, Ling et al., 2016). Other very important processing variables ultimately determining biodiesel yields are FA extraction yields and

FA to FAME conversion efficiencies. Most studies on the DT of yeast/fungal biomass reported FA yields but very few report on FA to FAME conversion efficiencies and interestingly, other than this study, none report on outcomes for both parameters, or provide information on FA extraction efficiencies, which could be used to calculate FA yields. For example, FA to FAME conversion efficiencies in this study ranged from <2% in the absence of a catalyst, ~25% at very low to ~97% at higher catalyst concentrations. Using this as an example of potential impact, a FA to FAME conversion efficiency of 95% would yield ~24 kg biodiesel per tonne dry biomass containing 25% total lipids (calculation based on best scenario from this study), whilst a similar biodiesel yield could be achieved for an organism with 50% total lipid content and a conversion efficiency of 50%.

The impact of water content on biodiesel production potential from fungal biomass has only been explored in four other studies for species with high lipid content (Cheirsilp and Louhasakul, 2013, Cui and Liang, 2014, Ward et al., 2017, Yellapu et al., 2017). Where reported, FA yields were slightly lower for fungal biomass with higher water content compared to yields achieved for *M. plumbeus* biomass with 50% water content in this study. Reported FA to FAME conversion efficiency for *Yarrowia lipolytica* with a total lipid content of 61 mg g^{-1} dry weight was, however, only 72 compared to ~91% achieved for *M. plumbeus* biomass achieved in this study despite similar water content (Cheirsilp and Louhasakul, 2013). Placing these outcomes into context of the much lower total lipid content of *M. plumbeus*, biodiesel yields for *M. plumbeus* would only approach half of the yields for *Y. lipolytica* (23 vs 44 kg $tonne^{-1}$ biomass dry weight).

Other than production parameters, time (reaction time, biomass drying and processing) and energy consumption (drying, reaction temperature, biomass processing) and reagent costs are also prime considerations for biodiesel production. Only one study was conducted with comparable FA yields at room temperature (Yellapu et al., 2017), while all others required reaction temperatures of between 50 to 100 °C to either assist in cell breakage and/or shorten the reaction time. In addition, except for one study reporting a reaction time of 4 min using *Cryptococcus curvatus* (Cui and Liang, 2014), typical reaction times were two orders of magnitude greater for the processing of dry fungal materials and at least 5 to 30 times longer for the processing of wet fungal biomass than reported here for *M. plumbeus*. The volumes of methanol used varied less, ranging from biomass to methanol ratios of 1:10 to 1:32 for the processing of dry fungal biomass (Liu and Zhao, 2007, Vicente et al., 2009, Venkata Subhash and Venkata Mohan, 2011, Cao et al., 2012, Koutinas et al., 2014, Thliveros et al., 2014, Zhang et al., 2014, Kakkad et al., 2015a,

Chopra et al., 2016, Ling et al., 2016, Carvalho et al., 2017, Katre et al., 2018) and 1:9 (this study) to 1:50 for the processing of wet fungal biomass (Cheirsilp and Louhasakul, 2013, Cui and Liang, 2014, Ward et al., 2017, Yellapu et al., 2017).

5.4.1.7 Energy consumption consideration

For economic assessment of energy requirements of the T^2FD-intensified DT of dry *M. plumbeus* biodiesel production at lab-scale, energy consumption of the T^2FD and the syringe pumps were roughly determined based on the energy (kWh) consumed in these small-lab scale experiments (Table 5.1). Energy consumption of the T^2FD increased with an increase of rotational speed. Thus, the energy consumption of the T^2FD was based on a rotational speed of 4,000 rpm (38.4 W), the setting for most parameter assessment for the T^2FD-intensified DT of dry *M. plumbeus* biomass. The energy consumption of the two syringe pumps was 20.4 W. As this study was conducted at room temperature, the total energy required for processing 2 g of biomass in T^2FD at 4,000 rpm for 5 min was 2.44 kWh kg^{-1} (Table 5.1), which is equivalent to 8.784 MJ kg^{-1} dry biomass. The energy consumption of the T^2FD was lower than for the magnetic stirrer hotplate, which is typically used for conventional heating processes at lab-scale. In comparison, biodiesel production from *Pichia guillermondii*, which used sonication for cell disruption prior to transesterification, using a magnetic stirrer hotplate in a two-step process (extraction and transesterification), requires 85.62 kWh kg^{-1} dry biomass (Table 5.1). Biodiesel production from wet biomass is certainly more energy-wise, saving 46% using a single step method instead of the traditional two-step method. The T^2FD-intensified DT, however, provides an energy saving of ~90% for the two-step dry biomass approach and ~94% for processing of wet biomass (Table 5.1). Using wet biomass as the raw material could also reduce processing time by at least 12 h, the time usually taken for biomass drying.

Table 5.1 Comparison of energy (kWh kg^{-1} biomass) consumed for different biodiesel production methods based on this study and Chopra et al. (2016).

Unit Operation / Process	**Methods**			
	Dry Biomass		**Wet Biomass**	
	Two Step	**T^2FD**	**Single Step Conventional**	**T^2FD**
Biomass drying	6	6	-	-
Cell Disruption	42.5	-	42.5	-
Lipid Extraction	34.72	-	-	-
Transesterification	2.4	2.44	3.6	2.44
Total	85.62	8.44	46.1	2.44

Cost of electricity[a] (AUS 43.67 c per KWh)	$37.33	$3.68	$20.09	$1.06

[a] Average electricity cost per kWh in South Australia is AUS 43.6 cents (O'Neill, 2018).

5.4.2 Conclusion

T^2FD-intensified DT combines oil extraction, cell disruption and transesterification of wet biomass into a single step process, operating at ambient temperature and pressure. This process is both energy- and time-efficient. Biodiesel production routinely occurred at >90% conversion at a base catalyst concentration of 3 wt./v %. Importantly, no significant effect of water content up to 50% was evident on FA to FAME conversion efficiency. A preliminary energy consumption assessment demonstrated that the T^2FD-intensified DT provides energy savings of >90%. Furthermore, the T^2FD operates in a continuous mode, a process that is suitable for up-scaling for commercial production.

Chapter 6
CONCLUSIONS, GENERAL DISCUSSION AND FUTURE DIRECTION

6.1 Summary of major findings

As a potential liquid renewable energy source, particularly for powering heavy machinery and the shipping industry, worldwide use of biodiesel is limited by high price, availability of sufficient feedstock at a guaranteed market price, often short bunker time, and particularly the debate on how green the fuel actually is (Haas et al., 2006, Aguieiras et al., 2015, Sheldon, 2018). In particular, choice of renewable feedstock that are not part of either the food vs. oil debate, or 'drink vs drive' debate (water usage/scarcity issues) especially for arid countries, demands the direct processing of feedstock with a high water content (Dominguez-Faus et al., 2009). In turn, such biomass requires large energy inputs for dewatering, as oils are not miscible with water (Lardon et al., 2009). To meet market demand for biodiesel, such sources must be exploited, but clearly require a novel approach to biodiesel production to reduce water and energy input, hence the cost.

Integration of extraction and transesterification into single-step process, termed direct transesterification (DT) has the potential to reduce biodiesel production costs, especially if wet microbial biomass can be used to eliminate energy and equipment costs for dewatering (Misra et al., 2014). DT of wet microbial biomass, however, requires higher reaction temperatures to avoid the water effect (Cao et al., 2013), while enzymatic processes that operate at moderately high temperatures (20-50 °C) demand prolonged reaction times (12 h) (Kim et al., 2016), and non-catalytic processes operate at very high temperatures (≥250 °C) and pressures (~2 MPa), whilst still requiring reaction times of ~1 h (Jazzar et al., 2015a). As reaction time, maintenance of pressure and temperature are energy-demanding, adding significantly to the cost of biodiesel, it is paramount to develop novel biomass processing strategies that operate at ambient pressure and temperature and produce high quality biodiesel directly from wet biomass.

Consequently, this research applied a novel micro-fluidic-based technology that operates at ambient temperature and pressure to intensify the DT of various oleaginous biomass and was the first to explore its capacity for continuous mode DT operation. This research

systematically explored in single and factorial design experiments the effect of water content, feedstock choice, operating mode (confined vs continuous) and process parameter settings (biomass to methanol ratio, rotational speed, flow rate, catalyst concentration) to unravel interactive effects of process parameters on fatty acid extraction and fatty acid to fatty acid methyl ester conversion efficiencies.

The VFD (Figure 3.1) is a novel mechano-energy processing platform which provides a large surface contact area between reactants, which enhances mass and heat transfer, and results in highly reduced processing times (Britton et al., 2017). VFD-intensified DT of wet and dry microalgal biomass of *C. pannonica*, conducted either in confined and continuous flow mode using sodium hydroxide in methanol as the catalyst, was investigated for the first time. A Box-Behnken experimental design determined the optimum reaction parameters. No significant impact of parameter setting, i.e. reaction time and catalyst concentration up to 7%, or mode of operation was detected for FA extraction or conversion to FAME efficiencies. Maximal conversion to biodiesel (96.9 ± 0.9%) was obtained at a ratio of biomass to methanol of 1:6 (wt./v), a flow rate 0.1 mL min^{-1} and a biomass water content of 50%. Average fatty extraction efficiencies of 41% were achieved while fatty acid to FAME conversion efficiencies were >90%. Fatty acid extraction efficiencies were comparable to most other DT of microbial biomass (Wahlen et al., 2011, Im et al., 2014, Kumar et al., 2014, Álvarez et al., 2017), but the VFD-intensified DT achieved this in ~41% of the normally required processing time and at ambient temperature, instead of 90% and 100 °C (Kim et al., 2015b). Moreover, these outcomes were achieved under continuous operation, which is a rarely considered parameter, yet of immediate importance for translation of research to industrial applications.

The new T^2FD microfluidic platform was developed recently in the Raston laboratory, based on a similar concept to the VFD. The T^2FD (Figure 3.2) consists of a motor connected to a blade and a base which, like the VFD, operates at ambient pressure and temperature, but is designed specifically for improving mass and heat transfer under continuous flow operation. This research was the first to systematically explore cell disruption capability and operating parameters for the T^2FD-intensified DT of wet and dry microbial and soybean seed biomass. Fatty acid to FAME conversion efficiencies for wet microalgal biomass of *C. pannonica* (water content 67.6%) routinely achieved >90% at a commonly used catalyst concentration of 3% sodium hydroxide at 2 min residence time. Results were similar for wet fungal *M. plumbeus* - and soybean seed meal biomass, demonstrating the efficiency of the device for simultaneous cell disruption and

transesterification. Outcomes were comparable to results achieved with the VFD for microalgal biomass and other DT processes of microbial biomass (see above), but up-scaling of the T^2FD for continuous mode operation at industrial scales is much more feasible. These studies were also the first to demonstrate that the novel T^2FD technology is relatively feedstock agnostic, which is another important criterion for translation to industrial applications.

It is well known that water has negative impacts on biodiesel production, as it inhibits transesterification reactions especially when using alkaline catalysts, or deteriorates the product (Atadashi et al., 2012). Therefore, for high yields of biodiesel, the water content should be below 0.06% (Kusdiana and Saka, 2004). This requirement however become a bottleneck in the utilization of oleaginous microbial biomass as feedstock (O'Connell et al., 2013), as dewatering consumed 90% of the total energy demand (Xu et al., 2011). This research was the first to demonstrate that wet microbial biomass can be used for biodiesel production using VFD- or T^2FD-itensified DT even at room temperature, ambient pressure, and, most importantly, under continuous flow operation, although higher than 50% water contents resulted in slightly reduced fatty acid to FAME conversion efficiencies (e.g. decreasing from ~98 to 90% for *C. pannonica* biomass with a water content of 75%). These negative effects of water were presumably due to saponification of free fatty acid, resulting in decreased catalyst concentration, as a base catalyst was used (Ma and Hanna, 1999). This research also demonstrated that negative effects of water could be compensated for by increasing methanol volumes. In conclusion, this research demonstrated that T^2FD- and VFD-intensified DT of wet microbial and traditional energy crops such as soy beans yields commonly achieved fatty acid extraction and high fatty acid to FAME conversion efficiencies, even when operated in continuous flow mode with residence (reaction) times of only 2 min at ambient temperature and pressure. Together with the outcomes of the systematic investigation on the interactive effects of processing parameters, the results lay the foundation for validating performance at pilot-scale, which was unfortunately beyond the scope of this research. As drying is avoided, a positive energy balance is achieved (section 6.2), but one area of concern is the requirement of the process for larger volumes of methanol (acting as a solvent and reactant in this process), which will be further concluded in a green metrics analysis in 6.3.

6.2 Energy consumption

The energy consumption for biodiesel production using two- and single-step processing was determined as kilowatt hour electricity consumption per kilogram biomass (Table 6.1). Direct biodiesel production from microalgal biomass was chosen as the model to determine the energy requirement of different processes and compare outcomes to the two-step approach, due to insufficient data on the DT of yeast/fungi and soybean crops. The energy consumption for biomass harvesting was set to 0.042 kWh kg^{-1} for all processes based on Evodos centrifugation (Collet et al., 2011, Klein-Marcuschamer et al., 2013), as this process consumed less energy compared to others and, most commonly no information on energy requirement for harvesting can be derived from published research. Even though an effect of species due to the nature of cell wall architecture cannot be completely excluded, outcomes should still be comparable, as energy consumption of different DT- processing methods, including thin film devices used in this thesis, are being evaluated. A further constraint is that energy consumptions of DT processes of microalgal biomass are based on lab-scale experiments, which will need further validation, once pilot-scale studies and outcomes are available.

Data used were derived from VFD- and T^2FD-intensified DT of *C. pannonica* operated in continuous flow mode while other DT processes were operated in batch mode (Table 6.1). Two syringe pumps, consuming 20.4 W were used to deliver reactants to the bottom of microfluidic device which rotated at 6,500 and 4,500 rpm for VFD and T^2FD, respectively. The total energy required for processing of wet microalgal biomass at room temperature using VFD and T^2FD were 2.012 and 2.482 kWh kg^{-1}, respectively. The energy consumption of VFD was slightly lower than for the T^2FD as the residence time of reactants in the VFD was shorter than in the T^2FD.

In general, the energy demand for microfluidic devices is 3, 21 and 125-fold lower than for the other two- and one-step biodiesel production pathways. The energy consumption of the transesterification process in the two-step biodiesel production was lower than for the microfluidic devices because it used pure extracted microalgal oil which required less energy and catalyst to produce biodiesel (Sivaramakrishnan and Incharoensakdi, 2017b). However, microfluidic device-intensified DT of *C. pannonica* saved 98% of energy consumption compared to the two-step method. In comparison to the single-step conventional method which usually uses magnetic stirrer and hotplates operated for 60

min at 100 ºC, the microfluidic devices saved 67 and 59% of energy for VFD and energy T2FD, respectively.

Table 6.1. Comparison energy consumption of some DT methods of microalgal biomass.

Process	Energy Consumption (kWh kg^{-1} Biomass)					
	Dry Biomass	Wet Biomass				
		One Step				
	Two Step Ultrasound Assisted	Ultrasound Assisted	Conventional	Microwave Assisted	VFD Assisted	T2FD Assisted
Species	*Scenedesmus*	*Scenedesmus*	*Nannochloropsis salina*	*Chlorella vulgaris*	*Choloroparva pannonica*	*Choloroparva pannonica*
Harvesting*	0.042	0.042	0.042	0.042	0.042	0.042
Drying	7.8	7.8	-	-	-	-
Cell disruption	33.2	33.2	-	-	-	-
Lipid extraction	85.7	-	-	-	-	-
Transesterification	0.3	85.7	6	43.75	1.97	2.44
Total Energy Consumption	**127.042**	**126.742**	**6.042**	**43.792**	**2.012**	**2.482**
References	(Sivaramakrishnan and Incharoensakdi, 2017b)	(Sivaramakrishnan and Incharoensakdi, 2017b)	(Kim et al., 2015b)	(Chen et al., 2015)	(Sitepu et al., 2018a)	(Sitepu et al., 2018a)

*****Harvesting process used Evodos centrifugation (Collet et al., 2011, Klein-Marcuschamer et al., 2013).

The microfluidic device-intensified DT saved 95 and 94% of energy compared to microwave-assisted DT of microalgal biomass. Energy consumption for DT is reduced further when using wet biomass. VFD- and T^2FD-intensified DT of wet *C. pannonica* saved 98% of energy compared to ultrasound-assisted DT of dry *Scenedesmus* biomass.

6.3 Green process metrics

Green chemistry metrics were established in the early 1990s and have been used worldwide to determine how green the chemistry of a process is (Curzons et al., 2001, Capello et al., 2007, Sheldon, 2018). This discussion part analyses the green chemistry metrics for one-step biodiesel production from microalgal biomass. Green metrics of DT of fungi and soybean seed biomass could not be calculated, due to insufficient comparable

published research, being further constrained by published data sets often lacking relevant detailed information. The E-factor was developed as the first green metric parameter to determine and set the relative reaction boundary to minimize waste generation for each product produced. Process mass intensity is defined as the ratio of total mass used in a process and mass of the desired product. Solvent intensity is used to determine the ratio of solvent used in a process to mass of product. The green metric parameters reaction mass efficiency, mass productivity and effective mass yield establish how efficient a process is compared to mass of reactants including hazardous reactants used. All of the green metrics equations (7.1-7.6) below were adopted from Sheldon (2018), replacing the term 'product' with the term 'biodiesel'.

$$E - factor = \frac{Total\ mass\ of\ waste}{Mass\ of\ biodiesel} \quad \text{(eq. 7.1)}$$

$$Process\ mass\ intensity = \frac{Total\ mass\ of\ materials\ in\ process}{Mass\ of\ biodiesel} \quad \text{(eq.7.2)}$$

$$Solvent\ intensity = \frac{Total\ mass\ of\ solvent}{Mass\ of\ biodiesel} \quad \text{(eq. 7.3)}$$

$$Reaction\ mass\ efficiency\ (\%) = \frac{Mass\ of\ biodiesel}{Total\ mass\ of\ reactants}\ x\ 100 \quad \text{(eq. 7.4)}$$

$$Mass\ productivity\ (\%) = \frac{Mass\ of\ biodiesel}{Total\ mass\ (including\ solvents)}\ x\ 100 \quad \text{(eq. 7.5)}$$

$$Effective\ mass\ yield\ (\%) = \frac{Mass\ of\ biodiesel}{Mass\ of\ hazardous\ reactants}\ x\ 100 \quad \text{(eq. 7.6)}$$

The first important aspect to notice is that the majority of published research does not provide all of the essential information, therefore limiting comparisons to those that do. This of course could bias conclusions drawn, as alternative production approaches could not be evaluated. For example, the required extraction cycles to obtained 44% oil yield from *Scenedesmus* were not specified (Sivaramakrishnan and Incharoensakdi, 2017b), therefore assuming a once only extraction cycle would give an E-factor of 16.78. However, the outcome would change to 50.34, if the traditional approach of three extraction cycles was applied. Furthermore, as mentioned previously, the quantity of methanol used in a continuous process is larger than for batch processes, as methanol was used to deliver biomass to the reactor. Unused methanol, however, can be easily recycled (Go et al., 2016, Giwa et al., 2018), and it therefore assumed here that unused methanol will be recovered and recycled in the process after separation from the product. Due to

incomplete information on water use in the published DT literature, water volumes typically used to purify biodiesel was set to 28% based on oil (v/v) (Atadashi et al., 2012).

Calculations of the green chemistry metrics of various DT microalgal biomass to biodiesel processes were based on the mass of reactants used in the process (Table 6.2).

Table 6.2. The mass of reactants used in the process.

Reactants (g)	**Batch System**		**Continuous Flow System**		
	Conventional	**Microwave Assisted**	**Reflux Extraction Reactor**	**VFD-Intensified**	**T^2FD-Intensified**
Species	*Chlorella pyrenoidosa*	*Chlorella vulgaris*	*Botryococcus braunii*	*Chloroparva pannonica*	*Chloroparva pannonica*
Biomass	0.1	0.79	10	0.65	0.65
Biomass residue	0.06	0.58	8.45	0.5	0.5
n-Hexane	5.24	7.68	26	0	0
Oil	0.05	0.21	1.55	0.15	0.15
Catalyst	0.20	0.04	1.6	0.36	0.12
Water	0.04	0.18	1.30	0.13	0.13
Methanol	3.17	6.34	55	9.50	9.50
Fatty Acid Methyl Esters	0.04	0.21	0.87	0.15	0.15

References (Chen et al., 2015, Hidalgo et al., 2015, Kim et al., 2015b, Sitepu et al., 2018a).

Green metrics outcomes for the DT processes of various microalgal biomass are shown in Table 6.3. The E-factor for microfluidic device-intensified DT is >80% lower than for all other processes, i.e. the novel processes applied for DT of wet microbial biomass produces 80% less waste. Process mass intensity for both VFD- and T^2FD-intensified DT was also more efficient, except for microwave-assisted DT of *Chlorella vulgaris*, presumably due to lower catalyst concentration used in that process (Chen et al., 2015). In terms of solvent intensity, the microfluidic devices were on par with microwave-assisted DT of *Chlorella vulgaris* and more efficient than use of the reflux extraction reactor for *Botryococcus braunii* biomass and conventional DT of *Chlorella pyrenoidosa*.

Reaction efficiencies based on the ratio of mass of product and total mass of reactants were similar for all DT methods, with microwave-assisted DT having the highest reaction

mass efficiency of 3.19%. All DT processing platform had low reaction mass efficiency and mass productivity, likely due to the large volumes of methanol used in DT to enable simultaneously extraction and transesterification (Kasim et al., 2010). The large volumes of hazardous reactants (catalysts, methanol, and hexane in some cases) required for DT also resulted in low effective mass yields for all examined processes.

Table 6.3. Green metrics of different DT process technologies.

Green Metrics	Batch System		Continuous Flow System		
	Conventional	Microwave Assisted	Reflux Extraction Reactor	VFD Assisted	T2FD Assisted
E-factor (g/g)	127.25	40.36	42.93	6.78	5.13
Process mass intensity (g/g)	201.12	71.54	107.93	73.11	71.46
Solvent intensity (g/g)	193.40	66.74	93.10	65.32	65.32
Reaction mass efficiency (%)	1.27	3.19	1.50	1.45	1.49
Mass productivity (%)	0.50	1.47	1.03	1.45	1.49
Effective mass yield (%)	0.52	1.50	1.07	1.53	1.53

To conclude, of all available current DT process information, microfluidic device-intensified DT offers significant reductions in the amount of waste products (E-factor 6.78 and 5.13 for VFD and T^2FD, respectively), being even superior to the two-step biodiesel production from, for example *Ricinus communis* (E-factor 24.40) (Martínez et al., 2018). This makes microfluidic device-intensified DT more environmental friendly. However, the amount of methanol used is still too high and the use of other methylene sources, such as dimethyl carbonate (DMC), identified as green solvent (Kreutzberer, 2001), offers further improvement opportunities for the green metrics of these DT processes. Unfortunately, implementation of DMC in DT requires a significant reduction in the price of this solvent, as it is presently more than twice the price of methanol.

6.4 Limitations of this research and future research directions

Microfluidic devices have been developed for greener processing and as intensified reaction platforms, simplifying processing, being also more time-, cost- and energy-efficient processes. Microfluidic devices have been shown in this research to improve process performance in the DT of wet oil-bearing materials to biodiesel. There are,

however, some limitations which could not be addressed/solved in this research, due to time and infrastructure constraints. First of all this study did not focus on generating crops / biomass as biodiesel raw materials. All the oil-bearing material used in this study was purchased or obtained from other collaborating laboratories, which did not focus on biomass production optimisation. For example, fungal biomass of *M. plumbeus* was obtained from the Centre for Tropical Crops and Biocommodities, Queensland University of Technology, Queensland, Australia, while soybean seed was purchased from the local market, Central Market, Adelaide, SA and microalgal biomass of *C. pannonica* was provided by a laboratory practical class in the Department of Medical Biotechnology, Flinders University. For this reason, relevant optimised biomass production data were not generated and impeded meaningful LCA and TEA investigations.

Likewise, validation of green metrics and performance of the microfluidic-intensified DT requires up scaling, as it is well recognised that extrapolation of laboratory scale data never lives up to promise (von Alvensleben et al., 2015). Up-scaling to industrial scales is often a major challenge for processes in general and it is reasonable to expect that it might also not be as straight forward for microfluidic-intensified DT. One perhaps more immediately feasible approach could be an implementation of parallel arrays of VFDs, which is cheaper and more reliable compared to the up-scaling of other microprocessor devices (Britton and Raston, 2014, Britton et al., 2015, Yuan et al., 2015). In fact, the VFD-intensified DT was conducted in continuous mode in this laboratory-scale research, which suggests that parallel array construction could provide sufficiently effective economics for commercial implementation. In addition rotating reactors are regularly used in continuous mode at large scale to facilitate reactions (Visscher et al., 2013). Therefore, it might be reasonable to expect that up-scaling of the T^2FD might be less problematic. Nonetheless it is imperative that process performance and parameter settings are validated at pilot-scale, as uptake by industry demands such proof of concept. Another point to underline is, to the best of our knowledge, no biodiesel manufacturer is presently using DT processes. To date, the biodiesel industry continues to use oil / lipid as raw material and most use alkaline transesterification. There is real potential for the implementation of other renewable catalysts, such as graphene oxide, for which the Raston laboratory has a patent pending for improved green production.

Even though microfluidic devices could produce biodiesel with a high conversion efficiency and yield, the product was not tested in a diesel engine, nor were the biodiesel quality parameters tested with recommended ASTM methods, due to limited amounts produced.

As this research focused on the development of a novel method to produce biodiesel directly using microfluidic devices, the determination of biodiesel properties and diesel engine tests were beyond of scope of the studies. Furthermore, diesel engine tests require special facilities to analyse engine performance, which unfortunately is very rare in Australia. However, to have complete knowledge on the microfluidic device-intensified DT process, it is suggested to determine the biodiesel properties of the product in future research to validate that the biodiesel product meets ASTM D6751 and EN 14214 requirements. It is further strongly recommended that the produced biodiesel be tested in suitable test engines to establish performance and emission profiles. All these recommendations require up-scaling of the devices to pilot scales.

Furthermore, biomass residue contains some valuable compounds such as polysaccharides and protein which can be used for other purposes. Utilization of the residual biomass through extraction and separation of value-adding compounds can improve techno-economics to the point where it makes biodiesel competitive to fossil fuel, but the question is how process residues such as methanol or sodium hydroxide can be removed cost-effectively with a guarantee of complete removal, as otherwise use of the biomass for feed and food products would be compromised. If residual biomass cannot be converted to product, this would negatively impact on LCA outcomes. One relatively easy way to deal with methanol toxicity would be to use ethanol instead. Likewise, micro-fluidic devices can be thinly coated on the rotating blade and base with an immobilised catalyst, such as green-produced graphene oxide. Once positive outcomes of such improvements on energy balances and processing costs have been demonstrated, only then can feedstock supplies be up-scaled to meet the growing demand, as markets are guaranteed not only in the biodiesel industry. Such bio-refinery concepts are particularly applicable to improve economic feasibility specifically of the microalgal industry.

Appendices

Appendix: Chapter 4

Vortex fluidic mediated direct transesterification of wet microalgae biomass to biodiesel

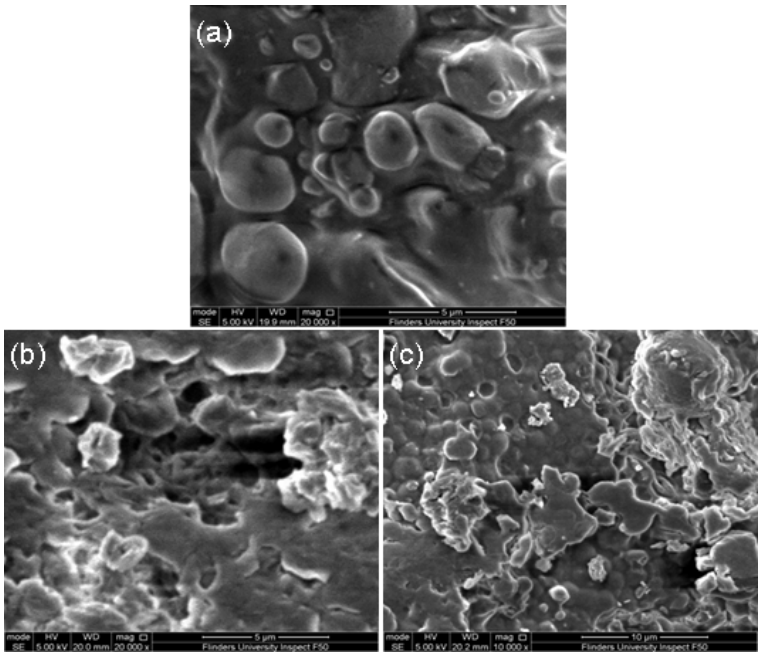

Figure 1 SEM images of raw microalgae biomass before (a) and after DT processing using (b) acid catalyst and (c) base catalyst using a biomass to methanol ratio of 1:5, 7% (wt./v) catalyst, reaction time 60 min, 45˚ tilt and rotational speed 7000 rpm, at room temperature in the confined mode of operation of the VFD.

Table 1. Quantified 1H-NMR spectra for C18:3, C18:1 and C16:0 of VFD-derived FAME samples of dry and wet biomass of *Chloroparva pannonica* operated in confined and continuous extraction mode.

					Polyunsaturated Fatty Acid		Monounsaturated Fatty Acid		Saturated Fatty Acid			ΣPUFA	ΣMUFA	ΣSFA	$\Sigma_{C18:3,C18:1,C16:0}$
					$C_{18:3}$	$C_{18:2}$	$C_{18:1}$	$C_{24:1}$	$C_{14:0}$	$C_{16:0}$	$C_{18:0}$				
GC	**Dry biomass non VFD**				21.9	24.7	30.2	0.7	0.4	16.7	0.7	48.6	33.1	18.2	
NMR	**Dry biomass confined mode acid catalyst**														
	Ratio biomass to methanol	**Reaction time (min)**	**Rotational speed (rpm)**	**% Catalyst concentration (wt/v)**											
	1:3.7	60	6000	7	16.88	b.d.l.	14.74	n.d.	n.d.	11.58	n.d.	n.d.	14.74	n.d.	43.21
	1:5	60	6000	7	20.00	b.d.l.	9.25	n.d.	n.d.	14.33	n.d.	n.d.	9.25	n.d.	43.58
	1:6.7	60	6000	7	14.00	b.d.l.	16.50	n.d.	n.d.	10.78	n.d.	n.d.	16.50	n.d.	41.28
	1:8	60	6000	7	14.12	b.d.l.	15.38	n.d.	n.d.	10.60	n.d.	n.d.	15.38	n.d.	40.10
	1:5	60	6000	**1**	16.84	b.d.l.	13.91	n.d.	n.d.	9.74	n.d.	n.d.	13.91	n.d.	40.49
	1:5	60	6000	**3**	18.87	b.d.l.	11.13	n.d.	n.d.	11.31	n.d.	n.d.	11.13	n.d.	41.31
	1:5	60	6000	**5**	17.10	b.d.l.	12.40	n.d.	n.d.	10.40	n.d.	n.d.	12.40	n.d.	39.90
	1:5	60	6000	**7**	20.00	b.d.l.	9.25	n.d.	n.d.	14.33	n.d.	n.d.	9.25	n.d.	43.58
acid	1:5	60	6000	**10**	17.03	b.d.l.	12.47	n.d.	n.d.	8.83	n.d.	n.d.	12.47	n.d.	38.33
catalyst	1:5	**15**	6000	7	16.85	b.d.l.	13.65	n.d.	n.d.	10.60	n.d.	n.d.	13.65	n.d.	41.10
	1:5	**30**	6000	7	12.87	b.d.l.	22.38	n.d.	n.d.	14.29	n.d.	n.d.	22.38	n.d.	49.54
	1:5	**60**	6000	7	20.00	b.d.l.	9.25	n.d.	n.d.	14.33	n.d.	n.d.	9.25	n.d.	43.58
	1:5	**75**	6000	7	14.90	b.d.l.	20.60	n.d.	n.d.	13.70	n.d.	n.d.	20.60	n.d.	49.20
	1:5	60	**4000**	7	17.25	b.d.l.	14.50	n.d.	n.d.	11.15	n.d.	n.d.	14.50	n.d.	42.90
	1:5	60	**5000**	7	17.65	b.d.l.	16.85	n.d.	n.d.	11.62	n.d.	n.d.	16.85	n.d.	46.12
	1:5	60	**6000**	7	20.00	b.d.l.	9.25	n.d.	n.d.	14.33	n.d.	n.d.	9.25	n.d.	43.58
	1:5	60	**7000**	7	17.97	b.d.l.	15.03	n.d.	n.d.	13.85	n.d.	n.d.	15.03	n.d.	46.85
	1:5	60	**8000**	7	8.73	b.d.l.	25.52	n.d.	n.d.	10.42	n.d.	n.d.	25.52	n.d.	44.67

Continued Table 1.

					Polyunsaturated Fatty Acid		Monounsaturated Fatty Acid		Saturated Fatty Acid			ΣPUFA	ΣMUFA	ΣSFA	$\Sigma_{C18:3,C18:1,C16:0}$
					$C_{18:3}$	$C_{18:2}$	$C_{18:1}$	$C_{24:1}$	$C_{14:0}$	$C_{16:0}$	$C_{18:0}$				
GC	**Dry biomass non VFD**				21.9	24.7	30.2	0.7	0.4	16.7	0.7	48.6	33.1	18.2	
	Dry biomass confined mode base catalyst														
base catalyst	**1:3.7**	60	6000	7											sample error
	1:5	60	6000	7	10.75	b.d.l.	22.25	n.d.	n.d.	8.95	n.d.	n.d.	22.25	n.d.	41.95
	1:6.7	60	6000	7	16.64	b.d.l.	14.99	n.d.	n.d.	10.80	n.d.	n.d.	14.99	n.d.	42.43
	1:8	60	6000	7	16.40	b.d.l.	15.35	n.d.	n.d.	11.13	n.d.	n.d.	15.35	n.d.	42.88
	1:5	60	6000	**1**	16.35	b.d.l.	14.40	n.d.	n.d.	11.32	n.d.	n.d.	14.40	n.d.	42.07
	1:5	60	6000	**3**	15.08	b.d.l.	15.79	n.d.	n.d.	10.75	n.d.	n.d.	15.79	n.d.	41.63
	1:5	60	6000	**5**											sample error
	1:5	60	6000	**7**	10.75	b.d.l.	22.25	n.d.	n.d.	8.95	n.d.	n.d.	22.25	n.d.	41.95
	1:5	60	6000	**10**											sample error
	1:5	**15**	6000	7											sample error
	1:5	**30**	6000	7	15.76	b.d.l.	14.49	n.d.	n.d.	10.27	n.d.	n.d.	14.49	n.d.	40.52
	1:5	**60**	6000	7	10.75	b.d.l.	22.25	n.d.	n.d.	8.95	n.d.	n.d.	22.25	n.d.	41.95
	1:5	**75**	6000	7											sample error
	1:5	60	**6000**	7	10.75	b.d.l.	22.25	n.d.	n.d.	8.95	n.d.	n.d.	22.25	n.d.	41.95
	1:5	60	**7000**	7	12.86	b.d.l.	17.39	n.d.	n.d.	9.33	n.d.	n.d.	17.39	n.d.	39.58
	1:5	60	**8000**	7	15.08	b.d.l.	16.42	n.d.	n.d.	10.05	n.d.	n.d.	16.42	n.d.	41.55

Continued Table 1.

					Polyunsaturated Fatty Acid		Monounsaturated Fatty Acid		Saturated Fatty Acid			ΣPUFA	ΣMUFA	ΣSFA	$\Sigma_{C18:3,C18:1,C16:0}$
					$C_{18:3}$	$C_{18:2}$	$C_{18:1}$	$C_{24:1}$	$C_{14:0}$	$C_{16:0}$	$C_{18:0}$				
GC	**Dry biomass non VFD**				21.9	24.7	30.2	0.7	0.4	16.7	0.7	48.6	33.1	18.2	
	Dry biomass continuos flow mode														
	Ratio biomass to methanol	**Flow rate (ml/min)**	**Rotational speed (rpm)**	**Angle (°)**											
	1:4	0.2	6000	45	18.59 ± 0.1	b.d.l.	9.91 ± 0.28	n.d.	n.d.	10.53 ± 0.08	n.d.	n.d.	9.91	n.d.	39.03
	1:6	0.2	6000	45	17.37 ± 3.8	b.d.l.	11.63 ± 3.62	n.d.	n.d.	10.34 ± 1.06	n.d.	n.d.	11.63	n.d.	39.34
	1:8	0.2	6000	45	19.39 ± 1.39	b.d.l.	11.04 ± 0.6	n.d.	n.d.	11.34 ± 0.43	n.d.	n.d.	11.04	n.d.	41.77
	1:10	0.2	6000	45	20.34 ± 2.5	b.d.l.	8.72 ± 2.23	n.d.	n.d.	11.27 ± 0.82	n.d.	n.d.	8.72	n.d.	40.33
	1:12	0.2	6000	45	17.44 ± 0.29	b.d.l.	11.87 ± 0.38	n.d.	n.d.	10.29 ± 0	n.d.	n.d.	11.87	n.d.	39.6
	1:10	**0.1**	6000	45	16.01 ± 0.55	b.d.l.	12.68 ± 0.25	n.d.	n.d.	9.88 ± 0.16	n.d.	n.d.	12.68	n.d.	38.57
	1:10	**0.2**	6000	45	20.34 ± 2.5	b.d.l.	8.72 ± 2.23	n.d.	n.d.	10.34 ± 1.06	n.d.	n.d.	8.72	n.d.	39.4
	1:10	**0.3**	6000	45	17.32 ± 0.93	b.d.l.	11.68 ± 0.13	n.d.	n.d.	9.94 ± 0.66	n.d.	n.d.	11.68	n.d.	38.94
	1:10	**0.4**	6000	45	21.06 ± 0.66	b.d.l.	8.94 ± 0.58	n.d.	n.d.	11.33 ± 0.2	n.d.	n.d.	8.94	n.d.	41.33
	1:10	**0.5**	6000	45	17.06 ± 8.27	b.d.l.	11.69 ± 8.09	n.d.	n.d.	10.88 ± 1.87	n.d.	n.d.	11.69	n.d.	39.63
	1:10	**0.75**	6000	45	16.12 ± 0.12	b.d.l.	13.51 ± 0.47	n.d.	n.d.	9.92 ± 0.08	n.d.	n.d.	13.51	n.d.	39.55
	1:10	**1**	6000	45	16.75 ± 0.44	b.d.l.	12.06 ± 0	n.d.	n.d.	10.07 ± 0.19	n.d.	n.d.	12.06	n.d.	38.88
	1:10	0.5	**5000**	45	15.52 ± 0.34	b.d.l.	14.05 ± 0.25	n.d.	n.d.	9.9 ± 0.08	n.d.	n.d.	14.05	n.d.	39.47
	1:10	0.5	**6000**	45	20.34 ± 2.5	b.d.l.	8.72 ± 2.23	n.d.	n.d.	10.34 ± 1.06	n.d.	n.d.	8.72	n.d.	39.4
	1:10	0.5	**7000**	45	14.73 ± 1.54	b.d.l.	14.77 ± 1.54	n.d.	n.d.	9.68 ± 0.32	n.d.	n.d.	14.77	n.d.	39.18
	1:10	0.5	**8000**	45	15.58 ± 2.21	b.d.l.	13.67 ± 3.09	n.d.	n.d.	9.86 ± 0.45	n.d.	n.d.	13.67	n.d.	39.11
	1:10	0.5	6000	**60**	16.18 ± 0.25	b.d.l.	13.2 ± 0.43	n.d.	n.d.	10.01 ± 0.06	n.d.	n.d.	13.20	n.d.	39.39
	1:10	0.5	6000	**45**	20.34 ± 2.5	b.d.l.	8.72 ± 2.23	n.d.	n.d.	10.34 ± 1.06	n.d.	n.d.	8.72	n.d.	39.4
	1:10	0.5	6000	**30**	16.15 ± 1.64	b.d.l.	13.17 ± 1.73	n.d.	n.d.	10.1 ± 0.5	n.d.	n.d.	13.17	n.d.	39.42

Continued Table 1.

				Polyunsaturated Fatty Acid		Monounsaturated Fatty Acid		Saturated Fatty Acid			ΣPUFA	ΣMUFA	ΣSFA	$\Sigma_{C18:3,C18:1,C16:0}$
				$C_{18:3}$	$C_{18:2}$	$C_{18:1}$	$C_{24:1}$	$C_{14:0}$	$C_{16:0}$	$C_{18:0}$				
GC	**Dry biomass non VFD**			21.9	24.7	30.2	0.7	0.4	16.7	0.7	48.6	33.1	18.2	
	Wet biomass confined mode													
	Ratio biomass to methanol	**Reaction time (min)**	**Water content (%,w/w)**											
	1:5	15	47.5	12.31	b.d.l.	18.44	n.d.	n.d.	9.67	n.d.	n.d.	18.44	n.d.	40.42
	1:5	30	90	15.03	b.d.l.	16.97	n.d.	n.d.	9.91	n.d.	n.d.	16.97	n.d.	41.91
	1:5	30	5	12.02	b.d.l.	18.23	n.d.	n.d.	9.54	n.d.	n.d.	18.23	n.d.	39.79
	1:5	**45**	**47.5**	11.87	b.d.l.	**21.38**	n.d.	n.d.	9.46	n.d.	n.d.	21.38	n.d.	42.71
	1:6.7	30	47.5	16.15	b.d.l.	15.23	n.d.	n.d.	10.75	n.d.	n.d.	15.23	n.d.	42.13
	1:6.7	30	47.5	12.87	b.d.l.	18.50	n.d.	n.d.	9.41	n.d.	n.d.	18.50	n.d.	40.79
	1:6.7	**30**	**47.5**	10.08	b.d.l.	**21.55**	n.d.	n.d.	9.34	n.d.	n.d.	21.55	n.d.	40.97
	1:6.7	15	5	14.47	b.d.l.	15.53	n.d.	n.d.	9.74	n.d.	n.d.	15.53	n.d.	39.74
	1:6.7	**15**	**90**	10.76	b.d.l.	**21.24**	n.d.	n.d.	9.31	n.d.	n.d.	21.24	n.d.	41.31
	1:6.7	45	5	14.77	b.d.l.	15.48	n.d.	n.d.	9.77	n.d.	n.d.	15.48	n.d.	40.02
	1:6.7	**45**	**90**	10.09	b.d.l.	**23.41**	n.d.	n.d.	9.45	n.d.	n.d.	23.41	n.d.	42.95
	1:8.3	30	90	13.75	b.d.l.	18.13	n.d.	n.d.	10.18	n.d.	n.d.	18.13	n.d.	42.06
	1:8.3	45	47.5	14.40	b.d.l.	17.85	n.d.	n.d.	9.77	n.d.	n.d.	17.85	n.d.	42.02
	1:8.3	15	47.5	14.82	b.d.l.	14.93	n.d.	n.d.	9.87	n.d.	n.d.	14.93	n.d.	39.62
	1:8.3	30	5	12.55	b.d.l.	18.82	n.d.	n.d.	9.46	n.d.	n.d.	18.82	n.d.	40.83

Continued Table 1.

				Polyunsaturated Fatty Acid		Monounsaturated Fatty Acid		Saturated Fatty Acid			ΣPUFA	ΣMUFA	ΣSFA	$\Sigma_{C18:3,C18:1,C16:0}$
				$C_{18:3}$	$C_{18:2}$	$C_{18:1}$	$C_{24:1}$	$C_{14:0}$	$C_{16:0}$	$C_{18:0}$				
GC	**Dry biomass non VFD**			21.9	24.7	30.2	0.7	0.4	16.7	0.7	48.6	33.1	18.2	
	Wet biomass continuous flow mode													
	Ratio biomass to methanol	**Flow rate (ml/min)**	**Water content (%,w/w)**											
	1:6	1	90	13.51	b.d.l.	17.12	n.d.	n.d.	9.63	n.d.	n.d.	17.12	n.d.	40.26
	1:6	0.55	100	13.80	b.d.l.	17.07	n.d.	n.d.	9.69	n.d.	n.d.	17.07	n.d.	40.57
	1:6	0.55	80	12.66	b.d.l.	18.34	n.d.	n.d.	9.38	n.d.	n.d.	18.34	n.d.	40.38
	1:6	**0.1**	**90**	12.01	b.d.l.	**20.74**	n.d.	n.d.	9.41	n.d.	n.d.	20.74	n.d.	42.16
	1:15	0.1	80	16.52	b.d.l.	13.73	n.d.	n.d.	10.46	n.d.	n.d.	13.73	n.d.	40.71
	1:15	0.1	100	13.40	b.d.l.	16.60	n.d.	n.d.	9.60	n.d.	n.d.	16.60	n.d.	39.60
	1:15	0.55	90	13.36	b.d.l.	19.39	n.d.	n.d.	10.53	n.d.	n.d.	19.39	n.d.	43.28
	1:15	0.55	90	16.46	b.d.l.	12.67	n.d.	n.d.	10.29	n.d.	n.d.	12.67	n.d.	39.42
	1:15	0.55	90	13.38	b.d.l.	17.12	n.d.	n.d.	9.65	n.d.	n.d.	17.12	n.d.	40.15
	1:15	**1**	**80**	10.21	b.d.l.	**21.41**	n.d.	n.d.	9.24	n.d.	n.d.	21.41	n.d.	40.87
	1:15	1	100	13.42	b.d.l.	17.96	n.d.	n.d.	10.24	n.d.	n.d.	17.96	n.d.	41.61
	1:24	0.1	90	12.76	b.d.l.	16.99	n.d.	n.d.	9.46	n.d.	n.d.	16.99	n.d.	39.21
	1:24	0.55	80	12.69	b.d.l.	18.56	n.d.	n.d.	9.66	n.d.	n.d.	18.56	n.d.	40.91
	1:24	**0.55**	**100**	11.55	b.d.l.	**23.70**	n.d.	n.d.	11.80	n.d.	n.d.	23.70	n.d.	47.05
	1:24	1	90	13.19	b.d.l.	17.43	n.d.	n.d.	9.67	n.d.	n.d.	17.43	n.d.	40.29

b.d.l.: below detection limit; n.d. not determinable

Table 2. Experimental design for Box-Behnken response surface method for direct transesterification of wet biomass.

Variables	Symbols	Levels		
		-1	0	1
Confined Mode				
Water content (wt%)	A	2.5	23.75	45
Reaction time (min)	B	15	30	45
Ratio biomass to methanol (wt/v)	C	1:5	1:6.7	1:8.3
Continuous Flow Mode				
Water content (wt%)	A	40	45	50
Flow rate (mL/min)	B	0.1	0.55	1.0
Ratio biomass to methanol (wt/v)	C	1:6	1:15	1:24

Supplementary Table 3. Correlation analysis of factors for the DT of wet microalgal biomass using VFD.

Term	Coefficient	Standard Error	Low Confidence	High Confidence	T Value	P Value
Confined Mode						
Intercept	94.25	1.386322	91.45649	97.04351	67.98563	1.30E-08
A: Water content	-1.7275	0.848946	-3.43817	-0.01683	-2.03488	0.097503
B: Reaction time	-0.9725	0.848946	-2.68317	0.738166	-1.14554	0.303838
C: Ratio of biomass : methanol	0.8075	0.848946	-0.90317	2.518166	0.95118	0.385193
A • B	-0.235	1.20059	-2.65425	2.184247	-0.19574	0.852522
A • C	0.81	1.20059	-1.60925	3.229247	0.674668	0.529818
B • C	-1.015	1.20059	-3.43425	1.404247	-0.84542	0.436454
A • A	0.1225	1.249614	-2.39553	2.640532	0.09803	0.925717
B • B	0.9175	1.249614	-1.60053	3.435532	0.734227	0.495777
C • C	-0.3575	1.249614	-2.87553	2.160532	-0.28609	0.786285
Continuous Flow						
Intercept	96.26667	1.051956	94.146926	98.386408	91.51208	2.95E-09

A:Water content (w/w)	-0.5125	0.644189	-1.810571	0.785571	-0.79557	0.46236
B:Flow rate	-0.975	0.644189	-2.273071	0.323071	-1.51353	0.190562
C:Ratio of biomass to methanol (wt./v)	-0.2875	0.644189	-1.585571	1.010571	-0.4463	0.674047
A • B	-1.475	0.91102	-3.31075	0.36075	-1.61906	0.166358
A • C	-0.85	0.91102	-2.68575	0.98575	-0.93302	0.393638
B • C	0.125	0.91102	-1.71075	1.96075	0.137209	0.89622
A • A	-0.98333	0.94822	-2.894042	0.927376	-1.03703	0.347248
B • B	0.341667	0.94822	-1.569042	2.252376	0.360324	0.733326
C • C	0.416667	0.94822	-1.494042	2.327376	0.43942	0.678699

Table 4. Analysis of variance for the DT of wet microalgal biomass using VFD

Source of Variation	Degrees of Freedom	Sum of Squares	Mean Squares	F Ratio	P Value
Confined Mode					
Model	9	47.43701	5.270779	0.914166	0.574001
A: Water content	1	23.87405	23.87405	4.140724	0.097503
B: Reaction time	1	7.56605	7.56605	1.312259	0.303838
C: Ratio of biomass to methanol	1	5.21645	5.21645	0.904743	0.385193
A • B	1	0.2209	0.2209	0.038313	0.852522
A • C	1	2.6244	2.6244	0.455177	0.529818
B • C	1	4.1209	4.1209	0.71473	0.436454
A • A	1	0.02541	0.02541	0.004407	0.949643
B • B	1	3.31695	3.31695	0.575293	0.482364
C • C	1	0.4719	0.4719	0.081847	0.786285
Residual	5	28.82835	5.76567		
Lack of Fit	3	2.28015	0.76005	0.057258	0.977756
Pure Error	2	26.5482	13.2741		
Total	14	76.26536			

Continuous Flow

Model	9	27.038167	3.004241	0.904937	0.578896
A: Water content (w/w)	1	2.10125	2.10125	0.632938	0.46236
B: Flow rate	1	7.605	7.605	2.290778	0.190562
C: Ratio of biomass to methanol (wt./v)	1	0.66125	0.66125	0.199182	0.674047
A • B	1	8.7025	8.7025	2.621367	0.166358
A • C	1	2.89	2.89	0.870526	0.393638
B • C	1	0.0625	0.0625	0.018826	0.89622
A • A	1	4.018583	4.018583	1.210477	0.321365
B • B	1	0.356058	0.356058	0.107252	0.756562
C • C	1	0.641026	0.641026	0.19309	0.678699
Residual	5	16.599167	3.319833		
Lack of Fit	3	9.4325	3.144167	0.877442	0.571638
Pure Error	2	7.166667	3.583333		
Total	14	43.637333			

Appendix: Chapter 5

Appendix Section 5.2. Continuous direct biodiesel production from soybean seeds by micro-fluidic turbo thin film processing

Table 1. Quantified ^{1}H-NMR spectra for $C_{18:2}$, $C_{18:1}$, $C_{16:0}$, and $C_{18:0}$ of T^{2}FD-derived FAME samples of soybean seed operating under continuous extraction processing.

					Polyunsaturated Fatty Acid		Monounsaturated Fatty Acid		Saturated Fatty Acid			SPUFA	SMUFA	SSFA	S_{total}
					$C_{18:3}$	$C_{18:2}$	$C_{18:1}$	$C_{24:1}$	$C_{14:0}$	$C_{16:0}$	$C_{18:0}$				
GC	**Dry biomass non T2FD**				8.2	39.2	20.3	0	7.4	8.9	3.9	47.4	20.3	20.2	87.9
NMR	**Soybean seed turbo thin film device using base catalyst**														
	Catalyst Conc. (%, wt/v)	**Ratio Biomass : MeOH (wt/v)**	**Flow Rate (mL/min)**	**Rotational Speed (rpm)**											
	Effect of Ratio Seed : Methanol														
	1	1:6	3	4000	n.d.	8.69 ± 0.44	21.35 ± 0.48	n.d.	n.d.	4.18 ± 0.03	2.14 ± 0.01	15.6 ± 0.32	21.35 ± 0.48	6.32 ± 0.02	43.26
	1	1:9	3	4000	n.d.	8.08 ± 0.5	21.63 ± 1.05	n.d.	n.d.	4.2 ± 0.02	2.15 ± 0.01	15.21 ± 0.45	21.63 ± 1.05	6.35 ± 0.02	43.19
	1	1:12	3	4000	n.d.	6.71 ± 1.24	23.1 ± 2.38	n.d.	n.d.	4.43 ± 0.33	2.26 ± 0.17	13.69 ± 0.77	23.1 ± 2.38	6.69 ± 0.25	43.48
	1	1:15	3	4000	n.d.	9.43 ± 0.86	26.47 ± 5	n.d.	n.d.	4.68 ± 0.95	2.39 ± 0.49	14.88 ± 0.84	26.47 ± 5	7.07 ± 0.72	48.42
	1	1:18	3	4000	n.d.	8.29 ± 0.87	21.15 ± 0.43	n.d.	n.d.	4.17 ± 0.05	2.13 ± 0.02	15.4 ± 0.65	21.15 ± 0.43	6.3 ± 0.04	42.85
	3	1:6	3	4000	n.d.	7.39 ± 0.55	20.86 ± 0.41	n.d.	n.d.	4.16 ± 0.03	2.13 ± 0.02	14.95 ± 0.42	20.86 ± 0.41	6.29 ± 0.03	42.10
	3	1:9	3	4000	n.d.	7.96 ± 0.33	21.15 ± 0.13	n.d.	n.d.	4.15 ± 0.01	2.12 ± 0.01	15.15 ± 0.18	21.15 ± 0.13	6.27 ± 0.01	42.57
	3	1:12	3	4000	n.d.	8.56 ± 0.83	21.61 ± 0.77	n.d.	n.d.	4.12 ± 0.03	2.11 ± 0.02	15.44 ± 0.69	21.61 ± 0.77	6.23 ± 0.03	43.29
	3	1:15	3	4000	n.d.	9.01 ± 0.73	21.84 ± 0.64	n.d.	n.d.	4.1 ± 0.03	2.09 ± 0.02	15.67 ± 0.57	21.84 ± 0.64	6.19 ± 0.03	43.70
	3	1:18	3	4000	n.d.	9 ± 0.19	22 ± 0.34	n.d.	n.d.	4.1 ± 0.02	2.09 ± 0.01	15.5 ± 0.14	22 ± 0.34	6.19 ± 0.02	43.69
	Effect of Flow Rate														

				Polyunsaturated Fatty Acid		Monounsaturated Fatty Acid		Saturated Fatty Acid			SPUFA	SMUFA	SSFA	S_{total}
				$C_{18:3}$	$C_{18:2}$	$C_{18:1}$	$C_{24:1}$	$C_{14:0}$	$C_{16:0}$	$C_{18:0}$				
1	1:9	1	4000	n.d.	7.34 ± 0.56	20.34 ± 0.34	n.d.	n.d.	4.19 ± 0.02	2.14 ± 0.01	15 ± 0.45	20.34 ± 0.34	6.33 ± 0.02	41.67
1	1:9	2	4000	n.d.	4.58 ± 1.3	17.37 ± 1.57	n.d.	n.d.	4.28 ± 0.1	2.19 ± 0.05	14.45 ± 1.11	17.37 ± 1.57	6.47 ± 0.08	38.30
1	1:9	3	4000	n.d.	8.08 ± 0.5	21.63 ± 1.05	n.d.	n.d.	4.2 ± 0.02	2.15 ± 0.01	15.21 ± 0.45	21.63 ± 1.05	6.35 ± 0.02	43.19
1	1:9	4	4000	n.d.	3.64 ± 0.79	17.48 ± 0.54	n.d.	n.d.	4.31 ± 0.05	2.2 ± 0.02	13.57 ± 0.6	17.48 ± 0.54	6.51 ± 0.04	37.57
1	1:9	5	4000	n.d.	3.89 ± 0.19	17.61 ± 0.17	n.d.	n.d.	4.28 ± 0.01	2.19 ± 0	13.7 ± 0.14	17.61 ± 0.17	6.47 ± 0.01	37.78
3	1:9	1	4000	n.d.	2.98 ± 0.23	16.66 ± 0.23	n.d.	n.d.	4.31 ± 0.02	2.2 ± 0.01	13.49 ± 0.17	16.66 ± 0.23	6.51 ± 0.02	36.66
3	1:9	2	4000	n.d.	2.4 ± 0.25	16.62 ± 0.18	n.d.	n.d.	4.34 ± 0.01	2.22 ± 0.01	13.12 ± 0.16	16.62 ± 0.18	6.56 ± 0.01	36.29
3	1:9	3	4000	n.d.	8.08 ± 0.5	21.63 ± 1.05	n.d.	n.d.	4.2 ± 0.02	2.15 ± 0.01	15.21 ± 0.45	21.63 ± 1.05	6.35 ± 0.02	43.19
3	1:9	4	4000	n.d.	3.89 ± 0.19	17.53 ± 0.23	n.d.	n.d.	4.27 ± 0.01	2.18 ± 0.01	13.7 ± 0.14	17.53 ± 0.23	6.45 ± 0.01	37.68
3	1:9	5	4000	n.d.	3.76 ± 0.11	17.63 ± 0.2	n.d.	n.d.	4.27 ± 0	2.18 ± 0	13.63 ± 0.08	17.63 ± 0.2	6.45 ± 0	37.71
Effect of Rotational Speed														
1	1:9	3	2000	n.d.	4.07 ± 0.19	17.37 ± 0.26	n.d.	n.d.	4.31 ± 0.01	2.2 ± 0.01	13.87 ± 0.16	17.37 ± 0.26	6.51 ± 0.01	37.76
1	1:9	3	2500	n.d.	3.43 ± 0.64	16.96 ± 0.48	n.d.	n.d.	4.33 ± 0.03	2.22 ± 0.02	13.63 ± 0.54	16.96 ± 0.48	6.55 ± 0.03	37.14
1	1:9	3	3000	n.d.	4.02 ± 0.62	17.17 ± 0.6	n.d.	n.d.	4.3 ± 0.03	2.2 ± 0.02	13.92 ± 0.47	17.17 ± 0.6	6.5 ± 0.03	37.59
1	1:9	3	3500	n.d.	4.07 ± 0.94	16.95 ± 0.43	n.d.	n.d.	4.3 ± 0.05	2.2 ± 0.02	13.95 ± 0.64	16.95 ± 0.43	6.5 ± 0.04	37.41
1	1:9	3	4000	n.d.	8.08 ± 0.5	21.63 ± 1.05	n.d.	n.d.	4.2 ± 0.02	2.15 ± 0.01	15.21 ± 0.45	21.63 ± 1.05	6.35 ± 0.02	43.19
1	1:9	3	4500	n.d.	3.53 ± 1.17	16.76 ± 0.58	n.d.	n.d.	4.33 ± 0.06	2.21 ± 0.03	13.76 ± 0.88	16.76 ± 0.58	6.54 ± 0.05	37.06
1	1:9	3	5000	n.d.	3.13 ± 0.32	16.4 ± 0.01	n.d.	n.d.	4.34 ± 0.02	2.22 ± 0.01	13.56 ± 0.24	16.4 ± 0.01	6.56 ± 0.02	36.53
1	1:9	3	5500	n.d.	4.17 ± 0.69	17 ± 0.48	n.d.	n.d.	4.3 ± 0.04	2.2 ± 0.02	14.09 ± 0.52	17 ± 0.48	6.5 ± 0.03	37.59
1	1:9	3	6000	n.d.	3.23 ± 0.78	16.37 ± 0.21	n.d.	n.d.	4.35 ± 0.03	2.22 ± 0.02	13.7 ± 0.56	16.37 ± 0.21	6.57 ± 0.03	36.63
3	1:9	3	2000	n.d.	4.16 ± 0.25	17.41 ± 0.06	n.d.	n.d.	4.27 ± 0.02	2.18 ± 0.01	14 ± 0.15	17.41 ± 0.06	6.45 ± 0.02	37.86
3	1:9	3	2500	n.d.	4.06 ± 0.46	17.45 ± 0.1	n.d.	n.d.	4.27 ± 0.02	2.19 ± 0.01	13.86 ± 0.28	17.45 ± 0.1	6.46 ± 0.02	37.77
3	1:9	3	3000	n.d.	3.48 ± 0.42	17.24 ± 0.24	n.d.	n.d.	4.3 ± 0.03	2.2 ± 0.02	13.57 ± 0.38	17.24 ± 0.24	6.5 ± 0.03	37.31
3	1:9	3	3500	n.d.	3.45 ± 1.59	16.98 ± 0.96	n.d.	n.d.	4.3 ± 0.07	2.2 ± 0.03	13.73 ± 1.19	16.98 ± 0.96	6.5 ± 0.05	37.20
3	1:9	3	4000	n.d.	7.96 ± 0.33	21.15 ± 0.13	n.d.	n.d.	4.15 ± 0.01	2.12 ± 0.01	15.15 ± 0.18	21.15 ± 0.13	6.27 ± 0.01	42.57
3	1:9	3	4500	n.d.	3.18 ± 0.11	16.84 ± 0.06	n.d.	n.d.	4.32 ± 0	2.21 ± 0	13.59 ± 0.09	16.84 ± 0.06	6.53 ± 0	36.95
3	1:9	3	5000	n.d.	3.11 ± 0.11	16.64 ± 0.13	n.d.	n.d.	4.32 ± 0.01	2.21 ± 0	13.56 ± 0.09	16.64 ± 0.13	6.53 ± 0.01	36.72

				Polyunsaturated Fatty Acid		Monounsaturated Fatty Acid		Saturated Fatty Acid			SPUFA	SMUFA	SSFA	S_{total}
				$C_{18:3}$	$C_{18:2}$	$C_{18:1}$	$C_{24:1}$	$C_{14:0}$	$C_{16:0}$	$C_{18:0}$				
3	1:9	3	5500	n.d.	3.62 ± 1.01	17.06 ± 0.51	n.d.	n.d.	4.29 ± 0.05	2.2 ± 0.02	13.81 ± 0.76	17.06 ± 0.51	6.49 ± 0.04	37.36
3	1:9	3	6000	n.d.	3.11 ± 0.11	16.64 ± 0.13	n.d.	n.d.	4.32 ± 0.01	2.21 ± 0.01	13.56 ± 0.09	16.64 ± 0.13	6.53 ± 0.01	36.72
Effect of Catalyst Concentration														
0	1:9	3	4000	n.d.	2.12 ± 0.73	16.98 ± 0.32	n.d.	n.d.	4.32 ± 0.03	2.21 ± 0.01	12.81 ± 0.55	16.98 ± 0.32	6.53 ± 0.02	36.33
0.5	1:9	3	4000	n.d.	5.29 ± 0.1	18.65 ± 0.05	n.d.	n.d.	4.22 ± 0.01	2.16 ± 0.01	14.15 ± 0.08	18.65 ± 0.05	6.38 ± 0.01	39.17
1	1:9	3	4000	n.d.	8.08 ± 0.5	21.63 ± 1.05	n.d.	n.d.	4.2 ± 0.02	2.15 ± 0.01	15.21 ± 0.45	21.63 ± 1.05	6.35 ± 0.02	43.19
3	1:9	3	4000	n.d.	7.96 ± 0.33	21.15 ± 0.13	n.d.	n.d.	4.15 ± 0.01	2.12 ± 0.01	15.15 ± 0.18	21.15 ± 0.13	6.27 ± 0.01	42.57
5	1:9	3	4000	n.d.	3.07 ± 0.11	17.2 ± 0.32	n.d.	n.d.	4.33 ± 0.01	2.21 ± 0	13.28 ± 0.08	17.2 ± 0.32	6.54 ± 0.01	37.02
7	1:9	3	4000	n.d.	3.19 ± 0.77	17.18 ± 0.53	n.d.	n.d.	4.31 ± 0.04	2.2 ± 0.02	13.35 ± 0.58	17.18 ± 0.53	6.51 ± 0.03	37.04
9	1:9	3	4000	n.d.	3.5 ± 0.87	17.42 ± 0.48	n.d.	n.d.	4.29 ± 0.04	2.2 ± 0.02	13.5 ± 0.65	17.42 ± 0.48	6.49 ± 0.03	37.41
12	1:9	3	4000	n.d.	3.7 ± 0.99	17.6 ± 0.72	n.d.	n.d.	4.28 ± 0.06	2.19 ± 0.03	13.6 ± 0.75	17.6 ± 0.72	6.47 ± 0.05	37.66

Table 2. ANOVA and Friedman ANOVA tests and Neuman-Keuls and Tukey post hoc tests for $C_{18:2}$, $C_{18:1}$, $C_{16:0}$, and $C_{18:0}$ of T^2FD-derived FAME samples of soybean seed operated in continuous extraction mode. Significance Values below $\alpha<0.05$ are colour coded in red.

	Univariate Tests of Significance for C18:2 [mol%] (catalyst concentration) Sigma-restricted parameterization Effective hypothesis decomposition				
Effect	SS	Degr. of	MS	F	p
Intercept	428.7242	1	428.7242	922.6018	0.000000
Catalyst Concentration [%,wt/v]	107.6546	6	17.9424	38.6116	0.000000
Error	6.5057	14	0.4647		

	Univariate Tests of Significance for C18:1 [mol%] (catalyst concentration) Sigma-restricted parameterization Effective hypothesis decomposition				
Effect	SS	Degr. of	MS	F	p
Intercept	7148.180	1	7148.180	21115.55	0.000000
Catalyst Concentration [%,wt/v]	73.486	6	12.248	36.18	0.000000
Error	4.739	14	0.339		

	Univariate Tests of Significance for C16:0 [mol%] (catalyst concentration) Sigma-restricted parameterization Effective hypothesis decomposition				
Effect	SS	Degr. of	MS	F	p
Intercept	382.8662	1	382.8662	318872.0	0.000000
Catalyst Concentration [%,wt/v]	0.0828	6	0.0138	11.5	0.000102
Error	0.0168	14	0.0012		

	Univariate Tests of Significance for C18:0 [mol%] (catalyst concentration) Sigma-restricted parameterization Effective hypothesis decomposition				
Effect	SS	Degr. of	MS	F	p
Intercept	100.0667	1	100.0667	318872.0	0.000000
Catalyst Concentration [%,wt/v]	0.0217	6	0.0036	11.5	0.000102
Error	0.0044	14	0.0003		

	Univariate Tests of Significance for C18:2 [mol%] (flow rate) Sigma-restricted parameterization Effective hypothesis decomposition				
Effect	SS	Degr. of	MS	F	p
Intercept	709.9703	1	709.9703	2112.576	0.000000
Catalyst Concentration [%,wt/v]	12.3002	1	12.3002	36.600	0.000006
Flow rate [mL/min]	87.8154	4	21.9539	65.326	0.000000
Catalyst Concentration [%,wt/v]*Flow rate [mL/min]	23.3920	4	5.8480	17.401	0.000003
Error	6.7214	20	0.3361		

	Univariate Tests of Significance for C18:1 [mol%] (flow rate) Sigma-restricted parameterization Effective hypothesis decomposition				
Effect	SS	Degr. of	MS	F	p
Intercept	10211.01	1	10211.01	19219.82	0.000000
Catalyst Concentration [%,wt/v]	5.72	1	5.72	10.78	0.003723
Flow rate [mL/min]	82.68	4	20.67	38.91	0.000000
Catalyst Concentration [%,wt/v]*Flow rate [mL/min]	15.43	4	3.86	7.26	0.000879
Error	10.63	20	0.53		

Univariate Tests of Significance for C16:0 [mol%] (flow rate)
Sigma-restricted parameterization
Effective hypothesis decomposition

Effect	SS	Degr. of	MS	F	p
Intercept	546.0240	1	546.0240	393855.9	0.000000
Catalyst Concentration [%,wt/v]	0.0040	1	0.0040	2.9	0.106029
Flow rate [mL/min]	0.0427	4	0.0107	7.7	0.000635
Catalyst Concentration [%,wt/v]*Flow rate [mL/min]	0.0228	4	0.0057	4.1	0.013579
Error	0.0277	20	0.0014		

Univariate Tests of Significance for C18:0 [mol%] (flow rate)
Sigma-restricted parameterization
Effective hypothesis decomposition

Effect	SS	Degr. of	MS	F	p
Intercept	142.7100	1	142.7100	393855.9	0.000000
Catalyst Concentration [%,wt/v]	0.0010	1	0.0010	2.9	0.106029
Flow rate [mL/min]	0.0112	4	0.0028	7.7	0.000635
Catalyst Concentration [%,wt/v]*Flow rate [mL/min]	0.0060	4	0.0015	4.1	0.013579
Error	0.0072	20	0.0004		

Univariate Tests of Significance for C18:2 [mol%] (rotational speed)
Sigma-restricted parameterization
Effective hypothesis decomposition

Effect	SS	Degr. of	MS	F	p
Intercept	909.5415	1	909.5415	1887.729	0.000000
Catalyst Concentration [%,wt/v]	0.4233	1	0.4233	0.879	0.354824
Rotational speed [rpm]	109.0713	8	13.6339	28.297	0.000000
Catalyst Concentration [%,wt/v]*Rotational speed [rpm]	1.8766	8	0.2346	0.487	0.857375
Error	17.3454	36	0.4818		

Univariate Tests of Significance for C18:1 [mol%] (rotational speed)
Sigma-restricted parameterization
Effective hypothesis decomposition

Effect	SS	Degr. of	MS	F	p
Intercept	16434.75	1	16434.75	76460.31	0.000000
Catalyst Concentration [%,wt/v]	0.10	1	0.10	0.48	0.493050
Rotational speed [rpm]	109.29	8	13.66	63.56	0.000000
Catalyst Concentration [%,wt/v]*Rotational speed [rpm]	0.81	8	0.10	0.47	0.866720
Error	7.74	36	0.21		

Univariate Tests of Significance for C16:0 [mol%] (rotational speed)
Sigma-restricted parameterization
Effective hypothesis decomposition

Effect	SS	Degr. of	MS	F	p
Intercept	996.0845	1	996.0845	890393.0	0.000000
Catalyst Concentration [%,wt/v]	0.0082	1	0.0082	7.4	0.010112
Rotational speed [rpm]	0.1065	8	0.0133	11.9	0.000000
Catalyst Concentration [%,wt/v]*Rotational speed [rpm]	0.0060	8	0.0007	0.7	0.714886
Error	0.0403	36	0.0011		

Univariate Tests of Significance for C18:0 [mol%] (rotational speed)
Sigma-restricted parameterization
Effective hypothesis decomposition

Effect	SS	Degr. of	MS	F	p
Intercept	260.3388	1	260.3388	890393.0	0.000000
Catalyst Concentration [%,wt/v]	0.0022	1	0.0022	7.4	0.010112
Rotational speed [rpm]	0.0278	8	0.0035	11.9	0.000000
Catalyst Concentration [%,wt/v]*Rotational speed [rpm]	0.0016	8	0.0002	0.7	0.714886
Error	0.0105	36	0.0003		

Univariate Tests of Significance for C18:2 [mol%] (biomass-mthanol ratio)
Sigma-restricted parameterization
Effective hypothesis decomposition

Effect	SS	Degr. of	MS	F	p
Intercept	2072.992	1	2072.992	4024.521	0.000000
Catalyst Concentration [%,wt/v]	0.148	1	0.148	0.287	0.598078
Soybean Seed : Methanol Ratio (wt/v)	9.345	4	2.336	4.535	0.009046
Catalyst Concentration [%,wt/v]*Biomass:Methanol ratio	8.562	4	2.140	4.155	0.013071
Error	10.302	20	0.515		

Univariate Tests of Significance for C18:1 [mol%] (biomass-mthanol ratio)
Sigma-restricted parameterization
Effective hypothesis decomposition

Effect	SS	Degr. of	MS	F	p
Intercept	14671.73	1	14671.73	4373.906	0.000000
Catalyst Concentration [%,wt/v]	11.65	1	11.65	3.474	0.077093
Soybean Seed : Methanol Ratio (wt/v)	36.33	4	9.08	2.707	0.059577
Catalyst Concentration [%,wt/v]*Biomass:Methanol ratio	25.60	4	6.40	1.908	0.148412
Error	67.09	20	3.35		

Univariate Tests of Significance for C16:0 [mol%] (biomass-mthanol ratio)
Sigma-restricted parameterization
Effective hypothesis decomposition

Effect	SS	Degr. of	MS	F	p
Intercept	536.6721	1	536.6721	5248.224	0.000000
Catalyst Concentration [%,wt/v]	0.3209	1	0.3209	3.138	0.091731
Soybean Seed : Methanol Ratio (wt/v)	0.2568	4	0.0642	0.628	0.648269
Catalyst Concentration [%,wt/v]*Biomass:Methanol ratio	0.3422	4	0.0856	0.837	0.517914
Error	2.0452	20	0.1023		

Univariate Tests of Significance for C18:0 [mol%] (biomass-mthanol ratio)
Sigma-restricted parameterization
Effective hypothesis decomposition

Effect	SS	Degr. of	MS	F	p
Intercept	140.2658	1	140.2658	5248.224	0.000000
Catalyst Concentration [%,wt/v]	0.0839	1	0.0839	3.138	0.091731
Soybean Seed : Methanol Ratio (wt/v)	0.0671	4	0.0168	0.628	0.648269
Catalyst Concentration [%,wt/v]*Biomass:Methanol ratio	0.0894	4	0.0224	0.837	0.517914
Error	0.5345	20	0.0267		

Tests of Homogeneity of Variances (catalyst concentration)
Effect: "Catalyst Concentration [%,wt/v]"

	Hartley	Cochran	Bartlett	df	p
C18:2 [mol%]	81.77869	0.303730	6.818138	6	0.337994

Tests of Homogeneity of Variances (catalyst concentration)
Effect: "Catalyst Concentration [%,wt/v]"

	Hartley	Cochran	Bartlett	df	p
C18:1 [mol%]	65.82326	0.468077	7.270334	6	0.296569

Tests of Homogeneity of Variances (catalyst concentration)
Effect: "Catalyst Concentration [%,wt/v]"

	Hartley	Cochran	Bartlett	df	p
C16:0 [mol%]	115.7952	0.407571	10.39536	6	0.108960

Tests of Homogeneity of Variances (catalyst concentration)
Effect: "Catalyst Concentration [%,wt/v]"

	Hartley	Cochran	Bartlett	df	p
C18:0 [mol%]	115.7952	0.407571	10.39536	6	0.108960

Tests of Homogeneity of Variances (flow rate)
Effect: "Catalyst Concentration [%,wt/v]"*"Flow rate [mL/min]"

	Hartley	Cochran	Bartlett	df	p
C18:2 [mol%]	135.4904	0.506496	16.20019	9	0.062817

Tests of Homogeneity of Variances (flow rate)
Effect: "Catalyst Concentration [%,wt/v]"*"Flow rate [mL/min]"

	Hartley	Cochran	Bartlett	df	p
C18:1 [mol%]	82.86884	0.466645	20.19620	9	0.016739

Tests of Homogeneity of Variances (flow rate)
Effect: "Catalyst Concentration [%,wt/v]"*"Flow rate [mL/min]"

	Hartley	Cochran	Bartlett	df	p
C16:0 [mol%]	432.8970	0.702969	26.13317	9	0.001943

Tests of Homogeneity of Variances (flow rate)
Effect: "Catalyst Concentration [%,wt/v]"*"Flow rate [mL/min]"

	Hartley	Cochran	Bartlett	df	p
C18:0 [mol%]	432.8970	0.702969	26.13317	9	0.001943

Tests of Homogeneity of Variances (rotational speed)
Effect: "Catalyst Concentration [%,wt/v]"*"Rotational speed [rpm]"

	Hartley	Cochran	Bartlett	df	p
C18:2 [mol%]	193.0064	0.289834	28.97299	17	0.034776

Tests of Homogeneity of Variances (rotational speed)
Effect: "Catalyst Concentration [%,wt/v]"*"Rotational speed [rpm]"

	Hartley	Cochran	Bartlett	df	p
C18:1 [mol%]	5480.216	0.286688	44.39611	17	0.000299

	Tests of Homogeneity of Variances (rotational speed) Effect: "Catalyst Concentration [%,wt/v]"*"Rotational speed [rpm]"				
	Hartley	Cochran	Bartlett	df	p
C16:0 [mol%]	24692.86	0.221705	31.35722	17	0.018064

	Tests of Homogeneity of Variances (biomass-mthanol ratio) Effect: "Catalyst Concentration [%,wt/v]*Biomass:Methanol ratio"				
	Hartley	Cochran	Bartlett	df	p
C18:2 [mol%]	44.83164	0.298977	7.252392	9	0.610860

	Tests of Homogeneity of Variances (rotational speed) Effect: "Catalyst Concentration [%,wt/v]"*"Rotational speed [rpm]"				
	Hartley	Cochran	Bartlett	df	p
C18:0 [mol%]	24692.86	0.221705	31.35722	17	0.018064

Tukey HSD test; variable C18:2 [mol%] (catalyst concentration)
Approximate Probabilities for Post Hoc Tests
Error: Between MS = .46469, df = 14.000

Cell No.	Catalyst Concentration [%,wt/v]	{1}	{2}	{3}	{4}	{5}	{6}	{7}
1	0		0.000174	0.000174	0.631397	0.501626	0.237595	0.138577
2	1	0.000174		0.999986	0.000176	0.000176	0.000181	0.000188
3	3	0.000174	0.999986		0.000176	0.000178	0.000185	0.000195
4	5	0.631397	0.000176	0.000176		0.999985	0.982516	0.908100
5	7	0.501626	0.000176	0.000178	0.999985		0.997014	0.965534
6	9	0.237595	0.000181	0.000185	0.982516	0.997014		0.999823
7	12	0.138577	0.000188	0.000195	0.908100	0.965534	0.999823	

Tukey HSD test; variable C18:1 [mol%] (catalyst concentration)
Approximate Probabilities for Post Hoc Tests
Error: Between MS = .33853, df = 14.000

Cell No.	Catalyst Concentration [%,wt/v]	{1}	{2}	{3}	{4}	{5}	{6}	{7}
1	0		0.000174	0.000176	0.998988	0.999423	0.961727	0.840037
2	1	0.000174		0.944154	0.000175	0.000175	0.000176	0.000178
3	3	0.000176	0.944154		0.000180	0.000180	0.000189	0.000204
4	5	0.998988	0.000175	0.000180		1.000000	0.999030	0.976351
5	7	0.999423	0.000175	0.000180	1.000000		0.998365	0.969722
6	9	0.961727	0.000176	0.000189	0.999030	0.998365		0.999697
7	12	0.840037	0.000178	0.000204	0.976351	0.969722	0.999697	

Tukey HSD test; variable C16:0 [mol%] (catalyst concentration)
Approximate Probabilities for Post Hoc Tests
Error: Between MS = .00120, df = 14.000

Cell No.	Catalyst Concentration [%,wt/v]	{1}	{2}	{3}	{4}	{5}	{6}	{7}
1	0		0.009737	0.000510	1.000000	0.998815	0.932580	0.718822
2	1	0.009737		0.537270	0.008630	0.023144	0.064486	0.147941
3	3	0.000510	0.537270		0.000473	0.000961	0.002391	0.005559
4	5	1.000000	0.008630	0.000473		0.997506	0.912311	0.680871
5	7	0.998815	0.023144	0.000961	0.997506		0.996752	0.929569
6	9	0.932580	0.064486	0.002391	0.912311	0.996752		0.998650
7	12	0.718822	0.147941	0.005559	0.680871	0.929569	0.998650	

Tukey HSD test; variable C18:0 [mol%] (catalyst concentration)
Approximate Probabilities for Post Hoc Tests
Error: Between MS = .00031, df = 14.000

Cell No.	Catalyst Concentration [%,wt/v]	{1}	{2}	{3}	{4}	{5}	{6}	{7}
1	0		0.009737	0.000510	1.000000	0.998815	0.932580	0.718822
2	1	0.009737		0.537270	0.008630	0.023144	0.064486	0.147941
3	3	0.000510	0.537270		0.000473	0.000961	0.002391	0.005559
4	5	1.000000	0.008630	0.000473		0.997506	0.912311	0.680871
5	7	0.998815	0.023144	0.000961	0.997506		0.996752	0.929569
6	9	0.932580	0.064486	0.002391	0.912311	0.996752		0.998650
7	12	0.718822	0.147941	0.005559	0.680871	0.929569	0.998650	

Tukey HSD test; variable C18:2 [mol%] (flow rate)
Approximate Probabilities for Post Hoc Tests
Error: Between MS = .33607, df = 20.000

Cell No.	Catalyst Concentration [%,wt/v]	Flow rate [mL/min]	{1}	{2}	{3}	{4}	{5}	{6}	{7}	{8}	{9}	{10}
1	1	1		0.000494	0.843242	0.000188	0.000194	0.000179	0.000179	0.843242	0.000194	0.000190
2	1	2	0.000494		0.000192	0.616273	0.896992	0.069922	0.005472	0.000192	0.896992	0.773472
3	1	3	0.843242	0.000192		0.000179	0.000179	0.000179	0.000179	1.000000	0.000179	0.000179
4	1	4	0.000188	0.616273	0.000179		0.999904	0.917746	0.278615	0.000179	0.999904	1.000000
5	1	5	0.000194	0.896992	0.000179	0.999904		0.653556	0.109586	0.000179	1.000000	1.000000
6	3	1	0.000179	0.069922	0.000179	0.917746	0.653556		0.961208	0.000179	0.653556	0.806476
7	3	2	0.000179	0.005472	0.000179	0.278615	0.109586	0.961208		0.000179	0.109586	0.178900
8	3	3	0.843242	0.000192	1.000000	0.000179	0.000179	0.000179	0.000179		0.000179	0.000179
9	3	4	0.000194	0.896992	0.000179	0.999904	1.000000	0.653556	0.109586	0.000179		1.000000
10	3	5	0.000190	0.773472	0.000179	1.000000	1.000000	0.806476	0.178900	0.000179	1.000000	

Newman-Keuls test; variable C18:1 [mol%] (flow rate)
Approximate Probabilities for Post Hoc Tests
Error: Between MS = .53127, df = 20.000

Cell No.	Catalyst Concentration [%,wt/v]	Flow rate [mL/min]	{1}	{2}	{3}	{4}	{5}	{6}	{7}	{8}	{9}	{10}
1	1	1		0.000995	0.042504	0.001046	0.000628	0.000226	0.000237	0.101590	0.000841	0.000334
2	1	2	0.000995		0.000165	0.851448	0.977093	0.243630	0.430808	0.000170	0.962360	0.991892
3	1	3	0.042504	0.000165		0.000153	0.000180	0.000163	0.000176	1.000000	0.000137	0.000147
4	1	4	0.001046	0.851448	0.000153		0.975052	0.364116	0.482077	0.000169	0.941447	0.994614
5	1	5	0.000628	0.977093	0.000180	0.975052		0.510705	0.565992	0.000140	0.890159	0.974647
6	3	1	0.000226	0.243630	0.000163	0.364116	0.510705		0.950540	0.000176	0.475408	0.584534
7	3	2	0.000237	0.430808	0.000176	0.482077	0.565992	0.950540		0.000186	0.556757	0.622921
8	3	3	0.101590	0.000170	1.000000	0.000169	0.000140	0.000176	0.000186		0.000154	0.000180
9	3	4	0.000841	0.962360	0.000137	0.941447	0.890159	0.475408	0.556757	0.000154		0.983849
10	3	5	0.000334	0.991892	0.000147	0.994614	0.974647	0.584534	0.622921	0.000180	0.983849	

Newman-Keuls test; variable C16:0 [mol%] (flow rate)
Approximate Probabilities for Post Hoc Tests
Error: Between MS = .00139, df = 20.000

Cell No.	Catalyst Concentration [%,wt/v]	Flow rate [mL/min]	{1}	{2}	{3}	{4}	{5}	{6}	{7}	{8}	{9}	{10}
1	1	1		0.077243	0.747567	0.018440	0.071614	0.019067	0.004009	0.943193	0.092300	0.092545
2	1	2	0.077243		0.114105	0.652712	0.933284	0.443112	0.357592	0.085577	0.929276	0.942382
3	1	3	0.747567	0.114105		0.030326	0.100715	0.030480	0.006742	1.000000	0.118373	0.102692
4	1	4	0.018440	0.652712	0.030326		0.765088	0.915736	0.436551	0.024302	0.719966	0.696929
5	1	5	0.071614	0.933284	0.100715	0.765088		0.666384	0.417649	0.069115	0.781873	0.883149
6	3	1	0.019067	0.443112	0.030480	0.915736	0.666384		0.645677	0.023447	0.664946	0.668199
7	3	2	0.004009	0.357592	0.006742	0.436551	0.417649	0.645677		0.005502	0.350999	0.316377
8	3	3	0.943193	0.085577	1.000000	0.024302	0.069115	0.023447	0.005502		0.070598	0.043001
9	3	4	0.092300	0.929276	0.118373	0.719966	0.781873	0.664946	0.350999	0.070598		0.846948
10	3	5	0.092545	0.942382	0.102692	0.696929	0.883149	0.668199	0.316377	0.043001	0.846948	

Newman-Keuls test; variable C18:0 [mol%] (flow rate)
Approximate Probabilities for Post Hoc Tests
Error: Between MS = .00036, df = 20.000

Cell No.	Catalyst Concentration [%,wt/v]	Flow rate [mL/min]	{1}	{2}	{3}	{4}	{5}	{6}	{7}	{8}	{9}	{10}
1	1	1		0.077243	0.747567	0.018440	0.071614	0.019067	0.004009	0.943193	0.092300	0.092545
2	1	2	0.077243		0.114105	0.652712	0.933284	0.443112	0.357592	0.085577	0.929276	0.942382
3	1	3	0.747567	0.114105		0.030326	0.100715	0.030480	0.006742	1.000000	0.118373	0.102692
4	1	4	0.018440	0.652712	0.030326		0.765088	0.915736	0.436551	0.024302	0.719966	0.696929
5	1	5	0.071614	0.933284	0.100715	0.765088		0.666384	0.417649	0.069115	0.781873	0.883149
6	3	1	0.019067	0.443112	0.030480	0.915736	0.666384		0.645677	0.023447	0.664946	0.668199
7	3	2	0.004009	0.357592	0.006742	0.436551	0.417649	0.645677		0.005502	0.350999	0.316377
8	3	3	0.943193	0.085577	1.000000	0.024302	0.069115	0.023447	0.005502		0.070598	0.043001
9	3	4	0.092300	0.929276	0.118373	0.719966	0.781873	0.664946	0.350999	0.070598		0.846948
10	3	5	0.092545	0.942382	0.102692	0.696929	0.883149	0.668199	0.316377	0.043001	0.846948	

Newman-Keuls test; variable C18:2 [mol%] (rotational speed)
Approximate Probabilities for Post Hoc Tests
Error: Between MS = .48182, df = 36.000

Cell No.	Catalyst Concentration [%,wt/v]	Rotational speed [rpm]	{1}	{2}	{3}	{4}	{5}	{6}	{7}	{8}	{9}	{10}	{11}	{12}	{13}	{14}	{15}	{16}	{17}	{18}
1	1	2000		0.962964	0.999628	0.998109	0.000125	0.925032	0.869119	0.983317	0.888206	0.880266	0.999564	0.938478	0.953366	0.000159	0.880501	0.883526	0.928371	0.904054
2	1	2500	0.962964		0.901472	0.942861	0.000134	0.998107	0.951844	0.959207	0.732990	0.948278	0.919816	0.995186	0.962936	0.000127	0.900950	0.981035	0.996975	0.993484
3	1	3000	0.999628	0.901472		0.994337	0.000132	0.666547	0.815704	0.999766	0.807005	0.999044	0.941133	0.781132	0.857140	0.000130	0.815272	0.843658	0.490311	0.875758
4	1	3500	0.998109	0.942861	0.994337		0.000132	0.868691	0.840856	0.998043	0.854908	0.987042	0.978108	0.898640	0.925725	0.000125	0.850184	0.859562	0.854278	0.884541
5	1	4000	0.000125	0.000134	0.000132	0.000132		0.000153	0.000145	0.000127	0.000141	0.000159	0.000130	0.000179	0.000127	0.829328	0.000138	0.000161	0.000140	0.000167
6	1	4500	0.925032	0.998107	0.666547	0.868691	0.000153		0.991592	0.942362	0.984863	0.917785	0.784825	0.935754	0.990978	0.000140	0.989545	0.995550	0.868993	0.998049
7	1	5000	0.869119	0.951844	0.815704	0.840856	0.000145	0.991592		0.840093	0.981633	0.825344	0.819089	0.988687	0.977998	0.000138	0.927302	0.980888	0.987030	0.999720
8	1	5500	0.983317	0.959207	0.999766	0.998043	0.000127	0.942362	0.840093		0.872840	0.981597	0.999621	0.945529	0.953667	0.000121	0.858262	0.851786	0.955822	0.872082
9	1	6000	0.888206	0.732990	0.807005	0.854908	0.000141	0.984863	0.981633	0.872840		0.854617	0.823976	0.971457	0.919486	0.000134	0.927426	0.996823	0.982452	0.999602
10	3	2000	0.880266	0.948278	0.999044	0.987042	0.000159	0.917785	0.825344	0.981597	0.854617		0.997869	0.926326	0.939392	0.000127	0.841915	0.839656	0.929343	0.862471
11	3	2500	0.999564	0.919816	0.941133	0.978108	0.000130	0.784825	0.819089	0.999621	0.823976	0.997869		0.844913	0.891273	0.000132	0.824532	0.842530	0.722654	0.871717
12	3	3000	0.938478	0.995186	0.781132	0.898640	0.000179	0.935754	0.988687	0.945529	0.971457	0.926326	0.844913		0.962486	0.000153	0.983687	0.994670	0.966900	0.997906
13	3	3500	0.953366	0.962936	0.857140	0.925725	0.000127	0.990978	0.977998	0.953667	0.919486	0.939392	0.891273	0.962486		0.000179	0.962499	0.990489	0.990985	0.996486
14	3	4000	0.000159	0.000127	0.000130	0.000125	0.829328	0.000140	0.000138	0.000121	0.000134	0.000127	0.000132	0.000153	0.000179		0.000141	0.000145	0.000132	0.000161
15	3	4500	0.880501	0.900950	0.815272	0.850184	0.000138	0.989545	0.927302	0.858262	0.927426	0.841915	0.824532	0.983687	0.962499	0.000141		0.992656	0.985750	0.999491
16	3	5000	0.883526	0.981035	0.843658	0.859562	0.000161	0.995550	0.980888	0.851786	0.996823	0.839656	0.842530	0.994670	0.990489	0.000145	0.992656		0.991981	1.000000
17	3	5500	0.928371	0.996975	0.490311	0.854278	0.000140	0.868993	0.987030	0.955822	0.982452	0.929343	0.722654	0.966900	0.990985	0.000132	0.985750	0.991981		0.995753
18	3	6000	0.904054	0.993484	0.875758	0.884541	0.000167	0.998049	0.999720	0.872082	0.999602	0.862471	0.871717	0.997906	0.996486	0.000161	0.999491	1.000000	0.995753	

Newman-Keuls test; variable C18:1 [mol%] (rotational speed)
Approximate Probabilities for Post Hoc Tests
Error: Between MS = .21494, df = 36.000

Cell No.	Catalyst Concentration [%,wt/v]	Rotational speed [rpm]	{1}	{2}	{3}	{4}	{5}	{6}	{7}	{8}	{9}	{10}	{11}	{12}	{13}	{14}	{15}	{16}	{17}	{18}
1	1	2000		0.931013	0.862815	0.952122	0.000125	0.836947	0.362030	0.867027	0.343965	0.910242	0.978828	0.731963	0.900688	0.000159	0.889476	0.733671	0.844467	0.694616
2	1	2500	0.931013		0.980303	0.979420	0.000179	0.951581	0.745384	0.993800	0.759618	0.929621	0.932527	0.976760	0.972278	0.000153	0.943200	0.954989	0.994082	0.911754
3	1	3000	0.862815	0.980303		0.991540	0.000130	0.955605	0.615219	0.894402	0.602216	0.920980	0.951471	0.863465	0.953151	0.000132	0.972775	0.915687	0.764686	0.886126
4	1	3500	0.952122	0.979420	0.991540		0.000127	0.870519	0.685055	0.999207	0.712191	0.947564	0.947250	0.987599	0.998025	0.000179	0.765913	0.920409	0.998612	0.841150
5	1	4000	0.000125	0.000179	0.000130	0.000127		0.000141	0.000161	0.000140	0.000167	0.000159	0.000127	0.000132	0.000153	0.214679	0.000134	0.000145	0.000132	0.000138
6	1	4500	0.836947	0.951581	0.955605	0.870519	0.000141		0.768941	0.987533	0.830601	0.816185	0.805999	0.936397	0.979474	0.000134	0.840697	0.943727	0.985071	0.747423
7	1	5000	0.362030	0.745384	0.615219	0.685055	0.000161	0.768941		0.797093	0.934794	0.326926	0.306986	0.542333	0.785920	0.000145	0.768349	0.524905	0.759192	0.797967
8	1	5500	0.867027	0.993800	0.894402	0.999207	0.000140	0.987533	0.797093		0.796234	0.884883	0.901819	0.923694	0.943260	0.000132	0.992411	0.977214	0.882405	0.959282
9	1	6000	0.343965	0.759618	0.602216	0.712191	0.000167	0.830601	0.934794	0.796234		0.307665	0.286510	0.525098	0.791345	0.000161	0.808248	0.750617	0.752668	0.886623
10	3	2000	0.910242	0.929621	0.920980	0.947564	0.000159	0.816185	0.326926	0.884883	0.307665		0.933765	0.890775	0.906070	0.000127	0.876763	0.699001	0.881751	0.662560
11	3	2500	0.978828	0.932527	0.951471	0.947250	0.000127	0.805999	0.306986	0.901819	0.286510	0.933765		0.947952	0.914551	0.000121	0.871992	0.678889	0.908922	0.645176
12	3	3000	0.731963	0.976760	0.863465	0.987599	0.000132	0.936397	0.542333	0.923694	0.525098	0.890775	0.947952		0.956107	0.000125	0.961541	0.878481	0.883481	0.846734
13	3	3500	0.900688	0.972278	0.953151	0.998025	0.000153	0.979474	0.785920	0.943260	0.791345	0.906070	0.914551	0.956107		0.000140	0.983652	0.972061	0.973564	0.946838
14	3	4000	0.000159	0.000153	0.000132	0.000179	0.214679	0.000134	0.000145	0.000132	0.000161	0.000127	0.000121	0.000125	0.000140		0.000127	0.000138	0.000130	0.000141
15	3	4500	0.889476	0.943200	0.972775	0.765913	0.000134	0.840697	0.768349	0.992411	0.808248	0.876763	0.871992	0.961541	0.983652	0.000127		0.951978	0.991647	0.858575
16	3	5000	0.733671	0.954989	0.915687	0.920409	0.000145	0.943727	0.524905	0.977214	0.750617	0.699001	0.678889	0.878481	0.972061	0.000138	0.951978		0.969001	1.000000
17	3	5500	0.844467	0.994082	0.764686	0.998612	0.000132	0.985071	0.759192	0.882405	0.752668	0.881751	0.908922	0.883481	0.973564	0.000130	0.991647	0.969001		0.950538
18	3	6000	0.694616	0.911754	0.886126	0.841150	0.000138	0.747423	0.797967	0.959282	0.886623	0.662560	0.645176	0.846734	0.946838	0.000141	0.858575	1.000000	0.950538	

Newman-Keuls test; variable C16:0 [mol%] (rotational speed)
Approximate Probabilities for Post Hoc Tests
Error: Between MS = .00112, df = 36.000

Cell No.	Catalyst Concentration [%,wt/v]	Rotational speed [rpm]	{1}	{2}	{3}	{4}	{5}	{6}	{7}	{8}	{9}	{10}	{11}	{12}	{13}	{14}	{15}	{16}	{17}	{18}
1	1	2000		0.956893	0.997137	0.800671	0.010696	0.984187	0.878871	0.943436	0.895658	0.853413	0.876563	0.987428	0.994246	0.000214	0.862063	0.987432	0.995783	0.951711
2	1	2500	0.956893		0.961311	0.924276	0.002147	0.751767	0.704454	0.935229	0.895654	0.543129	0.606455	0.956782	0.958779	0.000149	0.961717	0.864855	0.940940	0.947477
3	1	3000	0.997137	0.961311		0.999593	0.010217	0.991137	0.860690	0.999098	0.857565	0.736106	0.657556	0.990321	0.952152	0.000177	0.995010	0.996403	0.877286	0.994027
4	1	3500	0.800671	0.924276	0.999593		0.017400	0.969173	0.811822	0.943832	0.825619	0.916067	0.927908	0.996921	0.998877	0.000221	0.903594	0.976559	0.999122	0.944755
5	1	4000	0.010696	0.002147	0.010217	0.017400		0.004612	0.000867	0.017013	0.000832	0.017853	0.032601	0.013556	0.012338	0.062852	0.007905	0.006946	0.009831	0.006568
6	1	4500	0.984187	0.751767	0.991137	0.969173	0.004612		0.764269	0.977413	0.868853	0.717191	0.770416	0.988182	0.989694	0.000149	0.985032	0.846137	0.984566	0.972411
7	1	5000	0.878871	0.704454	0.860690	0.811822	0.000867	0.764269		0.822859	0.948220	0.335739	0.393410	0.859106	0.858813	0.000162	0.896739	0.806471	0.813526	0.884548
8	1	5500	0.943436	0.935229	0.999098	0.943832	0.017013	0.977413	0.822859		0.830639	0.903209	0.909556	0.996362	0.996770	0.000209	0.958453	0.985668	0.998364	0.970009
9	1	6000	0.895658	0.895654	0.857565	0.825619	0.000832	0.868853	0.948220	0.830639		0.323372	0.382136	0.862109	0.858462	0.000169	0.918549	0.870024	0.806930	0.917351
10	3	2000	0.853413	0.543129	0.736106	0.916067	0.017853	0.717191	0.335739	0.903209	0.323372		0.884011	0.853215	0.812788	0.000371	0.807583	0.797386	0.662883	0.778704
11	3	2500	0.876563	0.606455	0.657556	0.927908	0.032601	0.770416	0.393410	0.909556	0.382136	0.884011		0.848510	0.784515	0.000469	0.840398	0.839588	0.474896	0.818932
12	3	3000	0.987428	0.956782	0.990321	0.996921	0.013556	0.988182	0.859106	0.996362	0.862109	0.853215	0.848510		0.942376	0.000187	0.986361	0.994018	0.991511	0.988002
13	3	3500	0.994246	0.958779	0.952152	0.998877	0.012338	0.989694	0.858813	0.996770	0.858462	0.812788	0.784515	0.942376		0.000189	0.991905	0.995337	0.974662	0.991608
14	3	4000	0.000214	0.000149	0.000177	0.000221	0.062852	0.000149	0.000162	0.000209	0.000169	0.000371	0.000469	0.000187	0.000189		0.000150	0.000159	0.000185	0.000151
15	3	4500	0.862063	0.961717	0.995010	0.903594	0.007905	0.985032	0.896739	0.958453	0.918549	0.807583	0.840398	0.986361	0.991905	0.000150		0.986916	0.992420	0.901325
16	3	5000	0.987432	0.864855	0.996403	0.976559	0.006946	0.846137	0.806471	0.985668	0.870024	0.797386	0.839588	0.994018	0.995337	0.000159	0.986916		0.993393	0.976264
17	3	5500	0.995783	0.940940	0.877286	0.999122	0.009831	0.984566	0.813526	0.998364	0.806930	0.662883	0.474896	0.991511	0.974662	0.000185	0.992420	0.993393		0.990365
18	3	6000	0.951711	0.947477	0.994027	0.944755	0.006568	0.972411	0.884548	0.970009	0.917351	0.778704	0.818932	0.988002	0.991608	0.000151	0.901325	0.976264	0.990365	

Newman-Keuls test; variable C18:0 [mol%] (rotational speed)
Approximate Probabilities for Post Hoc Tests
Error: Between MS = .00029, df = 36.000

Cell No.	Catalyst Concentration [%,wt/v]	Rotational speed [rpm]	{1}	{2}	{3}	{4}	{5}	{6}	{7}	{8}	{9}	{10}	{11}	{12}	{13}	{14}	{15}	{16}	{17}	{18}
1	1	2000		0.956893	0.997137	0.800671	0.010696	0.984187	0.878871	0.943436	0.895658	0.853413	0.876563	0.987428	0.994246	0.000214	0.862063	0.987432	0.995783	0.951711
2	1	2500	0.956893		0.961311	0.924276	0.002147	0.751767	0.704454	0.935229	0.895654	0.543129	0.606455	0.956782	0.958779	0.000149	0.961717	0.864855	0.940940	0.947477
3	1	3000	0.997137	0.961311		0.999593	0.010217	0.991137	0.860690	0.999098	0.857565	0.736106	0.657556	0.990321	0.952152	0.000177	0.995010	0.996403	0.877286	0.994027
4	1	3500	0.800671	0.924276	0.999593		0.017400	0.969173	0.811822	0.943832	0.825619	0.916067	0.927908	0.996921	0.998877	0.000221	0.903594	0.976559	0.999122	0.944755
5	1	4000	0.010696	0.002147	0.010217	0.017400		0.004612	0.000867	0.017013	0.000832	0.017853	0.032601	0.013556	0.012338	0.062852	0.007905	0.006946	0.009831	0.006568
6	1	4500	0.984187	0.751767	0.991137	0.969173	0.004612		0.764269	0.977413	0.868853	0.717191	0.770416	0.988182	0.989694	0.000149	0.985032	0.846137	0.984566	0.972411
7	1	5000	0.878871	0.704454	0.860690	0.811822	0.000867	0.764269		0.822859	0.948220	0.335739	0.393410	0.859106	0.858813	0.000162	0.896739	0.806471	0.813526	0.884548
8	1	5500	0.943436	0.935229	0.999098	0.943832	0.017013	0.977413	0.822859		0.830639	0.903209	0.909556	0.996362	0.996770	0.000209	0.958453	0.985668	0.998364	0.970009
9	1	6000	0.895658	0.895654	0.857565	0.825619	0.000832	0.868853	0.948220	0.830639		0.323372	0.382136	0.862109	0.858462	0.000169	0.918549	0.870024	0.806930	0.917351
10	3	2000	0.853413	0.543129	0.736106	0.916067	0.017853	0.717191	0.335739	0.903209	0.323372		0.884011	0.853215	0.812788	0.000371	0.807583	0.797386	0.662883	0.778704
11	3	2500	0.876563	0.606455	0.657556	0.927908	0.032601	0.770416	0.393410	0.909556	0.382136	0.884011		0.848510	0.784515	0.000469	0.840398	0.839588	0.474896	0.818932
12	3	3000	0.987428	0.956782	0.990321	0.996921	0.013556	0.988182	0.859106	0.996362	0.862109	0.853215	0.848510		0.942376	0.000187	0.986361	0.994018	0.991511	0.988002
13	3	3500	0.994246	0.958779	0.952152	0.998877	0.012338	0.989694	0.858813	0.996770	0.858462	0.812788	0.784515	0.942376		0.000189	0.991905	0.995337	0.974662	0.991608
14	3	4000	0.000214	0.000149	0.000177	0.000221	0.062852	0.000149	0.000162	0.000209	0.000169	0.000371	0.000469	0.000187	0.000189		0.000150	0.000159	0.000185	0.000151
15	3	4500	0.862063	0.961717	0.995010	0.903594	0.007905	0.985032	0.896739	0.958453	0.918549	0.807583	0.840398	0.986361	0.991905	0.000150		0.986916	0.992420	0.901325
16	3	5000	0.987432	0.864855	0.996403	0.976559	0.006946	0.846137	0.806471	0.985668	0.870024	0.797386	0.839588	0.994018	0.995337	0.000159	0.986916		0.993393	0.976264
17	3	5500	0.995783	0.940940	0.877286	0.999122	0.009831	0.984566	0.813526	0.998364	0.806930	0.662883	0.474896	0.991511	0.974662	0.000185	0.992420	0.993393		0.990365
18	3	6000	0.951711	0.947477	0.994027	0.944755	0.006568	0.972411	0.884548	0.970009	0.917351	0.778704	0.818932	0.988002	0.991608	0.000151	0.901325	0.976264	0.990365	

Tukey HSD test; variable C18:2 [mol%] (biomass-mthanol ratio)
Approximate Probabilities for Post Hoc Tests
Error: Between MS = .51509, df = 20.000

Cell No.	Catalyst Concentration [%,wt/v]	Soybean Seed : Methanol Ratio (wt/v)	{1}	{2}	{3}	{4}	{5}	{6}	{7}	{8}	{9}	{10}
1	1	1:6		0.985648	0.067334	0.951134	0.999370	0.475090	0.954297	1.000000	0.999906	0.999935
2	1	1:9	0.985648		0.399374	0.428685	0.999997	0.967030	1.000000	0.997690	0.844365	0.854722
3	1	1:12	0.067334	0.399374		0.004735	0.233112	0.968717	0.520397	0.105891	0.022327	0.023443
4	1	1:15	0.951134	0.428685	0.004735		0.643169	0.056186	0.319443	0.878199	0.998962	0.998677
5	1	1:18	0.999370	0.999997	0.233112	0.643169		0.860201	0.999852	0.999980	0.960512	0.964828
6	3	1:6	0.475090	0.967030	0.968717	0.056186	0.860201		0.990827	0.616680	0.216109	0.224579
7	3	1:9	0.954297	1.000000	0.520397	0.319443	0.999852	0.990827		0.987735	0.735862	0.748923
8	3	1:12	1.000000	0.997690	0.105891	0.878199	0.999980	0.616680	0.987735		0.998302	0.998667
9	3	1:15	0.999906	0.844365	0.022327	0.998962	0.960512	0.216109	0.735862	0.998302		1.000000
10	3	1:18	0.999935	0.854722	0.023443	0.998677	0.964828	0.224579	0.748923	0.998667	1.000000	

Table 3. ANOVA and Friedman ANOVA tests and Tukey post hoc tests for FA to FAME conversion efficiency of T^2FD-derived FAME samples of soybean seed operated in continuous mode. Significance Values below $\alpha<0.05$ are colour coded in red.

	Univariate Tests of Significance for FA to FAME Conversion Efficiency (%) (Spreadsheet4) Sigma-restricted parameterization Effective hypothesis decomposition				
Effect	SS	Degr. of	MS	F	p
Intercept	146194.6	1	146194.6	350664.0	0.00
Catalyst Concentration (%,wt/v)	23971.6	6	3995.3	9583.1	0.00
Error	5.8	14	0.4		

	Univariate Tests of Significance for FA to FAME Conversion Efficiency (%) (Spreadsheet19) Sigma-restricted parameterization Effective hypothesis decomposition				
Effect	SS	Degr. of	MS	F	p
Intercept	287236.8	1	287236.8	545291.8	0.000000
Catalyst Concentration (%,wt/v)	1.0	1	1.0	2.0	0.176644
Soybean Seed : Methanol Ratio	1.6	4	0.4	0.8	0.561490
Catalyst Concentration (%,wt/v)*Soybean Seed : Methanol Ratio	6.7	4	1.7	3.2	0.036000
Error	10.5	20	0.5		

	Univariate Tests of Significance for FA to FAME Conversion Efficiency (%) (Spreadsheet15) Sigma-restricted parameterization Effective hypothesis decomposition				
Effect	SS	Degr. of	MS	F	p
Intercept	273294.0	1	273294.0	67435.94	0.000000
Catalyst Concentration (%,wt/v)	159.7	1	159.7	39.39	0.000004
Flow Rate (mL/min)	148.6	4	37.1	9.16	0.000224
Catalyst Concentration (%,wt/v)*Flow Rate (mL/min)	131.6	4	32.9	8.12	0.000465
Error	81.1	20	4.1		

	Univariate Tests of Significance for FA to FAME Conversion Efficiency (%) (Spreadsheet11) Sigma-restricted parameterization Effective hypothesis decomposition				
Effect	SS	Degr. of	MS	F	p
Intercept	511049.7	1	511049.7	375819.0	0.000000
Catalyst Concentration (%,wt/v)	3.1	1	3.1	2.3	0.139320
Rotational Speed (rpm)	26.1	8	3.3	2.4	0.034936
Catalyst Concentration (%,wt/v)*Rotational Speed (rpm)	23.5	8	2.9	2.2	0.055212
Error	49.0	36	1.4		

	Tests of Homogeneity of Variances (Spreadsheet4) Effect: "Catalyst Concentration (%,wt/v)"				
	Hartley	Cochran	Bartlett	df	p
FA to FAME Conversion Efficiency (%)		0.598581	4.534706	5	0.475253

	Tests of Homogeneity of Variances (Spreadsheet19) Effect: "Catalyst Concentration (%,wt/v)"*"Soybean Seed : Methanol Ratio"				
	Hartley	Cochran	Bartlett	df	p
FA to FAME Conversion Efficiency (%)		0.394306	8.176891	8	0.416385

	Tests of Homogeneity of Variances (Spreadsheet15) Effect: "Catalyst Concentration (%,wt/v)"*"Flow Rate (mL/min)"				
	Hartley	Cochran	Bartlett	df	p
FA to FAME Conversion Efficiency (%)		0.528030	10.10030	7	0.182961

	Tests of Homogeneity of Variances (Spreadsheet11) Effect: "Catalyst Concentration (%,wt/v)"*"Rotational Speed (rpm)"				
	Hartley	Cochran	Bartlett	df	p
FA to FAME Conversion Efficiency (%)		0.272186	12.12491	14	0.596272

Tukey HSD test; variable FA to FAME Conversion Efficiency (%) (Spreadsheet4)
Approximate Probabilities for Post Hoc Tests
Error: Between MS = .41691, df = 14.000

Catalyst Concentration (%,wt/v)	{1}	{2}	{3}	{4}	{5}	{6}	{7}
0		0.000174	0.000174	0.000174	0.000174	0.000174	0.000174
1	0.000174		0.194999	0.999995	0.984500	0.913822	0.913822
3	0.000174	0.194999		0.259356	0.545144	0.742822	0.742822
5	0.000174	0.999995	0.259356		0.996476	0.962106	0.962106
7	0.000174	0.984500	0.545144	0.996476		0.999819	0.999819
9	0.000174	0.913822	0.742822	0.962106	0.999819		1.000000
12	0.000174	0.913822	0.742822	0.962106	0.999819	1.000000	

Tukey HSD test; variable FA to FAME Conversion Efficiency (%) (Spreadsheet19)
Approximate Probabilities for Post Hoc Tests
Error: Between MS = .52676, df = 20.000

Cell No.	Catalyst Concentration (%,wt/v)	Soybean Seed : Methanol Ratio	{1}	{2}	{3}	{4}	{5}	{6}	{7}	{8}	{9}	{10}
1	1	1:6		0.173694	0.999895	0.792320	0.928780	0.815682	0.999858	0.928780	0.999944	1.000000
2	1	1:9	0.173694		0.406368	0.963213	0.861872	0.954002	0.417586	0.861872	0.067415	0.278893
3	1	1:12	0.999895	0.406368		0.974008	0.997673	0.980055	1.000000	0.997673	0.984486	1.000000
4	1	1:15	0.792320	0.963213	0.974008		0.999998	1.000000	0.976820	0.999998	0.494039	0.914533
5	1	1:18	0.928780	0.861872	0.997673	0.999998		1.000000	0.998081	1.000000	0.695687	0.983152
6	3	1:6	0.815682	0.954002	0.980055	1.000000	1.000000		0.982353	1.000000	0.521590	0.928659
7	3	1:9	0.999858	0.417586	1.000000	0.976820	0.998081	0.982353		0.998081	0.982388	1.000000
8	3	1:12	0.928780	0.861872	0.997673	0.999998	1.000000	1.000000	0.998081		0.695687	0.983152
9	3	1:15	0.999944	0.067415	0.984486	0.494039	0.695687	0.521590	0.982388	0.695687		0.997944
10	3	1:18	1.000000	0.278893	1.000000	0.914533	0.983152	0.928659	1.000000	0.983152	0.997944	

Tukey HSD test; variable FA to FAME Conversion Efficiency (%) (Spreadsheet15)
Approximate Probabilities for Post Hoc Tests
Error: Between MS = 4.0526, df = 20.000

Catalyst Concentration (%,wt/v)	Flow Rate (mL/min)	{1}	{2}	{3}	{4}	{5}	{6}	{7}	{8}	{9}	{10}
1	1		0.000403	0.000202	0.000205	0.011853	0.000191	0.000187	0.000187	0.000192	0.000189
1	2	0.000403		0.985990	0.990168	0.753984	0.888591	0.677426	0.686290	0.916136	0.786438
1	3	0.000202	0.985990		1.000000	0.205435	0.999984	0.996450	0.996881	0.999997	0.999506
1	4	0.000205	0.990168	1.000000		0.224302	0.999958	0.994500	0.995116	0.999991	0.999096
1	5	0.011853	0.753984	0.205435	0.224302		0.093447	0.040859	0.042122	0.108495	0.060306
3	1	0.000191	0.888591	0.999984	0.999958	0.093447		0.999989	0.999992	1.000000	1.000000
3	2	0.000187	0.677426	0.996450	0.994500	0.040859	0.999989		1.000000	0.999953	1.000000
3	3	0.000187	0.686290	0.996881	0.995116	0.042122	0.999992	1.000000		0.999964	1.000000
3	4	0.000192	0.916136	0.999997	0.999991	0.108495	1.000000	0.999953	0.999964		0.999999
3	5	0.000189	0.786438	0.999506	0.999096	0.060306	1.000000	1.000000	1.000000	0.999999	

Tukey HSD test; variable FA to FAME Conversion Efficiency (%) (Spreadsheet11)
Approximate Probabilities for Post Hoc Tests
Error: Between MS = 1.3598, df = 36.000

Catalyst Concentration (%,wt/v)	Rotational Speed (rpm)	{1}	{2}	{3}	{4}	{5}	{6}	{7}	{8}	{9}	{10}	{11}	{12}	{13}	{14}	{15}	{16}	{17}	{18}
1	2000		1.000000	1.000000	1.000000	0.959144	0.866908	0.999951	0.044649	0.148721	0.999998	1.000000	0.999564	0.999564	1.000000	1.000000	0.989894	0.997908	0.999951
1	2500	1.000000		1.000000	1.000000	0.985813	0.934296	0.999998	0.069591	0.215257	1.000000	1.000000	0.999962	0.999962	1.000000	1.000000	0.997691	0.999702	0.999998
1	3000	1.000000	1.000000		1.000000	0.996563	0.974529	1.000000	0.107375	0.303971	1.000000	1.000000	0.999999	0.999999	1.000000	1.000000	0.999682	0.999979	1.000000
1	3500	1.000000	1.000000	1.000000		0.918814	0.790174	0.999639	0.030538	0.107294	0.999975	1.000000	0.997908	0.997908	1.000000	1.000000	0.973735	0.992609	0.999639
1	4000	0.959144	0.985813	0.996563	0.918814		1.000000	0.999997	0.787993	0.973914	0.999931	0.996563	1.000000	1.000000	0.989674	0.996402	1.000000	1.000000	0.999997
1	4500	0.866908	0.934296	0.974529	0.790174	1.000000		0.999771	0.917533	0.996439	0.998114	0.974529	0.999979	0.999979	0.946884	0.973735	1.000000	0.999999	0.999771
1	5000	0.999951	0.999998	1.000000	0.999639	0.999997	0.999771		0.315605	0.648511	1.000000	1.000000	1.000000	1.000000	0.999999	1.000000	1.000000	1.000000	1.000000
1	5500	0.044649	0.069591	0.107375	0.030538	0.787993	0.917533	0.315605		1.000000	0.222186	0.107375	0.412753	0.412753	0.077710	0.106094	0.641524	0.510544	0.315605
1	6000	0.148721	0.215257	0.303971	0.107294	0.973914	0.996439	0.648511	1.000000		0.517525	0.303971	0.755374	0.755374	0.235387	0.301149	0.919212	0.838726	0.648511
3	2000	0.999998	1.000000	1.000000	0.999975	0.999931	0.998114	1.000000	0.222186	0.517525		1.000000	1.000000	1.000000	1.000000	1.000000	0.999999	1.000000	1.000000
3	2500	1.000000	1.000000	1.000000	1.000000	0.996563	0.974529	1.000000	0.107375	0.303971	1.000000		0.999999	0.999999	1.000000	1.000000	0.999682	0.999979	1.000000
3	3000	0.999564	0.999962	0.999999	0.997908	1.000000	0.999979	1.000000	0.412753	0.755374	1.000000	0.999999		1.000000	0.999982	0.999999	1.000000	1.000000	1.000000
3	3500	0.999564	0.999962	0.999999	0.997908	1.000000	0.999979	1.000000	0.412753	0.755374	1.000000	0.999999	1.000000		0.999982	0.999999	1.000000	1.000000	1.000000
3	4000	1.000000	1.000000	1.000000	1.000000	0.989674	0.946884	0.999999	0.077710	0.235387	1.000000	1.000000	0.999982	0.999982		1.000000	0.998520	0.999834	0.999999
3	4500	1.000000	1.000000	1.000000	1.000000	0.996402	0.973735	1.000000	0.106094	0.301149	1.000000	1.000000	0.999999	0.999999	1.000000		0.999661	0.999977	1.000000
3	5000	0.989894	0.997691	0.999682	0.973735	1.000000	1.000000	1.000000	0.641524	0.919212	0.999999	0.999682	1.000000	1.000000	0.998520	0.999661		1.000000	1.000000
3	5500	0.997908	0.999702	0.999979	0.992609	1.000000	0.999999	1.000000	0.510544	0.838726	1.000000	0.999979	1.000000	1.000000	0.999834	0.999977	1.000000		1.000000
3	6000	0.999951	0.999998	1.000000	0.999639	0.999997	0.999771	1.000000	0.315605	0.648511	1.000000	1.000000	1.000000	1.000000	0.999999	1.000000	1.000000	1.000000	

Appendix Section 5.3. Continuous flow biodiesel production from wet microalgae using a hybrid thin film microfluidic platform

1. Microalgae Cultivation

Microalgae *Chloroparva pannonica* (FC40) biomass was obtained from SARDI and was grown using F2SI media which consists of 75.0 g L^{-1} $CO(NH_2)_2$, 5.0 g L^{-1} NaH_2PO_4, 2.6 g L^{-1} $FeCl_3.6H_2O$, 8.7 g L^{-1} Na-EDTA, 40 mg L^{-1} $CuSO_4.5H_2O$, 25.2 mg L^{-1} $Na_2MoO_4.2H_2O$, 88 mg L^{-1} $ZnSO_4.7H_2O$, 40 mg L^{-1} CoCl2.6H_2O, 1.44 mg L^{-1} $MnCl_2.4H_2O$. The pH was adjusted to 4.5 by adding 1 M NaOH prior to autoclaving. The vitamin content per 100 mL of MilliQ water was 10 mg vitamin B_{12}, and 10 mg biotin. A 11 L photo-bioreactor with two cool white fluorescent lamps operating for 12 hours illumination was used in this cultivation. The CO_2 was augmented only during illumination. The cells were collected after 7 days of cultivation and harvested using centrifugation (6000×*g*, 10 min), then freeze-dried, ground to 250 µm and stored in a cold room until used. Methanol, sodium hydroxide, sulfuric acid and hexane were purchased from Sigma Aldrich and were of analytical grade (AR).

2. FT-IR and ^{1}H-NMR studies

The production of biodiesel was confirmed using a FT-IR spectrophotometer (Perkin Elmer FT-IR 400) equipped with an attenuated total reflectance (ATR) probe. The biodiesel spectra were observed in the range of 4000 – 400 cm^{-1}. Following the published method, a 600 MHz Bruker spectrometer ^{1}H-NMR with typical condition of 64 scans and 1 second D1 delay was used to measure the conversion yield based on the integration value of the specific chemical shift of methoxy protons (OMe) and α-methylene protons (α-CH_2), using equation 1 below (Mello et al., 2008, Satyarthi et al., 2009, Tariq et al., 2011, Choi et al., 2015).

$$C = \frac{2A_{Me}}{3A_{CH_2}} \times 100 \text{.....} \textit{Equation 1}$$

where C = percentage conversion of triglyceride (TG) to fatty acid methyl ester, A_{Me} = integration value of the methoxy protons of methyl ester and A_{CH_2} = integration value of α-methylene protons.

Table 1. The appearance of specific peaks of triglyceride and biodiesel in FT-IR spectra.(Siatis et al., 2006)

Absorption (cm^{-1})	Functional Group	Appearance	
		Triglyceride	Biodiesel
1445	CH_3 asymmetric	-	√
1238 - 1248	O-H deformation	√	√
1200	O-CH_3 stretching	-	√
1170	C-O-C symmetric stretching; C-C stretching	√	√
1100	O-CH_2-C asymmetric, -CH_2-OH	√	-

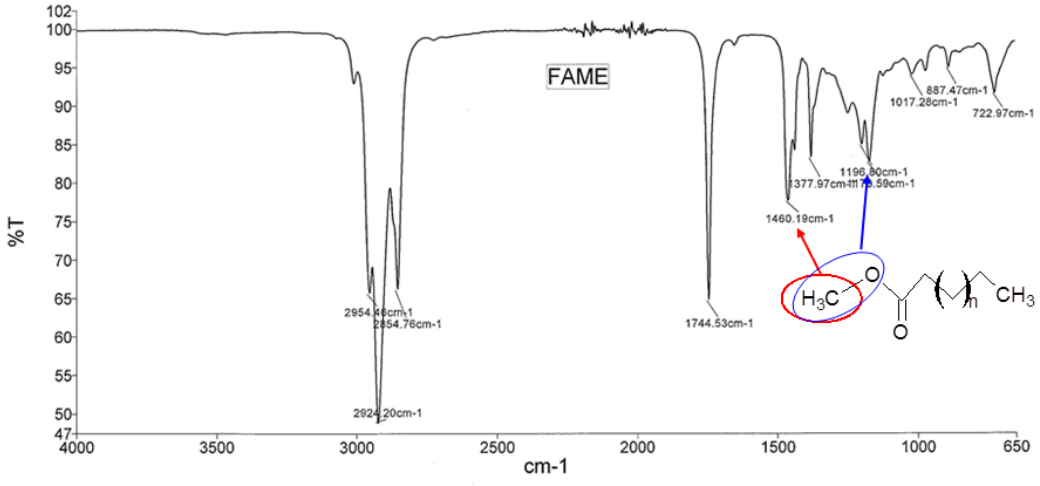

Figure 1 Representative FT-IR spectra of microalgae biodiesel produced in T^2FD-intensified DT of wet microalgae biomass.

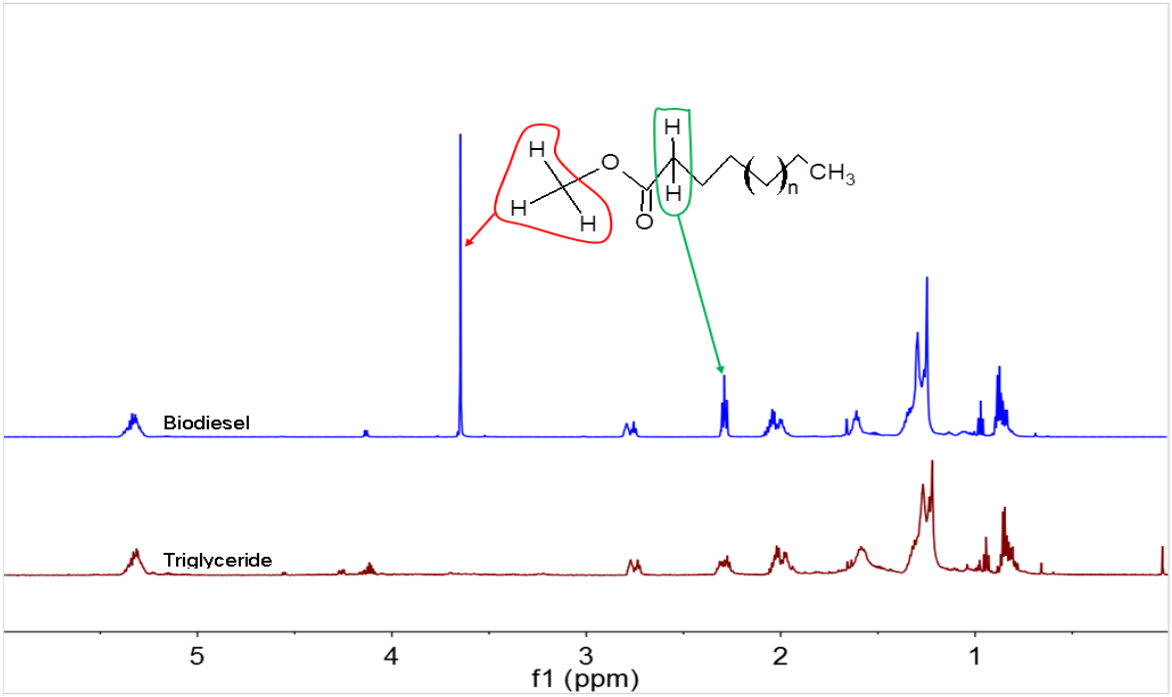

Figure 2 Comparison of ^{1}H-NMR spectra of triglyceride and biodiesel.

3. Lipid quantification

The Folch method (Folch et al., 1957) was used to quantify lipid content in the microalga *Chloroparva pannonica*. The dry biomass (0.05 g) was loaded into a conical polypropylene tube and stirred in a vortex mixer with a mixture of 1.4 mL 0.9% saline and 2 mL methanol. After standing for 5 min, 4 mL of chloroform was added to the mixture and shaken. The homogenate phase formed after 5 min standing was separated through centrifugation at 3000×*g* for 10 min. The chloroform layer containing the extracted lipid was removed and the solvent evaporated under a nitrogen stream. The mass of lipid obtained was determined gravimetrically.

The *Chloroparva pannonica* lipid content was determined to be 23.4%. Oleic acid ($C_{18:1}$) was the major constituent present in *Chloroparva pannonica*, with 30.2% of the total FAME content, followed by Linoleic acid ($C_{18:2}$) and α-Linolenic acid ($C_{18:3}$) and Palmitic acid ($C_{16:0}$) with 24.7, 21.9 and 16.7%, respectively (Table 2). The total saturated fatty acid content was 18.2%, of which palmitic acid ($C_{16:0}$) is the major compound. This profile was similar to other reported data.(Somogyi et al., 2011)

4. Scanning Electron Microscopy

SEM images of the fresh harvested microalgae biomass and solid residues after DT processing with sulfuric acid or sodium hydroxide as the catalyst were investigated using a FEI F50 Inspect FE-SEM. The dried sample was mounted on carbon tape and sputter-coated with 2 nm platinum, then examined at an accelerating voltage of 5 kV at a working distance of 19.9 mm. The images were captured at 20,000x magnification for a dwell time of 100 ms.

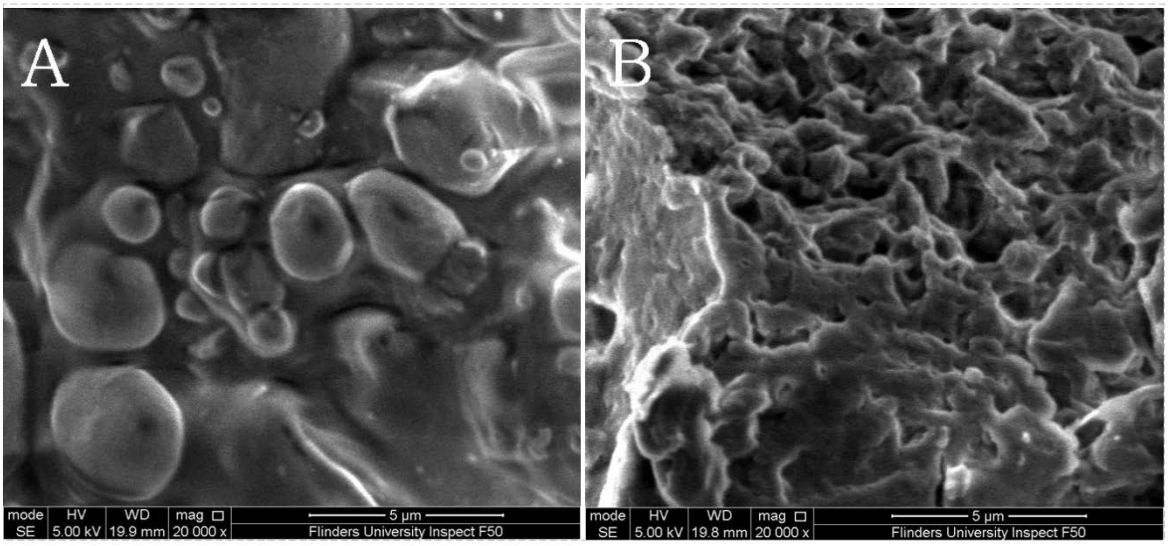

Figure 3 SEM images of microalgae *Chloroparva pannonica* biomass (A) before (reproduced from (Sitepu et al., 2018a) and (B) after T^2FD processing.

Table 2: Quantified ^{1}H-NMR spectra for C18:3, C18:1 and C16:0 of T^{2}FD-derived FAME samples of wet biomass of *Chloroparva pannonica* operated in continuous extraction mode. n.d. – not detected; b.d.l. – below detection limit.

						Polyunsaturated Fatty Acid		Monounsaturated Fatty Acid		Saturated Fatty Acid			ΣPUFA	ΣMUFA	ΣSFA	$\Sigma_{C18:3,C18:1,C16:0}$
						$C_{18:3}$	$C_{18:2}$	$C_{18:1}$	$C_{24:1}$	$C_{14:0}$	$C_{16:0}$	$C_{18:0}$				
GC	**Dry biomass non T^{2}FD**					21.9	24.7	30.2	0.7	0.4	16.7	0.7	48.6	33.1	18.2	
NMR	**Wet biomass turbo thin film device using base catalyst**															
	Ratio Biomass : MeOH (wt./v)	**Flow Rate (mL/min)**	**Rotation Speed (rpm)**	**Catalyst Conc. (wt.%/v)**	**Water Content (wt%)**											
	1:12	2	6,000	0	67.6	20.48 ± 0.9	b.d.l	7.77 ± 1.79	n.d.	n.d.	10.7 ± 0.18	n.d	n.d.	7.77 ± 1.79	n.d.	38.95
	1:12	2	6,000	0.5	67.6	22.03 ± 3.09	b.d.l	4.05 ± 4.61	n.d.	n.d.	10.66 ± 0.07	n.d	n.d.	4.05 ± 4.61	n.d.	36.74
	1:12	2	6,000	1	67.6	12.87 ± 2.89	b.d.l	17.55 ± 3.5	n.d.	n.d.	10.08 ± 0.23	n.d	n.d.	17.55 ± 3.5	n.d.	40.50
	1:12	2	6,000	3	67.6	25.06 ± 19.74	b.d.l	8.11 ± 20.14	n.d.	n.d.	11.57 ± 1.98	n.d	n.d.	8.11 ± 20.14	n.d.	44.74
	1:12	2	6,000	5	67.6	7.33 ± 0.92	b.d.l	25.5 ± 8.98	n.d.	n.d.	9.47 ± 0.86	n.d	n.d.	25.5 ± 8.98	n.d.	42.30
	1:12	2	6,000	7	67.6	11.71 ± 1.06	b.d.l	17.67 ± 0.88	n.d.	n.d.	10.03 ± 0.04	n.d	n.d.	17.67 ± 0.88	n.d.	39.41
	1:12	2	6,000	9	67.6	6.84 ± 1.21	b.d.l	25.79 ± 2.45	n.d.	n.d.	9.78 ± 0.12	n.d	n.d.	25.79 ± 2.45	n.d.	42.41
	1:12	2	6,000	12	67.6	n.d	b.d.l	n.d	n.d.	n.d.	n.d	n.d	n.d.	n.d	n.d.	NA
	1:12	1	6,000	1	67.6	12.96 ± 1.58	b.d.l	14.13 ± 2.99	n.d.	n.d.	10.02 ± 0.2	n.d	n.d.	14.13 ± 2.99	n.d.	37.11

					Polyunsaturated Fatty Acid		Monounsaturated Fatty Acid		Saturated Fatty Acid			ΣPUFA	ΣMUFA	ΣSFA	$\Sigma_{C18:3,C18:1,C16:0}$
					$C_{18:3}$	$C_{18:2}$	$C_{18:1}$	$C_{24:1}$	$C_{14:0}$	$C_{16:0}$	$C_{18:0}$				
1:12	2	6,000	1	67.6	12.87 ± 2.89	b.d.l	17.55 ± 3.5	n.d.	n.d.	10.08 ± 0.23	n.d	n.d.	17.55 ± 3.5	n.d.	40.50
1:12	3	6,000	1	67.6	15.28 ± 1.2	b.d.l	13.64 ± 1.7	n.d.	n.d.	10.3 ± 0.08	n.d	n.d.	13.64 ± 1.7	n.d.	39.22
1:12	4	6,000	1	67.6	17.21 ± 1.73	b.d.l	11.37 ± 1.35	n.d.	n.d.	10.35 ± 0.06	n.d	n.d.	11.37 ± 1.35	n.d.	38.93
1:12	5	6,000	1	67.6	14.21 ± 0.59	b.d.l	14.95 ± 0.78	n.d.	n.d.	10.26 ± 0.11	n.d	n.d.	14.95 ± 0.78	n.d.	39.42
1:12	3	2,000	1	67.6	11.68 ± 0.72	b.d.l	20.91 ± 0.6	n.d.	n.d.	10.53 ± 0.04	n.d	n.d.	20.91 ± 0.6	n.d.	43.12
1:12	3	2,500	1	67.6	11.41 ± 0.7	b.d.l	22.09 ± 0.7	n.d.	n.d.	10.57 ± 0.08	n.d	n.d.	22.09 ± 0.7	n.d.	44.07
1:12	3	3,000	1	67.6	10.87 ± 0.54	b.d.l	22.96 ± 0.67	n.d.	n.d.	10.55 ± 0.05	n.d	n.d.	22.96 ± 0.67	n.d.	44.38
1:12	3	3,500	1	67.6	10.28 ± 0.73	b.d.l	22.97 ± 0.53	n.d.	n.d.	10.48 ± 0.04	n.d	n.d.	22.97 ± 0.53	n.d.	43.73
1:12	3	4,000	1	67.6	10.4 ± 0.5	b.d.l	23.1 ± 0.81	n.d.	n.d.	10.48 ± 0.06	n.d	n.d.	23.1 ± 0.81	n.d.	43.98
1:12	3	4,500	1	67.6	10.56 ± 0.55	b.d.l	23.03 ± 1.1	n.d.	n.d.	10.5 ± 0.05	n.d	n.d.	23.03 ± 1.1	n.d.	44.09
1:12	3	5,000	1	67.6	11.49 ± 0.4	b.d.l	21.51 ± 1.01	n.d.	n.d.	10.47 ± 0.05	n.d	n.d.	21.51 ± 1.01	n.d.	43.47
1:12	3	5,500	1	67.6	11.35 ± 1.18	b.d.l	21.81 ± 1.56	n.d.	n.d.	10.5 ± 0.06	n.d	n.d.	21.81 ± 1.56	n.d.	43.66
1:12	3	6,000	1	67.6	15.28 ± 1.2	b.d.l	13.64 ± 1.7	n.d.	n.d.	10.3 ± 0.08	n.d	n.d.	13.64 ± 1.7	n.d.	39.22
1:12	3	6,500	1	67.6	14.99 ± 1.67	b.d.l	15.43 ± 1.99	n.d.	n.d.	10.3 ± 0.14	n.d	n.d.	15.43 ± 1.99	n.d.	40.72
1:12	3	7,000	1	67.6	15.22 ± 0.6	b.d.l	14.11 ± 0.76	n.d.	n.d.	10.25 ± 0.02	n.d	n.d.	14.11 ± 0.76	n.d.	39.58
1:12	3	2,000	0.5	67.6	15.13 ± 0.46	b.d.l	15.79 ± 0.54	n.d.	n.d.	10.55 ± 0.02	n.d	n.d.	15.79 ± 0.54	n.d.	41.47
1:12	3	3,000	0.5	67.6	16 ± 1.37	b.d.l	13.66 ± 1.89	n.d.	n.d.	10.5 ± 0.07	n.d	n.d.	13.66 ± 1.89	n.d.	40.16

					Polyunsaturated Fatty Acid		Monounsaturated Fatty Acid		Saturated Fatty Acid			ΣPUFA	ΣMUFA	ΣSFA	$\Sigma_{C18:3,C18:1,C16:0}$
					$C_{18:3}$	$C_{18:2}$	$C_{18:1}$	$C_{24:1}$	$C_{14:0}$	$C_{16:0}$	$C_{18:0}$				
1:12	3	4,000	0.5	67.6	17.45 ± 0.72	b.d.l	11.22 ± 0.83	n.d.	n.d.	10.51 ± 0.06	n.d	n.d.	11.22 ± 0.83	n.d.	39.18
1:12	3	5,000	0.5	67.6	17.56 ± 1.66	b.d.l	10.69 ± 2.01	n.d.	n.d.	10.49 ± 0.08	n.d	n.d.	10.69 ± 2.01	n.d.	38.74
1:12	3	2,000	0	67.6	23.63 ± 1.17	b.d.l	13.2 ± 0.89	n.d.	n.d.	10.98 ± 0.06	n.d	n.d.	13.2 ± 0.89	n.d.	47.81
1:12	3	3,000	0	67.6	24.03 ± 0.19	b.d.l	14.56 ± 1.55	n.d.	n.d.	11.14 ± 0.17	n.d	n.d.	14.56 ± 1.55	n.d.	49.73
1:12	3	4,000	0	67.6	23.83 ± 1.43	b.d.l	14.75 ± 1.01	n.d.	n.d.	11.27 ± 0.16	n.d	n.d.	14.75 ± 1.01	n.d.	49.85
1:12	3	5,000	0	67.6	23.28 ± 1.55	b.d.l	13.39 ± 1.17	n.d.	n.d.	11.32 ± 0.2	n.d	n.d.	13.39 ± 1.17	n.d.	47.99
1:6	3	4,000	1	67.6	14.19 ± 0.65	b.d.l	15.89 ± 1.19	n.d.	n.d.	10.22 ± 0.08	n.d	n.d.	15.89 ± 1.19	n.d.	40.30
1:9	3	4,000	1	67.6	14.11 ± 0.55	b.d.l	16.22 ± 0.66	n.d.	n.d.	10.24 ± 0.06	n.d	n.d.	16.22 ± 0.66	n.d.	40.57
1:15	3	4,000	1	67.6	13.66 ± 1.53	b.d.l	16.67 ± 1.25	n.d.	n.d.	10.39 ± 0.07	n.d	n.d.	16.67 ± 1.25	n.d.	40.72
1:12	3	4,000	1	67.6	10.4 ± 0.5	b.d.l	23.1 ± 0.81	n.d.	n.d.	10.48 ± 0.06	n.d	n.d.	23.1 ± 0.81	n.d.	43.98
1:18	3	4,000	1	67.6	12.32 ± 0.95	b.d.l	19.09 ± 2.58	n.d.	n.d.	10.35 ± 0.08	n.d	n.d.	19.09 ± 2.58	n.d.	41.76
1:12	3	4,000	1	67.6	10.4 ± 0.5	b.d.l	23.1 ± 0.81	n.d.	n.d.	10.48 ± 0.06	n.d	n.d.	23.1 ± 0.81	n.d.	43.98
1:12	3	4,000	1	75	15.32 ± 1.08	b.d.l	14.93 ± 1.14	n.d.	n.d.	10.6 ± 0.1	n.d	n.d.	14.93 ± 1.14	n.d.	40.85
1:12	3	4,000	1	80	15.76 ± 0.61	b.d.l	14.24 ± 0.68	n.d.	n.d.	10.51 ± 0.04	n.d	n.d.	14.24 ± 0.68	n.d.	40.51
1:12	3	4,000	1	85	16.66 ± 0.55	b.d.l	12.67 ± 0.62	n.d.	n.d.	10.53 ± 0.04	n.d	n.d.	12.67 ± 0.62	n.d.	39.86
1:12	3	4,000	1	90	16.05 ± 0.55	b.d.l	13.03 ± 0.76	n.d.	n.d.	10.31 ± 0.05	n.d	n.d.	13.03 ± 0.76	n.d.	39.39

Table 3: FA to FAME conversion efficiencies of the DT of wet biomass of *Chloroparva pannonica* in T^2FD operated in continuous extraction mode.

Ratio Biomass : MeOH (wt./v)	Flow Rate (mL/min)	Rotation Speed (rpm)	% Catalyst Concentration (wt./v)	Water Content (wt%)	Fatty Acid to FAME Conversion Efficiency (%)
Effect of catalyst concentration					
1:12	2	6,000	0	67.6	7.57 ± 1.34
1:12	2	6,000	0.5	67.6	84.04 ± 4.35
1:12	2	6,000	1	67.6	91.03 ± 1.28
1:12	2	6,000	3	67.6	93.44 ± 2.12
1:12	2	6,000	5	67.6	90.2 ± 5.07
1:12	2	6,000	7	67.6	94.46 ± 3.31
1:12	2	6,000	9	67.6	90.39 ± 2.86
1:12	2	6,000	12	67.6	52.9 ± 17.01
Effect of flow rate					
1:12	1	6,000	1	67.6	73.99 ± 8.53
1:12	2	6,000	1	67.6	91.03 ± 1.28
1:12	3	6,000	1	67.6	94.01 ± 1.19

Ratio Biomass : MeOH (wt./v)	Flow Rate (mL/min)	Rotation Speed (rpm)	% Catalyst Concentration (wt./v)	Water Content (wt%)	Fatty Acid to FAME Conversion Efficiency (%)
1:12	4	6,000	1	67.6	89.79 ± 1.96
1:12	5	6,000	1	67.6	89.75 ± 3.47
Effect of rotation speed					
1:12	3	2,000	1	67.6	91.49 ± 3.04
1:12	3	2,500	1	67.6	95.27 ± 1.65
1:12	3	3,000	1	67.6	92.49 ± 2.27
1:12	3	3,500	1	67.6	94.01 ± 2.32
1:12	3	4,000	1	67.6	96.56 ± 0.66
1:12	3	4,500	1	67.6	95.8 ± 1.54
1:12	3	5,000	1	67.6	89.43 ± 2.89
1:12	3	5,500	1	67.6	87.44 ± 3.51
1:12	3	6,000	1	67.6	94.01 ± 1.19
1:12	3	6,500	1	67.6	87.57 ± 0.55
1:12	3	7,000	1	67.6	89.49 ± 3.37
1:12	3	2,000	0.5	67.6	87.26 ± 3.42

Ratio Biomass : MeOH (wt./v)	Flow Rate (mL/min)	Rotation Speed (rpm)	% Catalyst Concentration (wt./v)	Water Content (wt%)	Fatty Acid to FAME Conversion Efficiency (%)
1:12	3	3,000	0.5	67.6	88.21 ± 1.92
1:12	3	4,000	0.5	67.6	88.19 ± 2.63
1:12	3	5,000	0.5	67.6	87.28 ± 2.1
1:12	3	2,000	0	67.6	14.39 ± 3.85
1:12	3	3,000	0	67.6	9.22 ± 2.58
1:12	3	4,000	0	67.6	8.34 ± 2.97
1:12	3	5,000	0	67.6	5.54 ± 1.57
Effect of ratio biomass to methanol					
1:6	3	4,000	1	67.6	90.75 ± 4.84
1:9	3	4,000	1	67.6	91.57 ± 2.64
1:12	3	4,000	1	67.6	96.56 ± 0.66
1:15	3	4,000	1	67.6	93.5 ± 3.37
1:18	3	4,000	1	67.6	90.48 ± 6.28
Effect of water content					
1:12	3	4,000	1	67.6	96.56 ± 0.66

Ratio Biomass : MeOH (wt./v)	Flow Rate (mL/min)	Rotation Speed (rpm)	% Catalyst Concentration (wt./v)	Water Content (wt%)	Fatty Acid to FAME Conversion Efficiency (%)
1:12	3	4,000	1	75	94.46 ± 0.98
1:12	3	4,000	1	80	90.28 ± 0.6
1:12	3	4,000	1	85	90.66 ± 1.79
1:12	3	4,000	1	90	91.58 ± 0.8

Table 4: Tukey test for C18:3, C18:1 and C16:0 of T^2FD-derived FAME samples of wet biomass of *Chloroparva pannonica* operated in continuous extraction mode. Significance Values below α<0.05 are colour coded in red.

Tukey HSD test; variable C18:3 (CC-T2FD microalgae biodiesel_FA extraction efficiency(5))
Approximate Probabilities for Post Hoc Tests
Error: Between MS = 2.5554, df = 8.0000

Cell No.	Cat. conc. [wt/v %]	{1}	{2}	{3}	{4}
1	0		0.001908	0.000247	0.000232
2	1	0.001908		0.012181	0.001169
3	5	0.000247	0.012181		0.231906
4	12	0.000232	0.001169	0.231906	

Tukey HSD test; variable C18:1 (2) (CC-T2FD microalgae biodiesel_FA extraction efficiency(5))
Approximate Probabilities for Post Hoc Tests
Error: Between MS = 32.050, df = 6.0000

Cell No.	Cat conc. [wt/v %]	{1}	{2}	{3}
1	0		0.166868	0.020237
2	1	0.166868		0.273135
3	5	0.020237	0.273135	

Tukey HSD test; variable C16:0 (CC-T2FD microalgae biodiesel_FA extraction efficiency(5))
Approximate Probabilities for Post Hoc Tests
Error: Between MS = .26648, df = 8.0000

Cell No.	Cat conc. [wt/v %]	{1}	{2}	{3}	{4}
1	0		0.505179	0.076266	0.000454
2	1	0.505179		0.505331	0.001310
3	5	0.076266	0.505331		0.006314
4	12	0.000454	0.001310	0.006314	

Tukey HSD test; variable C18:3 (Ratio-T2FD microalgae biodiesel_FA extraction efficiency)
Approximate Probabilities for Post Hoc Tests
Error: Between MS = .84607, df = 10.000

Cell No.	Ratio	{1}	{2}	{3}	{4}	{5}
1	1:18		0.432721	0.010072	0.972441	0.951982
2	1:15	0.432721		0.152932	0.198118	0.170920
3	1:12	0.010072	0.152932		0.004252	0.003690
4	1:9	0.972441	0.198118	0.004252		0.999971
5	1:6	0.951982	0.170920	0.003690	0.999971	

Tukey HSD test; variable C18:1 (Ratio-T2FD microalgae biodiesel_FA extraction efficiency)
Approximate Probabilities for Post Hoc Tests
Error: Between MS = 2.1463, df = 10.000

Cell No.	Ratio	{1}	{2}	{3}	{4}	{5}
1	1:18		0.321371	0.002360	0.995137	0.963133
2	1:15	0.321371		0.045881	0.192509	0.128956
3	1:12	0.002360	0.045881		0.001479	0.001069
4	1:9	0.995137	0.192509	0.001479		0.998585
5	1:6	0.963133	0.128956	0.001069	0.998585	

Tukey HSD test; variable C16:0 (Ratio-T2FD microalgae biodiesel_FA extraction efficiency)
Approximate Probabilities for Post Hoc Tests
Error: Between MS = .00533, df = 10.000

Cell No.	Ratio	{1}	{2}	{3}	{4}	{5}
1	1:18		0.937025	0.605121	0.165503	0.084954
2	1:15	0.937025		0.247048	0.451222	0.257874
3	1:12	0.605121	0.247048		0.017653	0.009062
4	1:9	0.165503	0.451222	0.017653		0.990711
5	1:6	0.084954	0.257874	0.009062	0.990711	

Tukey HSD test; variable C18:3 (RS-T2FD microalgae biodiesel_FA extraction efficiency)
Approximate Probabilities for Post Hoc Tests
Error: Between MS = 1.4418, df = 22.000

Cell No.	Rotational speed [rpm]	{1}	{2}	{3}	{4}	{5}	{6}	{7}	{8}	{9}	{10}	{11}
1	2000		1.000000	0.998695	0.930553	0.959715	0.983035	1.000000	0.999562	0.040428	0.074542	0.045997
2	2500	1.000000		0.999959	0.981797	0.991874	0.997783	1.000000	0.994113	0.022726	0.042895	0.025961
3	3000	0.998695	0.999959		0.999913	0.999989	1.000000	0.999861	0.890638	0.006664	0.012892	0.007639
4	3500	0.930553	0.981797	0.999913		1.000000	1.000000	0.971227	0.564909	0.001784	0.003382	0.002031
5	4000	0.959715	0.991874	0.999989	1.000000		1.000000	0.985933	0.640249	0.002314	0.004429	0.002640
6	4500	0.983035	0.997783	1.000000	1.000000	1.000000		0.995520	0.734590	0.003259	0.006293	0.003737
7	5000	1.000000	1.000000	0.999861	0.971227	0.985933	0.995520		0.996973	0.027060	0.050759	0.030880
8	5500	0.999562	0.994113	0.890638	0.564909	0.640249	0.734590	0.996973		0.168261	0.277915	0.187658
9	6000	0.040428	0.022726	0.006664	0.001784	0.002314	0.003259	0.027060	0.168261		1.000000	1.000000
10	6500	0.074542	0.042895	0.012892	0.003382	0.004429	0.006293	0.050759	0.277915	1.000000		1.000000
11	7000	0.045997	0.025961	0.007639	0.002031	0.002640	0.003737	0.030880	0.187658	1.000000	1.000000	

Tukey HSD test; variable C18:1 (RS-T2FD microalgae biodiesel_FA extraction efficiency)
Approximate Probabilities for Post Hoc Tests
Error: Between MS = 4.1087, df = 22.000

Cell No.	Rotational speed [rpm]	{1}	{2}	{3}	{4}	{5}	{6}	{7}	{8}	{9}	{10}	{11}
1	2000		0.999602	0.969838	0.969394	0.954564	0.963108	0.999999	0.996305	0.008374	0.085639	0.015914
2	2500	0.999602		0.999973	0.999971	0.999898	0.999948	0.999999	0.847754	0.001746	0.019041	0.003250
3	3000	0.969838	0.999973		1.000000	1.000000	1.000000	0.997672	0.545258	0.000628	0.005867	0.001070
4	3500	0.969394	0.999971	1.000000		1.000000	1.000000	0.997612	0.543556	0.000625	0.005831	0.001064
5	4000	0.954564	0.999898	1.000000	1.000000		1.000000	0.995262	0.495259	0.000550	0.004883	0.000911
6	4500	0.963108	0.999948	1.000000	1.000000	1.000000		0.996698	0.521272	0.000589	0.005375	0.000993
7	5000	0.999999	0.999999	0.997672	0.997612	0.995262	0.996698		0.960619	0.003732	0.040574	0.007087
8	5500	0.996305	0.847754	0.545258	0.543556	0.495259	0.521272	0.960619		0.063082	0.419275	0.111902
9	6000	0.008374	0.001746	0.000628	0.000625	0.000550	0.000589	0.003732	0.063082		0.988373	1.000000
10	6500	0.085639	0.019041	0.005867	0.005831	0.004883	0.005375	0.040574	0.419275	0.988373		0.999001
11	7000	0.015914	0.003250	0.001070	0.001064	0.000911	0.000993	0.007087	0.111902	1.000000	0.999001	

Tukey HSD test; variable C16:0 (RS-T2FD microalgae biodiesel_FA extraction efficiency)
Approximate Probabilities for Post Hoc Tests
Error: Between MS = .00497, df = 22.000

Cell No.	Rotational speed [rpm]	{1}	{2}	{3}	{4}	{5}	{6}	{7}	{8}	{9}	{10}	{11}
1	2000		0.999922	1.000000	0.998493	0.996654	0.999943	0.989943	0.822981	0.015949	0.015826	0.003138
2	2500	0.999922		1.000000	0.928516	0.901043	0.980254	0.843174	0.474479	0.004253	0.004220	0.000914
3	3000	1.000000	1.000000		0.987047	0.978140	0.998442	0.954221	0.676053	0.008856	0.008787	0.001775
4	3500	0.998493	0.928516	0.987047		1.000000	1.000000	1.000000	0.998010	0.092908	0.092270	0.020080
5	4000	0.996654	0.901043	0.978140	1.000000		1.000000	1.000000	0.999166	0.109633	0.108896	0.024182
6	4500	0.999943	0.980254	0.998442	1.000000	1.000000		0.999987	0.984831	0.054787	0.054390	0.011263
7	5000	0.989943	0.843174	0.954221	1.000000	1.000000	0.999987		0.999855	0.143252	0.142326	0.032850
8	5500	0.822981	0.474479	0.676053	0.998010	0.999166	0.984831	0.999855		0.403887	0.401948	0.120009
9	6000	0.015949	0.004253	0.008856	0.092908	0.109633	0.054787	0.143252	0.403887		1.000000	0.999512
10	6500	0.015826	0.004220	0.008787	0.092270	0.108896	0.054390	0.142326	0.401948	1.000000		0.999531
11	7000	0.003138	0.000914	0.001775	0.020080	0.024182	0.011263	0.032850	0.120009	0.999512	0.999531	

Tukey HSD test; variable C18:3 (RS-CC-FACTORIAL-T2FD microalgae biodiesel_FA extraction efficiency)
Approximate Probabilities for Post Hoc Tests
Error: Between MS = 1.4033, df = 16.000

Cell No.	Cat Conc. [%]	Rotational speed [rpm]	{1}	{2}	{3}	{4}	{5}	{6}	{7}	{8}
1	0	2000		0.981322	0.303902	0.256527	0.000175	0.000175	0.000175	0.000177
2	0	3000	0.981322		0.798727	0.738157	0.000181	0.000177	0.000179	0.000190
3	0	4000	0.303902	0.798727		1.000000	0.000340	0.000248	0.000287	0.000506
4	0	5000	0.256527	0.738157	1.000000		0.000380	0.000266	0.000313	0.000588
5	0.5	2000	0.000175	0.000181	0.000340	0.000380		0.999868	0.999999	0.999942
6	0.5	3000	0.000175	0.000177	0.000248	0.000266	0.999868		0.999999	0.992456
7	0.5	4000	0.000175	0.000179	0.000287	0.000313	0.999999	0.999999		0.998812
8	0.5	5000	0.000177	0.000190	0.000506	0.000588	0.999942	0.992456	0.998812	

Tukey HSD test; variable C18:1 (RS-CC-FACTORIAL-T2FD microalgae biodiesel_FA extraction efficiency)
Approximate Probabilities for Post Hoc Tests
Error: Between MS = 1.7726, df = 16.000

Cell No.	Cat Conc. [%]	Rotational speed [rpm]	{1}	{2}	{3}	{4}	{5}	{6}	{7}	{8}
1	0	2000		0.537413	0.012071	0.004756	0.313989	0.939678	0.974707	0.395692
2	0	3000	0.537413		0.374053	0.180915	0.999833	0.989109	0.968089	0.999995
3	0	4000	0.012071	0.374053		0.999595	0.612286	0.101771	0.074111	0.512654
4	0	5000	0.004756	0.180915	0.999595		0.344131	0.041812	0.029894	0.269676
5	0.5	2000	0.313989	0.999833	0.612286	0.344131		0.905782	0.834652	1.000000
6	0.5	3000	0.939678	0.989109	0.101771	0.041812	0.905782		1.000000	0.953018
7	0.5	4000	0.974707	0.968089	0.074111	0.029894	0.834652	1.000000		0.903173
8	0.5	5000	0.395692	0.999995	0.512654	0.269676	1.000000	0.953018	0.903173	

Tukey HSD test; variable C16:0 (RS-CC-FACTORIAL-T2FD microalgae biodiesel_FA extraction efficiency)
Approximate Probabilities for Post Hoc Tests
Error: Between MS = .01417, df = 16.000

Cell No.	Cat Conc. [%]	Rotational speed [rpm]	{1}	{2}	{3}	{4}	{5}	{6}	{7}	{8}
1	0	2000		0.999612	0.999856	0.997199	0.007722	0.000518	0.000197	0.000181
2	0	3000	0.999612		1.000000	1.000000	0.003104	0.000312	0.000182	0.000177
3	0	4000	0.999856	1.000000		0.999996	0.003514	0.000330	0.000184	0.000177
4	0	5000	0.997199	1.000000	0.999996		0.002259	0.000270	0.000180	0.000176
5	0.5	2000	0.007722	0.003104	0.003514	0.002259		0.760196	0.135690	0.046911
6	0.5	3000	0.000518	0.000312	0.000330	0.000270	0.760196		0.871365	0.553684
7	0.5	4000	0.000197	0.000182	0.000184	0.000180	0.135690	0.871365		0.998579
8	0.5	5000	0.000181	0.000177	0.000177	0.000176	0.046911	0.553684	0.998579	

Tukey HSD test; variable C18:3 (Water-T2FD microalgae biodiesel_FA extraction efficiency)
Approximate Probabilities for Post Hoc Tests
Error: Between MS = .48137, df = 10.000

Cell No.	Water content [%]	{1}	{2}	{3}	{4}	{5}
1	67		0.000198	0.000183	0.000177	0.000179
2	75	0.000198		0.931621	0.199139	0.699018
3	80	0.000183	0.931621		0.529696	0.983335
4	85	0.000177	0.199139	0.529696		0.813295
5	90	0.000179	0.699018	0.983335	0.813295	

Tukey HSD test; variable C18:1 (Water-T2FD microalgae biodiesel_FA extraction efficiency)
Approximate Probabilities for Post Hoc Tests
Error: Between MS = .67650, df = 10.000

Cell No.	Water content [%]	{1}	{2}	{3}	{4}	{5}
1	67		0.000176	0.000176	0.000176	0.000176
2	75	0.000176		0.837221	0.044394	0.101596
3	80	0.000176	0.837221		0.209160	0.422234
4	85	0.000176	0.044394	0.209160		0.981115
5	90	0.000176	0.101596	0.422234	0.981115	

Tukey HSD test; variable C16:0 (Water-T2FD microalgae biodiesel_FA extraction efficiency)
Approximate Probabilities for Post Hoc Tests
Error: Between MS = .00411, df = 10.000

Cell No.	Water content [%]	{1}	{2}	{3}	{4}	{5}
1	67		0.223202	0.982398	0.856240	0.060094
2	75	0.223202		0.440231	0.691747	0.002086
3	80	0.982398	0.440231		0.989635	0.026566
4	85	0.856240	0.691747	0.989635		0.013224
5	90	0.060094	0.002086	0.026566	0.013224	

Table 5: Tukey test of FA to FAME conversion efficiencies of the DT of wet biomass of *Chloroparva pannonica* in T^2FD operated in continuous extraction mode.

Cell No.	Catalyst concentration [%wt./v]	{1}	{2}	{3}	{4}	{5}	{6}	{7}
Tukey HSD test; variable FA to FAME conversion efficiency [%] (CC-T2FD microalgae biodiesel) Approximate Probabilities for Post Hoc Tests Error: Between MS = 48.865, df = 14.000								
1	0		0.000174	0.000174	0.000174	0.000174	0.000174	0.000186
2	1	0.000174		0.999421	0.999999	0.995792	1.000000	0.000310
3	3	0.000174	0.999421		0.996933	0.999996	0.997762	0.000234
4	5	0.000174	0.999999	0.996933		0.986822	1.000000	0.000349
5	7	0.000174	0.995792	0.999996	0.986822		0.989464	0.000217
6	9	0.000174	1.000000	0.997762	1.000000	0.989464		0.000340
7	12	0.000186	0.000310	0.000234	0.000349	0.000217	0.000340	

Cell No.	water content [wt. %]	{1}	{2}	{3}	{4}	{5}
Tukey HSD test; variable FA to FAME conversion efficiency [%] (Water-T2FD microalgae biodiesel) Approximate Probabilities for Post Hoc Tests Error: Between MS = 1.1222, df = 10.000						
1	67		0.183541	0.000334	0.000470	0.001444
2	75	0.183541		0.004912	0.009350	0.046816
3	80	0.000334	0.004912		0.990689	0.584197
4	85	0.000470	0.009350	0.990689		0.824089
5	90	0.001444	0.046816	0.584197	0.824089	

Cell No.	flow rate [mL/min]	{1}	{2}	{3}	{4}	{5}
Tukey HSD test; variable FA to FAME conversion efficiency [%] (FR-T2FD microalgae biodiesel) Approximate Probabilities for Post Hoc Tests Error: Between MS = 18.336, df = 10.000						
1	1		0.004637	0.001518	0.007751	0.007875
2	2	0.004637		0.908477	0.995979	0.995485
3	3	0.001518	0.908477		0.748070	0.742217
4	4	0.007751	0.995979	0.748070		1.000000
5	5	0.007875	0.995485	0.742217	1.000000	

Cell No.	Rotational speed [rpm]	{1}	{2}	{3}	{4}
Tukey HSD test; variable FA to FAME conversion efficiency [%] (RS-0%-T2FD microalgae biodiesel) Approximate Probabilities for Post Hoc Tests Error: Between MS = 8.1991, df = 8.0000					
1	2000		0.200442	0.119039	0.022457
2	3000	0.200442		0.980282	0.442846
3	4000	0.119039	0.980282		0.646466
4	5000	0.022457	0.442846	0.646466	

Tukey HSD test; variable FA to FAME conversion efficiency [%] (RS-1%-T2FD microalgae biodiesel)
Approximate Probabilities for Post Hoc Tests
Error: Between MS = 5.3713, df = 22.000

Cell No.	Rotational speed [rpm]	{1}	{2}	{3}	{4}	{5}	{6}	{7}	{8}	{9}	{10}	{11}
1	2000		0.651104	0.999972	0.952472	0.268571	0.478624	0.987713	0.564284	0.952931	0.606170	0.990269
2	2500	0.651104		0.915210	0.999773	0.999724	1.000000	0.131785	0.014752	0.999767	0.017136	0.140473
3	3000	0.999972	0.915210		0.998912	0.556796	0.795314	0.857627	0.273826	0.998935	0.304429	0.872170
4	3500	0.952472	0.999773	0.998912		0.948251	0.995688	0.397307	0.061985	1.000000	0.071131	0.416331
5	4000	0.268571	0.999724	0.556796	0.948251		0.999998	0.032967	0.003216	0.947762	0.003740	0.035475
6	4500	0.478624	1.000000	0.795314	0.995688	0.999998		0.076331	0.007888	0.995614	0.009174	0.081744
7	5000	0.987713	0.131785	0.857627	0.397307	0.032967	0.076331		0.990600	0.398452	0.994309	1.000000
8	5500	0.564284	0.014752	0.273826	0.061985	0.003216	0.007888	0.990600		0.062250	1.000000	0.988110
9	6000	0.952931	0.999767	0.998935	1.000000	0.947762	0.995614	0.398452	0.062250		0.071431	0.417504
10	6500	0.606170	0.017136	0.304429	0.071131	0.003740	0.009174	0.994309	1.000000	0.071431		0.992610
11	7000	0.990269	0.140473	0.872170	0.416331	0.035475	0.081744	1.000000	0.988110	0.417504	0.992610	

Tukey HSD test; variable FA to FAME conversion efficiency [%] (RS-0and0.5%-T2FD microalgae biodiesel)
Approximate Probabilities for Post Hoc Tests
Error: Between MS = 7.4312, df = 16.000

Cell No.	Rotational speed [rpm]	Catalyst concentration [%wt./v]	{1}	{2}	{3}	{4}	{5}	{6}	{7}	{8}
1	2000	0.0		0.000175	0.340571	0.000175	0.186419	0.000175	0.018918	0.000175
2	2000	0.5	0.000175		0.000175	0.999818	0.000175	0.999848	0.000175	1.000000
3	3000	0.0	0.340571	0.000175		0.000175	0.999891	0.000175	0.714455	0.000175
4	3000	0.5	0.000175	0.999818	0.000175		0.000175	1.000000	0.000175	0.999843
5	4000	0.0	0.186419	0.000175	0.999891	0.000175		0.000175	0.902419	0.000175
6	4000	0.5	0.000175	0.999848	0.000175	1.000000	0.000175		0.000175	0.999870
7	5000	0.0	0.018918	0.000175	0.714455	0.000175	0.902419	0.000175		0.000175
8	5000	0.5	0.000175	1.000000	0.000175	0.999843	0.000175	0.999870	0.000175	

Appendix Section 5.4. Turbo thin film continuous flow production of biodiesel from fungal biomass

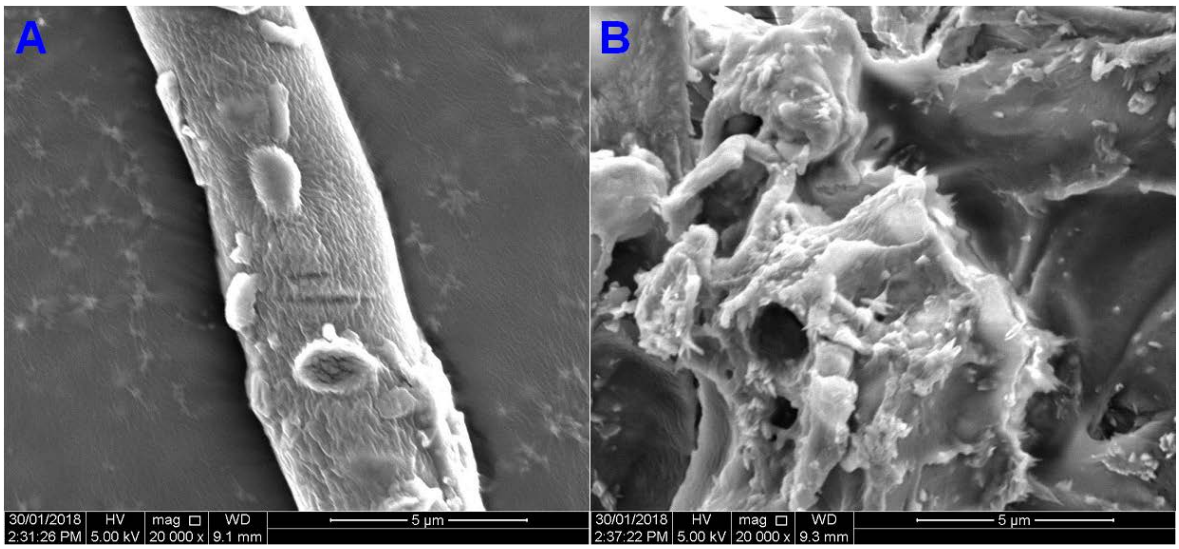

Figure 1 SEM images of (A) untreated fungal biomass and (B) treated with T^2FD.

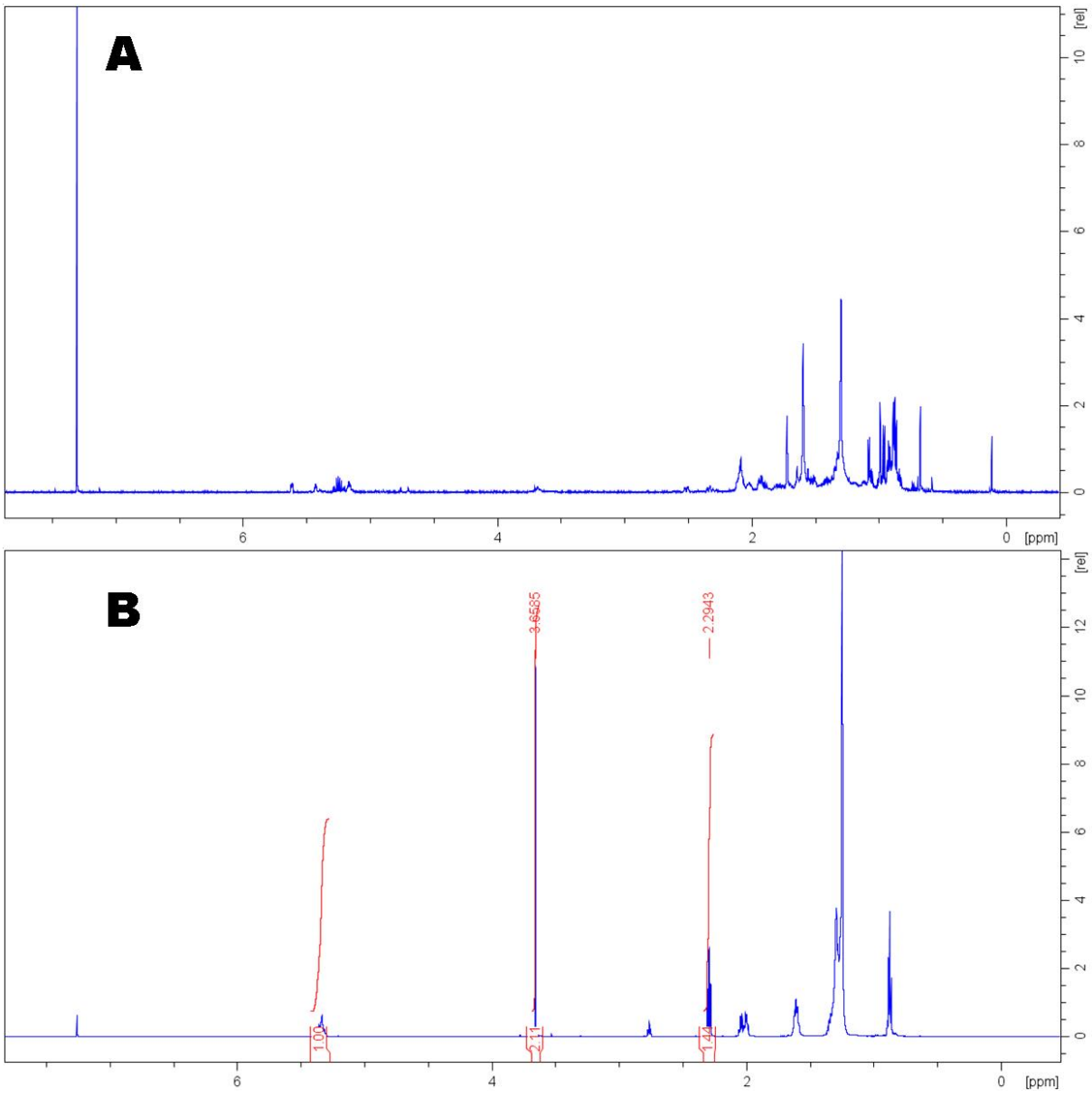

Figure 2 The FAME ^{1}H-NMR spectra of conventional direct transesterification (DT) of *Mucor plumbeus* using (A) sodium hydroxide (4% wt.v); and (B) sulphuric acid (4% v/v) as the catalysts.

Table 1. ANOVA and Friedman ANOVA tests and Neuman-Keuls and Tukey post hoc tests for $C_{18:2}$, $C_{18:1}$ and $C_{16:0}$ of T^2FD-derived FAME samples of *Mucor plumbeus* fungi biomass operated in continuous extraction mode. Significance Values below $\alpha<0.05$ are colour coded in red.

Univariate Tests of Significance for C18:2 (effect catalyst concentration on FA extraction)
Sigma-restricted parameterization
Effective hypothesis decomposition

Effect	SS	Degr. of	MS	F	p
Intercept	4634.260	1	4634.260	29659.27	0.000000
Catalyst Concentration (wt./v, %)	342.490	7	48.927	313.13	0.000000
Error	2.500	16	0.156		

Univariate Tests of Significance for C18:1 (effect catalyst concentration on FA extraction)
Sigma-restricted parameterization
Effective hypothesis decomposition

Effect	SS	Degr. of	MS	F	p
Intercept	35400.96	1	35400.96	79964.52	0.000000
Catalyst Concentration (wt./v, %)	338.02	7	48.29	109.07	0.000000
Error	7.08	16	0.44		

Univariate Tests of Significance for C16:0 Log (effect catalyst concentration on FA extraction)
Sigma-restricted parameterization
Effective hypothesis decomposition

Effect	SS	Degr. of	MS	F	p
Intercept	32.59580	1	32.59580	8372.506	0.000000
Catalyst Concentration (wt./v, %)	0.18899	7	0.02700	6.935	0.000681
Error	0.06229	16	0.00389		

Friedman ANOVA and Kendall Coeff. of Concordance (effect of ratio on FA extraction)
ANOVA Chi Sqr. (N = 35, df = 2) = 52.51429 p = .00000
Coeff. of Concordance = .75020 Aver. rank r = .74286

Variable	Average	Sum of	Mean	Std.Dev.
Catalyst concentration (wt./v %)	1.514286	53.0000	2.0286	1.014185
biomass to methanol ratio (wt./v)	3.000000	105.0000	103.5429	1.737863
C18:2 Log	1.485714	52.0000	1.1815	0.033865

Friedman ANOVA and Kendall Coeff. of Concordance (effect of ratio on FA extraction)
ANOVA Chi Sqr. (N = 35, df = 2) = 52.51429 p = .00000
Coeff. of Concordance = .75020 Aver. rank r = .74286

Variable	Average	Sum of	Mean	Std.Dev.
Catalyst concentration (wt./v %)	1.514286	53.0000	2.0286	1.014185
biomass to methanol ratio (wt./v)	3.000000	105.0000	103.5429	1.737863
C18:1 Log	1.485714	52.0000	1.5726	0.017368

Univariate Tests of Significance for C18:2 Log (effect of catalyst concentration and flow rate on C18:2 and C18:1 extraction)
Sigma-restricted parameterization
Effective hypothesis decomposition

Effect	SS	Degr. of	MS	F	p
Intercept	56.01257	1	56.01257	125346.9	0.000000
Catalyst concentration (wt./v)	0.04746	1	0.04746	106.2	0.000000
Flow rate [ml/min]	0.13085	6	0.02181	48.8	0.000000
Catalyst concentration (wt./v)*Flow rate [ml/min]	0.09745	6	0.01624	36.3	0.000000
Error	0.01251	28	0.00045		

Univariate Tests of Significance for C18:1 Log (effect of catalyst concentration and flow rate on C18:2 and C18:1 extraction)
Sigma-restricted parameterization
Effective hypothesis decomposition

Effect	SS	Degr. of	MS	F	p
Intercept	105.1890	1	105.1890	1831051	0.000000
Catalyst concentration (wt./v)	0.0081	1	0.0081	140	0.000000
Flow rate [ml/min]	0.0271	6	0.0045	79	0.000000
Catalyst concentration (wt./v)*Flow rate [ml/min]	0.0066	6	0.0011	19	0.000000
Error	0.0016	28	0.0001		

Friedman ANOVA and Kendall Coeff. of Concordance (Effect of catalyst concentration and rpm on FA extraction)
ANOVA Chi Sqr. (N = 53, df = 2) = 79.50943 p = .00000
Coeff. of Concordance = .75009 Aver. rank r = .74528

Variable	Average	Sum of	Mean	Std.Dev.
Catalyst concentration (wt/v %)	1.509434	80.0000	2.019	1.009
rotational speed [rpm]	3.000000	159.0000	3981.132	1308.119
C18:2 Log	1.490566	79.0000	1.171	0.034

Friedman ANOVA and Kendall Coeff. of Concordance (Effect of catalyst concentration and rpm on FA extraction)
ANOVA Chi Sqr. (N = 53, df = 2) = 79.50943 p = .00000
Coeff. of Concordance = .75009 Aver. rank r = .74528

Variable	Average	Sum of	Mean	Std.Dev.
Catalyst concentration (wt/v %)	1.509434	80.0000	2.019	1.009
rotational speed [rpm]	3.000000	159.0000	3981.132	1308.119
C18:1 Log	1.490566	79.0000	1.574	0.016

Tukey HSD test; variable C18:2 (effect catalyst concentration on FA extraction effiency)
Approximate Probabilities for Post Hoc Tests
Error: Between MS = .15625, df = 16.000

Cell No.	Catalyst concentration (wt./v %)	{1}	{2}	{3}	{4}	{5}	{6}	{7}	{8}
1	0		0.000175	0.000175	0.000175	0.000175	0.000175	0.000175	0.000175
2	0.5	0.000175		0.961972	0.999391	0.000413	0.771572	0.097364	0.231466
3	1	0.000175	0.961972		0.999391	0.000203	0.999391	0.473421	0.771572
4	3	0.000175	0.999391	0.999391		0.000261	0.961972	0.231466	0.473421
5	5	0.000175	0.000413	0.000203	0.000261		0.000184	0.000175	0.000175
6	7	0.000175	0.771572	0.999391	0.961972	0.000184		0.771572	0.961972
7	9	0.000175	0.097364	0.473421	0.231466	0.000175	0.771572		0.999391
8	12	0.000175	0.231466	0.771572	0.473421	0.000175	0.961972	0.999391	

Tukey HSD test; variable C18:1 (effect catalyst concentration on FA extraction effiency)
Approximate Probabilities for Post Hoc Tests
Error: Between MS = .44271, df = 16.000

Cell No.	Catalyst concentration (wt./v %)	{1}	{2}	{3}	{4}	{5}	{6}	{7}	{8}
1	0		0.000175	0.000175	0.000175	0.000175	0.000175	0.000175	0.000175
2	0.5	0.000175		0.979406	0.604637	1.000000	0.134235	0.001065	0.044268
3	1	0.000175	0.979406		0.979406	0.953633	0.514247	0.005635	0.222365
4	3	0.000175	0.604637	0.979406		0.514247	0.953633	0.033107	0.694897
5	5	0.000175	1.000000	0.953633	0.514247		0.102779	0.000835	0.033107
6	7	0.000175	0.134235	0.514247	0.953633	0.102779		0.222365	0.998152
7	9	0.000175	0.001065	0.005635	0.033107	0.000835	0.222365		0.514247
8	12	0.000175	0.044268	0.222365	0.694897	0.033107	0.998152	0.514247	

Newman-Keuls test; variable C18:2 Log (effect of ratio of biomass to methanol on FA extraction efficiency)
Approximate Probabilities for Post Hoc Tests
Error: Between MSE = .00075, df = 23.000

Cell No.	Catalyst concentration (wt./v %)	biomass to methanol ratio (wt./v)	{1}	{2}	{3}	{4}	{5}	{6}	{7}	{8}	{9}	{10}	{11}	{12}
1	1	1:6		0.997103	0.978067	0.995613	0.842544	0.979381	0.932024	0.299901	0.998381	0.993775	0.060665	1.000000
2	1	1:9	0.997103		1.000000	0.975369	1.000000	0.998609	0.982870	0.225703	0.976616	0.837456	0.048247	0.999637
3	1	1:12	0.978067	1.000000		0.993383	1.000000	0.994514	0.965040	0.288282	0.996812	0.976616	0.062167	0.997103
4	1	1:15	0.995613	0.975369	0.993383		0.998252	0.995352	0.962568	0.092452	0.837456	0.976616	0.032687	0.998299
5	1	1:18	0.842544	1.000000	1.000000	0.998252		0.978520	0.928583	0.347583	0.999587	0.996812	0.076651	0.978067
6	1	1:25	0.979381	0.998609	0.994514	0.995352	0.978520		0.691448	0.286696	0.998510	0.996091	0.054732	0.847333
7	3	1:6	0.932024	0.982870	0.965040	0.962568	0.928583	0.691448		0.161783	0.981471	0.968913	0.026274	0.823188
8	3	1:9	0.299901	0.225703	0.288282	0.092452	0.347583	0.286696	0.161783		0.144012	0.230500	0.352691	0.343310
9	3	1:12	0.998381	0.976616	0.996812	0.837456	0.999587	0.998510	0.981471	0.144012		1.000000	0.036668	0.999577
10	3	1:15	0.993775	0.837456	0.976616	0.976616	0.996812	0.996091	0.968913	0.230500	1.000000		0.054859	0.998381
11	3	1:18	0.060665	0.048247	0.062167	0.032687	0.076651	0.054732	0.026274	0.352691	0.036668	0.054859		0.071186
12	3	1:25	1.000000	0.999637	0.997103	0.998299	0.978067	0.847333	0.823188	0.343310	0.999577	0.998381	0.071186	

Newman-Keuls test; variable C18:1 Log (effect of ratio of biomass to methanol on FA extraction)
Approximate Probabilities for Post Hoc Tests
Error: Between MSE = .00027, df = 23.000

Cell No.	Catalyst concentration (wt./v %)	biomass to methanol ratio (wt./v)	{1}	{2}	{3}	{4}	{5}	{6}	{7}	{8}	{9}	{10}	{11}	{12}
1	1	1:6		0.981460	0.986871	0.994015	0.996069	0.880466	0.383896	0.698317	0.997755	0.939151	0.629861	0.991932
2	1	1:9	0.981460		0.982928	0.989561	0.970440	0.874833	0.709178	0.706880	0.994246	0.915446	0.651896	0.965581
3	1	1:12	0.986871	0.982928		0.836936	0.967086	0.584617	0.712150	0.590024	0.906224	0.984361	0.649631	0.973897
4	1	1:15	0.994015	0.989561	0.836936		0.972704	0.729038	0.778309	0.633673	0.831437	0.991767	0.645370	0.974836
5	1	1:18	0.996069	0.970440	0.967086	0.972704		0.835505	0.799466	0.665921	0.974948	0.988563	0.619211	0.831812
6	1	1:25	0.880466	0.874833	0.584617	0.729038	0.835505		0.422859	0.666980	0.762992	0.874616	0.811876	0.862202
7	3	1:6	0.383896	0.709178	0.712150	0.778309	0.799466	0.422859		0.242261	0.833295	0.605621	0.197137	0.768437
8	3	1:9	0.698317	0.706880	0.590024	0.633673	0.665921	0.666980	0.242261		0.625019	0.697084	0.857319	0.718313
9	3	1:12	0.997755	0.994246	0.906224	0.831437	0.974948	0.762992	0.833295	0.625019		0.996199	0.608912	1.000000
10	3	1:15	0.939151	0.915446	0.984361	0.991767	0.988563	0.874616	0.605621	0.697084	0.996199		0.634399	0.983686
11	3	1:18	0.629861	0.651896	0.649631	0.645370	0.619211	0.811876	0.197137	0.857319	0.608912	0.634399		0.685783
12	3	1:25	0.991932	0.965581	0.973897	0.974836	0.831812	0.862202	0.768437	0.718313	1.000000	0.983686	0.685783	

Tukey HSD test; variable C18:2 Log (effect of catalyst concentration and low rate on C18:2 and C18:1 extraction)
Approximate Probabilities for Post Hoc Tests
Error: Between MS = .00045, df = 28.000

Cell No.	Catalyst concentration (wt./v)	Flow rate [ml/min]	{1}	{2}	{3}	{4}	{5}	{6}	{7}	{8}	{9}	{10}	{11}	{12}	{13}	{14}
1	1	1		1.000000	1.000000	0.999998	0.999830	0.000151	0.000151	0.410230	1.000000	1.000000	0.999830	0.999830	0.999998	0.996531
2	1	2	1.000000		1.000000	1.000000	0.999998	0.000151	0.000151	0.266612	0.999999	1.000000	0.999998	0.999998	1.000000	0.999808
3	1	3	1.000000	1.000000		0.999998	0.999830	0.000151	0.000151	0.410230	1.000000	1.000000	0.999830	0.999830	0.999998	0.996531
4	1	4	0.999998	1.000000	0.999998		1.000000	0.000151	0.000151	0.161748	0.999848	1.000000	1.000000	1.000000	1.000000	0.999998
5	1	5	0.999830	0.999998	0.999830	1.000000		0.000151	0.000151	0.092800	0.997031	0.999998	1.000000	1.000000	1.000000	1.000000
6	1	8	0.000151	0.000151	0.000151	0.000151	0.000151		0.011401	0.000151	0.000151	0.000151	0.000151	0.000151	0.000151	0.000151
7	1	10	0.000151	0.000151	0.000151	0.000151	0.000151	0.011401		0.000151	0.000151	0.000151	0.000151	0.000151	0.000151	0.000151
8	3	1	0.410230	0.266612	0.410230	0.161748	0.092800	0.000151	0.000151		0.576252	0.266612	0.092800	0.092800	0.161748	0.049805
9	3	2	1.000000	0.999999	1.000000	0.999848	0.997031	0.000151	0.000151	0.576252		0.999999	0.997031	0.997031	0.999848	0.977448
10	3	3	1.000000	1.000000	1.000000	1.000000	0.999998	0.000151	0.000151	0.266612	0.999999		0.999998	0.999998	1.000000	0.999808
11	3	4	0.999830	0.999998	0.999830	1.000000	1.000000	0.000151	0.000151	0.092800	0.997031	0.999998		1.000000	1.000000	1.000000
12	3	5	0.999830	0.999998	0.999830	1.000000	1.000000	0.000151	0.000151	0.092800	0.997031	0.999998	1.000000		1.000000	1.000000
13	3	8	0.999998	1.000000	0.999998	1.000000	1.000000	0.000151	0.000151	0.161748	0.999848	1.000000	1.000000	1.000000		0.999998
14	3	10	0.996531	0.999808	0.996531	0.999998	1.000000	0.000151	0.000151	0.049805	0.977448	0.999808	1.000000	1.000000	0.999998	

Tukey HSD test; variable C18:1 Log (effect of catalyst concentration and low rate on C18:2 and C18:1 extraction)
Approximate Probabilities for Post Hoc Tests
Error: Between MS = .00006, df = 28.000

Cell No.	Catalyst concentration (wt./v)	Flow rate [ml/min]	{1}	{2}	{3}	{4}	{5}	{6}	{7}	{8}	{9}	{10}	{11}	{12}	{13}	{14}
1	1	1		0.615449	0.335739	0.194293	0.004265	0.000151	0.000151	0.000784	1.000000	0.876558	0.256898	0.330850	0.004203	0.027999
2	1	2	0.615449		1.000000	0.999907	0.470883	0.000151	0.000151	0.000152	0.721197	1.000000	0.999993	1.000000	0.467091	0.904209
3	1	3	0.335739	1.000000		1.000000	0.759921	0.000151	0.000151	0.000151	0.430624	0.999400	1.000000	1.000000	0.756562	0.991451
4	1	4	0.194293	0.999907	1.000000		0.908854	0.000151	0.000151	0.000151	0.262252	0.989883	1.000000	1.000000	0.906822	0.999542
5	1	5	0.004265	0.470883	0.759921	0.908854		0.000151	0.000151	0.000151	0.006496	0.226760	0.845080	0.765253	1.000000	0.999923
6	1	8	0.000151	0.000151	0.000151	0.000151	0.000151		0.778061	0.000151	0.000151	0.000151	0.000151	0.000151	0.000151	0.000151
7	1	10	0.000151	0.000151	0.000151	0.000151	0.000151	0.778061		0.000151	0.000151	0.000151	0.000151	0.000151	0.000151	0.000151
8	3	1	0.000784	0.000152	0.000151	0.000151	0.000151	0.000151	0.000151		0.000548	0.000154	0.000151	0.000151	0.000151	0.000151
9	3	2	1.000000	0.721197	0.430624	0.262252	0.006496	0.000151	0.000151	0.000548		0.934783	0.338787	0.425047	0.006402	0.041429
10	3	3	0.876558	1.000000	0.999400	0.989883	0.226760	0.000151	0.000151	0.000154	0.934783		0.997008	0.999335	0.224406	0.661362
11	3	4	0.256898	0.999993	1.000000	1.000000	0.845080	0.000151	0.000151	0.000151	0.338787	0.997008		1.000000	0.842325	0.997709
12	3	5	0.330850	1.000000	1.000000	1.000000	0.765253	0.000151	0.000151	0.000151	0.425047	0.999335	1.000000		0.761922	0.992007
13	3	8	0.004203	0.467091	0.756562	0.906822	1.000000	0.000151	0.000151	0.000151	0.006402	0.224406	0.842325	0.761922		0.999917
14	3	10	0.027999	0.904209	0.991451	0.999542	0.999923	0.000151	0.000151	0.000151	0.041429	0.661362	0.997709	0.992007	0.999917	

Tests of Homogeneity of Variances (effect of catalyst concentration and flow rate on C18:2 and C18:1 extraction)
Effect: "Catalyst concentration (wt./v)"*"Flow rate [ml/min]"

	Hartley	Cochran	Bartlett	df	p
C18:2 Log		0.800650	15.27165	8	0.054074

Tests of Homogeneity of Variances (effect of catalyst concentration and flow rate on C18:2 and C18:1 extraction)
Effect: "Catalyst concentration (wt./v)"*"Flow rate [ml/min]"

	Hartley	Cochran	Bartlett	df	p
C18:1 Log	57.94031	0.213948	10.84587	13	0.623728

Newman-Keuls test; variable C18:2 Log (Effect of catalyst concentration and rotational speed on FA extraction)
Approximate Probabilities for Post Hoc Tests
Error: Between MSE = .00013, df = 35.000

Cell No.	Catalyst concentration (wt/v %)	rotational speed [rpm]	{1}	{2}	{3}	{4}	{5}	{6}	{7}	{8}	{9}	{10}	{11}	{12}	{13}	{14}	{15}	{16}	{17}	{18}
1	1	2,000		0.616369	0.869127	0.969622	0.911063	0.957266	0.762472	0.847572	0.656122	0.869127	0.957266	0.246056	0.000133	0.986316	0.000131	0.000133	1.000000	0.947991
2	1	2,500	0.616369		1.000000	0.998649	0.986316	1.000000	0.941480	0.972167	0.889105	0.743960	0.848458	0.124654	0.000141	1.000000	0.000133	0.000131	0.869127	0.995683
3	1	3,000	0.869127	1.000000		0.995683	0.957266	1.000000	0.913952	0.951727	0.854890	0.848458	0.911063	0.157552	0.000154	1.000000	0.000141	0.000133	0.957266	0.986316
4	1	3,500	0.969622	0.998649	0.995683		1.000000	0.986316	0.744942	0.627571	0.762114	0.876235	0.904161	0.121930	0.000139	0.957266	0.000142	0.000135	0.982231	1.000000
5	1	4,000	0.911063	0.986316	0.957266	1.000000		0.869127	0.946972	0.960962	0.921516	0.793251	0.840058	0.093251	0.000135	0.616369	0.000128	0.000180	0.947991	1.000000
6	1	4,500	0.957266	1.000000	1.000000	0.986316	0.869127		0.873469	0.916389	0.810042	0.911063	0.947991	0.190701	0.000180	1.000000	0.000154	0.000141	0.986316	0.957266
7	1	5,000	0.762472	0.941480	0.913952	0.744942	0.946972	0.873469		0.808144	0.808144	0.526578	0.563572	0.027649	0.000162	0.814228	0.000146	0.000139	0.801917	0.882637
8	1	5,500	0.847572	0.972167	0.951727	0.627571	0.960962	0.916389	0.808144		0.876752	0.645787	0.686134	0.045005	0.000146	0.855711	0.000139	0.000142	0.882771	0.876752
9	1	6,000	0.656122	0.889105	0.854890	0.762114	0.921516	0.810042	0.808144	0.876752		0.407302	0.438359	0.016512	0.000169	0.751556	0.000162	0.000146	0.696240	0.862784
10	3	2,000	0.869127	0.743960	0.848458	0.876235	0.793251	0.911063	0.526578	0.645787	0.407302		1.000000	0.264693	0.000133	0.947991	0.000126	0.000160	0.616369	0.840058
11	3	2,500	0.957266	0.848458	0.911063	0.904161	0.840058	0.947991	0.563572	0.686134	0.438359	1.000000		0.121660	0.000126	0.969622	0.000160	0.000123	0.869127	0.876235
12	3	3,000	0.246056	0.124654	0.157552	0.121930	0.093251	0.190701	0.027649	0.045005	0.016512	0.264693	0.121660		0.000161	0.223653	0.000124	0.000123	0.175524	0.107500
13	3	3,500	0.000133	0.000141	0.000154	0.000139	0.000135	0.000180	0.000162	0.000146	0.000169	0.000133	0.000126	0.000161		0.000128	1.000000	0.998836	0.000131	0.000142
14	3	4,000	0.986316	1.000000	1.000000	0.957266	0.616369	1.000000	0.814228	0.855711	0.751556	0.947991	0.969622	0.223653	0.000128		0.000180	0.000154	0.995683	0.869127
15	3	4,500	0.000131	0.000133	0.000141	0.000142	0.000128	0.000154	0.000146	0.000139	0.000162	0.000126	0.000160	0.000124	1.000000	0.000180		0.962474	0.000133	0.000135
16	3	5,000	0.000133	0.000131	0.000133	0.000135	0.000180	0.000141	0.000139	0.000142	0.000146	0.000160	0.000123	0.000123	0.998836	0.000154	0.962474		0.000126	0.000128
17	3	5,500	1.000000	0.869127	0.957266	0.982231	0.947991	0.986316	0.801917	0.882771	0.696240	0.616369	0.869127	0.175524	0.000131	0.995683	0.000133	0.000126		0.969622
18	3	6,000	0.947991	0.995683	0.986316	1.000000	1.000000	0.957266	0.882637	0.876752	0.862784	0.840058	0.876235	0.107500	0.000142	0.869127	0.000135	0.000128	0.969622	

Newman-Keuls test; variable C18:1 Log (Effect of catalyst concentration and rotational speed on FA extraction)
Approximate Probabilities for Post Hoc Tests
Error: Between MSE = .00019, df = 35.000

Cell No.	Catalyst concentration (wt/v %)	rotational speed [rpm]	{1}	{2}	{3}	{4}	{5}	{6}	{7}	{8}	{9}	{10}	{11}	{12}	{13}	{14}	{15}	{16}	{17}	{18}
1	1	2,000		0.998277	0.139605	0.986932	0.999519	0.997160	0.989125	0.992532	0.993600	0.940337	0.755656	0.997050	0.415859	0.989609	0.690465	0.802352	0.994251	0.973909
2	1	2,500	0.998277		0.186819	0.996205	0.995628	0.935006	0.905568	0.992676	0.990481	0.999808	0.806597	0.993572	0.872607	0.956021	0.912911	0.917334	0.985661	0.979774
3	1	3,000	0.139605	0.186819		0.202501	0.163325	0.181100	0.299979	0.178451	0.214943	0.224273	0.244363	0.128009	0.022147	0.292566	0.024381	0.021740	0.238983	0.175123
4	1	3,500	0.986932	0.996205	0.202501		0.999767	0.998780	0.985986	0.997100	0.997005	1.000000	0.841044	0.941662	0.774516	0.990768	0.852704	0.873702	0.996570	0.988695
5	1	4,000	0.999519	0.995628	0.163325	0.999767		0.995827	0.677640	0.983146	0.975266	0.999986	0.759317	0.998241	0.911380	0.869329	0.939191	0.939732	0.957096	0.964309
6	1	4,500	0.997160	0.935006	0.181100	0.998780	0.995827		0.956896	0.993832	0.992915	0.999999	0.805921	0.987179	0.852432	0.975271	0.903822	0.913585	0.990806	0.981059
7	1	5,000	0.989125	0.905568	0.299979	0.985986	0.677640	0.956896		0.998989	0.998165	0.995552	0.904416	0.978871	0.761402	0.932119	0.805038	0.800495	0.995917	0.995313
8	1	5,500	0.992532	0.992676	0.178451	0.997100	0.983146	0.993832	0.998989		0.931856	0.998653	0.644449	0.988445	0.769001	0.998155	0.797831	0.780222	0.983716	0.800695
9	1	6,000	0.993600	0.990481	0.214943	0.997005	0.975266	0.992915	0.998165	0.931856		0.998756	0.758630	0.989441	0.785018	0.995824	0.815531	0.801106	0.931429	0.938192
10	3	2,000	0.940337	0.999808	0.224273	1.000000	0.999986	0.999999	0.995552	0.998653	0.998756		0.870309	0.742910	0.656619	0.996606	0.773935	0.814510	0.998753	0.993290
11	3	2,500	0.755656	0.806597	0.244363	0.841044	0.759317	0.805921	0.904416	0.644449	0.758630	0.870309		0.726532	0.279341	0.888605	0.300104	0.279781	0.819382	0.523457
12	3	3,000	0.997050	0.993572	0.128009	0.941662	0.998241	0.987179	0.978871	0.988445	0.989441	0.742910	0.726532		0.688752	0.981414	0.840601	0.891646	0.989804	0.964842
13	3	3,500	0.415859	0.872607	0.022147	0.774516	0.911380	0.852432	0.761402	0.769001	0.785018	0.656619	0.279341	0.688752		0.758286	0.999258	0.996456	0.797410	0.643614
14	3	4,000	0.989609	0.956021	0.292566	0.990768	0.869329	0.975271	0.932119	0.998155	0.995824	0.996606	0.888605	0.981414	0.758286		0.797449	0.788684	0.999191	0.992694
15	3	4,500	0.690465	0.912911	0.024381	0.852704	0.939191	0.903822	0.805038	0.797831	0.815531	0.773935	0.300104	0.840601	0.999258	0.797449		0.936609	0.830044	0.673934
16	3	5,000	0.802352	0.917334	0.021740	0.873702	0.939732	0.913585	0.800495	0.780222	0.801106	0.814510	0.279781	0.891646	0.996456	0.788684	0.936609		0.818920	0.650454
17	3	5,500	0.994251	0.985661	0.238983	0.996570	0.957096	0.990806	0.995917	0.983716	0.931429	0.998753	0.819382	0.989804	0.797410	0.999191	0.830044	0.818920		0.973417
18	3	6,000	0.973909	0.979774	0.175123	0.988695	0.964309	0.981059	0.995313	0.800695	0.938192	0.993290	0.523457	0.964842	0.643614	0.992694	0.673934	0.650454	0.973417	

Table 2. Kruskall-Wallis and Friedman ANOVA tests and Neuman-Keuls post hoc tests of significant effect of processing parameters on FA to FAME conversion efficiencies of the DT of *Mucor plumbeus* in T^2FD operated in continuous extraction mode.

Kruskal-Wallis ANOVA by Ranks; FA to FAME Conversion Efficiency [%] (Effect Catalyst conc on FA to FAME conversion efficiency)
Independent (grouping) variable: Catalyst Concentration [wt./v %]
Kruskal-Wallis test: H (7, N= 24) =18.17123 p =.0112

Depend.: FA to FAME Conversion Efficiency [%]	Code	Valid	Sum of	Mean
0	101	3	6.00000	2.00000
0.5	102	3	15.00000	5.00000
1	103	3	25.00000	8.33333
3	104	3	42.00000	14.00000
5	105	3	60.00000	20.00000
7	106	3	48.00000	16.00000
9	107	3	54.50000	18.16667
12	108	3	49.50000	16.50000

Kruskal-Wallis ANOVA by Ranks; FA to FAME conversion efficiency [%] (Effect water content on FA to FAME conversion efficiency)
Independent (grouping) variable: water content [wt. %]
Kruskal-Wallis test: H (4, N= 15) =12.40000 p =.0146

Depend.: FA to FAME conversion efficiency [%]	Code	Valid	Sum of	Mean
0	0	3	23.00000	7.66667
5	5	3	41.00000	13.66667
20	20	3	33.00000	11.00000
50	50	3	17.00000	5.66667
75	75	3	6.00000	2.00000

Friedman ANOVA and Kendall Coeff. of Concordance (Effect of cat conc and ratio on FA to FAME CE)
ANOVA Chi Sqr. (N = 36, df = 2) = 72.00000 p = .00000
Coeff. of Concordance = 1.0000 Aver. rank r = 1.0000

Variable	Average	Sum of	Mean	Std.Dev.
FA to FAME conversion efficiency [%]	2.000000	72.0000	91.7493	4.268731
Catalyst concentration [wt/v %]	1.000000	36.0000	2.0000	1.014185
Biomass to methanol ratio [w/v]	3.000000	108.0000	104.5000	1.732051

Friedman ANOVA and Kendall Coeff. of Concordance (Effect of cat conc and flow rate on FA to FAME CE)
ANOVA Chi Sqr. (N = 42, df = 2) = 72.44444 p = .00000
Coeff. of Concordance = .86243 Aver. rank r = .85908

Variable	Average	Sum of	Mean	Std.Dev.
Catalyst Concentration (wt/v %]	1.214286	51.0000	2.00000	1.012122
Flow rate [mL/min]	1.785714	75.0000	4.71429	3.046675
FA to FAME conversion efficiency [%]	3.000000	126.0000	89.32229	7.216043

Variable	Friedman ANOVA and Kendall Coeff. of Concordance (Effect of cat conc and rotational speed on FA to FAME CE) ANOVA Chi Sqr. (N = 54, df = 2) = 108.0000 p =0.00000 Average	Sum of	Mean	Std.Dev.
FA to FAME conversion efficiency [%]	2.000000	108.0000	88.395	8.538
Catalyst concentration [wt/v %]	1.000000	54.0000	2.000	1.009
Rotational speed [rpm]	3.000000	162.0000	4000.000	1303.117

Newman-Keuls test; variable FA to FAME Conversion Efficiency [%] (Effect Catalyst conc on FA to FAME conversion efficiency)
Approximate Probabilities for Post Hoc Tests
Error: Between MSE = 2.0463, df = 16.000

Cell No.	Catalyst Concentration [wt./v %]	{1}	{2}	{3}	{4}	{5}	{6}	{7}	{8}
1	0		0.000159	0.000168	0.000185	0.000175	0.000142	0.000163	0.000164
2	1	0.000159		0.000159	0.000168	0.000163	0.000185	0.000164	0.000142
3	1	0.000168	0.000159		0.005192	0.003083	0.002802	0.002767	0.003214
4	3	0.000185	0.000168	0.005192		0.631089	0.451132	0.580509	0.587500
5	5	0.000175	0.000163	0.003083	0.631089		0.918846	0.908914	0.912512
6	7	0.000142	0.000185	0.002802	0.451132	0.918846		0.862912	0.823217
7	9	0.000163	0.000164	0.002767	0.580509	0.908914	0.862912		0.773730
8	12	0.000164	0.000142	0.003214	0.587500	0.912512	0.823217	0.773730	

Newman-Keuls test; variable FA to FAME conversion efficiency [%] (Effect water content on FA to FAME conversion efficiency)
Approximate Probabilities for Post Hoc Tests
Error: Between MSE = 4.2041, df = 10.000

Cell No.	water content [wt. %]	{1}	{2}	{3}	{4}	{5}
1	0		0.322065	0.310913	0.476209	0.000199
2	5	0.322065		0.659138	0.171868	0.000176
3	20	0.310913	0.659138		0.216354	0.000205
4	50	0.476209	0.171868	0.216354		0.000187
5	75	0.000199	0.000176	0.000205	0.000187	

Newman-Keuls test; variable FA to FAME conversion efficiency [%] (Effect of cat conc and ratio on FA to FAME CE)
Approximate Probabilities for Post Hoc Tests
Error: Between MSE = 2.7600, df = 24.000

Cell No.	Catalyst concentration [wt/v %]	Biomass to methanol ratio [w/v]	{1}	{2}	{3}	{4}	{5}	{6}	{7}	{8}	{9}	{10}	{11}	{12}
1	1	1:6		0.789982	0.295171	0.717549	0.635924	0.000147	0.925647	0.966952	0.953680	0.771048	0.944118	0.935000
2	1	1:9	0.789982		0.542894	0.743780	0.808908	0.000126	0.842315	0.763497	0.771041	0.803027	0.806963	0.568323
3	1	1:12	0.295171	0.542894		0.573640	0.475963	0.000152	0.299167	0.176115	0.193384	0.380966	0.237670	0.331127
4	1	1:15	0.717549	0.743780	0.573640		0.772491	0.000161	0.752837	0.620620	0.639127	0.770365	0.693738	0.639742
5	1	1:18	0.635924	0.808908	0.475963	0.772491		0.000129	0.655460	0.487876	0.513482	0.718657	0.578966	0.631580
6	1	1:25	0.000147	0.000126	0.000152	0.000161	0.000129		0.000160	0.000143	0.000194	0.000144	0.000168	0.000138
7	3	1:6	0.925647	0.842315	0.299167	0.752837	0.655460	0.000160		0.946963	0.905704	0.920356	0.820771	0.970126
8	3	1:9	0.966952	0.763497	0.176115	0.620620	0.487876	0.000143	0.946963		0.905256	0.933547	0.946601	0.951475
9	3	1:12	0.953680	0.771041	0.193384	0.639127	0.513482	0.000194	0.905704	0.905256		0.923832	0.846571	0.950283
10	3	1:15	0.771048	0.803027	0.380966	0.770365	0.718657	0.000144	0.920356	0.933547	0.923832		0.925360	0.956353
11	3	1:18	0.944118	0.806963	0.237670	0.693738	0.578966	0.000168	0.820771	0.946601	0.846571	0.925360		0.960302
12	3	1:25	0.935000	0.568323	0.331127	0.639742	0.631580	0.000138	0.970126	0.951475	0.950283	0.956353	0.960302	

Newman-Keuls test; variable FA to FAME conversion efficiency [%] (Effect of cat conc and rotational speed on FA to FAME CE)
Approximate Probabilities for Post Hoc Tests
Error: Between MSE = 5.2660, df = 36.000

Cell No.	Catalyst concentration [wt/v %]	Rotational speed [rpm]	{1}	{2}	{3}	{4}	{5}	{6}	{7}	{8}	{9}	{10}	{11}	{12}	{13}	{14}	{15}	{16}	{17}	{18}
1	1	2,000		0.907107	0.002089	0.087004	0.036637	0.108241	0.256821	0.000132	0.000130	0.000357	0.000409	0.000319	0.000250	0.000423	0.000146	0.000227	0.000209	0.000231
2	1	2,500	0.907107		0.002144	0.115699	0.018753	0.123886	0.421005	0.000130	0.000132	0.000350	0.000391	0.000328	0.000271	0.000316	0.000203	0.000212	0.000207	0.000243
3	1	3,000	0.002089	0.002144		0.150157	0.000130	0.086835	0.027500	0.011242	0.011348	0.000179	0.000140	0.000153	0.000127	0.000132	0.000145	0.000138	0.000141	0.000134
4	1	3,500	0.087004	0.115699	0.150157		0.000400	0.881393	0.307437	0.000437	0.000274	0.000140	0.000130	0.000132	0.000153	0.000132	0.000141	0.000134	0.000127	0.000179
5	1	4,000	0.036637	0.018753	0.000130	0.000400		0.000368	0.003586	0.000132	0.000140	0.117756	0.088954	0.092973	0.086949	0.050531	0.033385	0.060735	0.063752	0.082640
6	1	4,500	0.108241	0.123886	0.086835	0.881393	0.000368		0.469153	0.000348	0.000291	0.000153	0.000132	0.000140	0.000179	0.000130	0.000138	0.000141	0.000134	0.000127
7	1	5,000	0.256821	0.421005	0.027500	0.307437	0.003586	0.469153		0.000141	0.000138	0.000138	0.000140	0.000135	0.000142	0.000135	0.000134	0.000128	0.000180	0.000155
8	1	5,500	0.000132	0.000130	0.011242	0.000437	0.000132	0.000348	0.000141		0.701881	0.000127	0.000153	0.000179	0.000134	0.000140	0.000161	0.000145	0.000138	0.000141
9	1	6,000	0.000130	0.000132	0.011348	0.000274	0.000140	0.000291	0.000138	0.701881		0.000134	0.000179	0.000127	0.000141	0.000153	0.000167	0.000161	0.000145	0.000138
10	3	2,000	0.000357	0.000350	0.000179	0.000140	0.117756	0.000153	0.000138	0.000127	0.000134		0.950619	0.945312	0.777813	0.967918	0.896157	0.946992	0.921236	0.907043
11	3	2,500	0.000409	0.000391	0.000140	0.000130	0.088954	0.000132	0.000140	0.000153	0.000179	0.950619		0.816112	0.935123	0.879176	0.870057	0.941455	0.934661	0.949335
12	3	3,000	0.000319	0.000328	0.000153	0.000132	0.092973	0.000140	0.000135	0.000179	0.000127	0.945312	0.816112		0.933603	0.920771	0.916864	0.965043	0.955034	0.960751
13	3	3,500	0.000250	0.000271	0.000127	0.000153	0.086949	0.000179	0.000142	0.000134	0.000141	0.777813	0.935123	0.933603		0.945289	0.937829	0.969240	0.935936	0.891897
14	3	4,000	0.000423	0.000316	0.000132	0.000132	0.050531	0.000130	0.000135	0.000140	0.000153	0.967918	0.879176	0.920771	0.945289		0.843354	0.929262	0.927533	0.949344
15	3	4,500	0.000146	0.000203	0.000145	0.000141	0.033385	0.000138	0.000134	0.000161	0.000167	0.896157	0.870057	0.916864	0.937829	0.843354		0.751581	0.906774	0.921020
16	3	5,000	0.000227	0.000212	0.000138	0.000134	0.060735	0.000141	0.000128	0.000145	0.000161	0.946992	0.941455	0.965043	0.969240	0.929262	0.751581		0.918668	0.947575
17	3	5,500	0.000209	0.000207	0.000141	0.000127	0.063752	0.000134	0.000180	0.000138	0.000145	0.921236	0.934661	0.955034	0.935936	0.927533	0.906774	0.918668		0.834875
18	3	6,000	0.000231	0.000243	0.000134	0.000179	0.082640	0.000127	0.000155	0.000141	0.000138	0.907043	0.949335	0.960751	0.891897	0.949344	0.921020	0.947575	0.834875	

Newman-Keuls test; variable FA to FAME conversion efficiency [%] (Effect of cat conc and flow rate on FA to FAME CE)
Approximate Probabilities for Post Hoc Tests
Error: Between MSE = 15.177, df = 28.000

Cell No.	Catalyst Concentration (wt/v %)	Flow rate [mL/min]	{1}	{2}	{3}	{4}	{5}	{6}	{7}	{8}	{9}	{10}	{11}	{12}	{13}	{14}
1	1	1		0.395554	0.432305	0.496562	0.305850	0.005447	0.002800	0.344285	0.194621	0.238952	0.222764	0.226798	0.323252	0.213074
2	1	2	0.395554		0.834210	0.951626	0.783150	0.000617	0.000569	0.914007	0.847170	0.887101	0.846437	0.864853	0.869827	0.814817
3	1	3	0.432305	0.834210		0.929783	0.876949	0.000522	0.000514	0.920242	0.900679	0.927545	0.882027	0.905090	0.845921	0.841179
4	1	4	0.496562	0.951626	0.929783		0.937779	0.000573	0.000565	0.849960	0.899339	0.921886	0.853577	0.890954	0.646469	0.785325
5	1	5	0.305850	0.783150	0.876949	0.937779		0.000788	0.000583	0.867574	0.738022	0.796182	0.759098	0.773405	0.833591	0.733472
6	1	8	0.005447	0.000617	0.000522	0.000573	0.000788		0.904009	0.000300	0.000192	0.000208	0.000252	0.000199	0.000293	0.000225
7	1	10	0.002800	0.000569	0.000514	0.000565	0.000583	0.904009		0.000311	0.000195	0.000215	0.000236	0.000262	0.000308	0.000220
8	3	1	0.344285	0.914007	0.920242	0.849960	0.867574	0.000300	0.000311		0.976043	0.980024	0.893019	0.953582	0.936066	0.697946
9	3	2	0.194621	0.847170	0.900679	0.899339	0.738022	0.000192	0.000195	0.976043		0.862412	0.992310	0.975370	0.981486	0.996960
10	3	3	0.238952	0.887101	0.927545	0.921886	0.796182	0.000208	0.000215	0.980024	0.862412		0.994125	0.970033	0.986956	0.998398
11	3	4	0.222764	0.846437	0.882027	0.853577	0.759098	0.000252	0.000236	0.893019	0.992310	0.994125		0.947873	0.949772	0.951153
12	3	5	0.226798	0.864853	0.905090	0.890954	0.773405	0.000199	0.000262	0.953582	0.975370	0.970033	0.947873		0.973773	0.991107
13	3	8	0.323252	0.869827	0.845921	0.646469	0.833591	0.000293	0.000308	0.936066	0.981486	0.986956	0.949772	0.973773		0.884399
14	3	10	0.213074	0.814817	0.841179	0.785325	0.733472	0.000225	0.000220	0.697946	0.996960	0.998398	0.951153	0.991107	0.884399	

References

Abdulkadir, B. A., Uemura, Y., Ramli, A., Osman, N. B., Kusakabe, K. & Kai, T. 2015. Production of biodiesel from rubber seeds *Hevea brasiliensis* by *in situ* transesterification method. *J. Japan Inst. Energ.,* 94**,** 763 - 768.

Abdullah, S. H. Y. S., Hanapi, N. H. M., Azid, A., Umar, R., Juahir, H., Khatoon, H. & Endut, A. 2017. A review of biomass-derived heterogeneous catalyst for a sustainable biodiesel production. *Renew. Sustain. Energ. Rev.,* 70**,** 1040 - 51.

Abo El-Enin, S. A., Attia, N. K., El-Ibiari, N. N., El-Diwani, G. I. & El-Khatib, K. M. 2013. *In situ* transesterification of rapeseed and cost indicators for biodiesel production. *Renew. Sustain. Energ. Rev.,* 18**,** 471 - 77.

Abu-Ghosh, S., Fixler, D., Dubinsky, Z. & Iluz, D. 2015. Energy-input analysis of the life-cycle of microalgal cultivation systems and best scenario for oil-rich biomass production. *Appl. Energ.,* 154**,** 1082 - 88.

Aguieiras, E. C. G., Cavalcanti-Oliveira, E. D. & Freire, D. M. G. 2015. Current status and new developments of biodiesel production using fungal lipases. *Fuel,* 159**,** 52 - 67.

Ahmad, A. L., Yasin, N. H. M., Derek, C. J. C. & Lim, J. K. 2011. Microalgae as a sustainable energy source for biodiesel production: A review. *Renew. Sustain. Energ. Rev.,* 15**,** 584 - 93.

Ahmad, F. B., Zhang, Z., Doherty, W. O. S., Te'o, V. S. J. & O'hara, I. M. 2017. Improved microbial oil production from oil palm empty fruit bunch by *Mucor plumbeus*. *Fuel,* 194**,** 180 - 7.

Alencar, E. R. d., Faroni, L. R. D., Peternelli, L. A., Silva, M. T. C. d. & Costa, A. R. 2010. Influence of soybean storage conditions on crude oil quality. *Rev. Bras. Eng. Agríc. Ambient.,* 14**,** 303 - 8.

Alipour, S., Omidvarborna, H. & Kim, D. S. 2017. A review on synthesis of alkoxymethyl furfural, a biofuel candidate. *Renew. Sustain. Energ. Rev.,* 71**,** 908 - 26.

Álvarez, P., Pérez, L., Salgueiro, J. L., Cancela, Á., Sánchez, Á. & Ortiz, L. 2017. Bioenergy use from *Pavlova lutheri* microalgae. *Int. J. Environ. Res.,* 11**,** 281 - 9.

Amalia Kartika, I., Yani, M., Ariono, D., Evon, P. & Rigal, L. 2013. Biodiesel production from jatropha seeds: Solvent extraction and *in situ* transesterification in a single step. *Fuel,* 106**,** 111 - 7.

Apostolakou, A. A., Kookos, I. K., Marazioti, C. & Angelopoulos, K. C. 2009. Techno-economic analysis of a biodiesel production process from vegetable oils. *Fuel Proces. Technol.,* 90**,** 1023 - 31.

Aranda, D. A. G., Santos, R. T. P., Tapanes, N. C. O., Ramos, A. L. D. & Antunes, O. A. C. 2008. Acid-catalyzed homogeneous esterification reaction for biodiesel production from palm fatty acids. *Catal. Letters,* 122**,** 20 - 5.

Asadi, M., Hooper, J. F. & Lupton, D. W. 2016. Biodiesel synthesis using integrated acid and base catalysis in continuous flow. *Tetrahedron,* 72**,** 3729 - 33.

Atabani, A. E., Silitonga, A. S., Ong, H. C., Mahlia, T. M. I., Masjuki, H. H., Badruddin, I. A. & Fayaz, H. 2013. Non-edible vegetable oils: A critical

evaluation of oil extraction, fatty acid compositions, biodiesel production, characteristics, engine performance and emissions production. *Renew. Sustain. Energ. Rev.,* 18**,** 211 - 45.

Atadashi, I. M., Aroua, M. K., Abdul Aziz, A. R. & Sulaiman, N. M. N. 2012. The effects of water on biodiesel production and refining technologies: A review. *Renew. Sustain. Energ. Rev.,* 16**,** 3456 - 70.

Barrows, F. T., Gaylord, T. G., Sealey, W. M., Haas, M. J. & Stroup, R. L. 2008. Processing soybean meal for biodiesel production; effect of a new processing method on growth performance of rainbow trout, *Oncorhynchus mykiss*. *Aquaculture,* 283**,** 141 - 7.

Bauer, G., Lima, S., Chenevard, J., Sugnaux, M. & Fischer, F. 2017. Biodiesel via *in situ* wet microalgae biotransformation: Zwitter-type ionic liquid supported extraction and transesterification. *ACS Sustain. Chem. Eng.,* 5**,** 1931 - 37.

Bernal, J. M., Lozano, P., García-Verdugo, E., Burguete, M. I., Sánchez-Gómez, G., López-López, G., Pucheault, M., Vaultier, M. & Luis, S. V. 2012. Supercritical synthesis of biodiesel. *Molecules,* 17**,** 8696 - 719.

Bhuiya, M. M. K., Rasul, M. G., Khan, M. M. K., Ashwath, N. & Azad, A. K. 2016. Prospects of 2nd generation biodiesel as a sustainable fuel—Part: 1 selection of feedstocks, oil extraction techniques and conversion technologies. *Renew. Sustain. Energ. Rev.,* 55**,** 1109 - 1128.

Bi, Z., He, B. B. & Mcdonald, A. G. 2015. Biodiesel production from green microalgae *Schizochytrium limacinum* via *in situ* transesterification. *Energ. Fuel,* 29**,** 5018 - 27.

Boey, P. L., Maniam, G. P. & Hamid, S. A. 2011. Performance of calcium oxide as a heterogeneous catalyst in biodiesel production: A review. *Chem. Eng. J.,* 168**,** 15-22.

Boon-Anuwat, N., Kiatkittipong, W., Aiouache, F. & Assabumrungrat, S. 2015. Process design of continuous biodiesel production by reactive distillation: Comparison between homogeneous and heterogeneous catalysts. *Chem. Eng. Process.,* 92**,** 33 - 44.

Boro, J., Deka, D. & Thakur, A. J. 2012. A review on solid oxide derived from waste shells as catalyst for biodiesel production. *Renew. Sustain. Energ. Rev.,* 16**,** 904 - 10.

Bourbon, E. 2018. Clean cities alternative fuel price report, July 2018. U.S. Department of Energy.

Brar, K. K., Sarma, A. K., Aslam, M., Polikarpov, I. & Chadha, B. S. 2017. Potential of oleaginous yeast *Trichosporon* sp., for conversion of sugarcane bagasse hydrolysate into biodiesel. *Bioresour. Technol.,* 242**,** 161 - 168.

Braunwald, T., French, W. T., Claupein, W. & Graeff-Hönninger, S. 2016. Economic assessment of microbial biodiesel production using heterotrophic yeasts. *Int. J. Green. Energ.,* 13**,** 274 - 82.

Brentner, L. B., Eckelman, M. J. & Zimmerman, J. B. 2011. Combinatorial life cycle assessment to inform process design of industrial production of algal biodiesel. *Environ. Sci. Technol.,* 45**,** 7060-7067.

Britton, J., Dalziel, S. B. & Raston, C. L. 2015. Continuous flow Fischer esterifications harnessing vibrational-coupled thin film fluidics. *RSC Adv.,* 5**,** 1655 - 60.

Britton, J., Dalziel, S. B. & Raston, C. L. 2016. The synthesis of di-carboxylate esters using continuous flow vortex fluidics. *Green Chem.,* 18**,** 2193 - 200.

Britton, J. & Raston, C. L. 2014. Continuous flow vortex fluidic production of biodiesel. *RSC Adv.,* 4**,** 49850 - 4.
Britton, J. & Raston, C. L. 2015. Rapid high conversion of high free fatty acid feedstock into biodiesel using continuous flow vortex fluidics. *RSC Adv.,* 5**,** 2276 - 80.
Britton, J., Stubbs, K. A., Weiss, G. A. & Raston, C. L. 2017. Vortex fluidic chemical transformations. *Chem. Eur. J.,* 23**,** 13270 - 8.
Canakci, M. 2007. The potential of restaurant waste lipids as biodiesel feedstocks. *Bioresour. Technol.,* 98**,** 183 - 90.
Cao, H., Zhang, Z., Wu, X. & Miao, X. 2013. Direct biodiesel production from wet microalgae biomass of *Chlorella pyrenoidosa* through *in situ* transesterification. *BioMed Res. Int.,* 2013**,** 1 - 6.
Cao, X., Xie, H., Wu, Z., Shen, H. & Jing, B. 2012. Phase-switching homogeneous catalysis for clean production of biodiesel and glycerol from soybean and microbial lipids. *ChemCatChem,* 4**,** 1272 - 8.
Capello, C., Fischer, U. & Hungerbühler, K. 2007. What is a green solvent? A comprehensive framework for the environmental assessment of solvents. *Green Chem.,* 9**,** 927 - 34.
Carvalho, A. K. F., Da Conceição, L. R. V., Silva, J. P. V., Perez, V. H. & De Castro, H. F. 2017. Biodiesel production from *Mucor circinelloides* using ethanol and heteropolyacid in one and two-step transesterification. *Fuel,* 202**,** 503 - 11.
Carvalho Júnior, R. M., Vargas, J. V. C., Ramos, L. P., Marino, C. E. B. & Torres, J. C. L. 2011. Microalgae biodiesel via *in situ* methanolysis. *J. Chem. Technol. Biotechnol.,* 86**,** 1418 - 27.
Castillo López, B., Esteban Cerdán, L., Robles Medina, A., Navarro López, E., Martín Valverde, L., Hita Peña, E., González Moreno, P. A. & Molina Grima, E. 2015. Production of biodiesel from vegetable oil and microalgae by fatty acid extraction and enzymatic esterification. *J. Biosci. Bioeng.,* 119**,** 706-711.
Chee Loong, T. & Idris, A. 2017. One step transesterification of biodiesel production using simultaneous cooling and microwave heating. *J. Clean. Prod.,* 146**,** 57 - 62.
Cheirsilp, B. & Louhasakul, Y. 2013. Industrial wastes as a promising renewable source for production of microbial lipid and direct transesterification of the lipid into biodiesel. *Bioresour. Technol.,* 142**,** 329 - 37.
Chen, C. L., Huang, C. C., Ho, K. C., Hsiao, P. X., Wu, M. S. & Chang, J. S. 2015. Biodiesel production from wet microalgae feedstock using sequential wet extraction/transesterification and direct transesterification processes. *Bioresour. Technol.,* 194**,** 179 - 86.
Chen, X., Dobson, J. F. & Raston, C. L. 2012. Vortex fluidic exfoliation of graphite and boron nitride. *ChemComm,* 48**,** 3703 - 5.
Chen, X., Smith, N. M., Iyer, K. S. & Raston, C. L. 2014. Controlling nanomaterial synthesis, chemical reactions and self assembly in dynamic thin films. *Chem. Soc. Rev.,* 43**,** 1387 - 99.
Cheng, J., Qiu, Y., Huang, R., Yang, W., Zhou, J. & Cen, K. 2016. Biodiesel production from wet microalgae by using graphene oxide as solid acid catalyst. *Bioresour. Technol.,* 221**,** 344 - 49.

Cheng, J., Qiu, Y., Zhang, J., Huang, R., Yang, W. & Fan, Z. 2017. Conversion of lipids from wet microalgae into biodiesel using sulfonated graphene oxide catalysts. *Bioresour. Technol.,* 244**,** 569 - 74.

Cheng, J., Yu, T., Li, T., Zhou, J. & Cen, K. 2013. Using wet microalgae for direct biodiesel production via microwave irradiation. *Bioresour. Technol.,* 131**,** 531 - 535.

Chisti, Y. 2007. Biodiesel from microalgae. *Biotechnol. Adv.,* 25**,** 294 - 306.

Choi, W. Y., Kang, D. H., Lee, S. Y. & Lee, H. Y. 2015. High quality biodiesel from marine microalga, *Scenedesmus* sp. through *in situ* acid transesterification. *J. Chem. Technol. Biotechnol.,* 90**,** 1245 - 52.

Choi, W. Y., Kim, G. V., Lee, S. Y. & Lee, H. Y. 2014. Biodiesel production from *Scenedesmus* sp. through optimized *in situ* acidic transesterification process. *Chem. Biochem. Eng. Q.,* 28**,** 367 - 74.

Chopra, J., Dineshkumar, R., Bhaumik, M., Dhanarajan, G., Kumar, R. R. & Sen, R. 2016. Integrated *in situ* transesterification for improved biodiesel production from oleaginous yeast: a value proposition for possible industrial implication. *RSC Adv.,* 6**,** 70364 - 73.

Christopher, L. P., Hemanathan, K. & Zambare, V. P. 2014. Enzymatic biodiesel: Challenges and opportunities. *Appl. Energ.,* 119**,** 497 - 520.

Collet, P., Hélias, A., Lardon, L., Ras, M., Goy, R. A. & Steyer, J. P. 2011. Life-cycle assessment of microalgae culture coupled to biogas production. *Bioresour. Technol.,* 102**,** 207 - 214.

Corsini, A., Marchegiani, A., Rispoli, F., Sciulli, F. & Venturini, P. 2015. Vegetable Oils as Fuels in Diesel Engine. Engine Performance and Emissions. *Energy Procedia,* 81**,** 942 - 9.

Cravotto, G., Boffa, L., Mantegna, S., Perego, P., Avogadro, M. & Cintas, P. 2008. Improved extraction of vegetable oils under high-intensity ultrasound and/or microwaves. *Ultrason. Sonochem.,* 15**,** 898 - 902.

Cui, Y. & Liang, Y. 2014. Direct transesterification of wet *Cryptococcus curvatus* cells to biodiesel through use of microwave irradiation. *Appl. Energ.,* 119**,** 438 - 44.

Curzons, A. D., Constable, D. J. C., Mortimer, D. N. & Cunningham, V. L. 2001. So you think your process is green, how do you know?—Using principles of sustainability to determine what is green–a corporate perspective. *Green Chem.,* 3**,** 1 - 6.

D´Agosto, M. A., Da Silva, M. A. V., Franca, L. S., De Oliveira, C. M., Alexandre, M. O. L., Da Costa Marques, L. G., Murta, A. L. S. & De Freitas, M. A. V. 2017. Comparative study of emissions from stationary engines using biodiesel made from soybean oil, palm oil and waste frying oil. *Renew. Sustain. Energ. Rev.,* 70**,** 1376 - 92.

Da Silva César, A., Conejero, M. A., Barros Ribeiro, E. C. & Batalha, M. O. 2019. Competitiveness analysis of “social soybeans” in biodiesel production in Brazil. *Renew. Energ.,* 133**,** 1147 - 57.

Dasari, S. R., Chaudhary, A. J., Goud, V. V., Sahoo, N. & Kulkarni, V. N. 2017. *In-situ* alkaline transesterification of castor seeds: Optimization and engine performance, combustion and emission characteristics of blends. *Energ. Convs. Manag.,* 142**,** 200 - 14.

De Luna, M. D. G., Doliente, L. M. T., Ido, A. L. & Chung, T. W. 2017. *In situ* transesterification of *Chlorella* sp. microalgae using LiOH-pumice catalyst. *J. Environ. Chem. Eng.,* 5**,** 2830 - 5.

Deeba, F., Pruthi, V. & Negi, Y. S. 2016. Converting paper mill sludge into neutral lipids by oleaginous yeast *Cryptococcus vishniaccii* for biodiesel production. *Bioresour. Technol.,* 213**,** 96 - 102.

Demirbas, M. F. & Balat, M. 2006. Recent advances on the production and utilization trends of bio-fuels: A global perspective. *Energ. Convs. Manag.,* 47**,** 2371 - 81.

Dianursanti, Religia, P. & Wijanarko, A. 2015. Utilization of n-hexane as co-solvent to increase biodiesel yield on direct transesterification reaction from marine microalgae. *Procedia Environ. Sci.,* 23**,** 412 - 20.

Dias, J. M., Alvim-Ferraz, M. C. M. & Almeida, M. F. 2008. Comparison of the performance of different homogeneous alkali catalysts during transesterification of waste and virgin oils and evaluation of biodiesel quality. *Fuel,* 87**,** 3572 - 8.

Dizge, N., Aydiner, C., Imer, D. Y., Bayramoglu, M., Tanriseven, A. & Keskinler, B. 2009. Biodiesel production from sunflower, soybean, and waste cooking oils by transesterification using lipase immobilized onto a novel microporous polymer. *Bioresour. Technol.,* 100**,** 1983 - 91.

Dominguez-Faus, R., Powers, S. E., Burken, J. G. & Alvarez, P. J. 2009. The water footprint of biofuels: A drink or drive issue? *Environ. Sci. Technol.,* 43**,** 3005 - 10.

Dong, T., Wang, J., Miao, C., Zheng, Y. & Chen, S. 2013. Two-step *in situ* biodiesel production from microalgae with high free fatty acid content. *Bioresour. Technol.,* 136**,** 8 - 15.

Du, W., Li, W., Sun, T., Chen, X. & Liu, D. 2008. Perspectives for biotechnological production of biodiesel and impacts. *Appl. Microbiol. Biotech.,* 79**,** 331 - 37.

Duncan, J. 2003. *Cost of biodiesel production* [Online]. Global Bioenergy Partnership. Available: http://www.globalbioenergy.org/uploads/media/0305_Duncan_-_Cost-of-biodiesel-production.pdf [Accessed October, 28 2015].

Dupont, J., Suarez, P. A. Z., Meneghetti, M. R. & Meneghetti, S. M. P. 2009. Catalytic production of biodiesel and diesel-like hydrocarbons from triglycerides. *Energ. Environ. Sci.,* 2**,** 1258 - 65.

Efavi, J. K., Kanbogtah, D., Apalangya, V., Nyankson, E., Tiburu, E. K., Dodoo-Arhin, D., Onwona-Agyeman, B. & Yaya, A. 2018. The effect of NaOH catalyst concentration and extraction time on the yield and properties of Citrullus vulgaris seed oil as a potential biodiesel feed stock. *South African J. Chem. Eng.,* 25**,** 98 - 102.

Ehimen, E. A., Sun, Z. F. & Carrington, C. G. 2010. Variables affecting the *in situ* transesterification of microalgae lipids. *Fuel,* 89**,** 677 - 84.

Ehimen, E. A., Sun, Z. F. & Carrington, G. C. 2012. Use of ultrasound and co-solvents to improve the *in-situ* transesterification of microalgae biomass. *Procedia Environ. Sci.,* 15**,** 47 - 55.

El-Shimi, H. I., Attia, N. K., El-Sheltawy, S. T. & El-Diwani, G. I. 2013. Biodiesel production from *Spirulina-platensis* microalgae by *in-situ* transesterification process. *J. Sustain. Bioenerg. Sys.,* 3**,** 224 - 33.

El Shimi, H. I. & Moustafa, S. S. 2018. Biodiesel production from microalgae grown on domestic wastewater: Feasibility and Egyptian case study. *Renew. Sustain. Energ. Rev.,* 82**,** 4238 - 44.

Eroglu, E., D'alonzo, N. J., Smith, S. M. & Raston, C. L. 2013. Vortex fluidic entrapment of functional microalgal cells in a magnetic polymer matrix. *Nanoscale,* 5**,** 2627 - 31.

Escobar, J. C., Lora, E. S., Venturini, O. J., Yáñez, E. E., Castillo, E. F. & Almazan, O. 2009. Biofuels: Environment, technology and food security. *Renew. Sustain. Energ. Rev.,* 13**,** 1275 - 87.

Fang, Y. R., Yeh, Y. & Liu, H. S. 2018. A novel strategy of biodiesel production from wet microalgae by direct saponification–esterification conversion (DSEC). *J. Taiwan Inst. Chem.,* 83**,** 23 - 31.

Fargione, J., Hill, J., Tilman, D., Polasky, S. & Hawthorne, P. 2008. Land Clearing and the Biofuel Carbon Debt. *Science,* 319**,** 1235-1238.

Faried, M., Samer, M., Abdelsalam, E., Yousef, R. S., Attia, Y. A. & Ali, A. S. 2017. Biodiesel production from microalgae: Processes, technologies and recent advancements. *Renew. Sustain. Energ. Rev.,* 79**,** 893 - 913.

Folch, J., Lees, M. & Sloane Stanley, G. H. 1957. A simple method for the isolation and purification of total lipides from animal tissues. *J. Biol. Chem.,* 226**,** 497 - 509.

Frankl, P. 2017. Role of bioenergy and transport biofuels in energy and climate scenarios.

Freedman, B., Pryde, E. H. & Mounts, T. L. 1984. Variables affecting the yields of fatty esters from transesterified vegetable oils. *J. Am. Oil Soc.,* 61**,** 1638 - 43.

Fukuda, H., Kondo, A. & Noda, H. 2001. Biodiesel fuel production by transesterification of oils. *J. Biosci. Bioeng.,* 92**,** 405 - 16.

García-Olivares, A., Solé, J. & Osychenko, O. 2018. Transportation in a 100% renewable energy system. *Energ. Convs. Manag.,* 158**,** 266 - 85.

Gebremariam, S. N. & Marchetti, J. M. 2018. Economics of biodiesel production: Review. *Energ. Convs. Manag.,* 168**,** 74 - 84.

Geldin, F., Volkman, J. K., Largeau, C., Derenne, S., Damste, J. S. S. & De Leeuw, J. W. 1999. Distribution of aliphatic, non-hydrolyzable biopolymers in marine microalgae. *Org. Geochem.,* 30**,** 147-159.

Georgogianni, K. G., Kontominas, M. G., Pomonis, P. J., Avlonitis, D. & Gergis, V. 2008. Conventional and *in situ* transesterification of sunflower seed oil for the production of biodiesel. *Fuel Proces. Technol.,* 89**,** 503 - 9.

Gerpen, J. V. 2005. Biodiesel processing and production. *Fuel Proces. Technol.,* 86**,** 1097 - 107.

Giwa, A., Adeyemi, I., Dindi, A., Lopez, C. G. B., Lopresto, C. G., Curcio, S. & Chakraborty, S. 2018. Techno-economic assessment of the sustainability of an integrated biorefinery from microalgae and Jatropha: A review and case study. *Renew. Sustain. Energ. Rev.,* 88**,** 239 - 57.

Go, A. W., Sutanto, S., Liu, Y. T., Nguyen, P. L. T., Ismadji, S. & Ju, Y. H. 2014a. *In situ* transesterification of *Jatropha curcas* L. seeds in subcritical solvent system. *J. Taiwan Inst. Chem.,* 45**,** 1516 - 22.

Go, A. W., Sutanto, S., Ong, L. K., Tran-Nguyen, P. L., Ismadji, S. & Ju, Y. H. 2016. Developments in *in-situ* (trans) esterification for biodiesel production: A critical review. *Renew. Sustain. Energ. Rev.,* 60**,** 284 - 305.

Go, A. W., Sutanto, S., Tran-Nguyen, P. L., Ismadji, S., Gunawan, S. & Ju, Y. H. 2014b. Biodiesel production under subcritical solvent condition using subcritical water treated whole *Jatropha curcas* seed kernels and possible use of hydrolysates to grow *Yarrowia lipolytica*. *Fuel,* 120**,** 46 - 52.

Godswill, N. N., Frank, N. E. G., Walter, A. N., Edson, M. Y. J., Kingsley, T. M., Arondel, V., Martin, B. J. & Emmanuel, Y. 2016. Oil palm. *In:* GUPTA, S. K. (ed.) *Breeding oilseed crops for sustainable production.* San Diego: Academic Press.

Gog, A., Roman, M., Toşa, M., Paizs, C. & Irimie, F. D. 2012. Biodiesel production using enzymatic transesterification – Current state and perspectives. *Renew. Energ.,* 39**,** 10 - 16.

Goh, B. H. H., Ong, H. C., Cheah, M. Y., Chen, W.-H., Yu, K. L. & Mahlia, T. M. I. 2019. Sustainability of direct biodiesel synthesis from microalgae biomass: A critical review. *Renew. Sustain. Energ. Rev.,* 107**,** 59-74.

Gouveia, J. D., Ruiz, J., Van Den Broek, L. A. M., Hesselink, T., Peters, S., Kleinegris, D. M. M., Smith, A. G., Van Der Veen, D., Barbosa, M. J. & Wijffels, R. H. 2017. *Botryococcus braunii* strains compared for biomass productivity, hydrocarbon and carbohydrate content. *J. Biotech.,* 248**,** 77-86.

Granados, M. L., Poves, M. D. Z., Alonso, D. M., Mariscal, R., Galisteo, F. C., Moreno-Tost, R., Santamaría, J. & Fierro, J. L. G. 2007. Biodiesel from sunflower oil by using activated calcium oxide. *Appl. Catal. B: Environ.,* 73**,** 317 - 26.

Griffiths, M. J., Van Hille, R. P. & Harrison, S. T. L. 2010. Selection of direct transesterification as the preferred method for assay of fatty acid content of microalgae. *Lipids,* 45**,** 1053 - 60.

Gu, H., Jiang, Y., Zhou, L. & Gao, J. 2011. Reactive extraction and *in situ* self-catalyzed methanolysis of germinated oilseed for biodiesel production. *Energ. Environ. Sci.,* 4**,** 1337 - 44.

Guldhe, A., Singh, B., Rawat, I. & Bux, F. 2014a. Synthesis of biodiesel from *Scenedesmus* sp. by microwave and ultrasound assisted *in situ* transesterification using tungstated zirconia as a solid acid catalyst. *Chem. Eng. Res. Des.,* 92**,** 1503 - 11.

Guldhe, A., Singh, B., Rawat, I., Ramluckan, K. & Bux, F. 2014b. Efficacy of drying and cell disruption techniques on lipid recovery from microalgae for biodiesel production. *Fuel,* 128**,** 46 - 52.

Gupta, A., Chaudhary, R. & Sharma, S. 2012. Potential applications of mahua (*Madhuca indica*) biomass. *Waste Biomass Valori.,* 3**,** 175 - 89.

Haagenson, D. M., Brudvik, R. L., Lin, H. & Wiesenborn, D. P. 2010. Implementing an *in situ* alkaline transesterification method for canola biodiesel quality screening. *J. Am. Oil Soc.,* 87**,** 1351 - 8.

Haas, M. J., Mcaloon, A. J., Yee, W. C. & Foglia, T. A. 2006. A process model to estimate biodiesel production costs. *Bioresour. Technol.,* 97**,** 671 - 78.

Haas, M. J. & Scott, K. M. 2007. Moisture removal substantially improves the efficiency of *in situ* biodiesel production from soybeans. *J. Am. Oil Soc.,* 84**,** 197 - 204.

Haas, M. J., Scott, K. M., Marmer, W. N. & Foglia, T. A. 2004. *In situ* alkaline transesterification: An effective method for the production of fatty acid esters from vegetable oils. *J. Am. Oil Soc.,* 81**,** 83 - 9.

Haas, M. J. & Wagner, K. 2011. Simplifying biodiesel production: The direct or *in situ* transesterification of algal biomass. *Eur. J. Lipid Sci. Tech.,* 113**,** 1219 - 29.

Hailegiorgis, S. M., Mahadzir, S. & Subbarao, D. 2013. Parametric study and optimization of *in situ* transesterification of *Jatropha curcas* L assisted by benzyltrimethylammonium hydroxide as a phase transfer catalyst via response surface methodology. *Biomass Bioenerg.,* 49**,** 63 - 73.

Hailegiorgis, S. M., Mahadzir, S. & Subbarao, D. 2015. Reaction kinetics study for microwave energy pretreated *Jatropha curcas* L *in-situ* transesterification. *In:* HASHIM, M. A. (ed.) *ICGSCE 2014.* Springer Singapore.

Harrington, K. J. & D'arcy-Evans, C. 1985. A comparison of conventional and in situ methods of transesterification of seed oil from a series of sunflower cultivars. *J. Am. Oil Soc.,* 62**,** 1009 - 13.

Harun, S. & Geok, S. K. 2016. Effect of sodium hydroxide pretreatment on rice straw composition. *Ind. J. Sci. Technol.,* 9**,** 1 - 9.

Hashimoto, T., Matsuzaka, K., Moses, E. & Onuki, A. 1995. String phase in phase-separating fluids under shear flow. *Phys. Rev. Lett.,* 74**,** 126 - 9.

Hawash, S., Kamal, N., Zaher, F., Kenawi, O. & Diwani, G. E. 2009. Biodiesel fuel from *Jatropha* oil via non-catalytic supercritical methanol transesterification. *Fuel,* 88**,** 579 - 82.

He, H., Wang, T. & Zhu, S. 2007. Continuous production of biodiesel fuel from vegetable oil using supercritical methanol process. *Fuel,* 86**,** 442 - 7.

He, Q., Yang, H. & Hu, C. 2016. Culture modes and financial evaluation of two oleaginous microalgae for biodiesel production in desert area with open raceway pond. *Bioresour. Technol.,* 218**,** 571 - 79.

Hegel, P., Martín, L., Popovich, C., Damiani, C., Pancaldi, S., Pereda, S. & Leonardi, P. 2017. Biodiesel production from *Neochloris oleoabundans* by supercritical technology. *Chem. Eng. Process.,* 121**,** 232 - 9.

Heimann, K. 2016. Novel approaches to microalgal and cyanobacterial cultivation for bioenergy and biofuel production. *Curr. Opin. Biotechnol.,* 38**,** 183 - 9.

Hidalgo, P., Ciudad, G., Schober, S., Mittelbach, M. & Navia, R. 2015. Biodiesel synthesis by direct transesterification of microalga *Botryococcus braunii* with continuous methanol reflux. *Bioresour. Technol.,* 181**,** 32 - 9.

Hidalgo, P., Toro, C., Ciudad, G., Schober, S., Mittelbach, M. & Navia, R. 2014. Evaluation of different operational strategies for biodiesel production by direct transesterification of microalgal biomass. *Energ. Fuel,* 28**,** 3814 - 20.

Ho, D. P., Ngo, H. H. & Guo, W. 2014. A mini review on renewable sources for biofuel. *Bioresour. Technol.,* 169**,** 742 - 49.

Hoarau, J., Caro, Y., Petit, T. & Grondin, I. 2016. Evaluation of direct wet transesterification methods on yeast and fungal biomass grown on sugarcane distillery spent wash. *Chem. Eng. Proc. Techniq.,* 2**,** 1032.

Huang, J., Xia, J., Jiang, W., Li, Y. & Li, J. 2015. Biodiesel production from microalgae oil catalyzed by a recombinant lipase. *Bioresour. Technol.,* 180**,** 47 - 53.

Im, H. J., Lee, H. S., Park, M. S., Yang, J. W. & Lee, J. W. 2014. Concurrent extraction and reaction for the production of biodiesel from wet microalgae. *Bioresour. Technol.,* 152**,** 534 - 37.

Ishak, M. A. M., Ismail, K., Nawawi, W. I., Jawad, A. H., Ani, A. Y. & Zakaria, Z. 2017. In-situ Transesterification of Jatropha curcas L. Seeds for Biodiesel Production using Supercritical Methanol. *MATEC Web Conf.,* 97**,** 01082.

Islam, M. A., Brown, R. J., Brooks, P. R., Jahirul, M. I., Bockhorn, H. & Heimann, K. 2015a. Investigation of the effects of the fatty acid profile on fuel properties using a multi-criteria decision analysis. *Energ. Convs. Manag.,* 98**,** 340 - 7.

Islam, M. A., Brown, R. J., O'hara, I., Kent, M. & Heimann, K. 2014. Effect of temperature and moisture on high pressure lipid/oil extraction from microalgae. *Energ. Convs. Manag.,* 88**,** 307 - 16.

Islam, M. A., Heimann, K. & Brown, R. 2017. Microalgae biodiesel: Current status and future needs for engine performance and emissions. *Renew. Sustain. Energ. Rev.,* 79**,** 1160 - 70.

Islam, M. A., Magnusson, M., Brown, R., Ayoko, G., Nabi, M. & Heimann, K. 2013. Microalgal species selection for biodiesel production based on fuel properties derived from fatty acid profiles. *Energies,* 6**,** 5676 - 702.

Islam, M. A., Rahman, M. M., Heimann, K., Nabi, M. N., Ristovski, Z. D., Dowell, A., Thomas, G., Feng, B., Von Alvensleben, N. & Brown, R. J. 2015b. Combustion analysis of microalgae methyl ester in a common rail direct injection diesel engine. *Fuel,* 143**,** 351 - 60.

Jairurob, P., Phalakornkule, C., Na-Udom, A. & Petiraksakul, A. 2013. Reactive extraction of after-stripping sterilized palm fruit to biodiesel. *Fuel,* 107**,** 282 - 89.

Jaliliannosrati, H., Amin, N. A. S., Talebian-Kiakalaieh, A. & Noshadi, I. 2013. Microwave assisted biodiesel production from *Jatropha curcas* L. seed by two-step *in situ* process: Optimization using response surface methodology. *Bioresour. Technol.,* 136**,** 565 - 73.

Jazzar, S., Olivares-Carrillo, P., Pérez De Los Ríos, A., Marzouki, M. N., Acién-Fernández, F. G., Fernández-Sevilla, J. M., Molina-Grima, E., Smaali, I. & Quesada-Medina, J. 2015a. Direct supercritical methanolysis of wet and dry unwashed marine microalgae (*Nannochloropsis gaditana*) to biodiesel. *Appl. Energ.,* 148**,** 210 - 19.

Jazzar, S., Quesada-Medina, J., Olivares-Carrillo, P., Marzouki, M. N., Acién-Fernández, F. G., Fernández-Sevilla, J. M., Molina-Grima, E. & Smaali, I. 2015b. A whole biodiesel conversion process combining isolation, cultivation and *in situ* supercritical methanol transesterification of native microalgae. *Bioresour. Technol.,* 190**,** 281 - 88.

Jiang, Y., Li, D., Li, Y., Gao, J., Zhou, L. & He, Y. 2013. *In situ* self-catalyzed reactive extraction of germinated oilseed with short-chained dialkyl carbonates for biodiesel production. *Bioresour. Technol.,* 150**,** 50 - 4.

Jones, D. B. & Raston, C. L. 2017. Improving oxidation efficiency through plasma coupled thin film processing. *RSC Adv.,* 7**,** 47111 - 5.

Kakkad, H., Khot, M., Zinjarde, S. & Ravikumar, A. 2015a. Biodiesel production by direct *in situ* transesterification of an oleaginous tropical mangrove fungus grown on untreated agro-residues and evaluation of its fuel properties. *BioEnergy Res.,* 8**,** 1788 - 99.

Kakkad, H., Khot, M., Zinjarde, S., Ravikumar, A., Ravi Kumar, V. & Kulkarni, B. D. 2015b. Conversion of dried *Aspergillus candidus* mycelia grown on waste

whey to biodiesel by *in situ* acid transesterification. *Bioresour. Technol.,* 197**,** 502 - 507.
Kasim, F. H. & Harvey, A. P. 2011. Influence of various parameters on reactive extraction of *Jatropha curcas* L. for biodiesel production. *Chem. Eng. J.,* 171**,** 1373 - 8.
Kasim, F. H., Harvey, A. P. & Zakaria, R. 2010. Biodiesel production by in situ transesterification. *Biofuels,* 1**,** 355 - 365.
Katre, G., Raskar, S., Zinjarde, S., Ravi Kumar, V., Kulkarni, B. D. & Ravikumar, A. 2018. Optimization of the *in situ* transesterification step for biodiesel production using biomass of *Yarrowia lipolytica* NCIM 3589 grown on waste cooking oil. *Energy,* 142**,** 944 - 52.
Kaul, S., Porwal, J. & Garg, M. O. 2010. Parametric study of jatropha seeds for biodiesel production by reactive extraction. *J. Am. Oil Soc.,* 87**,** 903 - 8.
Kaya, Y. 2016. Sunflower. *In:* GUPTA, S. K. (ed.) *Breeding oilseed crops for sustainable production.* San Diego: Academic Press.
Kildiran, G., Yücel, S. O. & Türkay, S. 1996. *In-situ* alcoholysis of soybean oil. *J. Am. Oil Soc.,* 73**,** 225 - 8.
Kim, B., Heo, H. Y., Son, J., Yang, J., Chang, Y.-K., Lee, J. H. & Lee, J. W. 2019. Simplifying biodiesel production from microalgae via wet in situ transesterification: A review in current research and future prospects. *Algal Res.,* 41**,** 101557.
Kim, B., Im, H. & Lee, J. W. 2015a. *In situ* transesterification of highly wet microalgae using hydrochloric acid. *Bioresour. Technol.,* 185**,** 421 - 25.
Kim, G. V., Choi, W. Y., Kang, D. H., Lee, S. Y. & Lee, H. Y. 2014. Enhancement of biodiesel production from marine alga, *Scenedesmus sp*. through *in situ* transesterification process associated with acidic catalyst. *BioMed Res. Int.,* 2014**,** 1 - 11.
Kim, K. H., Lee, O. K., Kim, C. H., Seo, J. W., Oh, B. R. & Lee, E. Y. 2016. Lipase-catalyzed *in-situ* biosynthesis of glycerol-free biodiesel from heterotrophic microalgae, *Aurantiochytrium* sp. KRS101 biomass. *Bioresour. Technol.,* 211**,** 472 - 7.
Kim, T. H., Suh, W. I., Yoo, G., Mishra, S. K., Farooq, W., Moon, M., Shrivastav, A., Park, M. S. & Yang, J. W. 2015b. Development of direct conversion method for microalgal biodiesel production using wet biomass of *Nannochloropsis salina*. *Bioresour. Technol.,* 191**,** 438 - 44.
Kittithammavong, V., Arponrnpong, N., Charoensaeng, A. & Khaodhiar, S. 2014. Environmental life cycle Assessment of palm oil-based biofuels production from transesterification: Greenhouse gas, energy and water balances. *International Conference on Advances in Engineering and Technology.* Singapore.
Klein-Marcuschamer, D., Turner, C., Allen, M., Gray, P., Dietzgen, R. G., Gresshoff, P. M., Hankamer, B., Heimann, K., Scott, P. T., Stephens, E., Speight, R. & Nielsen, L. K. 2013. Technoeconomic analysis of renewable aviation fuel from microalgae, *Pongamia pinnata,* and sugarcane. *Biofuel. Bioprod. Biorefin.,* 7**,** 416 - 428.
Knothe, G. 2010. Biodiesel and renewable diesel: A comparison. *Prog. Energy Combust. Sci.,* 36**,** 364 - 73.
Knothe, G. & Kenar, J. A. 2004. Determination of the fatty acid profile by ^{1}H-NMR spectroscopy. *Eur. J. Lipid Sci. Tech.,* 106**,** 88 - 96.

Koberg, M., Cohen, M., Ben-Amotz, A. & Gedanken, A. 2011. Bio-diesel production directly from the microalgae biomass of *Nannochloropsis* by microwave and ultrasound radiation. *Bioresour. Technol.,* 102**,** 4265 - 69.

Koberg, M. & Gedanken, A. 2012. Direct transesterification of castor and jatropha seeds for FAME production by microwave and ultrasound radiation using a SrO catalyst. *BioEnergy Res.,* 5**,** 958 - 68.

Koutinas, A. A., Chatzifragkou, A., Kopsahelis, N., Papanikolaou, S. & Kookos, I. K. 2014. Design and techno-economic evaluation of microbial oil production as a renewable resource for biodiesel and oleochemical production. *Fuel,* 116**,** 566 - 77.

Koutsouki, A. A., Tegou, E., Kontakos, S., Kontominas, M. G., Pomonis, P. J. & Manos, G. 2015. *In situ* transesterification of *Cynara cardunculus* L. seed oil via direct ultrasonication for the production of biodiesel. *Fuel Proces. Technol.,* 134**,** 122 - 9.

Kreutzberer, C. B. 2001. Chloroformates and Carbonates. *Kirk-Othmer Encyclopedia of Chemical Technology.*

Krohn, B. J., Mcneff, C. V., Yan, B. & Nowlan, D. 2011. Production of algae-based biodiesel using the continuous catalytic Mcgyan® process. *Bioresour. Technol.,* 102**,** 94 - 100.

Kumar, G. 2017. Ultrasonic-assisted reactive-extraction is a fast and easy method for biodiesel production from *Jatropha curcas* oilseeds. *Ultrason. Sonochem.,* 37**,** 634 - 9.

Kumar, V., Muthuraj, M., Palabhanvi, B., Ghoshal, A. K. & Das, D. 2014. Evaluation and optimization of two stage sequential in situ transesterification process for fatty acid methyl ester quantification from microalgae. *Renew. Energ.,* 68**,** 560 - 9.

Kumari, H., Kline, S. R., Kennedy, S. R., Garvey, C., Raston, C. L., Atwood, J. L. & Steed, J. W. 2016. Manipulating three-dimensional gel network entanglement by thin film shearing. *ChemComm,* 52**,** 4513 - 6.

Kusdiana, D. & Saka, S. 2004. Effects of water on biodiesel fuel production by supercritical methanol treatment. *Bioresour. Technol.,* 91**,** 289 - 95.

Lardon, L., Hélias, A., Sialve, B., Steyer, J. P. & Bernard, O. 2009. Life-cycle assessment of biodiesel production from microalgae. *Environ. Sci. Technol.,* 43**,** 6475 - 81.

Lee, D. W., Park, Y. M. & Lee, K. Y. 2009. Heterogeneous base catalysts for transesterification in biodiesel synthesis. *Catal. Surv. Asia,* 13**,** 63 - 77.

Leung, D. Y. C., Wu, X. & Leung, M. K. H. 2010. A review on biodiesel production using catalyzed transesterification. *Appl. Energ.,* 87**,** 1083 - 95.

Levine, R. B., Pinnarat, T. & Savage, P. E. 2010. Biodiesel production from wet algal biomass through *in situ* lipid hydrolysis and supercritical transesterification. *Energ. Fuel,* 24**,** 5235 - 43.

Li, L., Du, W., Liu, D., Wang, L. & Li, Z. 2006. Lipase-catalyzed transesterification of rapeseed oils for biodiesel production with a novel organic solvent as the reaction medium. *J. Mol. Catal. B Enzym.,* 43**,** 58 - 62.

Li, Y., Lian, S., Tong, D., Song, R., Yang, W., Fan, Y., Qing, R. & Hu, C. 2011. One-step production of biodiesel from *Nannochloropsis* sp. on solid base Mg–Zr catalyst. *Appl. Energ.,* 88**,** 3313 - 17.

Lim, S., Hoong, S. S., Teong, L. K. & Bhatia, S. 2010. Supercritical fluid reactive extraction of *Jatropha curcas* L. seeds with methanol: A novel biodiesel production method. *Bioresour. Technol.,* 101**,** 7169 - 72.

Lim, S. & Lee, K. T. 2013. Process intensification for biodiesel production from *Jatropha curcas* L. seeds: Supercritical reactive extraction process parameters study. *Appl. Energ.,* 103**,** 712 - 20.

Lim, S. & Teong, L. K. 2010. Recent trends, opportunities and challenges of biodiesel in Malaysia: An overview. *Renew. Sustain. Energ. Rev.,* 14**,** 938 - 54.

Lin, L., Cunshan, Z., Vittayapadung, S., Xiangqian, S. & Mingdong, D. 2011. Opportunities and challenges for biodiesel fuel. *Appl. Energ.,* 88**,** 1020 - 1031.

Ling, J., Nip, S., De Toledo, R. A., Tian, Y. & Shim, H. 2016. Evaluation of specific lipid production and nutrients removal from wastewater by *Rhodosporidium toruloides* and biodiesel production from wet biomass via microwave irradiation. *Energy,* 108**,** 185 - 94.

Liu, B. & Zhao, Z. 2007. Biodiesel production by direct methanolysis of oleaginous microbial biomass. *J. Chem. Technol. Biotechnol.,* 82**,** 775 - 80.

Liu, K., Wang, R. & Yu, M. 2017. Biodiesel production from soybean oils by a novel nano-magnetic solid base catalyst (K/ZrO2/γ-Fe2O3). *RSC Adv.,* 7**,** 51814 - 21.

Liu, X., He, H., Wang, Y. T., Zhu, S. & Piao, X. 2008. Transesterification of soybean oil to biodiesel using CaO as a solid base catalyst. *Fuel,* 87**,** 216 - 21.

Liu, Y., Lotero, E. & Goodwin Jr, J. G. 2006. Effect of water on sulfuric acid catalyzed esterification. *J. Mol. Catal. A Chem.,* 245**,** 132 - 40.

Luo, X., Smith, P. A., Raston, C. L. & Zhang, W. 2016. Vortex fluidic device-intensified aqueous two phase extraction of C-phycocyanin from *Spirulina maxima*. *ACS Sustain. Chem. Eng.,* 4**,** 3905-3911.

Ma, F. & Hanna, M. A. 1999. Biodiesel production: a review. *Bioresour. Technol.,* 70**,** 1 - 15.

Ma, G., Hu, W., Pei, H., Jiang, L., Ji, Y. & Mu, R. 2015a. Study of KOH/Al_2O_3 as heterogeneous catalyst for biodiesel production via in situ transesterification from microalgae. *Environ. Technol.,* 36**,** 622 - 7.

Ma, G., Hu, W., Pei, H., Jiang, L., Song, M. & Mu, R. 2015b. *In situ* heterogeneous transesterification of microalgae using combined ultrasound and microwave irradiation. *Energ. Convs. Manag.,* 90**,** 41 - 6.

Macías-Sánchez, M. D., Robles-Medina, A., Hita-Peña, E., Jiménez-Callejón, M. J., Estéban-Cerdán, L., González-Moreno, P. A. & Molina-Grima, E. 2015. Biodiesel production from wet microalgal biomass by direct transesterification. *Fuel,* 150**,** 14 - 20.

Marcon, N. S., Colet, R., Balen, D. S., Pereira De Pereira, C. M., Bibilio, D., Priamo, W., Bender, J. P., Steffens, C. & Rosa, C. D. 2017. Enzymatic biodiesel production from microalgae biomass using propane as pressurized fluid. *Can. J. Chem. Eng.,* 95**,** 1340 - 44.

Martinez-Guerra, E., Gude, V. G., Mondala, A., Holmes, W. & Hernandez, R. 2014a. Extractive-transesterification of algal lipids under microwave irradiation with hexane as solvent. *Bioresour. Technol.,* 156**,** 240 - 247.

Martinez-Guerra, E., Gude, V. G., Mondala, A., Holmes, W. & Hernandez, R. 2014b. Microwave and ultrasound enhanced extractive-transesterification of algal lipids. *Appl. Energ.,* 129**,** 354 - 63.

Martínez, A., Mijangos, G. E., Romero-Ibarra, I. C., Hernández-Altamirano, R. & Mena-Cervantes, V. Y. 2019. In-situ transesterification of Jatropha curcas L. seeds using homogeneous and heterogeneous basic catalysts. *Fuel,* 235**,** 277-287.

Martínez, A., Mijangos, G. E., Romero-Ibarra, I. C., Hernández-Altamirano, R., Mena-Cervantes, V. Y. & Gutiérrez, S. 2018. A novel green one-pot synthesis of biodiesel from *Ricinus communis* seeds by basic heterogeneous catalysis. *J. Clean. Prod.,* 196**,** 340 - 49.

Mckeon, T. A. 2016. Castor (*Ricinus communis* L.). *In:* MCKEON, T. A., HAYES, D. G., HILDEBRAND, D. F. & WESELAKE, R. J. (eds.) *Industrial Oil Crops.* AOCS Press.

Mello, V. M., Oliveira, F. C. C., Fraga, W. G., Do Nascimento, C. J. & Suarez, P. A. Z. 2008. Determination of the content of fatty acid methyl esters (FAME) in biodiesel samples obtained by esterification using ^{1}H-NMR spectroscopy. *Magn. Reson. Chem.,* 46**,** 1051 - 4.

Misra, R., Guldhe, A., Singh, P., Rawat, I. & Bux, F. 2014. Electrochemical harvesting process for microalgae by using nonsacrificial carbon electrode: A sustainable approach for biodiesel production. *Chem. Eng. J.,* 255**,** 327 - 33.

Mubarak, M., Shaija, A. & Suchithra, T. V. 2015. A review on the extraction of lipid from microalgae for biodiesel production. *Algal Res.,* 7**,** 117 - 123.

Muhammad, A. B., Obianke, M., Gusau, L. H. & Aliero, A. A. 2017. Optimization of process variables in acid catalysed *in situ* transesterification of *Hevea brasiliensis* (rubber tree) seed oil into biodiesel. *Biofuels,* 8**,** 585 - 94.

Murphy, E. J. 2016. Camelina (*Camelina sativa*). *In:* MCKEON, T. A., HAYES, D. G., HILDEBRAND, D. F. & WESELAKE, R. J. (eds.) *Industrial Oil Crops.* AOCS Press.

Murphy, J. D. & Thamsiriroj, T. 2011. What will fuel transport systems of the future? *Mater. Today,* 14**,** 518 - 24.

Nasreen, S., Nafees, M., Qureshi, L. A., Asad, M. S., Sadiq, A. & Ali, S. D. 2018. Review of catalytic transesterification methods for biodiesel production. *Biofuels-State of Development.* IntechOpen.

Nguyen, H. C., Liang, S.-H., Li, S.-Y., Su, C.-H., Chien, C.-C., Chen, Y.-J. & Huong, D. T. M. 2018. Direct transesterification of black soldier fly larvae (Hermetia illucens) for biodiesel production. *J. Taiwan Inst. Chem. Eng.,* 85**,** 165-169.

Niju, S., S. Begum, K. M. M. & Anantharaman, N. 2014. Continuous flow reactive distillation process for biodiesel production using waste egg shells as heterogeneous catalysts. *RSC Adv.,* 4**,** 54109 - 14.

Nikolić, N. Č., Cakić, S. M., Novaković, S. M., Cvetković, M. D. & Stanković, M. Z. 2009. Effect of extraction techniques on yield and composition of soybean oil. *Macedonian J. Chem. Chem. Eng.,* 28**,** 173 - 9.

Noureddini, H., Gao, X. & Philkana, R. S. 2005. Immobilized *Pseudomonas cepacia* lipase for biodiesel fuel production from soybean oil. *Bioresour. Technol.,* 96**,** 769 - 77.

O'neill, B. 2018. *Average electricity costs per kWh* [Online]. Australia. Available: https://www.canstarblue.com.au/energy/electricity/electricity-costs-kwh/ [Accessed 15/01/2018 2018].

O'connell, D., Savelski, M. & Slater, C. S. 2013. Life cycle assessment of dewatering routes for algae derived biodiesel processes. *Clean Technol. Envir. Policy,* 15**,** 567 - 77.

Pande, G., Akoh, C. C. & Lai, O. M. 2012. Food uses of palm oil and its components. *In:* LAI, O. M., TAN, C. P. & AKOH, C. C. (eds.) *Palm Oil.* AOCS Press

Patil, P. D., Gude, V. G., Mannarswamy, A., Cooke, P., Munson-Mcgee, S., Nirmalakhandan, N., Lammers, P. & Deng, S. 2011a. Optimization of microwave-assisted transesterification of dry algal biomass using response surface methodology. *Bioresour. Technol.,* 102**,** 1399 - 405.

Patil, P. D., Gude, V. G., Mannarswamy, A., Cooke, P., Nirmalakhandan, N., Lammers, P. & Deng, S. 2012a. Comparison of direct transesterification of algal biomass under supercritical methanol and microwave irradiation conditions. *Fuel,* 97**,** 822 - 31.

Patil, P. D., Gude, V. G., Mannarswamy, A., Deng, S., Cooke, P., Munson-Mcgee, S., Rhodes, I., Lammers, P. & Nirmalakhandan, N. 2011b. Optimization of direct conversion of wet algae to biodiesel under supercritical methanol conditions. *Bioresour. Technol.,* 102**,** 118 - 22.

Patil, P. D., Reddy, H., Muppaneni, T., Mannarswamy, A., Schuab, T., Holguin, F. O., Lammers, P., Nirmalakhandan, N., Cooke, P. & Deng, S. 2012b. Power dissipation in microwave-enhanced *in situ* transesterification of algal biomass to biodiesel. *Green Chem.,* 14**,** 809 - 18.

Patil, P. D., Reddy, H., Muppaneni, T., Schaub, T., Holguin, F. O., Cooke, P., Lammers, P., Nirmalakhandan, N., Li, Y., Lu, X. & Deng, S. 2013. *In situ* ethyl ester production from wet algal biomass under microwave-mediated supercritical ethanol conditions. *Bioresour. Technol.,* 139**,** 308 - 15.

Pham, L. J. 2016. Coconut (*Cocos nucifera*). *In:* MCKEON, T. A., HAYES, D. G., HILDEBRAND, D. F. & WESELAKE, R. J. (eds.) *Industrial Oil Crops.* AOCS Press.

Pinto, A. C., Guarieiro, L. L. N., Rezende, M. J. C., Ribeiro, N. M., Torres, E. A., Lopes, W. A., Pereira, P. A. d. P. & Andrade, J. B. d. 2005. Biodiesel: an overview. *J. Brazil Chem. Soc.,* 16**,** 1313 - 30.

Ponnusamy, S., Reddy, H. K., Muppaneni, T., Downes, C. M. & Deng, S. 2014. Life cycle assessment of biodiesel production from algal bio-crude oils extracted under subcritical water conditions. *Bioresour. Technol.,* 170**,** 454 - 61.

Pradhan, A., S. Shrestha, D., Mcaloon, A., Yee, W., Haas, M. & A. Duffield, J. 2011. Energy life-cycle assessment of soybean biodiesel revisited. *Transactions ASABE,* 54**,** 1031 - 39.

Pratap, A., Gupta, S. K., Kumar, J., Mehandi, S. & Pandey, V. R. 2016. Soybean. *In:* GUPTA, S. K. (ed.) *Breeding oilseed crops for sustainable production.* San Diego: Academic Press.

Priyadarshan, P. M., Hoa, T. T. T., Huasun, H. & De Gonçalves, P. S. 2005. Yielding potential of rubber (*Hevea brasiliensis*) in sub-optimal environments. *J. Crop Improv.,* 14**,** 221 - 47.

Qian, J., Wang, F., Liu, S. & Yun, Z. 2008. *In situ* alkaline transesterification of cottonseed oil for production of biodiesel and nontoxic cottonseed meal. *Bioresour. Technol.,* 99**,** 9009 - 12.

Raja, R., Shanmugam, H., Ganesan, V. & Carvalho, I. 2014. Biomass from microalgae: An overview. *J. Oceanogr. Mar. Sci.,* 2**,** 1 - 7.

Rashid, N., Ur Rehman, M. S., Sadiq, M., Mahmood, T. & Han, J. I. 2014. Current status, issues and developments in microalgae derived biodiesel production. *Renew. Sustain. Energ. Rev.,* 40**,** 760 - 78.

Razon, L. F. & Tan, R. R. 2011. Net energy analysis of the production of biodiesel and biogas from the microalgae: *Haematococcus pluvialis* and *Nannochloropsis*. *Appl. Energ.,* 88**,** 3507 - 14.

Reddy, H. K., Muppaneni, T., Patil, P. D., Ponnusamy, S., Cooke, P., Schaub, T. & Deng, S. 2014. Direct conversion of wet algae to crude biodiesel under supercritical ethanol conditions. *Fuel,* 115**,** 720 - 26.

Salam, K. A., Velasquez-Orta, S. B. & Harvey, A. P. 2016. A sustainable integrated in situ transesterification of microalgae for biodiesel production and associated co-product-a review. *Renew. Sustain. Energ. Rev.,* 65**,** 1179-1198.

Sander, K. & Murthy, G. S. 2010. Life cycle analysis of algae biodiesel. *Int. J. Life Cycle Assess.,* 15**,** 704 - 14.

Sangaletti-Gerhard, N., Cea, M., Risco, V. & Navia, R. 2015. *In situ* biodiesel production from greasy sewage sludge using acid and enzymatic catalysts. *Bioresour. Technol.,* 179**,** 63 - 70.

Sarpal, A. S., Teixeira, C. M. L. L., Silva, P. R. M., Da Costa Monteiro, T. V., Da Silva, J. I., Da Cunha, V. S. & Daroda, R. J. 2016. NMR techniques for determination of lipid content in microalgal biomass and their use in monitoring the cultivation with biodiesel potential. *Appl. Microbiol. Biotech.,* 100**,** 2471 - 2485.

Sathish, A., Smith, B. R. & Sims, R. C. 2014. Effect of moisture on in situ transesterification of microalgae for biodiesel production. *J. Chem. Tech. Biotech.,* 89**,** 137-142.

Satyarthi, J. K., Srinivas, D. & Ratnasamy, P. 2009. Estimation of free fatty acid content in oils, fats, and biodiesel by ^{1}H-NMR spectroscopy. *Energ. Fuel,* 23**,** 2273 - 7.

Sawada, M. M., Venâncio, L. L., Toda, T. A. & Rodrigues, C. E. C. 2014. Effects of different alcoholic extraction conditions on soybean oil yield, fatty acid composition and protein solubility of defatted meal. *Food Res. Int.,* 62**,** 662 - 70.

Sawangkeaw, R. & Ngamprasertsith, S. 2013. A review of lipid-based biomasses as feedstocks for biofuels production. *Renew. Sustain. Energ. Rev.,* 25**,** 97 - 108.

Schenk, P. M., Thomas-Hall, S. R., Stephens, E., Marx, U. C., Mussgnug, J. H., Posten, C., Kruse, O. & Hankamer, B. 2008. Second generation biofuels: High-efficiency microalgae for biodiesel production. *BioEnergy Res.,* 1**,** 20 - 43.

Schilde, C., Mages-Sauter, C., Kwade, A. & Schuchmann, H. P. 2011. Efficiency of different dispersing devices for dispersing nanosized silica and alumina. *Powder Technol.,* 207**,** 353 - 61.

Scholz, M. J., Weiss, T. L., Jinkerson, R. E., Jing, J., Roth, R., Goodenough, U., Posewitz, M. C. & Gerken, H. G. 2014. Ultrastructure and composition of the *Nannochloropsis gaditana* cell wall. *Eukaryotic Cell,* 13**,** 1450-1464.

Sedman, J., Gao, L., García-González, D., Ehsan, S. & Van De Voort, F. R. 2010. Determining nutritional labeling data for fats and oils by ^{1}H-NMR. *Eur. J. Lipid Sci. Tech.,* 112**,** 439 - 51.

Selmi, M., Gazzah, M. H. & Belmabrouk, H. 2017. Optimization of microfluidic biosensor efficiency by means of fluid flow engineering. *Sci. Rep.,* 7**,** 5721 - 32.

Sheldon, R. A. 2018. Metrics of green chemistry and sustainability: Past, present, and future. *ACS Sustain. Chem. Eng.,* 6**,** 32 - 48.

Shiu, P.-J., Gunawan, S., Hsieh, W.-H., Kasim, N. S. & Ju, Y.-H. 2010. Biodiesel production from rice bran by a two-step in-situ process. *Bioresour. Technol.,* 101**,** 984-989.

Shuba, E. S. & Kifle, D. 2018. Microalgae to biofuels: 'Promising' alternative and renewable energy, review. *Renew. Sustain. Energ. Rev.,* 81**,** 743 - 55.

Shuit, S. H., Lee, K. T., Kamaruddin, A. H. & Yusup, S. 2010. Reactive extraction and *in situ* esterification of *Jatropha curcas* L. seeds for the production of biodiesel. *Fuel,* 89**,** 527 - 30.

Siatis, N. G., Kimbaris, A. C., Pappas, C. S., Tarantilis, P. A. & Polissiou, M. G. 2006. Improvement of biodiesel production based on the application of ultrasound: Monitoring of the procedure by FT-IR spectroscopy. *J. Am. Oil Soc.,* 83**,** 53 - 57.

Sieverding, H. L., Bailey, L. M., Hengen, T. J., Clay, D. E. & Stone, J. J. 2015. Meta-analysis of soybean-based biodiesel. *J. Environ. Qual.,* 44**,** 1038 - 48.

Sitepu, E. K., Corbin, K., Luo, X., Pye, S. J., Tang, Y., Leterme, S. C., Heimann, K., Raston, C. L. & Zhang, W. 2018a. Vortex fluidic mediated direct transesterification of wet microalgae biomass to biodiesel. *Bioresour. Technol.,* 266**,** 488 - 97.

Sitepu, E. K., Heimann, K., Raston, C. L. & Zhang, W. 2020. Critical evaluation of process parameters for direct biodiesel production from diverse feedstock. *Renew. Sustain. Energ. Rev.,* 123**,** 109762.

Sitepu, E. K., Jones, D. B., Tang, Y., Leterme, S. C., Heimann, K., Zhang, W. & Raston, C. L. 2018b. Continuous flow biodiesel production from wet microalgae using a hybrid thin film microfluidic platform. *ChemComm,* 54**,** 12085 - 12088

Sitepu, E. K., Jones, D. B., Zhang, Z., Tang, Y., Leterme, S. C., Heimann, K., Raston, C. L. & Zhang, W. 2019. Turbo thin film continuous flow production of biodiesel from fungal biomass. *Bioresour. Technol.,* 273**,** 431 - 8.

Sitthithanaboon, W., Reddy, H. K., Muppaneni, T., Ponnusamy, S., Punsuvon, V., Holguim, F., Dungan, B. & Deng, S. 2015. Single-step conversion of wet *Nannochloropsis gaditana* to biodiesel under subcritical methanol conditions. *Fuel,* 147**,** 253 - 9.

Sivaramakrishnan, R. & Incharoensakdi, A. 2017a. Direct transesterification of *Botryococcus* sp. catalysed by immobilized lipase: Ultrasound treatment can reduce reaction time with high yield of methyl ester. *Fuel,* 191**,** 363-370.

Sivaramakrishnan, R. & Incharoensakdi, A. 2017b. Production of methyl ester from two microalgae by two-step transesterification and direct transesterification. *Environ. Sci. Pollut. R.,* 24**,** 4950 - 63.

Skorupskaite, V., Makareviciene, V. & Gumbyte, M. 2016. Opportunities for simultaneous oil extraction and transesterification during biodiesel fuel production from microalgae: A review. *Fuel Proces. Technol.,* 150**,** 78 - 87.

Somogyi, B., Felföldi, F., Solymosi, K., Makk, J., Homonnay, Z. G., Horváth, G., Turcsi, E., Böddi, B., Márialigeti, K. & Vörös, L. 2011. *Chloroparva pannonica* gen. et sp. nov. (*Trebouxiophyceae, Chlorophyta*) – a new picoplanktonic green alga from a turbid, shallow soda pan. *Phycologia,* 50**,** 1 - 10.

Son, J., Kim, B., Park, J., Yang, J. & Lee, J. W. 2018. Wet in situ transesterification of spent coffee grounds with supercritical methanol for the production of biodiesel. *Bioresour. Technol.,* 259**,** 465-468.

Souza, K. S. T., Ramos, C. L., Schwan, R. F. & Dias, D. R. 2017. Lipid production by yeasts grown on crude glycerol from biodiesel industry. *Prep. Biochem. Biotechnol.,* 47**,** 357 - 63.

Suganya, T., Kasirajan, R. & Renganathan, S. 2014. Ultrasound-enhanced rapid *in situ* transesterification of marine macroalgae *Enteromorpha compressa* for biodiesel production. *Bioresour. Technol.,* 156**,** 283 - 90.

Suh, W. I., Mishra, S. K., Kim, T. H., Farooq, W., Moon, M., Shrivastav, A., Park, M. S. & Yang, J. W. 2015. Direct transesterification of wet microalgal biomass for preparation of biodiesel. *Algal Res.,* 12**,** 405 - 411.

Sun, Z. F., Fang, X. P., Li, X. Y. & Zhou, Z. G. 2018. Oleaginous microalgae from dairy farm wastewater for biodiesel production: Isolation, characterization and mass cultivation. *Appl. Biochem. Biotech.,* 184**,** 524 - 537.

Suriya, A. C. N. P. 2016. Coconut. *In:* GUPTA, S. K. (ed.) *Breeding oilseed crops for sustainable production.* San Diego: Academic Press.

Suwannakarn, K., Lotero, E., Ngaosuwan, K. & Goodwin, J. G. 2009. Simultaneous free fatty acid esterification and triglyceride transesterification using a solid acid Catalyst with *in situ* removal of water and unreacted Methanol. *Ind. Chem Eng. Res.,* 48**,** 2810 - 18.

Taher, H., Al-Zuhair, S., Al-Marzouqi, A. H., Haik, Y. & Farid, M. 2014. Effective extraction of microalgae lipids from wet biomass for biodiesel production. *Biomass Bioenerg.,* 66**,** 159 - 167.

Talebian-Kiakalaieh, A., Amin, N. A. S. & Mazaheri, H. 2013. A review on novel processes of biodiesel production from waste cooking oil. *Appl. Energ.,* 104**,** 683 - 710.

Talha, N. S. & Sulaiman, S. 2018. In situ transesterification of solid coconut waste in a packed bed reactor with CaO/PVA catalyst. *Waste Management,* 78**,** 929-937.

Tamer, I. M., Moo-Young, M. & Chisti, Y. 1998. Optimization of poly(b-hydroxybutyric acid) recovery from *Alcaligenes latus*: combined mechanical and chemical treatments. *Bioprocess Eng.,* 19**,** 459 - 68.

Tan, L. F. 2016. *Enhancement of biomass and lutein production in Chloroparva pannonica.* Doctor of Philosphy, Flinders University.

Tarigan, J. B., Prakoso, H. T., Siahaan, D. & Kaban, J. 2017. Rapid biodiesel production from palm kernel through *in situ* transesterification reaction using CaO as catalyst. *Int. J. Appl. Chem.,* 13**,** 631 - 46.

Tariq, M., Ali, S., Ahmad, F., Ahmad, M., Zafar, M., Khalid, N. & Khan, M. A. 2011. Identification, FT-IR, NMR (^{1}H and ^{13}C) and GC/MS studies of fatty acid

methyl esters in biodiesel from rocket seed oil. *Fuel Proces. Technol.,* 92**,** 336 - 41.

Taufiq-Yap, Y. H. & Teo, S. H. 2014. Biodiesel production via transesterification of *Nannochloropsis oculata* microalga's oil using calcium methoxide as heterogeneous catalyst. *J. Japan Inst. Energ.,* 93**,** 995 - 9.

Teo, C. L. & Idris, A. 2014. Evaluation of direct transesterification of microalgae using microwave irradiation. *Bioresour. Technol.,* 174**,** 281 - 86.

Thliveros, P., Uçkun Kiran, E. & Webb, C. 2014. Microbial biodiesel production by direct methanolysis of oleaginous biomass. *Bioresour. Technol.,* 157**,** 181 - 87.

Tong, C. L., Stroeher, U. H., Brown, M. H. & Raston, C. L. 2015. Continuous flow vortex fluidic synthesis of silica xerogel as a delivery vehicle for curcumin. *RSC Adv.,* 5**,** 7953 - 8.

Tran, D. T., Chen, C. L. & Chang, J. S. 2013. Effect of solvents and oil content on direct transesterification of wet oil-bearing microalgal biomass of *Chlorella vulgaris* ESP-31 for biodiesel synthesis using immobilized lipase as the biocatalyst. *Bioresour. Technol.,* 135**,** 213 - 21.

Tran, D. T., Yeh, K. L., Chen, C. L. & Chang, J. S. 2012. Enzymatic transesterification of microalgal oil from *Chlorella vulgaris* ESP-31 for biodiesel synthesis using immobilized Burkholderia lipase. *Bioresour. Technol.,* 108**,** 119 - 27.

Tsigie, Y. A., Huynh, L. H., Ismadji, S., Engida, A. M. & Ju, Y. H. 2012. In situ biodiesel production from wet *Chlorella vulgaris* under subcritical condition. *Chem. Eng. J.,* 213**,** 104 - 8.

Velasquez-Orta, S. B., Lee, J. G. M. & Harvey, A. 2012. Alkaline *in situ* transesterification of *Chlorella vulgaris*. *Fuel,* 94**,** 544 - 50.

Velasquez-Orta, S. B., Lee, J. G. M. & Harvey, A. P. 2013. Evaluation of FAME production from wet marine and freshwater microalgae by *in situ* transesterification. *Biochem. Eng. J.,* 76**,** 83 - 9.

Venkata Subhash, G. & Venkata Mohan, S. 2011. Biodiesel production from isolated oleaginous fungi Aspergillus sp. using corncob waste liquor as a substrate. *Bioresour. Technol.,* 102**,** 9286 - 90.

Vicente, G., Bautista, L. F., Rodríguez, R., Gutiérrez, F. J., Sádaba, I., Ruiz-Vázquez, R. M., Torres-Martínez, S. & Garre, V. 2009. Biodiesel production from biomass of an oleaginous fungus. *Biochem. Eng. J.,* 48**,** 22 - 7.

Viêgas, C. V., Hachemi, I., Freitas, S. P., Mäki-Arvela, P., Aho, A., Hemming, J., Smeds, A., Heinmaa, I., Fontes, F. B., Da Silva Pereira, D. C., Kumar, N., Aranda, D. A. G. & Murzin, D. Y. 2015. A route to produce renewable diesel from algae: Synthesis and characterization of biodiesel via *in situ* transesterification of *Chlorella* alga and its catalytic deoxygenation to renewable diesel. *Fuel,* 155**,** 144 - 54.

Vimalanathan, K., Gascooke, J. R., Suarez-Martinez, I., Marks, N. A., Kumari, H., Garvey, C. J., Atwood, J. L., Lawrance, W. D. & Raston, C. L. 2016. Fluid dynamic lateral slicing of high tensile strength carbon nanotubes. *Sci. Rep.,* 6**,** 22865 - 9.

Visscher, F., Van Der Schaaf, J., Nijhuis, T. A. & Schouten, J. C. 2013. Rotating reactors – A review. *Chem. Eng. Res. Des.,* 91**,** 1923 - 40.

Volkman, J. K., Jeffrey, S. W., Nichols, P. D., Rogers, G. I. & Garland, C. D. 1989. Fatty acid and lipid composition of 10 species of microalgae used in mariculture. *J. Exp. Mar. Bio. Ecol.,* 128**,** 219 - 40.

Von Alvensleben, N., Magnusson, M. & Heimann, K. 2015. Salinity tolerance of four freshwater microalgal species and the effects of salinity and nutrient limitation on biochemical profiles. *J. Appl. Phycol.,* 28**,** 861 - 76.

Wahid, M. H., Eroglu, E., Chen, X., Smith, S. M. & Raston, C. L. 2013. Entrapment of *Chlorella vulgaris* cells within graphene oxide layers. *RSC Adv.,* 3**,** 8180 - 3.

Wahid, M. H., Eroglu, E., Lavars, S. M., Newton, K., Gibson, C. T., Stroeher, U. H., Chen, X., Boulos, R. A., Raston, C. L. & Harmer, S. L. 2015. Microencapsulation of bacterial strains in graphene oxide nano-sheets using vortex fluidics. *RSC Adv.,* 5**,** 37424 - 30.

Wahidin, S., Idris, A. & Shaleh, S. R. M. 2016. Ionic liquid as a promising biobased green solvent in combination with microwave irradiation for direct biodiesel production. *Bioresour. Technol.,* 206**,** 150 - 54.

Wahlen, B. D., Willis, R. M. & Seefeldt, L. C. 2011. Biodiesel production by simultaneous extraction and conversion of total lipids from microalgae, cyanobacteria, and wild mixed-cultures. *Bioresour. Technol.,* 102**,** 2724 - 30.

Ward, V. C. A., Munch, G., Cicek, N. & Rehmann, L. 2017. Direct conversion of the oleaginous yeast *Rhodosporidium diobovatum* to biodiesel using the ionic liquid [C2mim][EtSO4]. *ACS Sustain. Chem. Eng.,* 5**,** 5562 - 70.

Wyatt, V. T. & Haas, M. J. 2009. Production of fatty acid methyl esters via the *in situ* transesterification of soybean oil in carbon dioxide-expanded methanol. *J. Am. Oil Soc.,* 86**,** 1009 - 1016.

Xu, L., Brilman, D. W. F., Withag, J. A. M., Brem, G. & Kersten, S. 2011. Assessment of a dry and a wet route for the production of biofuels from microalgae: Energy balance analysis. *Bioresour. Technol.,* 102**,** 5113 - 22.

Xu, Q. Q., Li, Q., Yin, J. Z., Guo, D. & Qiao, B. Q. 2016. Continuous production of biodiesel from soybean flakes by extraction coupling with transesterification under supercritical conditions. *Fuel Proces. Technol.,* 144**,** 37 - 41.

Xu, R. & Mi, Y. 2011. Simplifying the process of microalgal biodiesel production through *in situ* transesterification technology. *J. Am. Oil Soc.,* 88**,** 91 - 9.

Yasmin, L., Chen, X., Stubbs, K. A. & Raston, C. L. 2013. Optimising a vortex fluidic device for controlling chemical reactivity and selectivity. *Sci. Rep.,* 3**,** 2282.

Yellapu, S. K., Kaur, R. & Tyagi, R. D. 2017. Detergent assisted ultrasonication aided *in situ* transesterification for biodiesel production from oleaginous yeast wet biomass. *Bioresour. Technol.,* 224**,** 365 - 72.

Yen, H. W., Hu, I. C., Chen, C. Y., Ho, S. H., Lee, D. J. & Chang, J. S. 2013. Microalgae-based biorefinery – From biofuels to natural products. *Bioresour. Technol.,* 135**,** 166 - 74.

Yousuf, A., Khan, M. R., Islam, M. A., Wahid, Z. A. & Pirozzi, D. 2017. Technical difficulties and solutions of direct transesterification process of microbial oil for biodiesel synthesis. *Biotechnol. Lett.,* 39**,** 13-23.

Yu, D., Tian, L., Wu, H., Wang, S., Wang, Y., Ma, D. & Fang, X. 2010. Ultrasonic irradiation with vibration for biodiesel production from soybean oil by Novozym 435. *Process Biochem.,* 45**,** 519 - 25.

Yu, N., Dieu, L. T. L., Harvey, S. & Lee, D. Y. 2015. Optimization of process configuration and strain selection for microalgae-based biodiesel production. *Bioresour. Technol.,* 193**,** 25c- 34.

Yuan, T., Akochi-Koble, E., Pinchuk, D. & Voort, v. d. 2014. FT-IR on-line monitoring of biodiesel transesterification. *Int. J. Renew. Energ. Biofuel.,* 2014**,** 1 - 13.

Yuan, T. Z., Ormonde, C. F. G., Kudlacek, S. T., Kunche, S., Smith, J. N., Brown, W. A., Pugliese, K. M., Olsen, T. J., Iftikhar, M., Raston, C. L. & Weiss, G. A. 2015. Shear stress mediated refolding of proteins from aggregates and inclusion bodies. *ChemBioChem,* 16**,** 393 - 6.

Zakaria, R. & Harvey, A. P. 2012. Direct production of biodiesel from rapeseed by reactive extraction/*in situ* transesterification. *Fuel Proces. Technol.,* 102**,** 53 - 60.

Zeng, J., Wang, X., Zhao, B., Sun, J. & Wang, Y. 2009. Rapid *in situ* transesterification of sunflower oil. *Ind. Chem Eng. Res.,* 48**,** 850 - 6.

Zhang, F., Fang, Z. & Wang, Y. T. 2015a. Biodiesel production direct from high acid value oil with a novel magnetic carbonaceous acid. *Appl. Energ.,* 155**,** 637 - 47.

Zhang, X., Ma, Q., Cheng, B., Wang, J., Li, J. & Nie, F. 2012. Research on KOH/La-Ba-Al_2O_3 catalysts for biodiesel production via transesterification from microalgae oil. *J. Nat. Gas Chem.,* 21**,** 774 - 9.

Zhang, X., Yan, S., Tyagi, R. D., Surampalli, R. Y. & Valéro, J. R. 2014. Ultrasonication aided *in-situ* transesterification of microbial lipids to biodiesel. *Bioresour. Technol.,* 169**,** 175 - 80.

Zhang, Y., Li, Y., Zhang, X. & Tan, T. 2015b. Biodiesel production by direct transesterification of microalgal biomass with co-solvent. *Bioresour. Technol.,* 196**,** 712 - 15.

Zhang, Y., Yang, L., Zu, Y., Chen, X., Wang, F. & Liu, F. 2010. Oxidative stability of sunflower oil supplemented with carnosic acid compared with synthetic antioxidants during accelerated storage. *Food Chem.,* 118**,** 656 - 62.

Zhang, Z., Ye, J., Fei, T., Ma, X., Xie, X., Huang, H. & Wang, Y. 2019. Interesterification of rice bran wax and palm olein catalyzed by lipase: Crystallization behaviours and characterization. *Food Chem.,* 286**,** 29-37.

Zhou, D., Qi, L., Qiao, B. Q., Xu, Q. Q. & Yin, J. Z. 2017. Continuous production of biodiesel from soybean flakes by extraction coupling with transesterification under supercritical conditions: Original research article. *J. Supercrit. Fluid,* 120**,** 395 - 402.